Aus dem Institut für Molekularbiologie und Tumorforschung
der Philipps-Universität Marburg
Geschäftsführender Direktor: Prof. Dr. Rolf Müller

The Role of the Mitotic Spindle Checkpoint in Chemotherapy-Induced Apoptosis

Inaugural-Dissertation

zur Erlangung des Doktorgrades
der Humanbiologie
(Dr. rer. physiol.)

dem Fachbereich Medizin der

Philipps Universität Marburg

vorgelegt von
Celia Vogel
aus Oldenburg

Marburg 2008

Angenommen vom Fachbereich Medizin
der Philipps-Universität Marburg am 05.08.2008.

Gedruckt mit Genehmigung des Fachbereichs.

Dekan: Prof. Dr. Matthias Rothmund
Referent: PD Dr. Holger Bastians
Korreferent: Prof. Dr. Czubayko

The only way of discovering the limits of the possible is to venture a little way past them into the impossible.

Arthur C. Clarke

Table of Contents

Summary

The mitotic spindle assembly checkpoint (SCP) is a signal transduction pathway that ensures proper chromosome segregation during mitosis by inhibiting the onset of anaphase until all chromosomes are properly aligned. It requires a group of highly conserved proteins including Mad1, Mad2, Bub1, BubR1, Mps1 and the so-called chromosomal passenger complex comprising survivin, borealin, INCENP and the Aurora B kinase.

The SCP ensures chromosomal stability during a normal mitosis, but it is also activated by chemotherapeutic drugs that interfere with chromosome alignment leading to a prolonged mitotic arrest. Subsequently tetraploid cells exit mitosis – a process termed "mitotic slippage –, thereby activating the so-called pseudo-G1 checkpoint, which arrests cells p53-dependently at the G1/S border. Failure of this second fail-safe mechanism might promote cancerogenesis via polyploidization and induction of genomic instability. The present work has defined the pseudo-G1 checkpoint as dependent on p53 and a functional SCP. Moreover, an additional SCP-independent checkpoint is activated in G2, which prevents polyploid cells from entering the next mitosis. Thus, multiple checkpoints cooperate to prevent further polyploidization after mitotic failure.

Antimitotic substances are among the most frequently used chemotherapeutics. However, the mechanisms of mitosis-associated apoptosis and chemotherapy resistance are largely unknown. During the course of my work I demonstrated that the SCP is required for the induction of apoptosis in response to various antimitotic drugs. Specifically, Mad2 was shown to be a central proapoptotic factor after treatment with drugs that impair kinetochore tension, which do not only include spindle poisons like taxol, but surprisingly also DNA damaging agents like topoisomerase II inhibitors.

A clinically relevant mitosis-associated chemotherapeutic strategy is the induction of “mitotic catastrophe”, a poorly defined form of cell death. Abrogation of the activated G2 DNA damage checkpoint by Chk1 kinase inhibitors selectively forces p53-negative cells into mitosis, resulting in mitosis-associated cell death. This work shows that “mitotic catastrophe” is a mitosis-specific form of apoptosis, which is associated with SCP activation and requires the proapoptotic function of Mad2. Surprisingly, I found that the proapoptotic pathway during mitosis was counteracted by survival pathways comprising survivin, Aurora B and Cdk1. Therefore, genetic or pharmacological abrogation of the survival pathways synergistically enhances mitotic apoptosis and suggests a highly improved strategy for anticancer chemotherapy.

My results, which demonstrate an important role of the SCP in mediating chemotherapy-induced apoptosis, suggest that SCP defects might account for drug resistance, posing a serious problem in the clinic. Therefore, alternative chemotherapeutic approaches independent of full SCP functionality are urgently needed. Interestingly, the observation that the SCP is essential for cancer cell viability gives rise to a novel concept of chemotherapy, which targets the SCP. In fact, our lab has identified a potent pharmacological SCP inhibitor and I was able to demonstrate that this inhibitor induces apoptosis in cancer cells, even those resistant to spindle poisons due to SCP defects.

Zusammenfassung

Der mitotische Spindelcheckpoint (SCP) ist ein Signalweg, der die ordnungsgemäße Chromosomentrennung in der Mitose dadurch sicherstellt, daß er die Anaphase solange hemmt bis alle Chromosomen korrekt ausgerichtet sind. Eine Gruppe von hochkonservierten Proteinen, wie Mad1, Mad2, Bub1, BubR1, Mps1 und der sogenannte „Chromosomal Passenger Complex“, bestehend aus Survivin, Borealin, INCENP und der Aurora B-Kinase, trägt zur Funktionalität des SCP bei.

Während einer normalen Mitose sichert der SCP die korrekte Verteilung der Chromatiden und dadurch die chromosomale Stabilität. Er wird jedoch auch durch Chemotherapeutika, die die Chromosomenaufreihung stören, aktiviert, was zunächst zu einem verlängerten mitotischen Arrest führt. Anschließend beobachtet man einen Austritt tetraploider Zellen aus der Mitose – ein als „mitotic slippage“ bezeichneter Prozeß –, wodurch nachfolgend ein sogenannter Pseudo-G1 Checkpoint aktiviert wird, der die Zellen p53-abhängig am G1/S-Übergang arretiert. Ein Versagen dieses zweiten Sicherungsmechanismus' könnte die Krebsentstehung durch Polyploidisierung und genomische Instabilität fördern. Die vorliegende Arbeit hat die Abhängigkeit des Pseudo-G1 Checkpoints sowohl von p53, als auch von einem funktionellen SCP nachgewiesen. Außerdem wird ein zusätzlicher SCP-unabhängiger Checkpoint in der darauffolgenden G2-Phase aktiviert, der den Eintritt von polyploiden Zellen in die nächste Mitose unterbindet. Somit kooperieren mehrere Checkpoints, um eine weitergehende Polyploidisierung infolge einer fehlerhaften Mitose zu verhindern.

Antimitotische Wirkstoffe gehören zu den am häufigsten verwendeten Chemotherapeutika. Allerdings sind die Mechanismen der mitoseassoziierten Apoptose und Chemotherapieresistenz weitgehend unbekannt. In meiner Arbeit habe ich gezeigt, daß der SCP für die Apoptoseauslösung durch diverse antimitotische Therapeutika notwendig ist. Insbesondere Mad2 erwies sich als ein zentraler proapoptotischer Faktor bei der Behandlung mit Wirkstoffen, die die Kinetochorspannung beeinträchtigen. Diese umfassen nicht nur Spindelgifte wie Taxol, sondern überraschenderweise auch DNA-schädigende Therapeutika wie Topoisomerase II-Hemmer.

Eine klinisch relevante mitoseassoziierte Chemotherapiestrategie ist die Auslösung der „mitotischen Katastrophe“, einer bislang nur unzureichend definierten Form des Zelltods. Die Ausschaltung des durch DNA-Beschädigung aktivierten G2 Checkpoints mittels Chk1-Kinaseinhibitoren führt selektiv für p53-negative Zellen zum mitotischen Eintritt,

der einen mitoseassoziierten Zelltod verursacht. Diese Arbeit weist nach, daß die „mitotische Katastrophe“ eine mitosespezifische Form der Apoptose ist, die mit einer SCP-Aktivierung einhergeht und die proapoptotische Funktion von Mad2 erfordert. Überraschenderweise habe ich festgestellt, daß der proapoptotische Signalweg während der Mitose durch Überlebenssignalwege mit den Komponenten Survivin, Aurora B und Cdk1 gehemmt wird. Daher verstärkt die genetische oder pharmakologische Hemmung dieser Überlebenssignalwege synergistisch die mitotische Apoptose und könnte eine erheblich verbesserte chemotherapeutische Strategie gegen Krebs darstellen.

Meine Ergebnisse zeigen, daß der SCP eine zentrale Rolle bei der chemotherapieaktivierten Apoptose spielt, und deuten darauf hin, daß SCP-Defekte Chemotherapieresistenzen verursachen können, was ein signifikantes Problem in der Krebstherapie darstellt. Deshalb sind alternative Behandlungsansätze dringend erforderlich, die unabhängig von der vollen SCP-Funktion wirksam sind. Interessanterweise ist der SCP essentiell für das Überleben von Tumorzellen, was ein neuartiges Chemotherapiekonzept nahelegt, in dem der SCP als Zielstruktur genutzt wird. In der Tat hat unser Labor einen effektiven pharmakologischen SCP-Inhibitor identifiziert, und ich konnte nachweisen, daß dieser Inhibitor Apoptose in Krebszellen auslöst, selbst wenn diese aufgrund von SCP-Defekten Resistenzen gegenüber Spindelgiften aufweisen.

Introduction

Cancer as medical and scientific problem

Cancer is one of the leading causes of death in the developed countries. The last decades have brought tremendous progress in understanding the molecular basis of cancer, but many open questions remain. The fields of cancer research include the transformation of a normal cell into a cancer cell (cancerogenesis), the means of diagnosis and prognosis, and the effective treatment of cancer, especially the combat of widespread chemotherapy resistance.

A tumor cell arises in a microevolutionary process. Most cancers are the result of spontaneous, acquired alterations, whereas hereditary cancer syndromes are rare. Factors facilitating transformation are the metabolism of the cell, physical mutagens like UV radiation or chemical mutagens found in cigarette smoke, food or the environment (Figure 1). Viral infections as a biological factor play a prominent role in cancer of certain organs like the liver or the cervix.

Cancer cells exhibit defects in regulatory pathways that govern normal cell proliferation and homeostasis. During cancerogenesis somatic cells abandon the functions typical for their tissue of origin due to de-differentiation and acquire capabilities which are referred to as hallmarks of cancer (Hanahan and Weinberg 2000). These include self-sufficiency in growth signals, limitless replicative potential, insensitivity to growth-inhibitors, evasion of programmed cell death, sustained angiogenesis and tissue invasion and metastasis.

Since most mutations are detrimental to the cell, evasion or counterbalancing of cell death signals by enhanced survival signaling might be the first alteration acquired (Vaux *et al.* 1998), before enhanced proliferation gives these cells a selective advantage. To exceed a tumor size of one millimeter in diameter, nutrient supply by the formation of new blood vessels (angiogenesis) has to be induced (Folkman 1995). A late step in cancerogenesis is metastasis by the activation of cell migration genes and cell-cell contact-independent growth, which allows cells to leave the tumor mass, travel through the blood or lymphatic vessels and leave them to initiate tumors at new sites (Figure 1).

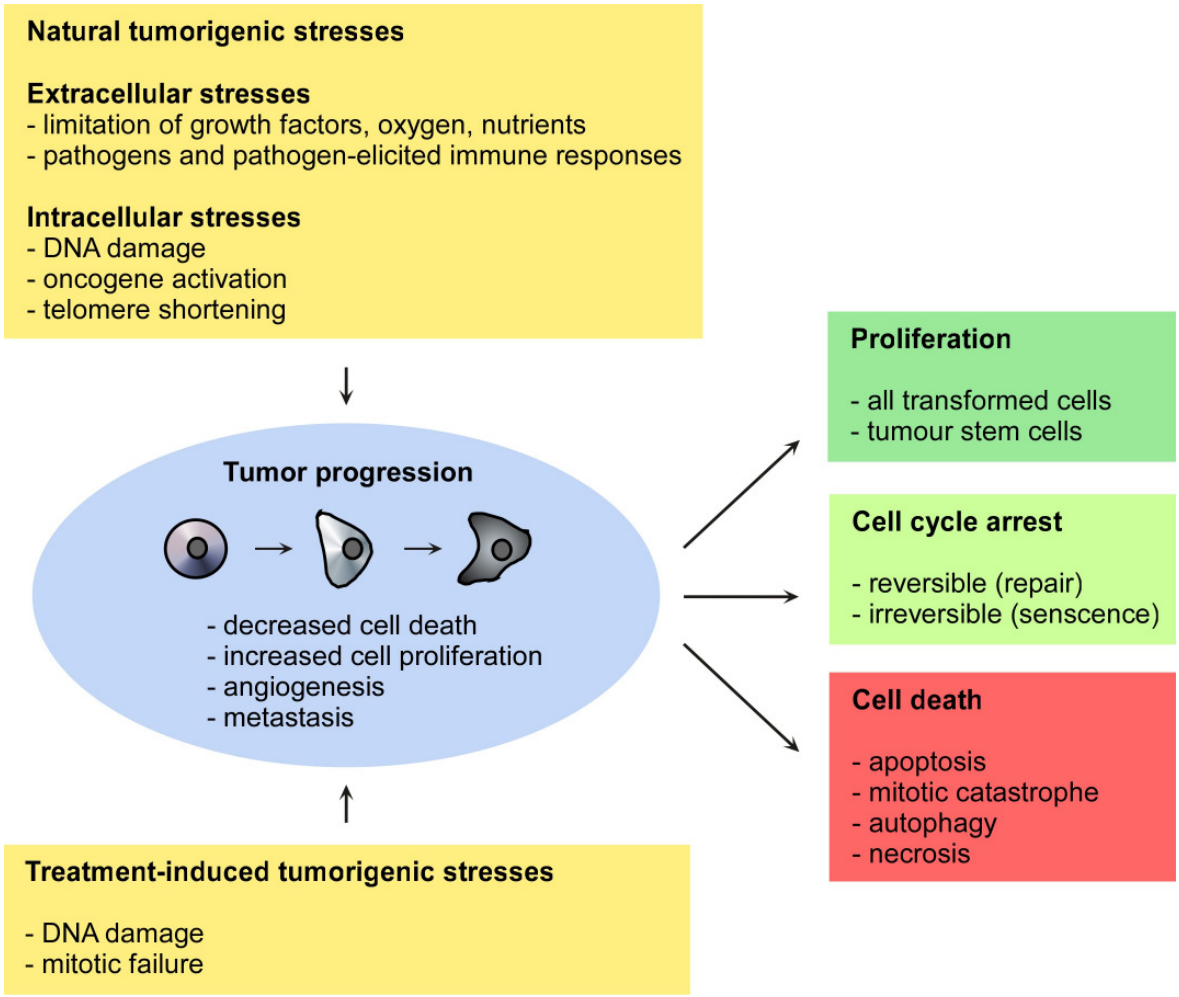

Figure 1: Oncogenic transformation and alternative cellular responses to natural and treatment-induced stresses. Cancerogenic stress originates from intracellular and extracellular events. Paradoxically, chemotherapeutic treatment itself can also be cancerogenic, because it often induces cellular damage to kill cells. Stressed cells will respond with a transient cell cycle arrest allowing the repair of the damage and will survive in a proliferative or senescent state. Upon irreparable damage cells will die by one of several pathways. Proliferating cancer cells display the hallmarks of cancer postulated by Hanahan and Weinberg: Growth is increased, whereas cell death is decreased. Later in tumor development tumors can induce angiogenesis and acquire the capability to metastasize. Adapted from Okada and Mak 2004 and Hanahan and Weinberg 2000.

Tumorigenesis is induced by multiple mechanisms

There is an ongoing debate about the mechanisms of cancerogenesis and their respective weight in the transformation of somatic cells to cancer cells, but it is widely accepted that a combination of several lesions is required to produce a cancer cell. Different theories favoring mutation, aneuploidization or polyploidization and combinations thereof as driving forces of cancerogenesis exist. Mutation based models assume that a few stochastic

events are sufficient to generate cancer. The "mutator hypothesis" postulates that genomic instability due to mutation of genes regulating DNA replication and metabolism or mitosis and the associated checkpoints arises early in tumorigenesis and increases the subsequent occurrence of tumor-promoting mutations and genetic lesions (Loeb 2001, Cahill *et al.* 1999). The discovery that most cancers are aneuploid made by Boveri almost a century ago (Boveri 1914) fuelled the hypothesis that the inherent instability of aneuploid karyotypes, which are induced either by a carcinogen or spontaneously, is sufficient for tumor formation (Duesberg and Li 2003). For instance, a rate of chromosome gains or losses of $1x10^{-2}$ per chromosome per cell division was shown for colorectal tumors (Lengauer *et al.*, 1997). Polyploidization is also claimed to precede aneuploidization in cancerogenesis, which would be produced by subsequent losses or gains of chromosomes due to the existence of supernumerary centrosomes (Meraldi *et al.* 2002, Fujiwara *et al.* 2005). The resulting genetic imbalance would alter the gene dosage and could accelerate malignant transformation as many mitosis-associated genes guarding genomic integrity are haplo-insufficient (Bharadwaj and Yu 2004).

The Eukaryotic Cell Cycle

Multicellular organisms have to duplicate their cells to maintain tissue homeostasis by replacing dead cells or to grow. Faithful transmission of the genetic information and the cell organelles requires an ordered sequence of events to take place, the cell cycle. The cell cycle is comprised of four phases. In G1 phase the cell grows, in S phase the chromosomes are duplicated, in G2 phase DNA synthesis is completed. In mitosis the chromosomes are distributed to two nuclei and after mitosis the cytoplasm is divided by cytokinesis generating two daughter cells. With a duration of only 30 to 60 min mitosis is the shortest cell cycle phase while completion of the whole cell cycle takes a human cell about 20 to 24 h. The resting state of a cell is termed G0 phase and cells can reenter from G0 into the cell cycle upon mitogenic stimulation by growth factors.

While the cell cycle phases have been described more than a century ago, the unraveling of their molecular basis in form of Cyclin dependent kinases (Cdks) and Cyclins began about 30 years ago in budding yeast (Hartwell *et al.* 1974), fission yeast (Nurse 1975), sea urchin eggs and clam (Evans *et al.* 1983, Swenson *et al.* 1986). The first Cdk/Cyclin complex to be detected was the mitosis or maturation promoting factor (MPF), which consists of Cdk1

and Cyclin B in vertebrates. The basic mechanisms of cell cycle regulation are conserved from yeast to man, but have acquired additional levels of complexity in multicellular organisms, especially in mammals (Johnson and Walker 1999). The phases of the cell cycle are characterized by the sequential activation of various Cdk/Cyclin complexes, which phosphorylate multiple substrates of the corresponding cell cycle phase. The catalytic subunit of the complex, the Cdk, has to be activated by a regulatory subunit, the Cyclin, which is expressed and degraded in a cell cycle specific manner. Moreover, the activity of the Cdk/Cyclin complexes is regulated by activating as well as inactivating phosphorylations. In addition, Cdk/Cyclin complexes can be inhibited by members of the two Cyclin dependent kinase inhibitor families (CKIs, Sherr and Roberts 1999). The INK4 (inhibitor of Cdk4) family of CKIs specifically inhibits Cdk4 or Cdk6 and includes p16INK4a, p15INK4b, p18INK4c and p19INK4d. The CIP/KIP (Cdk inhibitory polypeptides/kinase inhibitory proteins) family of CKIs has a broader spectrum and inhibits Cdks containing Cyclin D, Cyclin E and Cyclin A (Sherr and Roberts 1999). Its members are p21CIP1, p27KIP1 and p57KIP2.

The transition from G0 into the cell cycle is tightly regulated and depends on mitogenic signals that induce Cyclin D expression and accumulation (Cheng *et al.* 1999). Upon commitment to DNA replication at the restriction point, cells gain independence of growth signals. Cdk4 and Cdk6 are activated by the phosphatase Cdc25A (cell division cycle 25A), which removes two inhibitory phosphorylations conferred by Wee1 (WEE1 homolog (*S. pombe*)) and Myt1 (PKMYT1 protein kinase, membrane associated tyrosine/threonine 1), while the activating phosphorylation conferred by the large Cyclin activating complex (CAK) at threonine 161 is retained. Retinoblastoma protein (Rb) hyperphosphorylation is initiated by three D type Cyclins associated with Cdk4 (Cyclin D1 or D2) and Cdk6 (Cyclin D3) in early G1 phase, and is completed by Cdk2/Cyclin E. Rb hyperphosphorylation frees the transcription factor E2F-1 (E2F transcription factor 1), which in conjunction with DP-1 (transcription factor DP-1) induces the transcription of S phase genes, thus resulting in passage of the restriction point (Stevaux and Dyson 2002). The Cdk2/Cyclin E complex also regulates the transition from G1 to S phase by phosphorylation of its inhibitor p27KIP1, targeting it for proteasomal degradation (Sherr and Roberts 2004). Each chromosome has to be replicated exactly once per cell cycle to preserve genomic integrity. This is ensured by a licensing process that allows every origin of replication to initiate replication only once every S phase. Licensing occurs during phases with low Cdk activity (late mitosis, early G1) and is inhibited throughout phases

with high Cdk activity (late G1, S, G2 and early M phases, Blow and Tanaka 2005). Re-licensing, the repeated origin binding allowing the initiation of additional DNA replication cycles, is prevented by several mechanisms, which are often acting on the same proteins in parallel. The reduction of DNA binding affinity, the induction of nuclear export and of proteolytic degradation are regulated by Cdk-mediated phosphorylation of the substrates, whereas geminin-dependent inhibition of re-licensing is regulated by the availability of geminin, which is also Cdk-dependent.

The G2/M transition

In G2 phase, DNA synthesis is finished. Cyclin A switches from association with Cdk2 in S phase to Cdk1 in G2, where it promotes G2 phase events. Cdk1/Cyclin A activity rises during G2 phase and peaks in prophase, when Cdk1/Cyclin B is only marginally active, and Cyclin A is degraded in prometaphase (Rape *et al.* 2006). The active Cdk1/Cyclin A kinase complex is required for mitotic entry by promoting nuclear translocation and activation of Cdk1/Cyclin B through inactivation of Wee1 (Fung *et al.* 2007, Gong *et al.* 2007). In the nucleus Wee1 phosphorylates Cdk1 as part of the Cdk1/Cyclin B complex at Tyr15 leading to its export and sequestration in the cytoplasm by association with 14-3-3σ proteins and in the cytoplasm Myt1 phosphorylates Cdk1 at Thr14 and Tyr15, keeping Cdk1 catalytically inactive by inhibiting ATP binding (Figure 2, Malumbres and Barbacid 2005). Similar to the G1-S transition the G2-M transition depends on the addition of an activating phosphorylation to Cdk1 by CAK and the removal of inhibitory phosphorylations by the phosphatases Cdc25B and Cdc25C, whose activity is inhibited by the Chk1 kinase (Figure 2). It is still unknown how the initial activation of Cdk1/Cyclin B occurs, but recent data implicates centrosomally located Chk1 in the prevention of premature Cdk1/Cyclin B activation, but also in centrosomal recruitment of Cdc25B (Kramer *et al*. 2004). In some systems Plk1 was shown to activate Cdk1/Cyclin B at the centrosomes by phosphorylating Cyclin B and Cdc25C and by inducing Wee1 degradation (van Vugt and Medema 2005). In late G2 phase Ajuba kinase recruits and activates Aurora A kinase at the centrosomes (Hirota *et al.* 2003), where Aurora A phosphorylates Cdc25B at Ser353, committing the cell to mitotic entry (Dutertre *et al.* 2004). Aurora A also promotes separation of centrosomes, which is necessary for the establishment of spindle bipolarity, possibly via Nek2 kinase (NIMA (never in mitosis gene a)-related kinase 2), which is thought to phosphorylate the centrosomal protein CEP250 (centrosomal protein

250kDa), dissolving a dynamic structure that tethers duplicated centrosomes to each other (Marumoto *et al.* 2003). In late G2 phase and early mitosis the activated Cdk1/Cyclin B complex promotes centrosome separation, nuclear envelope breakdown, chromosomal condensation and cytoskeletal reorganization leading to cell shape changes by phosphorylating over 70 substrates, among them histone H1 and DNA binding proteins, lamin and centrosomal proteins (Figure 2, Malumbres and Barbacid 2005). Recently it was reported that low levels of Cdk1/Cyclin B activity are sufficient to allow mitotic entry, whereas higher levels are needed for mitotic progression, and gradually increasing activity levels during mitosis may by themselves regulate ordered progression through mitosis (Lindqvist *et al.* 2007).

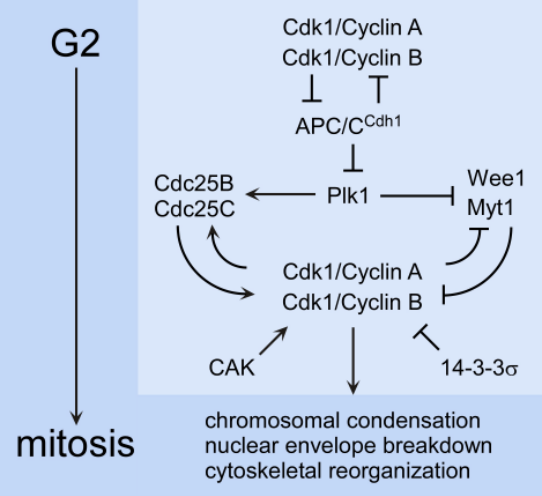

Figure 2: The G2/M transition. Cdk1 activity is required for mitotic entry. CAK confers an activating phosphorylation to Cdk1. Phosphorylation of Cdk1 by Wee1 and Myt1 leads to cytoplasmic localization mediated by binding to 14-3-3σ and catalytic inhibition of Cdk1, which can be alleviated by the phosphatases Cdc25B and C. The active Cdk1/Cyclin B complex phosphorylates G2 and mitotic substrates inducing chromosomal condensation, nuclear envelope breakdown and cytoskeletal reorganization leading to cell shape changes.

Mitosis is comprised of distinct phases and is regulated by phosphorylation

Mitosis can be divided into distinct phases: pro-, prometa-, meta-, ana- and telophase (Figure 3). Prophase is associated with the condensation of chromosomes and the duplicated centrosomes separate, migrate to opposite poles induced by the mitotic kinesin Eg5/KSP (kinesin spindle protein, Blangy *et al.* 1995), several other kinesin-related proteins and dynein (Nigg 2001) and begin to nucleate microtubules dependent on Aurora A kinase to build the mitotic spindle. Aurora A kinase recruits proteins regulating microtubule stability and also promotes mitotic progression in early mitosis (Marumoto *et al.* 2003). Cdk1/Cyclin A initiates chromosome condensation in prophase and promotes nuclear envelope breakdown (Gong *et al.* 2007), which is completed by Cdk1/Cyclin B in early prometaphase. At the same time, large proteinaceous structures, the kinetochores,

assemble on the centromeric DNA of the condensed chromosomes, which consist of two chromatids held together by the cohesin protein complexes at the centromeric DNA. The microtubules attach to the kinetochores and during metaphase the chromosomes are pushed to the metaphase plate by the microtubules, i.e. they align at one plane halfway between the poles. This process is dependent on numerous proteins regulating spindle microtubule stability and attachment of microtubules to the kinetochores, e.g. Aurora A and B (Kallio *et al.* 2002, Marumoto *et al.* 2003). Anaphase occurs upon full alignment of all chromosomes at the metaphase plate and can be divided into two stages, anaphase A and anaphase B. During anaphase A the chromatids are separated by the cleavage of cohesin complexes at the kinetochores and shortening of spindle microtubules, during anaphase B the chromatids move towards the spindle poles by elongation of polar microtubules. Similar to DNA replication, chromatid cohesion and segregation in mitosis have to be tightly regulated. The cohesin complex links the sister chromatids by its subunit Scc1 (*RAD21* homolog (*S. pombe*)) and is cleaved by separase (*ESPL1*, extra spindle pole bodies homolog 1 (*S. cerevisiae*)) upon destruction of its inhibitor securin (*PTTG1*, pituitary tumor-transforming 1). Securin is only degraded when all chromosomes are bipolarly attached to the mitotic spindle, upon deactivation of the mitotic spindle checkpoint, a mechanism ensuring equal distribution of the genetic material to the two daughter cells. Cohesin loading occurs in parallel to licensing in phases with low Cdk activity (late mitosis, early G1, Blow and Tanaka 2005) and depends on several components of the DNA replication machinery (Uhlmann 2003). Most of the cohesin dissociates from the chromosome arms during prophase, a process that is facilitated by the mitotic kinases Aurora B and Plk1 (Losada *et al*. 2002), while shugoshin maintains cohesin mediated attachment of the chromatids at the kinetochores in a Bub1 (budding uninhibited by benomyl 1)-dependent manner (Kitajima *et al*. 2005). Protein phosphatase 2A (PP2A) removes Plk1 mediated phosphorylations from shugoshin and cohesin, thereby preserving their localization to kinetochores (Rivera and Losada 2006). In telophase the nuclear membrane reforms into two nuclei and the chromosomes decondense. The spindle further elongates as the distance between poles increases and depolymerizes in late telophase. Cytokinesis occurs after mitosis, when a contractile actin ring separates the cytoplasm and membranes form between the two daughter cells.

The chromosomal passenger complex fulfils several important functions during mitosis. It consists of the kinase Aurora B (Giet and Prigent 1999) and three other subunits in humans, Borealin (Gassmann *et al.* 2004), INCENP (inner centromere protein, Cooke *et al.*

1987) and survivin (Li *et al.* 1998), that probably determine stability and localization, but maybe also activity and substrate specificity of Aurora B kinase. The chromosomal passenger complex participates in chromosome condensation, in the correction of misattachments of chromosomes to the spindle and in cytokinesis, depending on the typical alterations in subcellular localization, which gave the complex its name. The complex localizes to the chromosome arms at the onset of mitosis, subsequently to the centromeres in prometaphase, to the central spindle at the metaphase to anaphase transition and finally to the midbody in telophase (Bolton *et al*. 2002). Apparently, two chromosomal passenger complex subcomplexes exert different functions (Gassmann *et al*. 2004). The quaternary complex acts in chromosome alignment and cytokinesis, while a subcomplex containing Aurora B and INCENP phosphorylates histone H3 at Ser10 to dissociate HP-1 (hetero-chromatin protein-1) from the chromatin, thus facilitating chromosome condensation and cohesin binding (Fischle *et al*. 2005, Hirota *et al*. 2005).

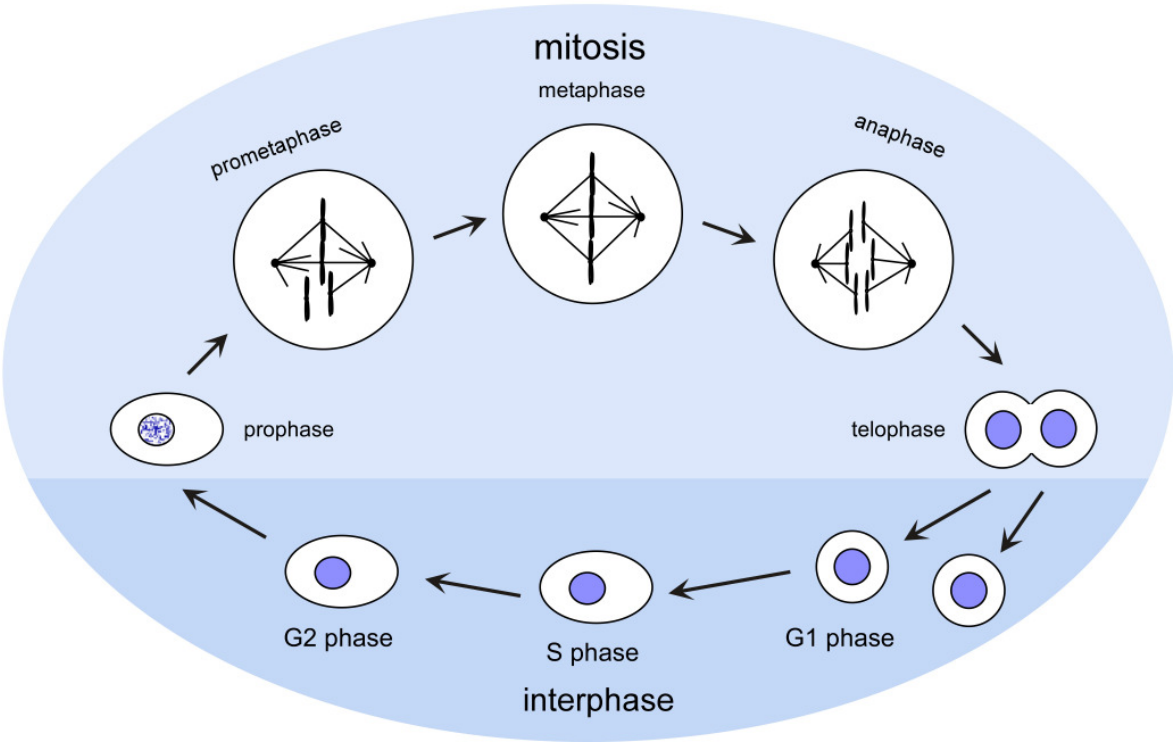

Figure 3: Schematic representation of the phases of mitosis. Chromosome condensation in prophase is followed by nuclear envelope breakdown and formation of the mitotic spindle in prometaphase. Chromatids are aligned at the cell equator in metaphase and separated and pulled towards the poles during anaphase. The nuclear envelope reforms and chromosomes decondense in telophase and the cytoplasm is divided by cytokinesis after mitosis. In interphase the cell grows and duplicates its chromosomes, which will be distributed to daughter cells during the next mitosis.

Regulation of mitosis by regulated protein proteolysis

The anaphase promoting complex or cyclosome (APC/C) is a large E3 ubiquitin ligase comprised of at least eleven subunits in humans, which has cell cycle regulatory functions by targeting cell cycle proteins for degradation (Castro *et al*. 2005, Acquaviva and Pines 2006, Pines 2006). Polyubiquitin chains linked at Lys48-Gly76 can serve as a signal for the proteasome to degrade proteins that are implicated in cell cycle functions or are damaged beyond repair, whereas monoubiquitination or polyubiquitin chains linked at Lys63-Gly76 can serve as a signal that does not lead to degradation (Mani and Gelmann 2005). Since the proteasome is constitutively active, substrates can be targeted for destruction throughout the whole cell cycle if they are polyubiquitinated, therefore this step has to be regulated at the substrate level. Polyubiquitination requires three enzymatic activities. First, ubiquitin is activated by an E1 ubiquitin activating enzyme, subsequently ubiquitin is transferred to an E2 ubiquitin conjugating enzyme (UBC), which acts together with an E3 ubiquitin ligase to add the ubiquitin molecule to the ε–amino group of a lysine residue in the substrate. Only 20 to 30 UBCs, but more than 600 E3 ubiquitin ligases, that confer higher substrate specificity to the E2 enzymes, are known to date in humans (Pray *et al*. 2002).

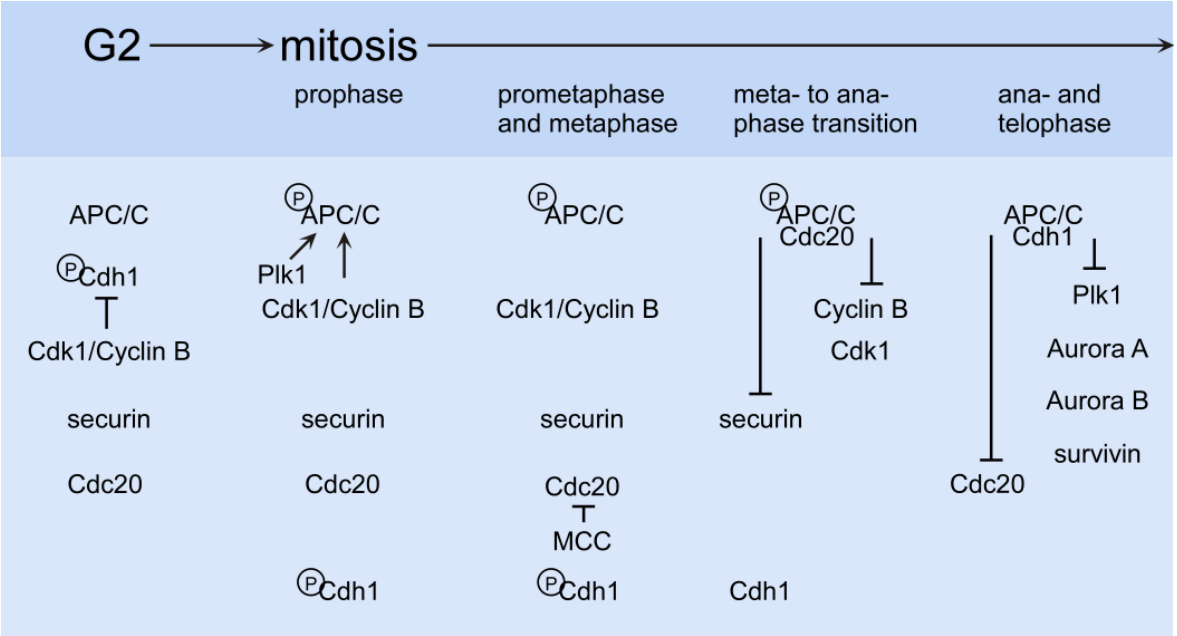

Figure 4: The APC/C controls mitotic progression. APC/C associated with Cdc20 first degrades securin and then Cyclin B when the spindle checkpoint is satisfied at the meta- to anaphase transition. APC/C associated with Cdh1 induces degradation of various mitotic substrates in ana- and telophase.

The substrate specificity of the APC/C depends on the cofactors Cdc20 or Cdh1 in vertebrates (Castro *et al*. 2005). Cdc20 associates with APC/C only during a short period

of time in mitosis in prometa- and metaphase and allows only the recognition of D box (destruction box) containing substrates (Figure 4). In contrast, Cdh1 binds to APC/C in anaphase and G1 phase (Figure 4) and permits destruction of substrates containing a D box, a KEN box (named after the recognized amino acid motif, Pfleger and Kirschner 2000) or a double motif consisting of a D box and a DAD box (D box activated domain box, Castro *et al*. 2002).

Cell cycle checkpoints

Cell cycle checkpoints are quality control mechanisms that ensure that a cell cycle phase has been successfully completed before the next is initiated and that ensure error-free propagation. A delay of the cell cycle mediated by cell cycle checkpoint signaling pathways allows time for repairs. The cells continue to cycle after the successful completion of the repairs or induce apoptosis, if a repair cannot be achieved. Cell cycle checkpoints maintain chromosomal stability and, thus, impairment of cell cycle checkpoints can drive cancerogenesis and determine the reaction of cancers to chemotherapy.

The DNA damage checkpoints

The DNA damage checkpoints at the G1/S and the G2/M transitions or in S phase detect the presence of DNA defects and prevent the replication or distribution of damaged chromosomes to daughter cells, respectively (Figure 5 and Figure 6). Multiple checkpoint pathways can be activated upon various kinds of DNA damage, e.g. stalled replication forks, strand breaks and adduct formations (Hoeijmakers 2001, Sancar *et al.* 2004). DNA damage is sensed by several protein complexes and kinases, most prominently ATM (ataxia telangiectasia mutated) and ATR (ataxia telangiectasia and Rad3 related), which signal to the Chk1 and Chk2 kinases and/or to p53. Ultimately, cell cycle arrest is induced by inhibition of Cdk activity.

The intra-S phase checkpoints

During S-phase the 9-1-1 complex consisting of Rad9, Rad1 and Hus1, the Rad17-RFC complex (replication factor C) and a complex of the ATR kinase and ATRIP (ATR

interacting protein) detect stalled replication forks during a normal S phase or upon inflicted damage (Bartek *et al.* 2004, Petermann and Caldecott 2006). Once activated the ATR kinase phosphorylates and activates the Chk1 kinase. The Chk1 kinase phosphorylates Cdc25A, leading to its degradation, the maintenance of an inactivated state of Cdk2/Cyclin E or Cdk2/Cyclin A and, thus, to S phase delay or arrest (Figure 5). Similarly, DNA double strand breaks activate the Chk2 kinase via ATM kinase, which results in Cdc25A degradation and S phase arrest (Figure 5). Conversely, ATR-mediated activation of Brca1 (breast cancer 1, early onset) or Nbs1 (Nijmegen breakage syndrome 1) leads to recovery of stalled, regressed or collapsed replication forks (Bartek *et al.* 2004, Sancar *et al*. 2004).

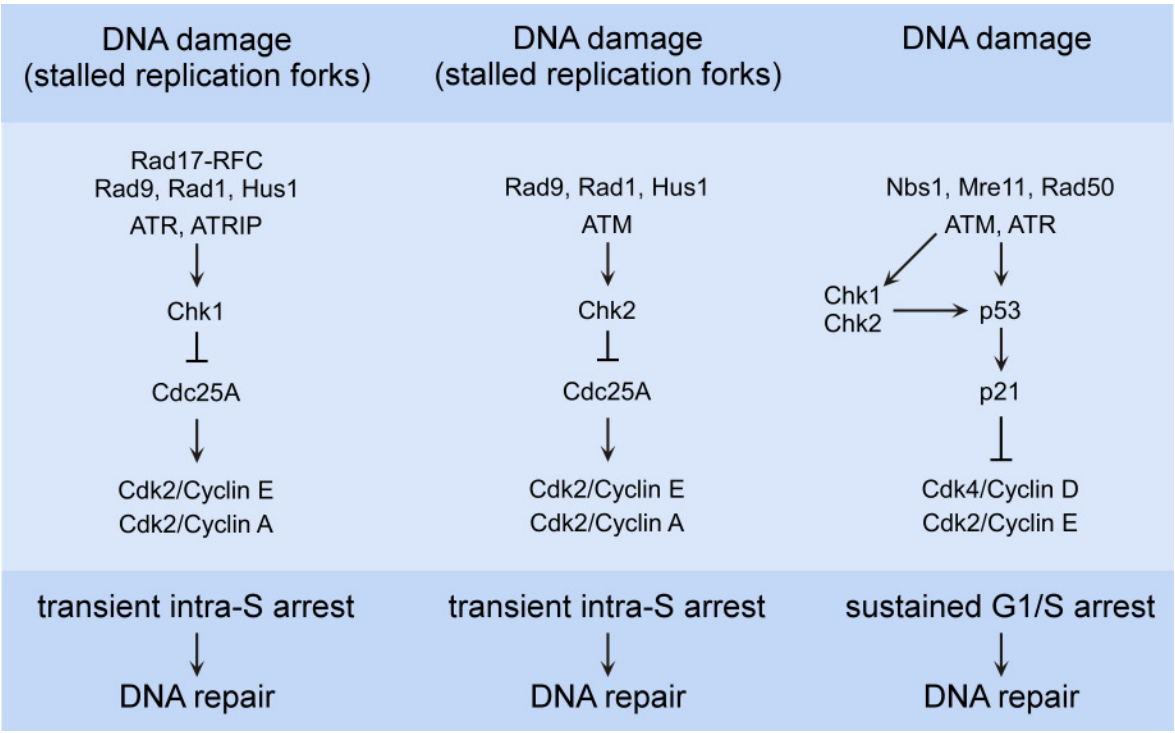

Figure 5: The G1/S and intra-S DNA damage checkpoints. DNA damage before and during S phase leads to G1 or intra-S phase arrest and the induction of repairs. ATM, ATR and other proteins sense and signal DNA damage directly to p53 or to Chk1 and Chk2, which induce cell cycle arrest by inhibition of Cdc25A phosphatase or indirectly by activating p53. p53-mediated transcription of p21 results in sustained cell cycle arrest.

The G1/S DNA damage checkpoint

Upon DNA damage in G1 phase the sensor kinase ATM – and to a lesser extent also ATR – act in concert with a complex of Nbs1, Mre11 (meiotic recombination 11 homolog) and Rad50 to activate the Chk1 and Chk2 effector kinases, which induce cell cycle arrest at the

G1/S border by direct inhibition of the Cdc25A phosphatase or by activating p53 through phosphorylation at serine 20 (Figure 5). ATM or ATR can also activate p53 directly by serine 15 phosphorylation. p53-mediated transcription of *CDKN1A* (p21) induces cell cycle arrest at the G1/S transition by inhibition of Cdk activity (Kastan and Bartek 2004).

The G2/M DNA damage checkpoint

DNA damage in G2 phase is sensed by ATM, ATR and Rad17-RFC, which activate Chk1, Chk2 or p53 and inhibit mitotic entry (Figure 6). ATM or ATR can arrest cells in G2 phase by Chk1 mediated phosphorylation of Cdc25C at Ser216, thereby promoting sequestration of Cdc25C by 14-3-3σ in the cytoplasm (Figure 6). Chk1 and Chk2 activate Wee1, which prevents mitotic entry by phosphorylating Cdk1/Cyclin B. The G2 DNA damage checkpoint inhibits Plk1 kinase activity and its transcription, thereby preventing activation of Cdc25C and inhibition of Myt1 and Wee1, thus leading to inhibition of Cdk1/Cyclin B and of mitotic entry (Figure 6, Smits *et al*. 2000, Nakajima *et al*. 2003).

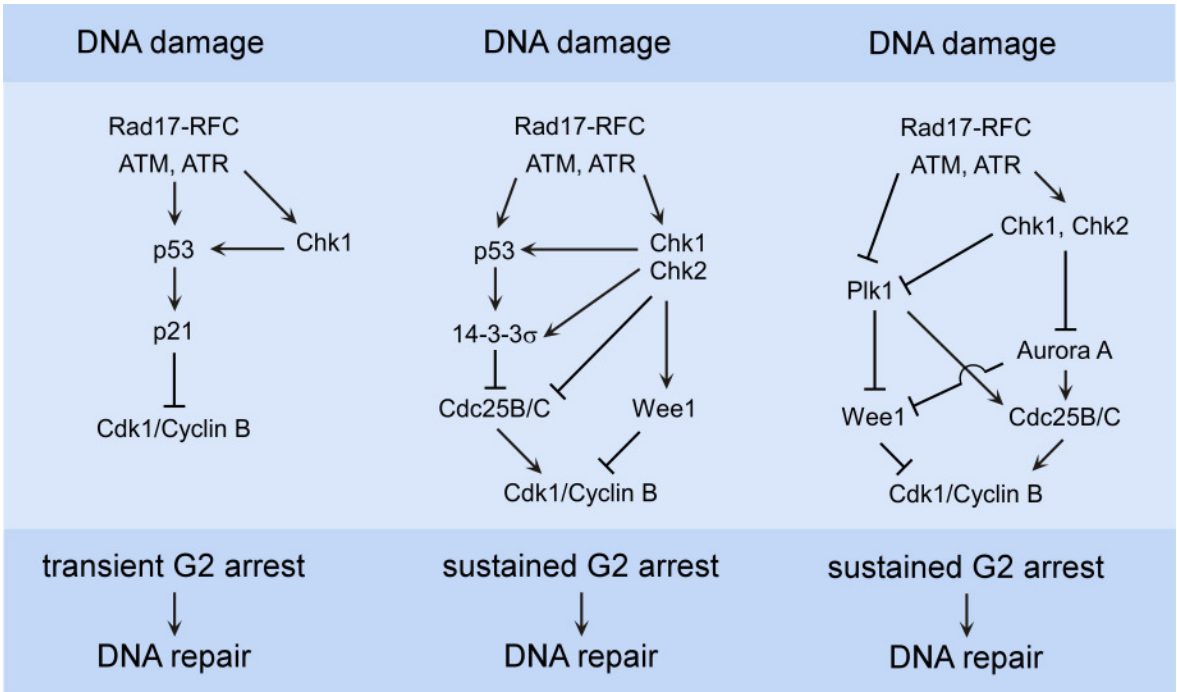

Figure 6: The G2 DNA damage checkpoints. DNA damage in G2 leads to p53-dependent or -independent G2 arrest. ATM, ATR and other proteins sense and signal DNA damage directly to p53 or to Chk1 and Chk2, which induce cell cycle arrest by inhibition of Cdc25B and C phosphatases or activation of Wee1. p53-mediated transcription of p21 or 14-3-3σ results in cell cycle arrest.

Plk1 inhibition prevents Nek2 activation, which is required for centrosome separation (Zhang *et al.* 2005). p53 induces G2 arrest leading to Cdk1/Cyclin B inhibition by transcription of *CDKN1A* ($p21^{CIP1}$), *14-3-3σ* and *GADD45* (growth arrest and DNA-damage-inducible 45) and transrepression of *CCNB1* (Cyclin B), *CDK1* or *CDC25C* (Taylor and Stark 2001). Aurora A activates Cdk1/Cyclin B indirectly via inhibition of Wee1 or activation of Cdc25B by Ser353 phosphorylation (Dutertre *et al.* 2004). It is currently unknown which proteins mediate the Chk1 signal that prevents Aurora A activation and, consequently, Cdc25B phosphorylation leading to mitotic entry (Cazales *et al.* 2005, Krystyniak *et al.* 2006).

p53 protects genomic integrity

p53 is a member of a small protein family of transcription factors comprising p53, p63 and p73. In contrast to p63 and p73, p53 is not required for normal development or cell viability, but prevents cancerogenesis upon genotoxic insults by induction of cell cycle arrest, repair or apoptosis. Unexpectedly, recent findings show a DNA damage response independent role of p53 in the suppression of irradiation induced lymphomagenesis (Christophorou *et al*. 2006). *TP53*$^{-/-}$ mice are viable, demonstrating that p53 is dispensable for normal growth and development, but develop early-onset spontaneous lymphomas and sarcomas (Donehower *et al*. 1992, Jacks *et al*. 1994), a phenotype that is much less pronounced in mice carrying p53 mutations (Toledo and Wahl 2006). The central importance of p53 in human cancers is underscored by the high incidence of mutations in the p53 pathway. About 50% of all human cancers carry mutated *TP53* and at least 7% of the cancers with wild type *TP53* have *MDM2* (mouse double minute 2 homolog, also known as Hdm2 in humans) amplifications leading to reduced p53 protein levels (Momand *et al*. 1998, Vousden and Lu 2002, Toledo and Wahl 2006). p53 is synthesized throughout the cell cycle, but its levels are nearly undetectable in nonstressed cells due to proteasomal degradation induced by the E3 ubiquitin ligase Mdm2, which itself and its regulators are transcriptional targets of p53. Thus, p53 and Mdm2 are part of a negative feedback loop that keeps p53 levels low. The p53 protein is 393 amino acids long in humans and is comprised of three domains. Sequence specific DNA binding leading to transactivation or -repression is conferred by the central domain of p53, whereas the amino- and carboxy-terminal domains of p53 control its localization and regulate transcription. The amino-terminus contains a transactivation domain required for transcription and a proline-rich

domain controlling protein-protein interactions like Mdm2 or p300/CBP binding, which inhibit or promote transactivation, respectively, and can induce ubiquitination or acetylation of the carboxy-terminal regulatory domain (Gomez-Lazaro *et al.* 2004, Toledo and Wahl 2006). The oligomerization of p53 into a tetramer enhances its activity and is mediated by the tetramerization domain, which is located at the carboxy-terminus together with a regulatory domain involved in DNA binding. p53 turnover is slowed down and its nuclear localization is induced by posttranslational modifications upon DNA damage or other genotoxic insults allowing accumulation of active p53 and induction of p53-driven responses (Gomez-Lazaro *et al.* 2004, Toledo and Wahl 2006). The most prominent posttranslational modifications of p53 include phosphorylation, but acetylation, sumoylation and other modifications are also added upon specific kinds of damage (Brooks and Gu 2003, Bode and Dong 2004, Lavin and Gueven 2006). However, the significance of some of these modifications is not clear at present and some, like ubiquitination, can either promote p53's degradation or its mediation of cell cycle arrest via regulation of its properties as transcription factor (Le Cam *et al*. 2006). More than a dozen residues, situated within 100 amino acids of the N- and C-terminal regions of p53, are phosphorylation targets and the same residues can be phosphorylated by several different kinases. Distinct subsets of amino acids in p53 are phosphorylated depending on the kind of damage, which is inflicted by various DNA damaging chemicals, UV or gamma radiation, hypoxia or spindle damaging agents. Different types of DNA damage induce similar phosphorylation patterns and lead to the most thorough phosphorylation of p53, whereas other stresses induce phosphorylation of a smaller subset of residues (Lavin and Gueven 2006). The most frequent phosphorylation of p53 occurs on serine 15 upon different stresses. The DNA damage signaling kinases ATM, ATR, Chk1, Chk2 and DNA-PK are the most prominent p53 kinases and kinases like ATM can phosphorylate up to six residues in p53 simultaneously. Other kinases phosphorylating p53 are stress related or cell cycle kinases (Akt, c-Abl, CAK, Cdk2, CK1/CK2, ERK2, GSK3β, HIPK2, JNK, MAPK, mTOR, PKC). Some p53 residues are constitutively phosphorylated and become dephosphorylated upon stress. The view that phosphorylation of p53 contributes to its stabilization upon stress or damaging conditions and can influence its transcriptional abilities is widely accepted, but has been challenged by some reports indicating that phosphorylation or acetylation are dispensable for transcriptional activation of p53 and that initial stabilization of p53 is achieved by disruption of the p53-Mdm2 complex (Lavin and Gueven 2006). In sum, it seems likely that an ordered pattern and interdependence of

stress-induced modifications to p53 exists, meaning that certain phosphorylations enable other residues to be phosphorylated as well (Lavin and Gueven, 2006).

Recent data derived from mouse models contradicts some of the *in vitro* data presented above, as mutation of residues critical for p53 function had no or only moderate effects *in vivo* with the exception of mutations in the central DNA binding domain, but confirms that Mdm2 regulates p53 stability and the related Mdm4/Mdmx (mouse double minute 4 homolog) regulates p53 activity. p53 accumulation after stress is possible, because Mdm2 switches from inducing p53 degradation to degradation of itself and Mdm4 (Toledo and Wahl 2006). As a note of caution, data derived from mouse models can deviate considerably from the situation found in humans, especially when considering the radically different lifespans of both species.

Mutations of p53 occur predominantly in the central domain as point mutations that hit a limited set of codons leading to amino acid exchanges, often resulting in enhanced protein stability and a dominant negative phenotype, since the mutated protein inhibits the wild typic protein in complexes. However, the occurrence of mutations in the terminal regions of p53 might be systematically underrated, as most often only exons 5 to 8, i.e. four of the ten coding exons, are analyzed for mutations (Vousden and Lu 2002). Besides mutations of p53 itself, the components upstream or downstream of p53 in the signaling pathways are also often mutated, leading to attenuation or abrogation mainly of proapoptotic responses that largely depend on the transactivation capabilities of p53, whereas transrepression of cell cycle progression genes (encoding Cdk1 and Cyclin B) by p53 induces arrest (Taylor and Stark 2001). Interestingly, besides its function as a transcription factor p53 seems also to be directly involved in the intrinsic pathway of apoptosis by translocation to the mitochondria in a manner similar to the proapoptotic BH3-only proteins, which negatively regulate mitochondrial membrane permeability, but this effect might also require transactivation of *PUMA*, a BH3-only protein (Chipuk *et al.* 2005, Yee and Vousden 2005).

The spindle checkpoint ensures genomic integrity by controlling chromatid segregation mediated by the APC/C^{Cdc20}

The mitotic spindle checkpoint is a control mechanism ensuring that the replicated chromosomes are distributed evenly to daughter cells so that each receives a full complement of the genome. To this end the spindle checkpoint monitors the attachment of

kinetochores to the mitotic spindle and the bipolar attachment of chromatids to opposite spindle poles via the tension generated between kinetochores. The spindle checkpoint prevents chromatid separation and mitotic exit followed by cytokinesis until all chromatids are attached properly to the spindle.

The spindle checkpoint signaling proteins, the Mad1-3 (mitotic arrest deficient) and Bub1-3 (budding uninhibited by benomyl, a benzimidazole) proteins have first been identified in *S. cerevisiae* screens for mitotic arrest deficiencies (Li and Murray 1991, Hoyt *et al*. 1991). Mad1, Mad2, Bub1 and Bub3 possess vertebrate homologs (Chen *et al.* 1996, Li and Benezra 1996, Taylor and McKeon 1997, Chen *et al.* 1998, Taylor *et al.* 1998), whereas the vertebrate protein BubR1 (*BUB1B*: budding uninhibited by benzimidazoles 1 homolog beta (yeast)) has homologies in the N-terminus to both yeast Bub1 and Mad3, but its kinase domain is different from Bub1 and other kinases (Taylor *et al*. 2004). Bub2 has a role independent from the other spindle checkpoint proteins in the separately operating spindle positioning checkpoint and the mitotic exit network (MEN) in budding yeast or the septation initiation network (SIN) in fission yeast (Glotzer 2001, Guertin *et al*. 2002). Bub1, Bub3, BubR1, Mps1 (monopolar spindle 1, Abrieu *et al.* 2001, Stucke *et al*. 2002), Plk1 (Golsteyn *et al.* 1994), Aurora A and B are mitotic kinases (Giet and Prigent 1999), whereas Mad1, Mad2, Borealin (Gassmann *et al.* 2004), CENP-E (centromere protein E, Yen *et al*. 1991), INCENP (inner centromere protein, Cooke *et al.* 1987) and survivin (Li *et al.* 1998) have no known kinase activity. CENP-E is a kinesin-like motor protein (Yen *et al.* 1991), which – like other proteins implicated in spindle checkpoint signaling, but unlike other centromeric proteins – is only transiently associated with the kinetochores and might function as a sensor for microtubule attachment to the kinetochores, which upon contact deactivates the BubR1 kinase (Mao *et al*. 2003). Rae1 (RNA export 1 homolog (*S. pombe*)) is a novel spindle checkpoint protein with high homology to Bub3, as both contain WD-40 repeats and a GLEBS domain, and apparently cooperates with Bub3 in Bub1 binding. The proteins comprising the RZZ complex consisting of Rod (rough deal homolog (*D. melanogaster*), Chan *et al.* 2000), Zw10 (zeste white 10 homolog (*D. melanogaster*), Chan *et al.* 2000) and Zwilch (homolog (*D. melanogaster*), Williams *et al.* 2003) were first identified in flies, have no yeast homologs and no obvious structural motifs and are indispensable for spindle checkpoint function (Karess 2005). Tao1 kinase (thousand and one-amino acid protein kinase 1, Hutchison *et al.* 1998) has recently been shown to participate in spindle checkpoint signaling and regulation of spindle dynamics, but not in

mitotic timing, by interaction with BubR1 and promotion of Mad2 accumulation at unattached kinetochores (Draviam *et al*. 2007).

Checkpoint independent functions of several spindle checkpoint proteins have also been reported. For instance, BubR1 is implicated in aging and fertility (Baker *et al.* 2004), apoptosis (Baek *et al.* 2005, Kim *et al.* 2005, Shin *et al.* 2003) and its homolog Mad3 is implicated the DNA damage response and gross chromosomal rearrangements, as are Bub3 and Mad2 in *Saccharomyces cerevisiae* (Myung *et al.* 2004). Bub3 and Cdc20 associate with histone deacetylases leading to transcriptional repression (Yoon *et al.* 2004). Mad2 is found at the nuclear envelope and nuclear pores together with Mad1 (Campbell *et al.* 2001, Iouk *et al.* 2002) and could participate in the DNA replication checkpoint in fission yeast (Sugimoto *et al.* 2004).

Mechanism of spindle checkpoint signaling

It remains a matter of controversy what exactly the spindle checkpoint senses. The observed differences are likely to be the consequence of different experimental systems: cells originating from different species, cancer cells or untransformed cells, mitotic or meiotic cells, cells treated with spindle damaging agents or traversing an undisturbed mitosis. Kinetochores lacking microtubule attachment or tension across the kinetochores emit a signal inhibiting the APC/C^{Cdc20}-mediated destruction of securin and Cyclin B (Sudakin *et al*. 2001). On the one hand it was shown that even a single unattached kinetochore is sufficient to activate the spindle checkpoint and arrest cells in metaphase, a conclusion drawn from an experiment where all kinetochores were attached and the connection between spindle fibers and a single kinetochore was severed by a laser in rat kangaroo PtK1 cells (Rieder *et al*. 1995), on the other hand the spindle checkpoint might not be on or off, but activated to a greater or lesser extent, depending on the number of unattached or tension-lacking kinetochores or the amount of signaling molecules generated at the kinetochores (Kops *et al.* 2005). Thus, spindle checkpoint proficiency or deficiency cannot be clearly defined, as it is a matter of definition which duration of mitotic arrest still qualifies for spindle checkpoint proficiency.

Premature APC/C^{Cdc20} activation is prevented by a Mad2- and BubR1-dependent cytosolic mitotic timer mechanism until kinetochore maturation is completed and a spindle checkpoint signal can be generated (Meraldi *et al*. 2004). Then the microtubules come in contact with the kinetochores by a process termed dynamic instability, a stochastic process

of alternating phases of slow microtubule outgrowth from the spindle poles and rapid microtubule shrinkage until all kinetochores are bound to microtubules, which is markedly faster in mitotic than in interphase cells (Mitchison and Kirschner 1984, Belmont *et al*. 1990). Upon capture by the kinetochores this kinetochore-bound microtubules are stabilized, whereas non-attached microtubules tend to depolymerize.

Although an ordered assembly of spindle checkpoint proteins at the kinetochores is likely and has been proposed based on several studies, a major problem is that most of these are based on siRNA mediated depletion of proteins possibly altering the stoichiometry in the complexes involved. Thus, the proposed order has to be regarded with caution. Also, the exact nature of the spindle checkpoint signal, also called "wait-anaphase signal", and the mode of its transmission remain mysterious. Apparently, only a subset of the spindle checkpoint proteins present at the kinetochore inhibit the APC/C^{Cdc20} after they have been assembled in the cytoplasm or at the kinetochore and have been activated at the kinetochore. APC/C^{Cdc20} is localized to the spindle, especially to the spindle poles, and to unattached kinetochores in pro- and prometaphase, but its precise localization upon inhibition by the spindle checkpoint is still unclear (Pines 2006). Several complexes have been reported by different groups to constitute the "wait-anaphase signal". A mitotic checkpoint complex (MCC) comprised of Mad2-BubR1-Bub3 and Cdc20 has been described (Sudakin *et al*. 2001, Figure 7), yet subcomplexes consisting of Mad2-Cdc20 or BubR1-Bub3-Cdc20 have also been reported (Chen 2002, Fang *et al*. 1998, Tang *et al*. 2001). The existence of the MCC and the smaller complexes might not be mutually exclusive. Phosphorylation of Cdc20 at the kinetochore might activate the MCC (Chung and Chen 2003). Cyclin B is recruited to kinetochores by Mad2 and Hec1 (highly expressed in cancer 1, Chen *et al.* 1997) by Cdk1-dependent and -independent pathways, where it promotes chromosome attachment, whereas Cyclin B localization to centrosomes and chromatin is Cdk1-independent (Bentley *et al.* 2007). Plk1 phosphorylates BubR1 upon lack of tension between the kinetochores (Elowe *et al.* 2007). At prometaphase the RZZ is recruited to the kinetochore by its receptor Zwint-1 (Zw10 interacting protein-1, Wang *et al.* 2004), which becomes a part of the outer plate of the kinetochore at the beginning of prophase and is associated with inner plate proteins of the kinetochore and the Ndc80 complex containing Ndc80/Hec1. The RZZ stabilizes Mad1-Mad2 at unattached kinetochores (Buffin *et al.* 2005), thus promoting spindle checkpoint signaling, but also silences the spindle checkpoint upon attachment by recruiting the microtubule motor

protein complex dynein-dynactin, which transports Mad2 and BubR1 away from the kinetochores (Howell *et al.* 2001).

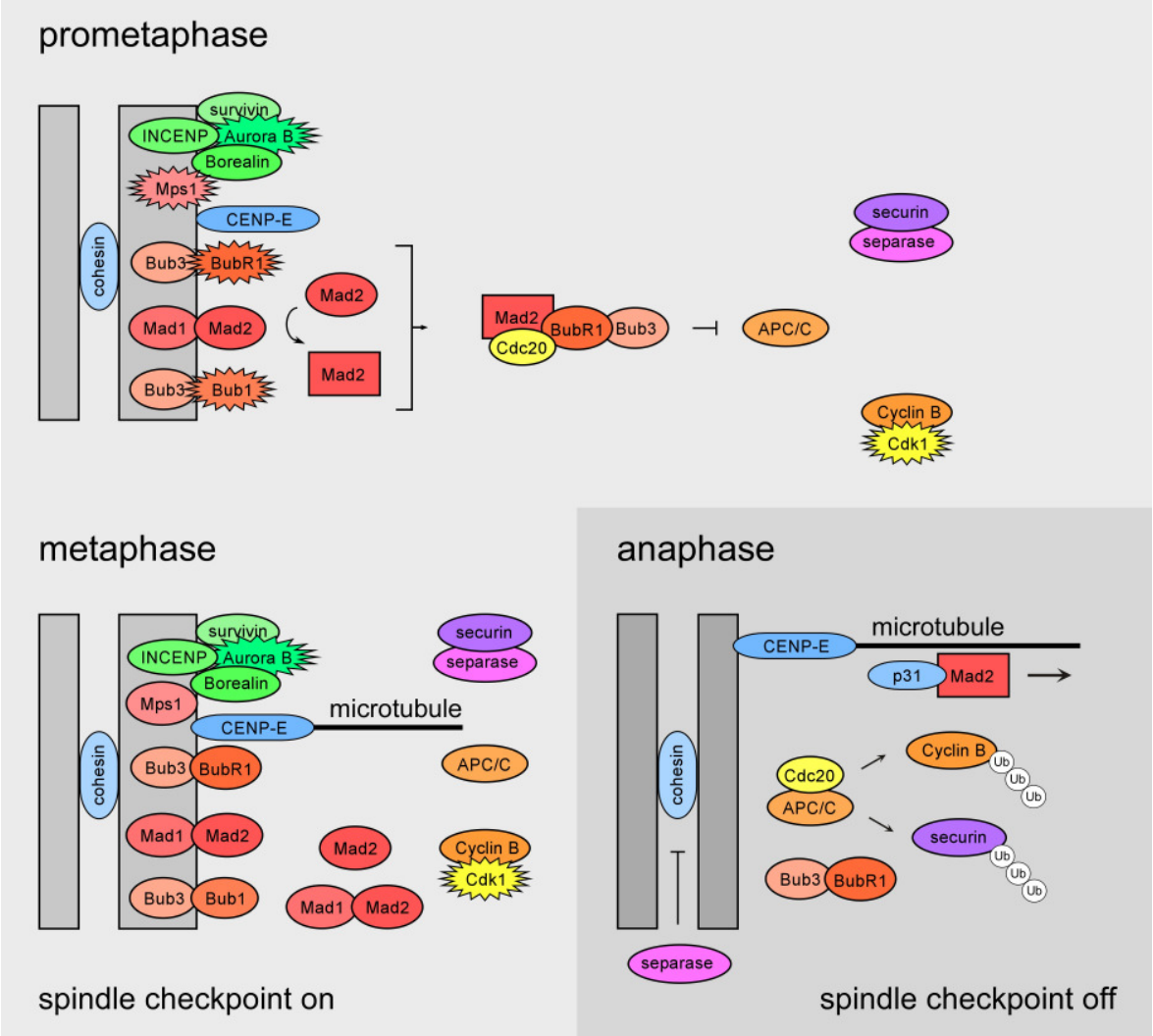

Figure 7: The mitotic spindle checkpoint ensures euploidy by controlling the metaphase to anaphase transition. The spindle checkpoint is active until microtubule attachment to the kinetochores and tension across the kinetochores is achieved and inhibits the ubiquitin ligase APC/C^{Cdc20} responsible for proteasomal degradation of Cyclin B and securin and, thus, sister chromatid segregation and anaphase onset. Mitotic signaling depends on the mitotic checkpoint complex consisting of Mad2, BubR1, Bub3 and Cdc20 which inhibits Cdc20, the mitotic specificity factor for APC/C. Active kinases are indicated as spiked symbols, active Mad2 (C-Mad2) as rectangles, inactive Mad2 (O-Mad2) as ovals, kinetochores as grey rectangles. For details see text.

Upon satisfaction of the spindle checkpoint its silencing probably occurs by several additional mechanisms (Figure 7): Downregulation of BubR1 kinase activity upon microtubule binding of CENP-E (Mao *et al.* 2003), removal of Cdk1/Cyclin B from correctly attached kinetochores by the dynein/dynactin complex (Chen *et al.* 2008),

phosphorylation of Mad2 rendering it incapable to bind Mad1 or Cdc20 thus inhibiting MCC formation (Wassmann *et al.* 2003) and $p31^{comet}$ binding of Mad1- or Cdc20-bound Mad2, which inhibits Mad2's activation and promotes disassembly of MCCs (Yang *et al.* 2007). Recently, a switch of the ubiquitination status of Cdc20 was shown to regulate its association with Mad2 and BubR1 and, thus, the APC/C activation status (Reddy *et al*. 2007, Stegmeier *et al*. 2007). Furthermore, mutual repression of APC/C^{Cdc20} and Mps1 was identified in budding yeast: while Mps1 inhibits APC/C^{Cdc20} via the spindle checkpoint in metaphase, it is degraded by APC/C^{Cdc20} in anaphase. Mps1 degradation in anaphase might explain why the spindle checkpoint cannot be reactivated (Palframan *et al.* 2006).

Mad2 activation

Recently, a model incorporated several observations connected to the activation of Mad2, the most downstream component of the spindle checkpoint, involving conformational changes (open (O-Mad2) and closed (C-Mad2) conformation), its homooligomerization and its binding to Mad1, which is mutually exclusive to Cdc20 binding, because it is mediated by the same domain (Luo *et al*. 2002). According to De Antoni and coworkers' "Mad2 template model" stable complexes of C-Mad2/Mad1 at the kinetochore might be required to convert cytosolic O-Mad2 to C-Mad2 enabling complex formation of C-Mad2/Cdc20 (De Antoni *et al*. 2005, Yu 2006). $p31^{comet}$ binds O-Mad2 at the dimerization interface, thereby inhibiting dimerization of Mad2 and its conversion to the active form C-Mad2 (Yang *et al.* 2007).

Altered expression of spindle checkpoint genes can lead to aneuploidy, cancer and premature aging in mice and men

A knockout of spindle checkpoint genes is lethal in early mouse embryogenesis and in human cancer cells upon experimentally induced deletion or even upon downregulation below a threshold level. This might be due to spindle checkpoint inactivation, but it cannot be ruled out that the loss of other spindle checkpoint independent functions of spindle checkpoint proteins is lethal. Viable mice with only one functional allele of a spindle checkpoint gene have been generated. So far only the $MAD2^{+/-}$ (Michel *et al.* 2001) and the $MAD1^{+/-}$ (Iwanaga *et al.* 2007) mouse lines show an increase in spontaneous tumors, which appear after a long latency period and are restricted to the lung in the case of $MAD2^{+/-}$ mice

(Michel *et al.* 2001). In all other cases tumors only develop after treatment with carcinogens (in *RAE1*$^{+/-}$, *BUB3*$^{+/-}$, *BUB3*$^{+/-}$/*RAE1*$^{+/-}$ and *BUB1B*$^{+/-}$ mice; Baker *et al.* 2004, Dai *et al.* 2004, Baker *et al.* 2006). Surprisingly, mice with hypomorphic *BUB1B* alleles leading to reduced BubR1 levels and *BUB3*/*RAE1* doubly haploinsufficient mice age prematurely, implicating BubR1 in fertility and in the prevention of aging and hinting to a function of Bub3 in cooperation with Rae1 in the prevention of aging (Baker *et al.* 2004, Baker *et al.* 2006). Loss of one spindle checkpoint allele induces moderate to substantial aneuploidy (Baker *et al.* 2004, Baker *et al.* 2006, Iwanaga *et al.* 2007), which is probably a consequence of a weakened spindle checkpoint. Aneuploidy is a hallmark of cancers, but it remains a matter of debate whether aneuploidy is the cause or consequence of transformation. However, the rate of aneuploidy might also exceed limits for viability leading to so-called mutational meltdown and therefore counteract cancer as shown for the spindle checkpoint protein CENP-E (Weaver *et al.* 2007).

Interestingly, genes involved in mitotic regulation are deregulated in human cancers. For instance, 29 out of 70 genes associated with a so-called CIN signature are mitosis and centrosome cycle regulators (Carter *et al.* 2006). In human cancers most alterations in spindle checkpoint gene expression leading to spindle checkpoint impairment and chemotherapy resistance are probably due to epigenetic mechanisms (Shichiri *et al.* 2002), since intragenic mutations seem to be rare (Bharadwaj and Yu 2004). Overexpression due to gene amplification or increased transcription independent of gene amplification has been shown for several kinases involved in mitosis: Aurora A in breast, colon, gastric, ovarian and pancreatic cancers (Keen and Taylor 2004, Li and Li 2006) and its regulator and substrate TPX2 (targeting protein for Xklp2, Perez de Castro *et al.* 2007) and Aurora B in breast, colon, prostate and non-small cell lung cancer (Chieffi *et al.* 2006, Vischioni *et al.* 2006), concomitant overexpression of Bub1, Bub3 and BubR1 in gastric cancer (Grabsch *et al.* 2003) and BubR1 in breast cancer (Yuan *et al.* 2006), Plk1 in breast, ovary, endometrium, prostate, the digestive tract, lung, skin, head and neck, mouth and pharynx and brain (Eckerdt *et al.* 2005, Takai *et al.* 2005). Overexpression has also been shown for Tao1 kinase and other mitotic proteins like Rod, Zw10, Zwilch, Cdc20, securin (Perez de Castro *et al.* 2007) and survivin (Wheatley and McNeish 2005). Upregulation of Mad2 was found in gastric, bladder and ovarian cancers and neuroblastomas (Wang *et al.* 2002, Hernando *et al*. 2004, Wu *et al.* 2004) and can have a similarly detrimental effect on spindle checkpoint function as Mad2 downregulation, which is found in breast, lung, nasopharyngeal and ovarian cancers, hepatomas and testicular germ cell tumors (Li and

Benezra 1996, Takahashi *et al.* 1999, Wang *et al.* 2000, Wang *et al.* 2002, Sze *et al.* 2004, Fung *et al.* 2007). Downregulation was demonstrated for CHFR (checkpoint with forkhead and ring finger domains), which is part of a poorly characterized stress-activated checkpoint acting in prophase independently of the spindle checkpoint, which depends on p38 MAP kinase (Scolnick and Halazonetis 2000). CHFR is an ubiquitin ligase implicated in negative regulation of Aurora A and is frequently downregulated in human cancer via epigenetic mechanisms (Scolnick and Halazonetis 2000, Yu *et al.* 2005). Furthermore, reduced levels of BubR1 were detected in human colon adenocarcinoma samples (Shin *et al.* 2003). Tumor associated point mutations have been reported for *BUB1*, *BUB1B* (encoding BubR1) and *PLK1*, *CHFR*, *MAD1*, *MAD2*, *ROD*, *ZW10* and *ZWILCH* (Cahill *et al.* 1998, Scolnick and Halazonetis 2000, Perez de Castro *et al.* 2007). A notable exception to the usually non-hereditary cancers is a rare recessive disease, mosaic variegated aneuploidy syndrome (MVA), which is characterized by the occurrence of childhood cancers, constitutional mosaicism for chromosomal gains and losses, microcephaly and growth retardation (Hanks *et al.* 2004). The identification of truncating and missense mutations of *BUB1B* is the first report of a human disorder linked to a hereditary mutation of a spindle checkpoint gene and provides evidence for an anticancer function of the spindle checkpoint by maintaining euploidy (Hanks *et al.* 2004).

In sum, some spindle checkpoint genes like Aurora A, Plk1 and securin appear to act mainly as oncogenes and some like CHFR as tumor suppressor genes, whereas others like Mad2 or BubR1 cannot be easily classified as either oncogenes or tumor suppressor genes since their deregulation leads to tumorigenesis regardless of their up- or downregulation (Michel *et al.* 2004, Perez de Castro *et al.* 2007).

The postmitotic G1 checkpoint prevents propagation of tetraploid cells generated by a failed mitosis

Spindle checkpoint activation due to a disturbed mitosis is only transient and is followed by an unscheduled exit from mitosis, a process known as mitotic slippage – the resolution of mitotic arrest, which results in the generation of tetraploid cells (Andreassen *et al.* 1996, Chen *et al.* 2003, Blagosklonny 2006, Brito and Rieder 2006). Those tetraploid cells display G1 phase characteristics in the presence of an abnormally high chromosome content and arrest at G1/S due to activation of the tetraploidy checkpoint. The postmitotic or pseudo-G1 checkpoint or tetraploidy checkpoint functions by p53 accumulation during a

prolonged mitosis leading to p21 induction, which arrests cells before the next S phase and, thus, prevents replication of the DNA to octaploidy (Andreassen *et al.* 1996, Stewart and Pietenpol 2001, Chen *et al.* 2003, Vogel *et al.* 2004). Recent findings indicate a novel role for the DNA damage checkpoint kinase ATM in mediating the mitotic centrosomal localization of p53 by Ser15 phosphorylation. During an undisturbed mitosis p53's Ser15 phosphorylation is ablated upon association with the centrosomes, whereas it persists upon spindle depolymerization, leading to sequestration of activated ATM (phosphorylated at Ser1981) and activated p53 (phosphorylated at Ser15) in cytoplasmic spots (Oricchio *et al.* 2006). Upon nuclear reformation, p53 enters the nucleus, dissociates from ATM and becomes further activated by phosphorylation at Ser46, allowing p53 to transmit the information of a perturbed mitosis and to activate the tetraploidy checkpoint (Oricchio *et al.* 2006). This explains why loss of functional p53 or p21 can lead to polyploidization (Lanni and Jacks 1998). However, controversy persists about what exactly the postmitotic G1 checkpoint actually measures, as it does not appear to sense tetraploidy, an aberrant centrosome number or a failed cytokinesis, or about its existence *per se* (Stewart and Pietenpol 2001, Uetake and Sluder 2004, Wong and Stearns 2005, Blagosklonny 2006).

Apoptosis and other forms of cell death

Apoptosis

Regulated cell death is necessary for development, tissue homeostasis and protection from disease. Apoptosis has important functions in morphogenesis during embryonic development, in the removal of damaged or virally infected cells, in the elimination of self-reactive clones from the immune system and in the maintenance of tissue homeostasis (Okada and Mak 2004). Impaired apoptosis is a hallmark of cancer, can drive cancerogenesis and impede anti-cancer treatment (Hanahan and Weinberg 2000), whereas the aberrant activation of apoptosis may contribute to AIDS, neurodegenerative disorders, and ischemic injury (Thompson 1995). The morphological features of apoptosis include blebbing of the plasma membrane, shrinking of the cytoplasm and nucleus and cellular fragmentation by budding of apoptotic bodies containing nuclear chromatin without producing an inflammatory response (Kerr *et al.* 1972). The most prominent biochemical feature of apoptosis is the activation of caspases (cysteine-dependent aspartate-specific proteases) in an amplification cascade. To avoid untimely execution of apoptosis the caspases are synthesized as precursors that have to be activated by autocatalytic or hetero-

catalytic cleavage. When initiator caspases (caspases 2, 8, 9) are activated by oligomerization, they cleave effector caspases (caspases 3, 6, 7) which in turn digest a wide variety of cellular substrates that determine the integrity and shape of the organelles (Budihardjo *et al.* 1999). Typical caspase 3 substrates are the nuclear lamins, PARP (a member of the poly-ADP ribose polymerase family of DNA repair enzymes, Schreiber *et al.* 2006), or ICAD (inhibitor of caspase activated DNase), which inhibits the caspase activated DNase (CAD) responsible for internucleosomal cleavage of chromatin.

Apoptosis can be triggered by two pathways sharing some of the caspases involved, the cell surface death receptor pathway and the mitochondria-associated pathway, also known as extrinsic and intrinsic pathways, respectively (Figure 8; Budihardjo *et al.* 1999). Whereas the extrinsic pathway is induced by cell-cell interactions e.g. upon viral infection detected by immune cells, the intrinsic pathway responds to intracellular stresses like nutrient starvation, chemotherapeutic agents, physical stimuli like UV- or γ-radiation or oxidative stress induced by reactive oxygen species (ROS). The extrinsic pathway is mediated by death ligand-death receptor interactions on the cell surface which recruit the death-induced signaling complex (DISC) consisting of adaptor proteins and procaspase 8. Caspase 8 is activated by the DISC and stimulates downstream caspases by direct cleavage in type I cells or indirectly by cleaving bid, which then induces cytochrome C release from the mitochondria in type II cells. In the intrinsic pathway, effector caspase activation is triggered by the formation of the apoptosome, a multimeric Apaf-1/cytochrome C/ caspase 9 complex stimulating autocatalytic cleavage of procaspase 9 (Figure 8). Activated caspase 9 will then cleave and activate effector caspases 3, 6 and 7. This pathway is regulated at several steps, including the release of cytochrome C from the mitochondria, the binding and hydrolysis of dATP/ATP by Apaf-1 and the inhibition of caspase activation by proteins like survivin that belong to the inhibitors of apoptosis (IAP) family (Okada and Mak 2004). The IAPs, in turn, can be inhibited by Smac/DIABLO (second mitochondria-derived activator of caspase/direct IAP-binding protein with low pI), a protein also released from the mitochondria upon a proapoptotic signal. Only XIAP (X-linked IAP) is a *bona fide* caspase inhibitor, whereas all other IAPs inhibit caspases by indirect, unknown mechanisms (Eckelman *et al.* 2006). Two special features separate survivin from other IAPs, its structure – it shares the BIR domain (baculovirus IAP repeat), but no other domains with them – and its dual function in mitosis as part of the chromosomal passenger complex (Lens *et al.* 2006) and in cell survival. It appears that mitotic regulation is survivin's main function in nontransformed cells and adult tissues.

Survivin's role in cell survival is restricted to transformed cells, in which survivin overexpression is frequent and its expression lacks the cell cycle-dependent periodicity seen in normal cells (Altieri 2006). Survivin can inhibit apoptosis by several mechanisms: Cytosolic survivin translocates to the mitochondria and then back into the cytoplasm, where it binds cofactors such as HBXIP (hepatitis B virus x interacting protein) leading to inhibition of apoptosome formation and of caspase 9 and it increases XIAP stability, thereby enhancing XIAP-mediated direct caspase inhibition (Altieri 2006).

Mitochondrial outer membrane permeabilization is a process that disrupts the cellular energy supply by stopping ATP production due to the collapse of the pH gradient across the mitochondrial membranes and the cytoplasm. Proteins like cytochrome C from the respiratory chain are released into the cytoplasm and act as apoptotic activators. From this step on the caspase cascade is irreversible. Mitochondrial membrane permeability is regulated by the bcl-2 protein family, which consists of about 30 members in humans. The bcl-2 family is comprised of antiapoptotic members containing four bcl-2 homology (BH) domains like bcl-2 (B-cell CLL/lymphoma 2) and bcl-X_L (BCL-2 like 1) and proapoptotic members with different domain structures (Reed 2006). Bid, bad, Puma and Noxa belong to the family of BH3-only proteins with sequence homology restricted to one domain that is sufficient to induce apoptosis, whereas the multi-domain bax-like subfamily proteins bax and bak contain three BH domains (Reed 2006). The bcl2 family proteins can homo- or heterodimerize and the ratio of pro- and antiapoptotic members or the ratio of molecules in their active conformation of this family can tip the scale towards cell death or survival (Willis *et al.* 2003, Reed 2006). Bcl-2 is the most prominent of the antiapoptotic bcl-2 proteins and can counteract bax and bak (Willis *et al.* 2003). However, the mechanism of mitochondrial membrane permeabilization is still unresolved (Antignani and Youle 2006, Reed 2006). Since several bcl-2 family proteins can insert into membranes and these insertions can be modulated by conformational changes occurring upon their activation, they might form channels through the outer mitochondrial membrane permitting diffusion or transport of mitochondrial proteins into the cytoplasm (Antignani and Youle 2006). So far there is only circumstantial evidence, mostly gained from systems using artificial membranes to support these models (Antignani and Youle 2006). Some members of the bcl-2 family are transcriptional targets of p53, which is upregulated upon many stresses and checkpoint mediated arrests.

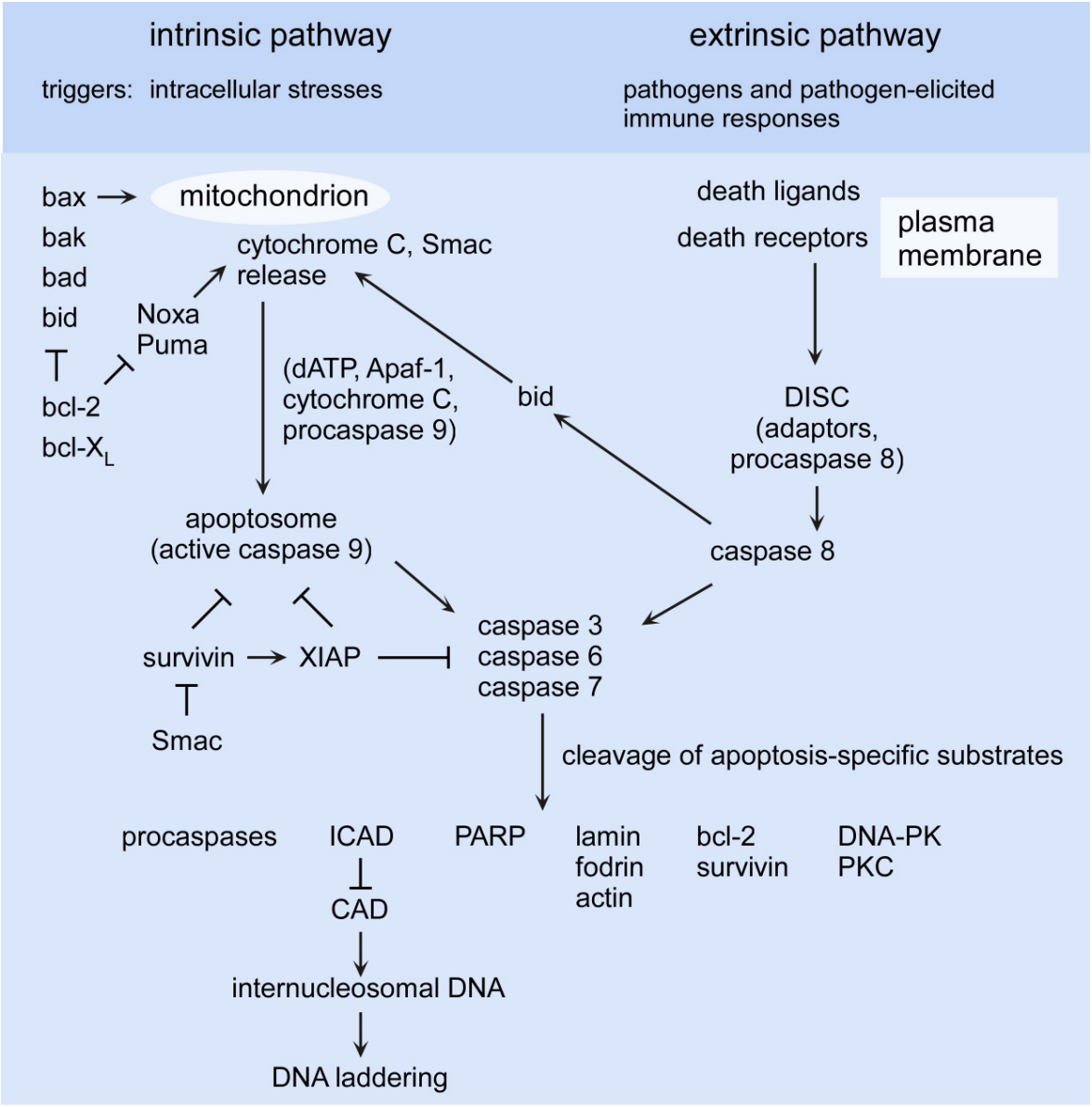

Figure 8: The intrinsic and extrinsic pathways of apoptosis. Intracellular stresses like nutrient deprivation, irradiation or chemicals (including chemotherapeutic agents) trigger apoptosis via the intrinsic pathway, whereas the extrinsic pathway is primarily induced by the immune system. The intrinsic pathway is characterized by the permeabilization of the mitochondrial outer membrane, leading to cytochrome C release – a prerequisite for apoptosome formation – activating caspase 9. The ratio of activated pro- and antiapoptotic members of the bcl-2 protein family is a main determinant of mitochondrial permeability that is often deregulated in cancer cells favouring cell survival. The extrinsic pathway is activated via death ligand-death receptor interactions, which activate caspase 8 via adaptor proteins. Besides inducing effector caspases (in type I cells), caspase 8 can also trigger the intrinsic pathway via bid cleavage (in type II cells), resulting in cytochrome C release from the mitochondria. Both pathways lead to the activation of effector caspases 3, 6 and 7 via the initiator caspases 8 or 9. The activation of effector caspases leads to the cleavage of PARP and DNA, cell and organelle shrinking and finally the disintegration of the cells into apoptotic bodies without eliciting an inflammatory response.

The proapoptotic bcl2-proteins bax, Noxa and Puma are transcriptionally upregulated by p53 (Vousden and Lu 2002), while the antiapoptotic proteins bcl-2 and bcl-X_L or the IAP survivin are repressed (Wu *et al.* 2001, Hoffman *et al.* 2002).
Interestingly, there are only a few studies addressing the incidence of caspase mutations in human tumors and these indicate a similar situation as in the case of spindle checkpoint genes: Mutations appear to be rare, but impairment of expression and function by epigenetic mechanisms seems to be frequent (Jin and El-Deiry 2005).

Other forms of cell death

Necrosis, autophagy and mitotic catastrophe are considered to be nonapoptotic cell death pathways (Okada and Mak 2004, Broker *et al.* 2005, Jin and El-Deiry 2005, Kim *et al.* 2006). Kroemer and Martin list three possible relationships between cell death and caspase activation: cell death through caspase activation, cell death with concomitant but not causative caspase activation and cell death without caspase activation (Kroemer and Martin 2005).
Cell death by necrosis is characterized by membrane distortion, organelle degradation and cellular swelling leading to the release of intracellular contents into the cytoplasm triggering inflammation. Recent results indicate that necrosis is the result of a chain of biochemical reactions with some similarities to apoptosis (Broker *et al.* 2005). Under some conditions necrosis can substitute for apoptotic cell death if apoptosis is suppressed, e.g. by the inhibition of caspases (Broker *et al.* 2005). Autophagy is a process by which long-lived proteins and organelle components are directed to the lysosomes by the autophagosome and degraded there. Its function in yeast is to enable survival during nutrient starvation, but its role in mammalian cells is only poorly understood. Significantly, autophagy is required for cellular remodeling upon differentiation, stress or cytotoxin induced damage and can promote survival of cancer cells upon chemotherapy (Degenhardt *et al.* 2006). However, cancerogenesis can be counteracted by the autophagy pathway as evidenced by monoallelic deletion of the conserved autophagy gene *BECN1*, encoding the protein beclin 1, in several cancers (Liang *et al.* 1999). Beclin 1 is reported to interact with bcl-2 and recent findings link bcl-2 and autophagy via bcl-2 mediated regulation of intracellular calcium levels, which are known to mediate apoptosis (Liang *et al.* 1999, Hoyer-Hansen *et al.* 2007). Mitotic catastrophe – also termed mitotic cell death – is categorized as a distinct form of cell death. Evidence for this claim, however, is scarce. Death of mammalian cells

caused by an aberrant mitosis is often called mitotic catastrophe. The term is used heterogeneously, as it can refer to cell death executed directly in mitosis, but also to cell death subsequently to an aberrant mitosis. Its hallmarks are multinucleated, sometimes giant cells containing fragmented nuclei and abnormally high Cdk1/Cyclin B levels (Okada and Mak 2004). One group has recently reported caspase 2 and 3 activation and an involvement of mitochondria, suggesting that mitotic catastrophe might be a variant of apoptotic cell death (Castedo *et al.* 2004).

Apoptosis is an increasingly complex field of research, but other forms of cell death are gaining attention, and all forms of cell death are now viewed under the aspect of mutual interdependence and substitution especially under chemotherapy conditions (Kroemer and Martin 2005). This new view and novel insights into nonapoptotic forms of cell death could improve anti-cancer drug development and treatment strategies substantially.

Chemotherapy

Introduction

Modern cancer therapy mainly relies on chemotherapy, surgery and radiation therapy, which can be applied together in combined modality chemotherapy. Chemotherapeutic agents can be administered alone or in combination. Combination chemotherapy employs drugs differing in their mechanism of action, thereby creating synergies and minimizing the chances of resistance developing to any one agent, and is therefore the most commonly used form of chemotherapy. Many different combination chemotherapies of several anti-cancer agents and other medications aiding the effects of the chemotherapeutic drugs or alleviating their side effects exist.

Chemotherapeutic agents induce DNA damage, interfere with DNA replication or induce damage to the mitotic spindle. Treated cells detect the damage and activate the corresponding cell cycle checkpoints at the G1/S or G2/M transitions or in mitosis leading to cell cycle arrest and initiate repair, and, if the damage is too severe, induce apoptosis. However, due to the genetic heterogeneity of cancer cells it is likely that tumor regrowth in response to the selective pressure exerted by treatment is initiated by cells carrying a mutation conferring resistance to a certain agent. Obstacles to reaching clinically relevant drug concentrations in cancer cells are the multiple resistance mechanisms, which are inherent or acquired during treatment and result in drug exclusion or inactivation, limited

accessibility of the tumor due to reduced blood flow near solid tumors, binding of the agents to blood plasma, fast excretion of the agents by the urinary tract or degradation by the liver and encompass probably additional unknown mechanisms (Kinsella and Smith 1998, Lee and Schmitt 2003, Zhou and Giannakakou 2005). For instance, multidrug resistance (MDR) – resistance of cancer cells to structurally diverse drugs – can be mediated by several mechanisms, most frequently the overexpression of drug efflux pumps belonging to the ABC (ATP-binding cassette) superfamily (Ross and Doyle 2004, Brooks *et al.* 2005). Cross-resistance is a major problem in chemotherapy, because the ABC pumps transport drugs with different structures and cellular targets (Ozben 2006). Preferential substrates are drugs derived from naturally occurring substances with amphipathic or hydrophobic properties like anthracyclines, epipodophyllotoxins, antimetabolites, taxanes and *Vinca* alkaloids, all widely used chemotherapeutics (Ross and Doyle 2004, Ozben 2006). Significantly, MDR can be intrinsic or acquired within days of chemotherapeutic treatment, e.g. by overexpression of MDR genes and downregulation of drug target genes like topoisomerase II (Di Nicolantonio *et al.* 2005).

The side effects of chemotherapy can be severe and are mainly the result of adverse effects on tissues with rapidly proliferating cells. The spectrum and kind of side effects depend on the chemotherapeutic agent. Common side effects are nausea and vomiting, diarrhea or constipation, mucositis, myelosuppression resulting in anemia, immunosuppression and thrombocytopenia, alopecia, neurological symptoms, toxicity to other organs and the elevated risk to develop secondary neoplasms. The latter is due to the mutagenic and therefore possibly cancerogenic effect of many classical chemotherapeutics.

DNA damaging agents

Many different forms of DNA damage are induced by the chemotherapeutic agents currently in clinical use. DNA single or double strand breaks are created by the inhibition of topoisomerase I or II, respectively. Alkylating agents form DNA adducts, whereas antimetabolites deplete the nucleotide pools and, thus, lead to DNA damage indirectly.

Topoisomerase inhibitors

Supercoiling of DNA is relieved by topoisomerases. Topoisomerase I introduces a DNA single strand break in an ATP-independent manner through which the other DNA strand is passed and religated, whereas topoisomerase II cuts both strands ATP-dependently,

creating a DNA-linked protein gate through which the other DNA double strand is passed. Topoisomerase I mainly functions in DNA replication and transcription, whereas topoisomerase IIα is also required for chromosome decatenation, condensation and segregation and is the only cell cycle dependently expressed topoisomerase with levels peaking in G2 phase and mitosis (Cortes *et al.* 2003). Most clinically used topoisomerase inhibitors are non-catalytic and prevent religation of the cut DNA by the enzyme, which is covalently bound to the DNA during the reaction. Catalytic topoisomerase II inhibitors can interfere with the enzymatic activity of topoisomerases before DNA scission, thus not creating DNA strand breaks *per se*. However, inhibition of catalytic topoisomerase activity may lead to DNA strand break formation, if a cell accumulates torsional stresses by continued traversal of the cell cycle, e.g. the attempt to replicate DNA or to pull still catenated or uncondensed chromatids apart in mitosis (Cortes *et al.* 2003). Non-catalytic topoisomerase inhibitors block the religation of DNA strands cleaved by these enzymes, leading to accumulation of DNA breaks that are detected by the DNA damage checkpoints in a p53-dependent and a p53-independent manner (Shapiro and Harper 1999, Shiloh 2001, Eastman 2004, Kastan and Bartek 2004). In addition, some agents commonly categorized as topoisomerase inhibitors also exert toxicity by intercalation between bases of DNA or RNA (anthracyclines), formation of DNA adducts (adriamycin, in a sequence specific manner), DNA crosslinks (mitoxantrone) or free radicals (adriamycin).

To date, more topoisomerase II than topoisomerase I inhibitors are used in the clinic. The first topoisomerase I inhibitors to be discovered and still the most prominent are the camptothecins. The semisynthetic derivatives of camptothecin, which was isolated from the Asian tree *Camptotheca acuminata*, irinotecan (a prodrug that is enzymatically converted into the active metabolite SN-38 by a carboxylesterase-converting enzyme) and topotecan are non-catalytic topoisomerase I inhibitors and were approved for clinical use in 1996. Topoisomerase II inhibitors are chemically diverse and can be divided into more than two dozen chemical classes, but progress in finding new clinically applicable inhibitors is slow, therefore research concentrates on improving drug delivery (Wang *et al.* 1997, Giles and Sharma 2005). Adriamycin/doxorubicin, daunorubicin, epirubicin, idarubicin and mitoxantrone are members of the anthracycline family, most of them are semisynthetic derivatives of adriamycin, which was first isolated from the fungus *Streptococcus peucetius var. caesius* and were approved for clinical use in the 1970s and 1980s. Etoposide, teniposide and amsacrine are semisynthetic derivatives of epipodophyllotoxins, alkaloids from the root of the American Mayapple, *Podophyllum*

peltatum. Whereas amsacrine is a catalytic inhibitor and an intercalator, the other two agents are not, illustrating that small chemical alterations can change the mechanism of action of epipodophyllotoxins, but also anthracyclines, substantially (Jensen and Sehested 1997). Doxorubicin is effective against a broad spectrum of malignancies: breast, ovarian, endometrial, testicular, thyroid, lung, bladder, gastric and liver cancer, soft tissue sarcoma, Wilm's tumor, neuroblastoma, acute leukemia, Hodgkin's and Non-Hodgkin's lymphoma. Daunorubicin is used to treat acute myeloic and acute lymphatic leukemias. Etoposide is employed against various cancers, e.g. lung, testicular and gastric cancers and leukemias. Topotecan is used to treat metastatic ovarian cancer and small cell lung cancer, and irinotecan is employed against metastatic colorectal cancer. All these agents cause diarrhea and immunosuppression, doxorubicin also exhibits cardiotoxicity.

Alkylating agents

The alkylating agents cisplatin, carboplatin and oxaliplatin form adducts to the DNA and intra- and interstrand crosslinks, which inhibit DNA replication and transcription and can arrest cells at the G1/S or G2/M border (Wang and Lippard 2005). Cisplatin was approved for clinical use in 1978, carboplatin in 1989 and oxaliplatin in 1999 in the EU and in 2004 in the USA. Several chemically distinct alkylating agents are known and in clinical use, among them several nitrogen mustard derivatives like cyclophosphamide, a prodrug that is activated by liver enzymes and was approved in 1959. Nitrogen mustards are used to treat both solid tumors and leukemias. The platinum compounds are employed against a wide variety of malignancies of the ovary, endometrium, cervix, prostate, testis, esophagus, bladder, lung, germ cell tumors, Non-Hodgkin's lymphoma, relapsed and refractory acute leukemia. Cisplatin is used most often in lung cancer and testicular cancer, and can cause severe kidney damage. This nephrotoxic effect is reduced in carboplatin and absent in oxaliplatin, which can lead to severe neuropathies.

Antimetabolites

Drugs mimicking folates, purines and pyrimidines are called antimetabolites and are successful chemotherapeutics against a number of diseases including cancer (Peters *et al.* 2000). Methotrexate mimics folate and inhibits the synthesis of tetrahydrofolate by binding to dihydrofolate reductase, which is needed for the synthesis of purines and pyrimidines required for DNA and RNA synthesis (Kinsella and Smith 1998). The effect of

5-fluorouracil (approved in 1962), a pyrimidine analog, which inhibits dTMP synthesis by thymidylate synthase, and, thus, DNA synthesis and repair, depends on functional p53 to induce apoptosis at the G1/S border (Kinsella and Smith 1998). Its prodrug capecitabine, and cytidine analogs cytarabine and gemcitabine are other examples for this class of drugs. Methotrexate is employed to treat hematological malignancies like leukemias and lymphomas and solid tumors of the breast, bones, head and neck, colon, bladder and choriocarcinomas. 5-Fluorouracil has a major role in the treatment of gastrointestinal cancers and bladder, breast, ovary, head and neck carcinomas. Capecitabine is used in the treatment of metastatic colon or breast cancer, cytarabine is employed against leukemias and gemcitabine is effective in solid cancers, e.g. of the pancreas, ovary or lung.

Spindle damaging agents

Interference with the mitotic spindle of cancer cells has been a successful chemo-therapeutic strategy for over 40 years (Schmidt and Bastians 2007). Until recently it was believed that the depolymerization of microtubules by *Vinca* alkaloids (Jordan *et al.* 1992) or their stabilization by taxanes or epothilones (Jordan *et al.* 1996) would activate the spindle checkpoint, induce mitotic arrest and cell death. However, subtle repression of microtubule dynamics is now recognized as the common mechanism of action of spindle damaging agents. The agent concentrations sufficient to disturb microtubule dynamics are 10-100 fold lower (in the nanomolar range), but clinically relevant, than the ones required to change the amount of tubulin polymerized into microtubules, meaning that the effect of spindle damaging agents on microtubule dynamics will often be more powerful in chemotherapy than the effect on microtubule mass (Jordan and Wilson 2004). Not only are undisturbed microtubule dynamics indispensable for the proper execution of mitosis, microtubules are also involved in axon formation and neuronal transport, which is probably the reason for the neurotoxicity of several antimicrotubule agents. Most spindle damaging agents inhibit microtubules by binding to the *Vinca* domain, the paclitaxel site or the colchicine domain of β-tubulin. A certain specificity of antimicrotubule agents for mitotic cells is probably due to the greater dynamicity of mitotic over interphase microtubules (Belmont *et al.* 1990). Synergy effects of combination of spindle damaging agents with distinct or similar mechanisms of action are observed, e.g. for taxanes and *Vinca* alkaloids and could be the basis for improved chemotherapies (Jordan and Wilson 2004).

Vinca alkaloids

Vinca alkaloids were first isolated from the Madagascar periwinkle, *Cataranthus roseus*, formerly known as *Vinca rosea*. In 1961, vinblastine was approved for chemotherapy, in 1963 vincristine and in 1994 vinorelbine/navelbine, which exhibits reduced neurotoxicity probably due to reduced axonal microtubule binding *in vitro*. However, besides the interaction with the *Vinca* domain of β-tubulin, *Vinca* alkaloids may also interfere with amino acid, cyclic AMP and glutathione metabolism, the calmodulin-dependent Ca^{2+} transport ATPase activity, cellular respiration and nucleic acid and lipid biosynthesis. Other microtubule depolymerizing agents of diverse chemical classes include the *Vinca* domain binding cryptophycins, halichondrins, dolastatins and hemiasterlins and the colchicine domain binding colchicine, whereas estramustine (a combination of estradiol and the nitrogen mustard mechlorethamine) has a distinct tubulin binding mechanism. Many of these agents are in several stages of clinical development as anticancer drugs (Mollinedo and Gajate 2003, Jordan and Wilson 2004, Zhou and Giannakakou 2005, Schmidt and Bastians 2007). The various *Vinca* alkaloids are distinct in their effect on cancers, their pharmacokinetics and toxicity profiles. *Vinca* alkaloids are used to treat both hematological malignancies like leukemias and lymphomas and solid tumors of the breast, ovary, testis, lung, colon, central nervous system, melanomas and Kaposi sarcomas. While vincristine and vinorelbine are mainly neurotoxic, vinblastine and vindesine are lowering the blood counts.

Taxanes

Taxanes are very successful chemotherapeutic agents. The taxane paclitaxel/taxol is derived from the Pacific yew tree, *Taxus brevifolia*, and docetaxel/taxotere is a semisynthetic derivative of a compound from the European yew tree, *Taxus baccata*. The former was approved for anticancer treatment in 1992, the latter in 1996. Both agents stabilize microtubules by binding the paclitaxel binding site of β-tubulin, practically lining the inside of microtubules (Jordan and Wilson 2004). Interestingly, the effects of taxol or taxotere on additional cellular targets enhance their anticancer activity by promoting apoptosis and inflammation and inhibiting angiogenesis. Resistance mechanisms to taxol include mutation of the paclitaxel binding site of β-tubulin, followed by loss of the wild type allele, lower stability of microtubules (Wang *et al.* 2005, Hari *et al.* 2006) and export by the MDR (multi drug resistance) proteins like the MDR1 P-glycoprotein drug efflux

pump (Brooks *et al.* 2003). Taxanes are employed against a broad range of cancers, namely of the breast, ovary, prostate, lung, head and neck, esophagus, stomach, bladder and Kaposi's sarcoma and are generally used when other chemotherapy regimens have failed. The most common side effect of these drugs is the lowering of the blood counts.

Epothilones

Epothilones are promising anticancer agents undergoing clinical trials during the past years. They were first isolated from the myxobacterium *Sorangium cellulosum* 20 years ago and derivatives have been synthesized. Epothilones stabilize microtubules by binding the paclitaxel site of β-tubulin, but in a unique manner different from taxol, with only one amino acid overlap in the binding site and, thus, have been shown to target taxane-resistant cells for apoptosis, which is further aided by their reduced susceptibility to MDR efflux pumps (Nettles *et al.* 2004).

New mitotic targets

Since microtubule poisons used in anti-cancer chemotherapy also target non-proliferating and differentiated cells, novel agents are now undergoing clinical tests to achieve greater specificity and less side effects in mitosis-targeting chemotherapy. Commercial drug development concentrates on Cdks and also mitotic kinases like members of the Aurora and the Plk families, but the mitotic kinesin Eg5/KSP is also an attractive target (for a review see Schmidt and Bastians 2007).

Cyclin dependent kinase inhibitors

The human genome encodes more than 500 kinases (Noble *et al.* 2004). Most kinase inhibitors developed for chemotherapy block the ATP binding site, although this often leads to reduced specificity for a certain kinase, especially if several closely related kinases exist, for example the Cdk family members (Blagden and de Bono 2005, Shapiro 2006). The available Cdk inhibitors show relatively great promiscuity in their targets, but since it is unknown – albeit likely –, if it would be advantageous to inhibit only one Cdk instead of several Cdks simultaneously, this is not necessarily detrimental to the success of a treatment. So far, toxicity of agents like flavopiridol has been a problem, therefore novel Cdk inhibitors are currently in clinical trials (Shapiro 2006). Blocking substrate binding or

blocking cofactor or ligand binding required to induce an activating conformational change or mimicking inhibitor binding required to induce an inactivating conformational change are other strategies to inhibit kinases (Noble *et al.* 2004). However, these strategies might not work if the cancer cell has acquired mutations conferring resistance to these inhibitors like constitutively active forms of a kinase or receptor kinase.

Aurora inhibitors

The Aurora family of serine/threonine kinases fulfils several important functions in mitosis (Marumoto *et al.* 2005, Vader *et al.* 2006). *S. cerevisiae* possesses only one Aurora kinase, *D. melanogaster* has two and mammals have three Aurora kinases, namely Aurora A, B and C. Aurora A kinase is required for centrosome maturation and separation and for proper spindle formation, stabilization and bipolarity in prophase (Marumoto *et al.* 2003), whereas Aurora B is part of the chromosomal passenger complex and functions in chromosome condensation, chromosome alignment and cytokinesis and takes part in spindle checkpoint signaling (Vader *et al.* 2006). Aurora C is a kinase with unknown function, which is unique to mammals and is expressed in the testis and some cancer cell lines. Recent reports about Aurora C's localization and function claim it to have a similar function in mitosis as Aurora B; Aurora C interacts with Borealin and phosphorylates it and CENP-A and binds survivin and INCENP (Yan *et al*. 2005, Tang *et al.* 2006, Slattery *et al.* 2007). Overexpression of Aurora A due to gene amplification or other mechanisms was found in breast, colon, gastric, ovarian and pancreatic cancers and often correlates with aneuploidy (Keen and Taylor 2004, Li and Li 2006), whereas Aurora B overexpression was found in breast, colon and prostate cancer and non-small cell lung carcinoma (Chieffi *et al.* 2006, Vischioni *et al.* 2006). Therefore, the Aurora kinases appear as alternative targets for chemotherapy. The first Aurora inhibitors described, VX-680 (Vertex, Harrington *et al.* 2004), ZM447439 (AstraZeneca; Ditchfield *et al.* 2003) and Hesperadin/BIBI1489 (Boehringer Ingelheim; Hauf *et al.* 2003) inhibit both, Aurora A and B kinases *in vitro*, but display an Aurora B inhibition phenotype *in vivo*. Polyploidization due to suppression of cytokinesis occurs in cells treated with Aurora kinase inhibitors or siRNAs directed against Aurora B while cell cycle progression is unimpeded (Hauf *et al.* 2003, Ditchfield *et al.* 2005). Recently, inhibitors with greater specificity for Aurora A kinase were developed, e.g. ZM-3, a derivative of ZM447439, VX-528 (Vertex) and MLN8054 (Manfredi *et al.* 2006). Several Aurora kinase inhibitors are currently

undergoing clinical trials and many more are in preclinical development by over two dozen companies. Interestingly, CYC116 (Cyclacel) inhibits both Aurora B and angiogenesis and showed promise against solid tumors and hematological malignancies in preclinical studies. These inhibitors might overcome the taxol resistance associated with Aurora A overexpression induced spindle checkpoint override (Anand *et al.* 2003, Gizatullin *et al.* 2006). Interestingly, Aurora B inhibitors are now joined by inhibitors of survivin, which have recently entered first clinical trials (Pennati *et al.* 2007), broadening the spectrum of targets in the chromosomal passenger complex.

Plk inhibitors

The members of the Plk family of serine/threonine kinases function in centrosome maturation, Cdk1 activation, mitotic spindle formation, regulation of the APC/C, chromosome segregation and cytokinesis (Eckerdt *et al.* 2005, Takai *et al.* 2005). Whereas *S. cerevisiae*, *S. pombe* and *D. melanogaster* possess only one Plk, which is homologous to human Plk1, four Plks exist in vertebrates (Eckerdt *et al.* 2005). All Plks share a 30 amino acids large polo box situated at the noncatalytic C-terminus that regulates kinase activity primarily by influencing subcellular localization and to a lesser extent autoinhibition of the Plk (van de Weerdt and Medema 2006). The best characterized Plk is Plk1, whereas less is known about Plk2, 3 and 4 (Eckerdt *et al.* 2005). Plk1, 2 and 4 are expressed in a cell cycle-specific manner, promote cell cycle progression and are therefore mainly detectable in highly proliferating tissues, whereas Plk3 is constitutively expressed and arrests cells upon DNA damage (Eckerdt *et al.* 2005, Takai *et al.* 2005, Winkles and Alberts 2005). Additionally, Plk1, 2 and 3 are stress-regulated (Winkles and Alberts 2005). Interestingly, an inverse correlation of Plk1 and Plk3 expression exists during cancerogenesis in lung and head and neck cancers, where Plk1 levels are increased while Plk3 levels are decreased, probably leading to enhanced proliferation and genomic instability (Eckerdt *et al.* 2005, Takai *et al.* 2005, Winkles and Alberts 2005). However, concomitant overexpression of Plk1 and Plk3 was also reported in ovarian tumors, correlating with high proliferation and bad prognosis (Weichert *et al.* 2004). Plk1 is overexpressed in cancers of the breast, ovary, endometrium, prostate, the digestive tract, lung, skin, head and neck, mouth and pharynx and brain (Eckerdt *et al.* 2005, Takai *et al.* 2005). So far Plk2 and 4 expression was not thoroughly analyzed in human cancers, but both appear to regulate centrosome duplication, which is often altered in tumors (Warnke *et al.* 2004, Habedanck *et al.* 2005, van de

Weerdt and Medema 2006). Plk inhibitor development for chemotherapy concentrates on targeting Plk1, which is often overexpressed in higher stage cancers with bad prognosis, and employs small molecule inhibitors and siRNA based approaches, whereas cell culture experiments also made use of introduction of polo-box containing peptides or antibodies or the expression of dominant negative Plk1 (Takai *et al.* 2005). Pharmacological inhibition or depletion of Plk1 leads to metaphase arrest induced by unstably attached chromosomes due to spindle defects caused by impaired centrosomal microtubule nucleation, and pharmacological Plk1 inhibition specifically leads to monoastral spindles (van Vugt *et al.* 2004, McInnes *et al.* 2006). Phase II clinical trials are underway for the Plk1 inhibitors BI 2536 (Boehringer Ingelheim; Steegmaier *et al.* 2007) and GSK461364A (GlaxoSmith-Kline) and many more Plk1 inhibitors are currently being developed.

Eg5/KSP inhibitors

Microtubule motor proteins can be divided into kinesins and dyneins, which both can move cargo along the microtubule network of the cell in an ATP-dependent manner. Dyneins move towards the minus end of microtubules, whereas kinesins move to the plus end. The mitotic kinesin motor protein Eg5/KSP establishes spindle bipolarity by moving the duplicated centrosomes to opposite sides of the cell (Blangy *et al.* 1995). Inhibition of Eg5/KSP leads to formation of a monoastral spindle, which activates the spindle checkpoint and leads to mitotic arrest. Inhibition of Eg5/KSP is expected to be mitosis-specific and, thus, effective solely in proliferating cells. Therefore, Eg5/KSP inhibitors should not have the side effects associated with interference with microtubule stability, which also affect quiescent cells. Monastrol was the first Eg5/KSP inhibitor to be identified (Mayer *et al.* 1999). Subsequently, more potent inhibitors like KSP-IA (Tao *et al.* 2005), Ispinesib (SB-715992 and its derivative SB-743921, GlaxoSmithKline; Davis *et al.* 2006), MK-0731 (Merck; Stein *et al.* 2006) and ARRY-520 (Array Biopharma; Woessner *et al.* 2007) were identified and are currently evaluated in phase I trials. At least thirteen other mitotic kinesins are currently known and might become valuable chemotherapeutic targets in the future (Schmidt and Bastians 2007).

G2 CP abrogation

A promising strategy to target tumor cells lacking functional p53 is the concept of “G2 checkpoint abrogation” (Kawabe 2004, Figure 9). In response to DNA damage, p53

deficient cells are only able to arrest in G2 phase via activation of the p53-independent DNA damage pathway, whereas cells containing wild type p53 will also arrest at the G1/S border. Therefore, p53 deficient cancer cells will be targeted for death selectively, since the G2 arrest will only be overridden in these cells, whereas nontransformed cells containing wild type p53 will maintain the p53-dependent G1/S and G2/M arrests and, hence, side effects may be minimized. Although the concept of G2 checkpoint abrogation is widely accepted, the mechanisms and nature of this form of cell death – often termed "mitotic catastrophe" or "mitotic cell death" – are largely unknown (Okada and Mak 2004).

Clinical trials of UCN-01 as "stand-alone therapy" or combining UCN-01 with DNA damaging agents like the topoisomerase I inhibitors irinotecan or topotecan, cisplatin or with the antimetabolites cytarabine or 5-fluorouracil are currently under way (5-fluorouracil and UCN-01: Blagden and de Bono 2005, Kortmansky *et al.* 2005, cisplatin and UCN-01: Perez *et al.* 2006 and Lara *et al.* 2005, topotecan and UCN-01: Hotte *et al.* 2006, cytarabine and UCN-01: Sampath *et al.* 2006).

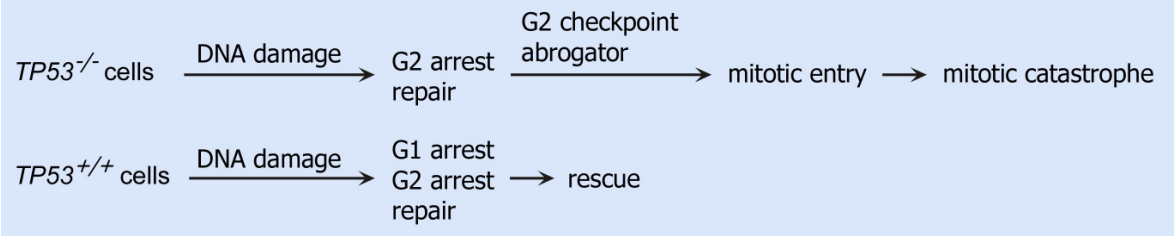

Figure 9: G2 checkpoint abrogation is a novel strategy to overcome chemotherapy resistance in p53 negative cancer cells. Upon DNA damage cancer cells lacking functional p53 rely solely on the p53-independent G2 DNA damage checkpoint pathway, which can be overcome by G2 abrogators. Thus, these cells enter mitosis in the presence of DNA damage and die by mitotic catastrophe, whereas cells with functional p53 are protected G1 and G2 phase arrest and repairs.

Aims of the study

Spindle checkpoint function, cancerogenesis and cancer cell responses to chemotherapy appear to be intimately linked. However, relatively little is known about the underlying molecular mechanisms. Therefore, I set out to elucidate the role of the spindle checkpoint in response to widely employed chemotherapeutics – spindle damaging and DNA damaging agents – and also in two novel chemotherapeutic strategies to combat chemotherapy resistance: G2 checkpoint abrogation and spindle checkpoint abrogation.

Mechanisms of cancerogenesis were analyzed. Mitotic slippage and its possible outcomes, cell cycle arrest in G1 phase, progression into S phase accompanied by endoreduplication or the desired outcome, apoptosis, were investigated focusing on the contribution of the spindle checkpoint and p53.

The role of the spindle checkpoint in chemotherapy resistance was elucidated. A possible requirement of the spindle checkpoint-mediated mitotic arrest for successful apoptosis induction upon treatment with fundamentally distinct spindle damaging agents was studied. Differential roles of the spindle checkpoint proteins Mad1 and Mad2 in this response were analyzed. Furthermore, in a novel approach the role of the spindle checkpoint in apoptosis induction upon DNA damage and a conceivable connection between spindle checkpoint impairment and resistance to DNA damaging chemotherapeutics were assessed.

New strategies to counteract chemotherapy resistance were investigated. Cell death by "mitotic catastrophe" due to G2 checkpoint abrogation in p53-deficient cells was characterized. I tested innovative chemotherapeutic strategies to improve G2 checkpoint abrogation, which enhance cell death by tipping the scales between opposing pro- and antiapoptotic pathways, while providing cancer cell selectivity of the treatment. In addition, pharmacological abrogation of the spindle checkpoint was evaluated as a novel chemotherapeutic approach, based on the fact that loss of spindle checkpoint function is lethal. Therefore, pharmacological inhibition of the spindle checkpoint should preferentially kill cancer cells with already impaired spindle checkpoint function, which are resistant to several conventional chemotherapies.

Materials and Methods

Materials

Chemicals, antibodies and probes

All chemicals were of highest purity and purchased from Roth (Karlsruhe, Germany), Sigma-Aldrich Chemie GmbH (Steinheim, Germany) and Merck (Darmstadt, Germany). Special categories of items are listed in form of tables: kits, chemical inhibitors, antibodies (primary and secondary) and probes for Northern blotting.

Table 1: Kits

purpose	**kit**	**company**
DNA isolation from agarose gel	NucleoSpin ExtractII	Machery & Nagel, Düren, Germany
DNA isolation from bacteria (small, medium, large scale)	Nucleobond Plasmid DNA Purification	Machery & Nagel, Düren, Germany
DNA isolation from bacteria (small scale)	Wizard Plus Minipreps DNA Purification System	Promega Corporation, Madison, WI, USA
DNA labeling	DECAprime II Random Primed DNA Labeling Kit	Ambion, Huntingdon, Cambridgeshire, UK
DNA probe purification	Qiaquick Nucleotide Removal Kit	Qiagen, Hilden, Germany
RNA isolation	GenElute Mammalian Total RNA Kit	Sigma-Aldrich, Steinheim, Germany

All kits were used following the manufacturer's instructions.

Table 2: Chemical inhibitors

chemical inhibitor	**stock solution**	**final concen-tration**	**target, effect**	**company**	**ordering number**
α-amanitin-oleate	50 mg/ml	50 µg/ml; 10 µM	RNA polymerase II	Calbiochem, Schwalbach Ts., Germany	454559

chemical inhibitor	**stock solution**	**final concen-tration**	**target, effect**	**company**	**ordering number**
adriamycin (= doxorubicin hydrochloride)	1 mM in H_2O at 4°C	300-750 nM	topoisomerase II (religation step)	Sigma-Aldrich, Steinheim, Germany	D1515
ALLN (calpain inhibitor I)	40 mM	200 µM	proteasome	Alexis, Grünberg, Germany	260-037
actinomycin D	1 mg/ml	10 µg/ml	RNA polymerases I, II, III	Alexis, Grünberg, Germany	380-009
caffeine	100 mM	1.2, 2 mM	ATM, partially ATR, not DNA-PK	Alexis, Grünberg, Germany	550-322
cycloheximide	10 mg/ml = 35 mM	50 µg/ml = 175 µM	inhibits translation and RNA polymerase I	Calbiochem, Schwalbach Ts., Germany	239763
etoposide (= VP-16)	10 mM	200 µM	topoisomerase II (religation step)	Calbiochem, Schwalbach Ts., Germany	341205
5-fluorouracil	50 mg/ml	50 µg/ml	pyrimidine synthesis => depletion of intracellular dTTP pool	Sigma-Aldrich, Steinheim, Germany	F6627
Gö6976	5 mM	2-20 µM	Unknown mitotic target, PKC, PDK1, S6K1, MSK1, Chk1, MAPKAP-K16, PHK	Calbiochem, Schwalbach Ts., Germany	365250
H89	50 mM	10 µM	PKA	Sigma-Aldrich, Steinheim, Germany	B1427
hygromycin B	400 mg/ml	1 mg/ml	translation (translocation of 70S ribosome)	Calbiochem, Schwalbach Ts., Germany	400051
LY294002	20 mM	50 µM	PI_3K	Calbiochem, Schwalbach Ts., Germany	M8515
monastrol	70 mM	70 µM	Eg5 kinesin => centrosome migration, formation of a bipolar spindle	Sigma-Aldrich, Steinheim, Germany	M8515
nocodazole	2 mM	150 nM	microtubule stability, microtubule dynamics, kinetochore attachment	Sigma-Aldrich, Steinheim, Germany	M1404
olomoucine	20 mM	50 µM	Cdk1, Cdk2, Cdk5	Alexis, Grünberg, Germany	I-800-900-0065

chemical inhibitor	**stock solution**	**final concen-tration**	**target, effect**	**company**	**ordering number**
PD98059	18.7 mM	50 µM	MEK	Calbiochem, Schwalbach Ts., Germany	538000
puromycin	20 mg/ml in H_2O	1-5 µg/ml; 40 µg/ml	translation (premature release of nascent polypeptide chain)	Sigma, Steinheim, Germany	P8833
purvalanol A	10 mM	10 µM	Cdk1	Alexis, Grünberg, Germany	270-246
Ro-318220	1 mM	1 µM	PKC	Calbiochem, Schwalbach Ts., Germany	557520
Ro-320432	1 mM	200 nM	PKC	Calbiochem, Schwalbach Ts., Germany	557525
roscovitine	20 mM	20-50 µM	Cdk1, Cdk2, Cdk5, not Cdk4, Cdk6	Calbiochem, Schwalbach Ts., Germany	557360
rottlerin	20 mM	20 µM	PKC, CaM kinase	Calbiochem, Schwalbach Ts., Germany	557370
SB202190	3 mM	15 µM	p38 (MAPK)	Calbiochem, Schwalbach Ts., Germany	559397
SB203580	10 mM	20 µM	p38 (MAPK)	Alexis, Grünberg, Germany	270-179
SP600125	100 mM	50, 500 nM	JNK, p38, ERK, Mps1	Tocris Cockson Ltd, Bristol, UK	1496
staurosporine	10 µM	20 nM	broad spectrum kinase inhibitor	Calbiochem, Schwalbach Ts., Germany	569397
taxol	1 mM	100 nM	binds N-terminal region of β-tubulin, inhibits microtubule instability, inhibits tension across kinetochores	Sigma-Aldrich, Steinheim, Germany	T7402
UCN-01	1 mM	100 nM	Chk1, PKC, cTAK1, Cdk1, PAK4, PDK1, Lck, MAPKAP-K2	NCI (National Cancer Institute, Bethesda, MD, USA)	-
wortmannin	1 mM	1 µM	ATM and DNA-PK, PI_3K, not ATR	Calbiochem, Schwalbach Ts., Germany	681675
Y27632	5 mM	10, 100 µM	ROCK I, ROCK II	Calbiochem, Schwalbach Ts., Germany	688001

All stock solutions were prepared in DMSO and stored at -20°C, if not stated otherwise.

Table 3: Primary antibodies

name of the antibody, clone number	**species**	**company**	**appli-cation**	**concen-tration of antibody**	**dilution**	**ordering number**
β-actin AC-15	mouse ascites	Sigma-Aldrich, Steinheim, Germany	WB	-	1:10000	A5441
bak (Ab-1)	mouse monoclonal (TC-100)	Calbiochem, Schwalbach Ts., Germany	FACS	0.1 µg/µl	2-3 µl / 10 µl	AM03
bax (Ab-6)	mouse monoclonal (6A7)	Calbiochem, Schwalbach Ts., Germany	IP	0.1 µg/µl	5 µl / 500 µg protein	AM44
bax	rabbit polyclonal	BD Pharmingen, Erebodegem, Belgium	WB	serum	1:1000	554104 (13666E)
bcl-2	rabbit polyclonal	BD Pharmingen, Erebodegem, Belgium	WB	1 µg/µl	1:1000	554160
BrDU ZBU30	mouse monoclonal	Zymed, San Francisco, CA, USA	FACS	1 µg/µl	1:200 - 1:400	03-3900
Bub1 (SB1.3)	sheep polyclonal	Dr Stephen Taylor, Manchester (Johnson *et al.* 2004)	IF	-	1:400	-
BubR1 (SBR1.3)	sheep polyclonal	Dr Stephen Taylor, Manchester (Johnson *et al.* 2004)	IF	-	1:400	-
Cdc2 = Cdk1 (PSTAIRE)	rabbit polyclonal	Santa Cruz, Santa Cruz, CA, USA	WB	0.1 µg/µl	1:1000	sc-53
Cdk2 (M2) agarose conjugate	rabbit polyclonal	Santa Cruz, Santa Cruz, CA, USA	IP	500 µg/ 250 µl agarose	5 µl (per 200 µg protein)	sc-163 AC
Cdk2 (M2)	rabbit polyclonal	Santa Cruz, Santa Cruz, CA, USA	WB, IP	0.1 µg/µl	1:1000	sc-163
CREST (ANA-centromere)	human autoantibody	Europa Bioproducts, Wicken, Ely, Cambridge, UK	IF	-	1:500	CS1058
Cyclin B (GNS-1)	mouse monoclonal	Santa Cruz, Santa Cruz, CA, USA	WB, IP	0.1 µg/µl	1:1000, 5 µl (per 200 µg protein)	sc-245

name of the antibody, clone number	**species**	**company**	**appli-cation**	**concen-tration of antibody**	**dilution**	**ordering number**
cytochrome C	mouse monoclonal	BD Pharmingen, Erebodegem, Belgium	WB	1 µg/µl	1:1000	556433 (65981A)
phospho-H2A.X (Ser319)	mouse monoclonal clone: JBW301	Upstate, Lake Placid, NY, USA	IF, WB	0.7 µg/µl	1:350, 1:1000	05-636
Mad1	mouse monoclonal	Tim J. Yen, Philadelphia, PA, USA (Campbell *et al.* 2001)	WB	-	1:1000	-
Mad2	rabbit polyclonal	Berkeley Antibody Company, Richmond, CA, USA	WB, IF	crude antiserum	1:1000	PRB-452C
MPM2 (mitotic protein monoclonal 2)	mouse monoclonal	Upstate, Lake Placid, NY, USA	FACS	1 µg/µl	1:1600	05-368
Mps1 (TTK (C-19))	rabbit polyclonal	Santa Cruz, Santa Cruz, CA, USA	WB	0.2 µg/µl	1:1000	sc-540
p21 (WAF1 (Ab-1))	mouse monoclonal clone EA10	Oncogene, San Diego, CA, USA	WB	0.1 µg/µl	1:1000	OP64
p53(DO-1) (Ab-6)	mouse monoclonal	Oncogene, San Diego, CA, USA	WB	0.1 µg/µl	1:1000	OP43
p53(DO-1) (Ab-2, PAb1801)	mouse monoclonal	Santa Cruz, Santa Cruz, CA, USA	WB	0.1 µg/µl	1:1000	sc-126
p53(DO-1) agarose conjugate	mouse monoclonal	Santa Cruz, Santa Cruz, CA, USA	IP	500 µg/ 250 µl agarose	1:1000	sc-126 AC
p53(pSer15) 16G8	mouse monoclonal	Cell Signaling, Frankfurt a. M., Germany	WB	-	1:500	9286
PARP	mouse monoclonal	BD Pharmingen, Erebodegem, Belgium	WB	0.5 µg/µl	1:1000	551024
survivin	rabbit polyclonal	Research & Development Systems, San Diego, CA, USA	WB	1 µg/µl	1:2000	AF886
α-tubulin	mouse monoclonal	Sigma-Aldrich, Steinheim, Germany	IF	2 µg/µl	1:800	T6074

name of the antibody, clone number	**species**	**company**	**appli-cation**	**concen-tration of antibody**	**dilution**	**ordering number**
γ-tubulin	rabbit IgG fraction of antiserum	Sigma-Aldrich, Steinheim, Germany	IF	-	1:600	T 3559

Table 4: Secondary antibodies

name of the antibody	**conjugated to**	**species**	**company**	**appli-cation**	**concen-tration of antibody**	**dilution**	**ordering number**
anti-human	rhodamine RedX	donkey polyclonal	Dianova, Eugene, OR, USA	IF	1.4 µg/µl	1:600	709-295-128
anti-mouse	AlexaFluor488	goat polyclonal	Molecular Probes, Leiden, the Netherlands	IF, FACS	2 µg/µl	1:800 - 1:1000	A11029
anti-mouse	HRP	goat polyclonal	Jackson Immuno Research, West Grove, PA, USA	WB	0.4 µg/µl	1:4000 - 1:5000	115-035-146
anti-mouse	DTAF	goat polyclonal	Jackson Immuno Research, West Grove, PA, USA	FACS	0.75 µg/µl	1:400	115-016-062
anti-rabbit	AlexaFluor488	goat polyclonal	Molecular Probes, Leiden, the Netherlands	IF	2 µg/µl	1:800 - 1:1000	A-11034
anti-rabbit	HRP	goat polyclonal	Jackson Immuno Research, West Grove, PA, USA	WB	0.4 µg/µl	1:4000 - 1:5000	111-035-045
anti-sheep	AlexaFluor488	donkey polyclonal	Molecular Probes, Leiden, the Netherlands	IF	2 µg/µl	1:1000	A-11015

Table 5: Probes for Northern Blotting

target mRNA	**production of DNA for probe generation**			**size of probe (in bp)**	**amount of DNA used for labeling**
	vector, restriction enzymes or PCR template	**PCR: primer names**	**PCR: primer sequences**		
BAX	human brain cDNA library	#170 bax-3‘, #171 bax-5‘	CCAGATGGTGAGCGAGGC, GGACGGGTCCGGGGAGC	574	100ng
*GAPDH**	-	-	-	316	25ng
GAPDH	human brain cDNA library	#147 GAPDH-RT-5‘, #148 GAPDH-RT-3‘	GGGGAAGGTGAAGCTC, CCTTGGCCAGGGGTGC	485	25ng
MAD2	#351 pEFT7MCS-Mad2, *Eco*RI/*Xba*I	-	-	ca. 620	100ng
CDKN1A/ WAF1	#49 pBluescript-p21(T7), *Eco*RI	-	-	1010	100ng
CDKN1A/ WAF1	human brain cDNA library	#151 p21-RT-2-3‘, #152 p21-RT-2-5‘	GGATGTCCGTCAGAACCCA, CAGGTCCACATGGTCTTCC	323	100ng

*: DNA from DECAprime kit (10ng/µl).

Table 6: Probes for promoter fragments isolated by chromatin immunoprecipitation

target promoter	**primer names**	**primer sequences**	**size of probe (in bp)**
CDKN1A/ WAF1	#119 p21 reverse, #127 p21 Promotor II	GGGAGGAAGGGGATGGTA, CTGAAGAAGGCAAGGGAGCA	180
CDC25C	#26 CDC25C-promotor 5´ #27 CDC25C-promotor 3´	GGCGCGGTTTAAATCTCCCGGGGTTCG, CCCTGAGCAGAAGGCCAAAGTTACGGC	397

Lab ware

Lab ware like plastic reaction tubes was bought from Sarstedt (Nümbrecht, Germany), glass ware from Schott (Mainz, Germany), cell culture-related plastic ware from Greiner

(Frickenhausen, Germany) and Nunc (Wiesbaden, Germany) and filtering devices from Millipore (Schwalbach, Germany), if not stated otherwise. Specifications about other items can be found under the corresponding methods.

Equipment

Information about the manufacturers and handling parameters of the machines used can be found under the corresponding methods.

Table 7: Equipment

equipment	**name**	**company**
blotting machine, for Northern blot	PosiBlot 30-30 pressure blotter	Stratagene, Amsterdam Zuidoost, the Netherlands
blotting machine, for Western blot	semi-dry electroblotter	BioRad, Hercules, CA, USA
camera, for DNA or RNA gel photos	CCD camera	part of the GelDoc EQ System BioRad, Hercules, CA, USA
camera, for immunofluorescence photos	digital CCD camera	Hamamatsu, Hamamatsu City, Japan
cell culture hood	Heraeus LaminAir HA 2448	Heraeus, Osterode, Germany
centrifuge, mid-sized	Beckmann GP Centrifuge	Beckmann, Munich, Germany
centrifuge, mid-sized, cooled	Multifuge 3 L-R	Heraeus, Osterode, Germany
centrifuge, table-top	Biofuge pico	Heraeus, Osterode, Germany
centrifuge, table-top, cooled	Biofuge fresco	Heraeus, Osterode, Germany
centrifuge, ultra-centrifuge, cooled	Beckmann J2-21M/E Centrifuge	Beckmann, Munich, Germany
Electroporator, for human cells	Gene Pulser	BioRad, Hercules, CA, USA
FACS/fluorocytometer	BD FACSCalibur	Becton Dickinson, San Jose, CA, USA
fluorometer, for caspase assays	Victor^2 1420 Multilabel Counter	Wallac Oy, Turku, Finland and Perkin Elmer, Freiburg, Germany
gel dryer	Model 583 Gel Dryer BioRad	BioRad, Hercules, CA, USA
hybridization oven	-	Bachofer, Reutlingen, Germany
incubator, bacteria	Heraeus B6120	Heraeus, Hanau, Germany
incubator, cell culture	Cytoperm 8080 or BBD 6620	Heraeus, Hanau, Germany
microscope, fluorescence (for fixed cells)	Leitz Axiovert 40 CFC	Leica Geosystems GmbH, Munich, Germany

equipment	**name**	**company**
microscope, fluorescence (for living cells)	Zeiss Axiovert 40 CFL	Carl Zeiss AG, Oberkochen, Germany
microscope, light (for living cells)	Leitz Labovert FS	Leica Geosystems GmbH, Munich, Germany
PCR machine	PTC-200	MJ Research (via BioRad, Hercules, CA, USA)
phosphoimager	Fujifilm FLA-3000	Fujifilm, Düsseldorf, Germany
photometer, for DNA or RNA concentration measurements	Ultrospec 3000 UV/Visible Spectrophotometer	Pharmacia Biotech, Uppsala, Sweden
photometer, for protein concentration measurements, ELISA plate reader	SpectraMax 340	MWG-Biotech, Ebersberg, Germany
pipette	Pipetman P2, P20, P200, P1000	Gilson International B.V. Deutschland, Limburg-Offheim, Germany
pipetting aid, cell culture	Pipetboy plus	Integra Biosciences, Fernwald, Germany
pipetting aid, lab	Pipetboy acu	Integra Biosciences, Fernwald, Germany
power supply	BioRad PowerPac 300 or Model 100/200	BioRad, Hercules, CA, USA
shaker, bacteria	HT Multitron	Infors, Einsbach, Germany
sonifier, for cell lysis	Branson Sonic Power sonifier model S125	Branson, Danbury, CT, USA
UV crosslinker, for Northern blots	UV Stratalinker 2400	Stratagene, Amsterdam Zuidoost, the Netherlands
UV illumination desk	BioRad Mini-Transilluminator	part of the GelDoc EQ System BioRad, Hercules, CA, USA
X-ray film developing machine	KODAK X-OMAT 2000 Processor machine	Kodak, New Haven, CT, USA

Plasmids

Table 8: Plasmids

plasmid name	plasmid number	generated by or obtained from	reference
pBabepuro	-	Martin Eilers, IMT	Morgenstern and Land 1990
pBluescript-p21(T7)	#49	Ed Harlow, Boston, MD, USA	-
pcDNA3.1	-	Invitrogen, Karlsruhe, Germany	-
pcDNA3-bcl2	#476	Martin Eilers, IMT	-
pcDNA3-HA-p53DD	#339	Holger Bastians, IMT	-
pcDNA-GFP-Mad1	#389	Holger Bastians, IMT	-
pcDNA-survivin	#478	Simone Fulda, Ulm, Germany	-
pCMV-bcl2-SV40-H2BGFP	#477	Martin Eilers, IMT	-
pEFT7MCS-Mad2	#351	Tim Hunt, South Mimms, UK	Geley *et al*. 2001

Table 9: pSUPER shRNA constructs

plasmid name	plasmid number	shRNA sequence	position (nt.)	generated by or obtained from	reference for target sequence
pSUPER	#419	-	-	Thijn Brummelkamp, Amsterdam, the Netherlands	Brummelkamp *et al*. 2002
pSUPER-Bub1-628	#474	GAGTGATCACG ATTTCTAA	628 ff	this work	Meraldi and Sorger 2005
pSUPER-BubR1-2925	#471	AGATCCTGGCT AACTGTTC	2925 ff	this work	Lens *et al*. 2003
pSUPER-Mad1 si1(391)	#426	CAGGCAGTGTC AGCAGAAC	391 ff	Holger Bastians, IMT	Luo *et al*. 2002
pSUPER-Mad1 si2(992)	#427	GACCTTTCCAG ATTCGTGG	992 ff	Holger Bastians, IMT	-
pSUPER-Mad2	#460	GGAAGAGTCGG GACCACAG	501 ff	Rene Medema, Amsterdam, the Netherlands	van Vugt *et al*. 2004
pSUPER-Mps1-1362	#464	GCAGCAATACC TTGGATGA	1362 ff	Holger Bastians, IMT	Yuan *et al*. 2004
pSUPER-survivin	#472	GAGGCTGGCTT CATCCACT	167 ff	this work	Lens *et al*. 2003

Bacteria

The *Escherichia coli* strain DH5α (Hanahan 1985) was used for transformation and plasmid DNA generation.

Cell lines

Table 10: Human cancer cell lines

name	**tissue**	***TP53* status**	**SCP status**	**special features**	**culture medium**	**source (line obtained from)**
A2780	breast cancer	wt	SCP impaired (our findings)	p21 normal	RPMI, DMEM	Matthias Dobbelstein, Göttingen, Germany
A549	lung cancer	wt	SCP normal	p21, bax, bcl-2, caspases 2, 3, 9 okay	RPMI	ATCC
C33A	cervix carcinoma	mutated, stabilized	SCP impaired	Rb deficient	DMEM	Matthias Dobbelstein, Göttingen, Germany
CaCo-2	colon carcinoma	truncated	SCP normal	CIN	DMEM	ATCC
H1299	lung cancer (NSCLC)	homozygous partial deletion, no expression	SCP impaired		RPMI	Matthias Dobbelstein, Göttingen, Germany
HCT116 wild type	colon carcinoma	wt	SCP normal	MIN, ras mutated, no ARF, no CHFR expression	RPMI	Bert Vogelstein, Baltimore, MD, USA

name	**tissue**	***TP53* status**	**SCP status**	**special features**	**culture medium**	**source (line obtained from)**
HCT116 *CHK2*$^{-/-}$	colon carcinoma	wt	SCP normal	MIN, ras mutated, no ARF, no CHFR expression	RPMI	Bert Vogelstein, Baltimore, MD, USA (Jallepalli *et al*. 2003)
HCT116 *MAD1*^{kd}	colon carcinoma	wt	SCP impaired	MIN, ras mutated, no ARF, no CHFR expression	RPMI	this work
HCT116 *MAD2*$^{+/-}$	colon carcinoma	wt	SCP impaired	MIN, ras mutated, no ARF, no CHFR expression	RPMI	Robert Benezra, New York, USA (Michel *et al*. 2001)
HCT116 *TP53*$^{-/-}$	colon carcinoma	null	SCP normal	MIN, ras mutated, no ARF, no CHFR expression	RPMI	Bert Vogelstein, Baltimore, MD, USA (Bunz *et al*. 1998)
HeLa	cervix carcinoma	wt, low expression due to E6-mediated degradation	SCP normal	Rb expression normal	DMEM	ATCC
HT29	colon carcinoma	mutated	SCP normal	CIN	DMEM	ATCC
Ovca 420	ovarian cancer	wt	SCP impaired	reduced Mad1 and Mad2 protein levels (70-80% less)	RPMI	Xianghong Wang, Hong Kong, China (Wang *et al.* 2002)
Ovca 429	ovarian cancer	wt	SCP normal	Mad1 and Mad2 levels normal	RPMI	Xianghong Wang, Hong Kong, China (Wang *et al.* 2002)
Ovca 432	ovarian cancer	mutated	SCP impaired	reduced Mad2 protein levels (70-80% less), Mad1 normal	RPMI	Xianghong Wang, Hong Kong, China (Wang *et al.* 2002)
Ovca 433	ovarian cancer	wt	SCP impaired	reduced Mad2 protein levels (70-80% less), Mad1 normal	RPMI	Xianghong Wang, Hong Kong, China (Wang *et al.* 2002)

name	**tissue**	***TP53* status**	**SCP status**	**special features**	**culture medium**	**source (line obtained from)**
SaOS-2	osteo-sarcoma	null	SCP impaired	Rb truncated, E2F-1, Mdm2 interaction defective	DMEM	ATCC
T47D	breast cancer	mutated	SCP impaired	50% of normal Mad2 level	RPMI	ATCC
U2OS	osteo-sarcoma	wt	SCP impaired (our findings), normal (literature)	Rb positive	DMEM	Matthias Dobbelstein, Göttingen, Germany

SCP status: spindle checkpoint status. Normal: fully functional. Impaired: reduced function.

CIN: chromosome instability, MIN: microsatellite instability.

CIN is a process of chromosome gains or losses, which generates aneuploidy. Microsatellites are short repetitive nucleotide stretches in the DNA. Their length differs interindividually, but is constant intraindividually. MIN is the appearance of uncommonly short or long microsatellites in an individual, which is caused by DNA repair defects.

Table 11: Human primary or non-transformed cell lines

name	**tissue**	***TP53* status**	**SCP status**	**culture medium**	**source (line obtained from)**
BJ-tert	fibroblasts	wt	normal	DMEM (15% FCS)	Reuven Agami, Amsterdam, Netherlands
HUVEC	human umbilical vein endothelial cells	wt	normal	EBM	Jürgen Adamkiewicz, IMT

Data bases, software

Nucleotide and protein sequences were retrieved from the sequence data base of the National Institutes of Health (http://www.ncbi.nlm.nih.gov). Microsoft Office programs

Word, Excel and PowerPoint were used (Microsoft, Unterschleißheim, Germany). Agfa FotoLook 3.0 (Agfa-Gevaert, Mortsel, Belgium), Adobe Photoshop 5.0 (Adobe, Munich, Germany) and Canvas 10.0 (ACD Systems, Saanichton, BC, Canada) were employed for photography and graphics applications. Equipment software is described under the corresponding methods.

Methods

Molecular Biology

Generation of transformation competent bacteria

Transformation ultracompetent *Escherichia coli* DH5α were generated according to Inoue *et al*. 1990.

Transformation of bacteria

50-100 µl ultracompetent *Escherichia coli* DH5α were transformed by heat shock for 2 min at 42°C with 0.5-1 µg plasmid DNA or 5 µl of a ligation reaction. The bacteria transformed with a ligation reaction were plated out or a liquid culture was inoculated for plasmid DNA isolation upon retransformation. Selection medium or plates contained a concentration of 100 µg/ml ampicillin or 30 µg/ml kanamycin.

Plasmid DNA preparation from bacteria

Small scale DNA preparations were done from 5 ml liquid *Escherichia coli* DH5α culture in LB medium (1% w/v peptone, 0.5% yeast extract, 1% NaCl, pH 7.5) using the Nucleobond Plasmid DNA Purification kit (Macherey & Nagel, Düren, Germany). Bacterial pellets were resuspended in 150 µl buffer S1, mixed with 150 µl buffer S2 and then with 150 µl buffer S3. The supernatant produced by centrifugation was transferred to a new tube, mixed by vortexing with 500 µl phenol/chloroform/isoamylalcohol (24:24:1) and spun down. The upper phase was transferred to a new tube and precipitated with 2.5

volumes of isopropanol. Then the pellet was washed with 0.5 volume of 70% ethanol, air dried and resuspended in 20 µl H_2O.

For Northern probe generation or sequencing the Wizard Plus Minipreps DNA Purification System kit (Promega, Madison, WI, USA) was used according to the manufacturer's instructions. DNA content and purity of 1 µl DNA in 99 µl H_2O was determined photometrically at 260 and 280 nm.

Medium and large scale DNA preparations for cloning or transfection were carried out with the Nucleobond Plasmid DNA Purification kit (Macherey & Nagel, Düren, Germany) according to the manufacturer's instructions. 100 ml bacterial culture normally yielded 200 µg DNA for high copy plasmids or 100 µg for low copy plasmids.

Restriction digest

Typically 10 µg DNA were digested with 5-10 units of restriction endonucleases (Gibco, Karlsruhe, Germany) at 37°C for 2-16 h in a Heraeus B6120 incubator (Heraeus, Hanau, Germany).

PCR

DNA fragments were amplified in a polymerase chain reaction in the PTC-200 PCR machine (MJ Research, purchased via BioRad, Hercules, CA, USA). A mix of template DNA (50 ng plasmid or 1-3 µl cDNA library), 300 nM primer x (MWG, Ebersberg, Germany), 300 nM primer y (MWG, Ebersberg, Germany), 200 nM of each dNTP (Gibco, Karlsruhe, Germany), 1.5 mM $MgCl_2$ (Gibco, Karlsruhe, Germany), 1x Taq polymerase buffer (Roche, Penzberg, Germany) and 5 units of Taq polymerase (Roche, Penzberg, Germany) was incubated with a standard program (10 min 95°C, 30 cycles of: denaturation: 1 min 95°C, annealing: 1 min 55-62°C, elongation: 1 min 72°C; final elongation step: 10 min 72°C; 4°C for ever).

PCR purification

PCR reactions were purified with a Qiaquick Nucleotide Removal Kit (Qiagen, Hilden, Germany) following the manufacturer's instructions.

Cloning

30 µg of the pSUPER plasmid were subjected to two rounds of restriction digests for 16 h with 25 units of both *Bgl*II and *Hin*dIII. After the first digest the sample was purified with NucleoSpin ExtractII kit columns (Macherey & Nagel, Düren, Germany). Subsequently to the second digest the plasmid was extracted from a 1% agarose gel with the NucleoSpin ExtractII kit (Macherey & Nagel, Düren, Germany) according to the manufacturer's instructions. The DNA content and purity was determined.

The insert was generated by annealing a pair of 64mer oligonucleotides (MWG, Ebersberg, Germany) in a PTC-200 PCR machine (MJ Research, via BioRad, Hercules, CA, USA). A mix of 20 µM forward oligonucleotide, 20 µM reverse oligonucleotide and 1x T4 DNA ligase buffer (Roche, Penzberg, Germany) in 50 µl was incubated (program: 4 min 95°C, 10 min 70°C, 5 min 60°C, 5 min 50°C, 5 min 40°C, 5 min 30°C, 5 min 20°C, 5 min 10°C, 4°C for ever). The annealed oligonucleotides were diluted with H_2O at different ratios (1:600-1:2000). 1 µl of the diluted oligonucleotide was mixed with 90 ng *Bgl*II/*Hin*dIII digested pSUPER vector in a 10 µl reaction containing 1x T4 DNA ligase buffer and 5 units of T4 DNA ligase (Roche, Penzberg, Germany). The ligation was performed at RT for 2-4 h or over night at 16°C in a water bath. Competent bacteria were transformed with 5 µl of the ligation reaction as described. Positive clones were identified by analytical restriction digest with *Eco*RI and *Hin*dIII.

Agarose gel electrophoresis

DNA fragments were applied in loading buffer (50% (v/v) glycerol, 6.25 mM EDTA, 0.25% (w/v) bromophenol blue) and separated on 1-1.5% agarose gels in 1x TAE buffer (40 mM Tris-acetate pH 8.0, 1 mM EDTA pH 8.0) at 100V.

Gel extraction

DNA fragments were isolated from agarose gels with the NucleoSpin ExtractII kit (Macherey & Nagel, Düren, Germany) according to the manufacturer's instructions.

DNA Sequencing

0.6 µg plasmid DNA were sequenced with 2.86 µM primer by Seqlab (Göttingen, Germany).

Chromatin immunoprecipitation for PCR of promoter fragments

Cells were harvested from 10 cm dishes in parallel without crosslinking directly in RIPA buffer (50 mM Tris/HCl pH 8.0, 150 mM NaCl, 5 mM EDTA pH 8.0, 1% NP-40, 0,5% sodium desoxycholate, 0,1% SDS, 50 mM NaF, 0,2 mM Na_3VO_4, 5 µM trichostatin A, plus freshly added Complete EDTA-free Protease Inhibitor Cocktail Tablets diluted 1:25 (from Roche, Penzberg, Germany, stock: one tablet per 2 ml)) or with crosslinking as follows: Treated cells on a 10 cm dish were overlaid with 5 ml 0.37% formaldehyde in PBS for 5 min, washed once with PBS, overlaid with 5 ml PBS and 1 ml 2.5 M glycine (in H_2O) for 5 min and washed twice with PBS. All following steps were performed on ice. The cells were scraped off in 1 ml RIPA buffer and sonicated four to five times for 15-20 sec at setting 2 on a Branson sonifier. A fragment size between 200 and 1000 bp was verified on an 1% agarose gel by checking 10 µl of the sample. Debris were pelleted at 13000 rpm for 10 min and the protein concentration determined by a Lowry assay kit according to the manufacturer's instructions. For immunoprecipitation 2 mg lysate in 1 ml RIPA buffer were precleared with 10 µl equilibrated protein G agarose beads for 2 h at 4°C on a rotator. The precleared lysate was incubated with 10 µl anti-p53 antibody-agarose conjugate (p53(DO-1) 0.2 µg/µl Santa Cruz, Santa Cruz, CA, USA) over night at 4°C on a rotator and as control mouse IgG is used. The beads were washed three times in RIPA buffer, four times in IP wash buffer (100 mM Tris/HCl pH 8.5, 500 mM LiCl, 1% NP-40, 1% Na-desoxycholate) and twice in RIPA buffer by rotating for 5 min at 4°C for each step. To isolate DNA for the PCR reaction, the beads were incubated at 95°C for 30 min in 300 µl crosslinking reversal buffer (125 mM Tris/HCl pH 6.8, 10% mercaptoethanol, 4% SDS) and mixed with 300 µl phenol-chloroform by vortexing. The phases were separated by spinning for 5 min at 13000 rpm and the upper phase was precipitated in a new tube with 900 µl 100% ethanol for 2 h at -80°C. Samples were spun for 1 h at 13000 rpm at 4°C, washed once with 70% ethanol and resuspended in 20 µl H_2O. The PCR reaction was performed in the PTC-200 PCR machine (MJ Research, purchased via BioRad, Hercules, CA, USA). A mix of 2 µl DNA as template, 300 nM primer x (MWG, Ebersberg,

Germany), 300 nM primer y (MWG, Ebersberg, Germany), 200 nM of each dNTP (Gibco, Karlsruhe, Germany), 1.5 mM $MgCl_2$ (Gibco, Karlsruhe, Germany), 1x Taq polymerase buffer (Gibco, Karlsruhe, Germany) and 5 units of Taq polymerase (Gibco, Karlsruhe, Germany) was incubated with the ChIP program (3 min 95°C, 36 cycles of: denaturation: 30 sec 95°C, annealing: 45 sec 58°C, elongation: 45 sec 72°C; 4°C for ever). For analysis 15 µl sample in 5 µl DNA loading buffer were run on an 1.5% agarose gel.

Northern blotting

RNA isolation

RNA isolation from cultured mammalian cancer cells was carried out with the GenElute Mammalian total RNA kit (Sigma-Aldrich, Steinheim, Germany) according to the manufacturer's instructions. Shredder columns were used to homogenize the cells in lysis buffer prior to application onto the RNA isolation columns. After binding, washing and eluting RNA in DEPC-H_2O (a 0.1% (v/v) solution of DEPC (Sigma-Aldrich, Steinheim, Germany) in H_2O was stirred well and autoclaved), the RNA was precipitated with 2.5 volumes of 100% ethanol and 0.1 volume of 3 M Na-acetate (pH 5.1) at -80°C for at least 30 min. The pellet produced by centrifugation was washed with 70% ethanol (ethanol diluted with DEPC-H_2O), air dried and resuspended in DEPC-H_2O. RNA content and purity was determined photometrically as described above for DNA. RNA integrity was checked by analytical denaturing agarose gel electrophoresis (see below), which makes the ribosomal bands of the isolated RNA visible. Typical yields were 100-150 µg total RNA from a 10 cm dish or 150-300 µg from a 14 cm dish of cultured HCT116 cells.

RNA agarose gel electrophoresis and blotting

Samples were prepared for the gel run by aliquoting 30 µg of RNA, air-drying it and resuspending it in 4.5 µl DEPC-H_2O plus sample buffer (2 µl 5x MOPS buffer (25 mM Na-acetate, 100 mM MOPS, 50 mM EDTA), 3.5 µl 37% filtered formaldehyde, 10 µl deionized formamide (procedure: 1 g mixed bed ion exchange resin (BioRad 501-X8 or AG 501-X8) and 20 ml formamide were stirred well at RT over night. The deionized formamide was filtered through a Whatman no.1 paper filter (Whatman GmbH, Dassel,

Germany)) and denaturation for 10-15 min at 60-65°C. After cooling on ice the RNA was mixed with 2 µl ethidium bromide solution (100 µg/ml) and 3 µl loading buffer (50% (v/v) glycerol, 6.25 mM EDTA, 0.25% (w/v) bromophenol blue) and applied to the gel.
A medium-sized denaturing 1% agarose gel was poured by adding 6% of a filtered formaldehyde solution and 1x MOPS-buffer to a partially cooled agarose solution. The gel was run until the blue dye had migrated about 3-4 cm, i.e. for 4-6 h at 50V.
RNA samples were transferred on the nylon membrane (Hybond N, Amersham Pharmacia Biotech, Little Chalfont, Buckinghamshire, UK) using a PosiBlot 30-30 pressure blotter (Stratagene, Amsterdam Zuidoost, the Netherlands). One sheet of Whatman paper, the membrane, the mask, the gel, one sheet of Whatman paper and a sponge were stacked onto each other. Paper, membrane and sponge were pre-wetted with blotting buffer (20x SSC: 3 M NaCl, 300 mM Na_3-citrate). Transfer was carried out for 1.5-2 h at 80 mm Hg. The transferred RNA was crosslinked to the membrane by UV light in a UV Stratalinker 2400 (Stratagene, Amsterdam Zuidoost, the Netherlands) at 254 nm and 1200 J/m^2.

Radioactive labeling of DNA

Radioactive probes were generated from 25-100 ng DNA of either PCR products or DNA fragments from digested plasmids. The DNA fragments were labeled with α-P^{32}dATP (Amersham, Braunschweig, Germany) with the DECAprime II kit (Ambion, Huntingdon, Cambridgeshire, United Kingdom). Then they were purified with the Qiaquick Nucleotide Removal Kit (Qiagen GmbH, Hilden, Germany), both according to the manufacturer's instructions. The probe's activity was determined by measuring 1 µl out of 100 µl probe in the scintillation counter LS1701 (Beckmann, Munich, Germany). Probes were used freshly or stored at -20°C and re-used several times, if necessary.

Hybridization of RNA

The membrane with crosslinked RNA was pre-hybridized in a rotating glass tube for 2-4 h at 50-65°C with hybridization buffer (500 mM Na-phosphate buffer pH 7.2, 7% SDS (w/v), 1 mM EDTA pH 8.0) supplemented with 50 µg/ml salmon sperm DNA denatured for 5 min at 95°C. The hybridization probe was denatured for 2 min at 95°C, added to the hybridization buffer to a final activity of 1-4x10^6 cpm/ml and hybridized for 16 h at 50-

65°C. The blot was washed at the hybridization temperature with pre-warmed wash buffer (40 mM Na-phosphate buffer pH 7.2, 0.1% SDS (w/v)). An imaging screen (Fujifilm BAS-MP2040, Fujifilm, Düsseldorf, Germany) was exposed to the blot. The signal was quantitated with a Fujifilm FLA-3000 reader using the ImageGauge V3.1 software (both from Fujifilm, Düsseldorf, Germany).

Protein biochemistry

Protein lysate preparation for Western blotting

Lysis conditions are described for generation of whole cell lysates to be used directly for Western blotting. FACS samples were taken after the washing step and the remaining cells lysed. For very stringent cell lysis, treated mammalian cells were harvested with trypsin/EDTA or PBS/EDTA (PBS: 6.5 mM Na_2HPO_4, 1.5 mM KH_2PO_4, 2.5 mM KCl, 140 mM NaCl, pH 7.25, autoclaved; plus 0.5 mM EDTA pH 8.0) and washed once with PBS. They were lysed for 10 min on ice in Boehringer lysis buffer (1% (v/v) Nonidet-P-40, 0.1% (w/v) SDS, 50 mM Tris/HCl pH 7.4, 150 mM NaCl, 5 mM EDTA, 5 mM EGTA, 0.1% (w/v) sodium desoxycholate, plus freshly added Complete EDTA-free Protease Inhibitor Cocktail Tablets diluted 1:25 (from Roche, Penzberg, Germany, stock: one tablet per 2 ml)). The lysate was spun at 13000 rpm for 15 min in a cooled table top centrifuge to remove debris and the supernatant was transferred to a new 1.5 ml tube. Its protein concentration was determined photometrically at 405 nm with a Spectramax 340 Microplate Reader (Molecular Devices Co., Sunnyvale, Ca, USA; with Softmax Pro 1.1 software) using a Lowry assay kit (BioRad, Hercules, CA, USA) according to the manufacturer's instructions. For preservation of phosphorylations on the isolated proteins a less stringent method was used. Treated mammalian cells were harvested with PBS/EDTA, washed once with PBS and lysed for 15 min on ice in modified Matsumoto lysis buffer (1% (v/v) Nonidet-P-40, 50 mM HEPES pH 7.4, 250 mM NaCl, 0.2 mM EDTA, 5 mM β-glycerophosphate, 2 mM Na_3VO_4, 10 mM NaF, plus freshly added Complete protease inhibitors diluted 1:25, 500 nM microcystin, 1 mM DTT; Habu *et al.* 2002). Then the samples were sonicated on ice in an 1.5 ml or 15 ml tube with 3 x 20 pulses at setting 2 with a Branson Sonic Power sonifier model S125 (Branson, Danbury, CT, USA). The lysate was spun at 13000 rpm for 15 min at 4°C, the supernatant transferred to a new 1.5 ml tube and its protein concentration determined as described above.

Immunoprecipitation

Treated cells were harvested with trypsin/EDTA and washed once with PBS. Harvested cells were lysed for 15 min on ice in Matsumoto or NP-40 buffer (0.7% NP-40, 20 mM HEPES pH 7.4, 175 mM NaCl, 10 mM EDTA, plus freshly added Complete protease inhibitors diluted 1:25) and sonicated with 3 x 20 pulses at setting 2 with a Branson sonifier. The lysate was spun at 13000 rpm for 20 min at 4°C, the supernatant transferred to a new 1.5 ml tube and its protein concentration determined by a Lowry assay kit as described above. 200 µg protein in NP-40 buffer adjusted to a concentration of 1 µg/µl were precleared with 10-20 µl equilibrated protein G sepharose beads from Santa Cruz (Santa Cruz, Santa Cruz, CA, USA; equaling 5-10 µl original slurry of the beads) for 30 min. For Cdk2 kinase assays the supernatant was mixed with 5 µl Cdk2(M2) antibody coupled to agarose beads (0.2 µg/µl; Santa Cruz, Santa Cruz, CA, USA), and rotated at 4°C for at least 2.5 h. Alternatively for Cdk1 kinase assays 5 µl anti-Cyclin B(GNS-1) antibody (0.1 µg/µl; Santa Cruz, Santa Cruz, CA, USA) were added and rotated at 4°C for at least 1 h and 20 µl equilibrated protein G sepharose beads were added for another hour. To check the quality of the immunoprecipitation, the beads were divided into two halves before the last washing step with NP-40 buffer. One half of the beads was run on a 12% or 14% gel for Cdk1/Cyclin B or for Cdk2 Westerns blots. The other half was employed for the kinase assay.

Kinase assay

Immunoprecipitation of Cdk2 or Cyclin B/Cdk1 was carried out as outlined above. After five washes with 500 µl NP-40 buffer, followed by one wash with 500 µl kinase buffer (20 mM HEPES pH 7.4, 10 mM $MgCl_2$), the beads were incubated for the kinase reaction with 20 µl kinase master mix (20 mM HEPES pH 7.4, 10 mM $MgCl_2$ and freshly added 1 mM DTT, 10 µM PKC inhibitor, 7.5 µg histone H1, 0.2 mM ATP, 0.5 µl [^{32}P]γ-ATP (5000Ci/mmol)) for 10-20 min at 37°C. The reaction was stopped with 30 µl pre-heated 5x SDS sample buffer (15% (w/v) SDS, 15% (v/v) β-mercaptoethanol, 50% (v/v) glycerol, 0.25% (w/v) bromophenol blue), the proteins denatured at 95°C for 5 min, snap-frozen and stored at -20°C. For SDS-PAGE the beads were boiled again and 10 µl of the samples (of a total of 50 µl) run at 20 mA for 3 h on an 18% SDS-PAGE gel. Free radioactivity was removed after the run and the gel dried onto a Whatman paper with a Model 583 Gel Dryer

(BioRad, Hercules, CA, USA) at 80°C for 45 min. Radioactive signals were detected with a PhosphoImager screen for quantitation as described under Hybridization of RNA and visualized on X-ray film.

Western blotting

SDS-PAGE: The resolving gel buffer (3 M Tris/HCl, 27.7 mM SDS, pH 8.8) was mixed with 7 volumes of acrylamide diluted in H_2O to the desired percentage and the stacking gel buffer (313 mM Tris/HCl, 6.9 mM SDS, pH 6.8) was mixed with 1 volume of acrylamide diluted in H_2O to a final concentration of 6% acrylamide. Protein samples (usually 50 µg per lane) were mixed with 0.2 volumes of 5x SDS sample buffer (15% (w/v) SDS, 15% (v/v) β-mercaptoethanol, 50% (v/v) glycerol, 0.25% (w/v) bromophenol blue) and denatured at 95°C for 5 min. Samples were run into the stacking gel at 25 mA and through the resolving gel at 30-35 mA.

Western blotting: Proteins were transferred from the gel to the Protran nitrocellulose transfer membrane (Whatman Schleicher & Schuell, Dassel, Germany) with a semi-dry electroblotter (BioRad, Hercules, CA, USA). Two sheets of Whatman 3MM chromatography paper (Whatman, Dassel, Germany), the membrane, the gel and two sheets of Whatman paper were stacked onto each other, all pre-wetted with 1x Western blotting buffer (0.1% SDS, 25 mM Tris/HCl, 192 mM glycine, 20% methanol, pH 8.3). The transfer was carried out for 1.5-2.5 h at 0.7-1 mA/cm^2 and checked by Ponceau S staining (0.2% Ponceau S in 3% TCA). The blot was blocked with 5% skimmed milk powder in TBS (50 mM Tris/HCl pH 7.2, 160 mM NaCl) for 1 h at RT. After thorough washing with TBST (0.1% Tween-20 in TBS) for five times the primary antibody in 5% BSA (fraction V, Sigma-Aldrich, Steinheim, Germany) in TBS was added over night at 4°C on a shaker. The blot was washed three times with TBST at RT. Incubation with the secondary antibody (HRP coupled) in 2% skimmed milk powder in TBS was performed for 2 h at RT and the blot was washed three times with TBST, then two times with TBS. The fluorescent signal was detected by incubating the blot for 1 min in enhanced chemi-luminescence solutions (Super Signal West Pico or Femto chemiluminescent substrate from Pierce, Rockford, IL, USA or the luminol solutions described below). Fuji Medical X-Ray Film (Fujifilm, Düsseldorf, Germany) was exposed to the blot for a few seconds to

a few minutes and developed with a KODAK X-OMAT 2000 Processor machine (Kodak, New Haven, CT, USA).

Luminol-based chemiluminescence system

1 ml of solutions A and B were mixed immediately before incubation of the membrane. Solution A contained 100 mM Tris/HCl pH 8.5, 25 mM luminol and 0.4 mM β-hydroxy-coumaric acid, solution B contained 100 mM Tris/HCl pH 8.5 and 0.03% H_2O_2.

Cell culture

Cell culture of mammalian cells

Mammalian cancer cells were cultured in DMEM or RPMI medium (both from PAA, Cölbe, Germany) supplemented with 10% fetal calf serum (Invitrogen, Karlsruhe, Germany), 1% glutamine, 100 U/ml penicillin, and 100 µg/ml streptomycin (all from Cambrex Bioscience, Verviers, Belgium) in a Cytoperm 8080 or BBD 6620 (Heraeus, Hanau, Germany) at 37°C in a humidified atmosphere of 95% H_2O containing 5% CO_2. For subcultivation most cancer cell lines were split three times a week with an average ratio of 1:5. For splitting the cells were washed once with PBS and detached with trypsin/EDTA (Cambrex Bioscience, Verviers, Belgium) at 37°C. Cells were then resuspended in PBS, pelleted by centrifugation, resuspended in medium and seeded.
Human primary cells (HUVEC) were cultured under the same conditions in EGM-2 medium (Cambrex Bioscience, Verviers, Belgium) containing 2% serum and BJ-tert cells in DMEM with 15% FCS, both were split three times a week from plate to plate by trypsinization at RT and resuspension in culture medium with a ratio of 1:2.
The cells were seeded one day prior to the treatment to achieve the desired confluence in the desired format, either by estimation of the split ratio or by counting cells with a Neubauer improved chamber (La Fontaine, Forst, Germany).

Preparation of freezing stocks

Pelleted cells were resuspended in freezing medium (culture medium with 20% FCS and 10% DMSO). 50% of a confluent 10 cm dish per freezing vial were resuspended in 1 ml freezing medium. The vials were put in styrofoam boxes and cooled to -80°C for several days before storage in the liquid nitrogen tank.

Transfection of human cancer cells

Electroporation

HeLa cells were split one day prior to transfection. On the day of transfection the cells were harvested by trypsinization, spun down, resuspended in PBS and counted with a Neubauer improved chamber (La Fontaine, Forst, Germany). 4 x 10^6 cells/ml were resuspended in DMEM. 400 µl of the cell suspension was mixed thoroughly with plasmid DNA in a 1.5 ml tube by pipetting up and down 20 times with a 1000 µl pipette and transferred to a 4 mm electroporation cuvette (BioRad, Hercules, CA, USA). Cells were transfected with a Gene Pulser (BioRad, Hercules, CA, USA). Electroporation parameters were 300 V and 960 µF for 20 ms. The transfected cells were mixed with pre-warmed medium, distributed to culture dishes for experiments and washed three times with PBS 6 h after transfection to remove dead cells.

Generation of stable cell lines

One day prior to transfection 8 x 10^5 HCT116 wild type cells were seeded into a 6 cm dish. 5 µg plasmid DNA were diluted in 150 µl medium (without FCS, L-glutamine, antibiotics) and thoroughly mixed with 20 µl SuperFect transfection reagent (Qiagen, Hilden, Germany) in a 1.5 ml tube by pipetting up and down five times. Complex formation took place at RT for 10 min. Cells were washed once with PBS, then overlaid with 1 ml growth medium mixed with the complexes and incubated for 3 h. After several washes with PBS and addition of 4 ml fresh medium cells were allowed to express the constructs for 48 h before starting selection with puromycin (5 µg/ml). One day after transfection cells were split from one 6 cm dish into four 10 cm dishes and cultured in normal medium. Single

colonies were picked, freezing stocks made and clones tested for shRNA expression with FACS based assays and Western blots.

Mad1 shRNA expressing cells lines: HCT116 wt cells were cotransfected either with 4.5 µg pSUPER-Mad1 si1 (#426) or si2 (#427) of each plasmid or the empty pSUPER vector plus 0.5 µg pBabepuro vector, or both plasmids at once with 2.25 µg of each plasmid plus 0.5 µg pBabepuro vector.

Dominant p53 expressing cells lines: HCT116 wt and HCT116 *MAD2*$^{+/-}$ cells were co-transfected with 4.5 µg pcDNA3-HA-p53DD vector or the empty pcDNA3 vector and 0.5 µg pBabepuro vector and selected with 5 µg/ml puromycin. HCT116 *MAD1*^{kd} cells were transfected with the pcDNA3-HA-p53DD vector or the empty pcDNA3 vector and selected with 300 µg/ml neomycin.

Synchronization of cell populations

Thymidine (Sigma-Aldrich, Steinheim, Germany) was added to a final concentration of 2 mM for 16-24 h, washed out by at least three washes with PBS for 5 min each and replaced by new medium. 8-9 h later thymidine was added as before and washed out 16 h later as described. Cells were released in drug-free or drug-containing medium. FACS samples were taken during and at several time points after release from the block. The method was performed essentially as described by Kramer *et al*. 2000.

Treatment with spindle damaging agents

Standard concentrations of 150 nM nocodazole, 100 nM taxol or 70 µM monastrol were added to the culture medium in a working dilution prepared in medium for the desired span of time. To enrich the amount of mitotically arrested cells – particularly to minimize the differences between spindle checkpoint proficient and impaired cell lines – a mitotic shake-off was performed. To this end cells were grown and treated in flasks and mitotic cells were detached from the surface by tapping the flask. The medium containing the floating cells was spun down to isolate the mitotic cells for harvesting or seeding for further treatments.

Treatment with UV light

After removal of the culture medium, the cells were exposed in opened dishes to UV light of 254 nm of the desired energy in a UV Stratalinker 2400 (Stratagene, Amsterdam Zuidoost, the Netherlands), fresh medium was added and the cells were cultivated until harvesting.

Treatment with DNA damaging agents or antimetabolites

Topoisomerase inhibitors: Standard concentrations of 300 nM adriamycin on HeLa cells or 350 nM adriamycin on HCT116 cell lines were added to the culture medium in a working dilution prepared in medium to induce a cell cycle arrest. Apoptosis was induced by treatment with 750 nM adriamycin. Etoposide was diluted in medium and added at the indicated concentrations.
Antimetabolites: 5-fluorouracil was diluted in medium and added at the indicated concentrations.

G2 DNA damage checkpoint abrogation

Cells arrested in G2 phase with 300 or 350nM adriamycin were subsequently treated with 100 nM UCN-01 or 1.2 mM caffeine. To separate cell sub-populations arrested in G2 phase or in mitosis, a mitotic shake-off was performed as described above.

FACS methods

Determination of DNA content

The DNA content was determined by PI FACS analysis. Treated cells were harvested with trypsin/EDTA or PBS/EDTA, washed once with PBS and resuspended in a 15 ml tube in 200-500 µl PBS by pipetting up and down 20 times. 1-2 ml of ice-cold 75% ethanol was added dropwise to the cell suspension under vigorous vortexing and the cells were fixed at 4°C over night. To remove RNA before PI staining, cells were resuspended in 100 µl PBS with 1 µg/ml RNase at 4°C over night. 50 µg/ml PI (propidium iodide, Sigma-Aldrich,

Steinheim, Germany) in PBS was added 15 min before measurement of the samples. Samples were measured with a FACSCalibur (BectonDickinson, San Jose, CA, USA) fluorocytometer with BD CellQuestPro software. FACS measurement parameters were: FSC and SSC adjusted, channel F3 linear on the x-axis, with the number of counted events on the y-axis. Display of the data as histogram.

MPM2 staining

The mitotic index was determined by MPM2 FACS analysis. Fixation of treated cells was executed as described for PI FACS analysis. The pellet of fixed cells was resuspended in MPM2 wash buffer (0.05% Triton X-100 in PBS) and spun down at 4000 rpm for 5 min at 4°C. The cells were incubated for at least 2 h on ice in 60-100 µl staining solution (2% FCS, 0.2% Triton X-100 in PBS) with anti-MPM2 antibody (Upstate, Lake Placid, NY, USA, 1 µg/µl) diluted 1:1600. After washing twice with 1 ml MPM2 wash buffer, the cells were incubated for at least 1 h on ice in 60-100 µl staining solution with anti-mouse AlexaFluor488 antibody (Molecular Probes, Leiden, the Netherlands, 2 µg/µl) diluted 1:2400 or anti-mouse DTAF antibody (Jackson Immuno Research, West Grove, PA, USA, 0.75 µg/µl) diluted 1:400. Before being handled like PI samples (see *Determination of DNA content*, i.e. over night RNase digest, PI staining), cells were washed once with MPM2 wash buffer and once with PBS. Samples were measured with a FACSCalibur (BectonDickinson, San Jose, CA, USA) fluorocytometer with BD CellQuestPro software. FACS measurement parameters were: FSC and SSC adjusted. For the MPM2 signal: channel F1 logarithmic on the x-axis (with the positive population being to the right of the scale), for the PI signal: channel F3 linear on the y-axis. Display of the data as dot plot. The mitotic index is calculated as the percentage of MPM2-positive 4N cells of the total population.

Determination of DNA synthesis

The DNA synthesis was determined by BrdU FACS analysis. Cells were pulse-labeled by adding BrDU (Sigma-Aldrich, Steinheim, Germany) to a final concentration of 50 µM to the culture medium 30 min prior to harvesting. Ethanol fixed cells were rehydrated in wash buffer (0.5% BSA in PBS) and denatured in 1 ml 2 M HCl in H_2O for 25 min at RT. The

cells were washed twice with wash buffer and once with dilution buffer (0.5% BSA, 0.5% Tween in PBS), followed by incubation for at least 1.5 h at RT in 100 µl dilution buffer with 1:200-1:400 diluted anti-BrDU antibody (Zymed, San Francisco, CA, USA, 1 µg/µl). After two washes with wash buffer cells were incubated for at least 1.5 h at RT in 100 µl dilution buffer with 1:100 diluted anti-mouse DTAF antibody (Jackson Immuno Research, West Grove, PA, USA, 0.75 µg/µl). Then they were washed twice with wash buffer and once with PBS before being handled like PI samples (see *Determination of DNA content*, i.e. over night RNase digest, PI staining). FACS measurement parameters were: FSC and SSC adjusted. For the BrDU signal: channel F1 logarithmic on the x-axis (with the positive population being to the right of the scale), for the PI signal: channel F3 linear on the y-axis. Display of the data as dot plot.

Immunofluorescence

Preparation of coverslips

Coverslips were sterilized with ethanol and air dried under the hood. They were put on 1 mg/ml polylysine drops (Sigma-Aldrich, Steinheim, Germany) on parafilm for 15 min and washed five times with filtered H_2O to remove excess polylysine. Cells were harvested, resuspended in PBS, dropped onto the coated coverslips and allowed to attach for 10 min.

Fixation and antibody staining

Cells were fixed with 1% paraformaldehyde in 1x PHEM solution (60 mM PIPES pH 7.0, 27 mM HEPES, 10 mM EGTA, 4 mM $MgSO_4$) for 10 min at RT and permeabilized for 10 min with 1% CHAPS in PHEM solution. The coverslips were washed once with MBST (0.05% Tween-20 in MBS (10 mM MOPS pH 7.2, 150 mM NaCl)). Blocking was performed in 20% bNGS (boiled normal goat serum, B304, Rockland, Gilbertsville, PA, USA) in MBST for 30 min with the slides put upside down on parafilm in a wet chamber at RT. After washing once with MBST the slides were incubated with the primary antibody (or antibodies) diluted in 5% bNGS in MBS for at least 60 min at RT in a wet chamber as described above. The coverslips were washed three times with MBST afterwards and the

following steps were performed in the dark. Incubation with the secondary antibody (or antibodies) diluted in 5% bNGS in MBS was done for at least 60 min at RT in a wet chamber. DNA was stained Hoechst 33258 and the coverslips were sealed like described under Morphological examination of apoptotic cells. Slides were stored protected from light at 4°C or -20°C. Photos were taken with a digital CCD camera (Hamamatsu, Hamamatsu City, Japan) mounted on a Leitz Axiovert 40 CFC microscope (Leica Geosystems GmbH, Munich, Germany) and were processed with Wasabi and Adobe Photoshop 5.0 (Adobe, Munich, Germany).

Apoptosis assays

Caspase assay

One day prior to treatment, transfected or untransfected cells were counted and seeded to the desired density, usually 1 x 10^5 cells per well of a 6- or 12-well dish. After treatment floating and attached cells were harvested in 15 ml tubes with PBS/EDTA, washed once with PBS and put on ice during processing. The PBS was removed and the cell pellet resuspended in 135 µl PBS by pipetting up and down 20 times with a 200 µl pipette. The cell suspension was transferred in triplicates (40 µl per well) into a white microtiter plate with lid. After all samples were pipetted into the plate, a fluorogenic peptide caspase substrate was added to a final concentration of 25 µM substrate (caspase 2, 3 and 9 substrates: Ac-VDVAD-AMC, Ac-DEVD-AMC, Ac-LEHD-AMC; Alexis, Grünberg, Germany). 10 µl of a 125 µM substrate working dilution in PBS was added and mixed with the cells by pipetting up and down twice with a 200 µl pipette. The plate was put in a cell culture incubator and only taken out for each measurement. Fluorescence was measured at 485 nm (with an excitation wavelength of 355 nm) using a Victor^2 1420 Multilabel Counter (Wallac Oy, Turku, Finland and Perkin Elmer, Freiburg, Germany) at 30-60 min intervals for 3 h to check linearity of the reaction. The 150 or 180 min-values were used to calculate the results with Excel. Mean values for each sample were calculated from triplicates. A value diverging more than 10% from the other values of a triplicate was omitted from the calculation. Values for untreated cells were subtracted from values of treated cells, because cells emit autofluorescence signals independently from caspase activity.

Cytochrome C release

Subcellular fractionation was performed essentially as described in Juin *et al.* 1999, but with several modifications. Cells were seeded one day prior to treatment. Floating and attached treated cells from a 10 cm dish were harvested using PBS/EDTA and washed once with PBS. All following steps were done on ice or at 4°C. The cell pellet was resuspended gently in 1 ml SCEB (sucrose-supplemented cell extract buffer: 300 mM sucrose, 10 mM HEPES pH 7.4, 50 mM KCl, 5 mM $MgCl_2$, 5 mM EGTA, plus freshly added Complete protease inhibitors diluted 1:25, 1 mM DTT, 1 mM PMSF, 10 µM cytochalasin B (Sigma-Aldrich, Steinheim, Germany)), swollen on ice for 30 min and homogenized on ice with a douncer with a B pestle with 30 strokes. The suspension was transferred into a 1.5 ml tube and spun at 2000 rpm for 5 min at 4°C. The supernatant was transferred to a new 1.5 ml tube and centrifuged at 13000 rpm for 15 min at 4°C, whereas the remaining pellet (fraction P1, containing the nuclei), was lysed with SCEB buffer. Then the supernatant (fraction C, containing the cytoplasm) was transferred to a new 1.5 ml tube and the remaining pellet (fraction P2, containing the mitochondria) was lysed like the first pellet. Alternatively, to prepare a cytosolic fraction, the homogenized cells were centrifuged at 13000 rpm for 15 min at 4°C and the supernatant would be used for Western blotting. The protein concentration was determined and 50 µg of protein was resolved on a thick 15% SDS-PAGE gel. Cytochrome C was detected using a mouse monoclonal antibody (BD Pharmingen, Erebodegem, Belgium) at a 1:1000 dilution on Western blots.

DNA laddering

DNA laddering assays were performed essentially as described in Herrmann *et al.* 1994, but with several modifications. Cells were seeded one day prior to treatment. Floating and attached treated cells from a 10 cm dish were harvested with PBS/EDTA, washed once with PBS and the cell pellet was resuspended gently in 50-100 µl extraction buffer (1% NP-40, 20 mM EDTA, 50 mM Tris/HCl pH 7.5). The cells were incubated on ice for 10 min, centrifuged at 2000 rpm for 5 min at 4°C and the supernatant was transferred into a new 1.5 ml tube. The extraction was repeated, the supernatant pooled with the supernatant from the first extraction step and SDS was added to a final concentration of 1%. To remove RNA and protein the sample was first digested with RNase A (1 µg/µl final) for 2 h at 56°C and subsequently with Proteinase K (1 µg/µl final) for 4 h at 37°C. The DNA

was then precipitated with 2.5 volumes of ice-cold 100% ethanol and 0.1 volume of 3 M Na-acetate (pH 5.1) over night at -80°C. The resulting pellet was dissolved in 60 µl H_2O. 15 µl of the sample were mixed with 5 µl DNA loading buffer and run on a 2 % agarose gel until the blue dye had migrated about 3-4 cm, i.e. for 2-3 h at 50 V. Photos were taken on a Mini-Transilluminator with a CCD camera using QuantityOne software (all from BioRad, Hercules, CA, USA), and the images were processed with Adobe Photoshop 5.0 (Adobe, Munich, Germany).

Bax activation

Immunoprecipitation of activated bax was essentially performed as described by Yamaguchi *et al*. 2003. Treated cells were harvested with PBS/EDTA, washed once with PBS and lysed for 15 min on ice in IP buffer (immunoprecipitation buffer: 1% Triton X-100 or CHAPS, 150 mM NaCl, 10 mM HEPES pH 7.5, plus freshly added Complete protease inhibitors diluted 1:25 and 0.1 mM PMSF). The lysate was centrifuged at 13000 rpm for 15 min at 4°C, the supernatant was transferred into a new 1.5 ml tube and its protein concentration was determined with a Lowry assay kit. 500 µg protein in IP buffer was adjusted to a concentration of 2 µg/µl and pre-cleared with 20 µl equilibrated protein G sepharose beads for 1 h. The supernatant was mixed with 5 µl conformation specific anti-bax antibody (Calbiochem, 6A7, 0.1 µg/µl) and rotated at 4°C for at least 3 h. To precipitate the antibody-bax complexes, 20 µl equilibrated protein G sepharose beads were added and the mixture rotated end-over-end at 4°C for at least 2 h. Beads were washed five times for 2 min with IP buffer with enhanced salt concentration (250 mM NaCl instead of 150 mM) by adding 500 µl buffer and spinning at 2000 rpm at 4°C. The pelleted beads were boiled at 95°C for 5 min in 20 µl 5x sample buffer, snap-frozen and stored at -80°C. For Western blotting the whole volume of the samples was run on a 16% SDS-PAGE gel and blotted for 1.5-2 h. The blot was incubated with anti-bax antibody 554104 from BD Pharmingen or 6A7 from Calbiochem and developed as described above.

Bak activation

Detection of activated bak was essentially carried out as described by Panaretakis *et al*. 2002. Treated cells from a 10 cm dish were harvested with PBS/EDTA, fixed in a 15 ml

tube with 200 µl 0.25% paraformaldehyde in PBS for 5 min at RT and washed twice with 500 µl PBS. Cells were incubated with 0.2-0.3 µl anti-bak antibody (Calbiochem, Ab1, 0.1 µg/µl) in 100 µl staining solution (500 µg/ml digitonin in PBS, Sigma-Aldrich, Steinheim, Germany) for at least 3 h on ice. After two washes with PBS cells were incubated with 100 µl staining solution with anti-mouse AlexaFluor488 antibody diluted 1:400 for at least 3 h on ice in the dark. Following one wash with PBS the cells were resuspended in PBS and measured immediately. FACS measurement parameters were: FSC and SSC adjusted. For the bak signal: channel F1 linear on the x-axis (with the positive population being to the right of the scale or a shift of the whole population to the right). For a dot plot: FSC-Height on the y-axis, for a histogram: counts on the y-axis.

SubG1 PI FACS

Cells were fixed with 75% ethanol for 16-24 h. To remove RNA before PI staining, cells were resuspended in 100 µl PBS with 1 µg/ml RNase at 4°C over night. 50 µg/ml PI (Sigma-Aldrich, Steinheim, Germany) in PBS was added 15 min before measurement of the samples. FACS measurement parameters were: FSC and SSC adjusted, channel F3 linear on the x-axis, with the number of counted events on the y-axis. Events found left of the G1 peak were interpreted as cells containing a subG1 DNA content, which were dead or dying.

TMRE FACS

Treated cells were harvested with PBS/EDTA, washed once with PBS, resuspended in PBS with 125 nM TMRE (tetramethylrhodamine ethyl ester perchlorate, Sigma-Aldrich, Steinheim, Germany) and incubated in the dark in the cell culture incubator for 15 min. Samples were measured immediately thereafter. FACS measurement parameters were: FSC linear and SSC logarithmic, channel F3 logarithmic on the x-axis (with the positive population being to the right of the scale) with the number of counted events on the y-axis. Living cells accumulate the dye in their mitochondria and constitute the TMRE-positive population, while dying cells lose mitochondrial integrity and dye retention capability. Thus, TMRE-negative cells are defined as apoptotic.

Morphological examination of apoptotic cells

Cells were seeded on polylysinized coverslips and fixed with 1-2% paraformaldehyde in 1x PHEM solution for 5 min at RT, followed by fixation with ice-cold methanol for 5 min at -20°C. After three washes with MBST, DNA was stained with Hoechst 33258 (1 µg/ml in 1x PHEM, Fluka BioChemika via Sigma-Aldrich, Munich, Germany) for 5 min at RT in the dark. The coverslips were washed twice with MBST and once with MBS. The dried coverslips were put upside down in Vectashield mounting medium onto slides and sealed with nail polish.

Results

1. Generation and characterization of stable *MAD1* knock down cell lines

Spindle checkpoint impairment is frequently observed in human cancer (Bharadwaj and Yu 2004), but intragenic mutations in the known spindle checkpoint genes appear to be rather rare (Bharadwaj and Yu 2004). However, diminished spindle checkpoint protein levels can lead to compromised checkpoint function and were found to be associated with cancer (Bharadwaj and Yu 2004) and to correlate with resistance to certain chemotherapeutic drugs (Masuda *et al.* 2003, Nitta *et al.* 2004, Sudo *et al.* 2004, Tao 2005, Vogel *et al.* 2005). Specifically, reduced protein levels of Mad1 or Mad2 in human cancers can occur alone or in combination (Wang *et al.* 2002), which suggests non-redundant functions of these proteins. Investigation of these non-redundant functions requires cell lines containing reduced Mad1 or Mad2 levels. Severe repression of spindle checkpoint proteins or homozygous deletion of spindle checkpoint genes leads to cell death indicating that their products are essential for viability (Kalitsis *et al.* 2000, Michel *et al.* 2001, Kops *et al.* 2004, Iwanaga *et al*. 2007). Therefore, previous studies could not investigate the consequences of Mad1 inactivation. Our approach was to mimic conditions in human cancers by reduction of Mad1 to a level compatible with long-term cell survival.
HCT116 colon carcinoma cells were particularly attractive for the generation of stable *MAD1* knock down cell lines, because isogenic derivatives with a heterozygous gene deletion of *MAD2* (Michel *et al.* 2001) or a homozygous deletion of *TP53* (Bunz *et al.* 1998) were already available. These cell lines allowed functional comparisons in an isogenic background.

Stable HCT116 *MAD1* knock down cells are spindle checkpoint impaired

For stable downregulation of *MAD1* by expression of shRNAs which downregulate mRNA levels I cloned two constructs targeting different regions of the *MAD1* mRNA into the pSUPER vector (Brummelkamp *et al.* 2002). HCT116 wt cells were stably co-transfected with the pSUPER-*MAD1* and the pBabepuro vector coding for resistance to puromycin to allow selection with 5 µg/µl puromycin. As controls HCT116 wt cells were co-transfected with the empty pSUPER vector and the pBabepuro vector. The pSUPER vector containing sequence si1 (targeting nucleotides 391 to 399, Luo *et al.* 2002) did not yield any cell lines,

which might indicate that the level of *MAD1* downregulation reached was lethal to the cells. However, 31 independent cell clones of HCT116 wt cells transfected with the vector containing sequence si2 (targeting nucleotides 992 to 1010) and three independent cell clones for the controls containing the empty pSUPER vector were isolated. To identify cell lines with sufficient downregulation of *MAD1* to impair spindle checkpoint function a functional screen was employed. Since Mad1 is an essential spindle checkpoint component (Vigneron *et al.* 2004), the spindle checkpoint activity in cells with reduced Mad1 levels should be markedly decreased compared to control cells expressing the empty vector.

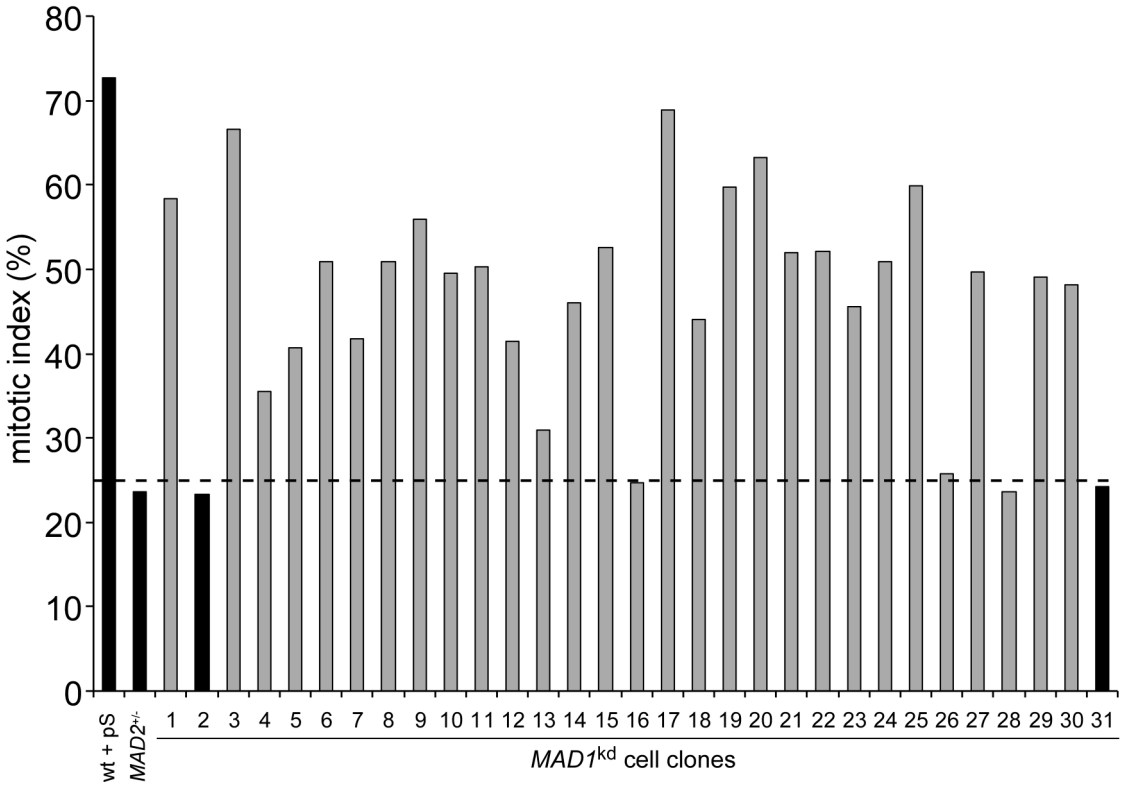

Figure 10: Determination of spindle checkpoint impairment of stable HCT116 *MAD1* knock down cell clones. HCT116 *MAD1* knock down clones (*MAD1*^{kd}) were generated by stable co-transfection of HCT116 wt cells with pSUPER-*MAD1* and pBabepuro vectors. As controls HCT116 wt cells were co-transfected with pSUPER and pBabepuro vectors. The spindle checkpoint function of 31 independent HCT116 *MAD1*^{kd} cell clones (numbered 1-31), HCT116 wt + pSUPER cell clone 1 (wt + pS) and HCT116 *MAD2*$^{+/-}$ cells was assessed by treatment with 150 nM nocodazole for 14 h and determination of the mitotic index by MPM2 FACS analysis. The controls and the *MAD1*^{kd} cell clones 2-2 and 2-31 are highlighted in black. The horizontal line marks a mitotic index of 25% indicating an ideal degree of spindle checkpoint impairment for further experiments. One representative experiment is shown.

A total of 31 independent *MAD1* knock down cell lines as well as HCT116 wt + pSUPER (clone 1) and HCT116 *MAD2*$^{+/-}$ cells were treated with 150 nM nocodazole for 14 h and

the mitotic index was determined by MPM2 FACS analysis. In agreement with previous results the HCT116 wt cell line 1 carrying the control vector exhibited a mitotic index of 72.8% and the HCT116 *MAD2*$^{+/-}$ cells had a mitotic index of 23.7% (Figure 10). The mitotic indices of the 31 *MAD1* knock down (*MAD1*^{kd}) cell clones varied from 23.3% to 68.8% (Figure 10). Five HCT116 *MAD1*^{kd} cell clones showed spindle checkpoint impairment comparable to the HCT116 *MAD2*$^{+/-}$ cells: HCT116 *MAD1*^{kd} 2-2, 2-16, 2-26, 2-28 and 2-31 (mitotic index of 23.3%, 24.7%, 25.7%, 23.0%, 24.2%, respectively, (Figure 10). Two of these cell lines were selected for all following experiments: *MAD1*^{kd} 2-2 and 2-31. The HCT116 wt + pSUPER (clone 1) was chosen as a control.

The level of Mad1 protein downregulation was determined by Western blotting. Expression levels of HCT116 *MAD1*^{kd} 2-2 and 2-31 cell clones were quantified compared to control cells (HCT116 + pSUPER clone 1), and parental cells (HCT116 wt). Mad1 signals were normalized for actin expression and the Mad1 protein level was calculated. HCT116 *MAD1*^{kd} cell lines 2-2 and 2-31 showed a 35.3% and 49.6% reduction of protein levels respectively (Figure 11), while HCT116 *MAD2*$^{+/-}$ cells displayed a loss of 20% on protein level (Michel *et al.* 2001) and also on mRNA level (my own Northern blot data, not shown). Surprisingly, the degree of Mad1 protein downregulation had to exceed that of Mad2 to yield an identical degree of spindle checkpoint impairment in the FACS-based functional assay.

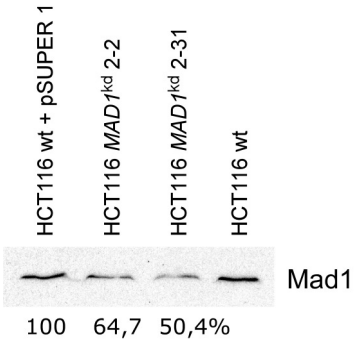

Figure 11: Quantitation of reduced Mad1 protein levels in HCT116 *MAD1* knock down cells on Western blot. Western blots of lysates from asynchronously growing cells of two independent HCT116 *MAD1*^{kd} cell clones (2-2, 2-31), empty vector control cells (HCT116 + pSUPER clone 1) and parental cells (HCT116 wt) were used to calculate the mean of four independent experiments. Mad1 signals were normalized for actin expression and the Mad1 protein level was calculated in percent of HCT116 wt + pSUPER expression (indicated below the blot). The Western blot was probed with antibodies directed against Mad1 (Campbell *et al.* 2001) and actin. One representative Western blot is shown.

Asynchronously growing HCT116 *MAD1*^{kd} cells clones 2-2 and 2-31 and control cell lines were analyzed for their DNA content and their mitotic index to detect possible cell cycle defects.

Initial characterization of untreated HCT116 *MAD1*^{kd} cell lines revealed no gross growth defects. The overall cell cycle distribution was undisturbed including the amount of mitotic cells compared to controls (Figure 12). Subcultivation ratios for HCT116 *MAD1*^{kd} cells 2-2 and 2-31 were identical to the ratios for the other HCT116 cell lines, indicating unaltered growth rates (data not shown).

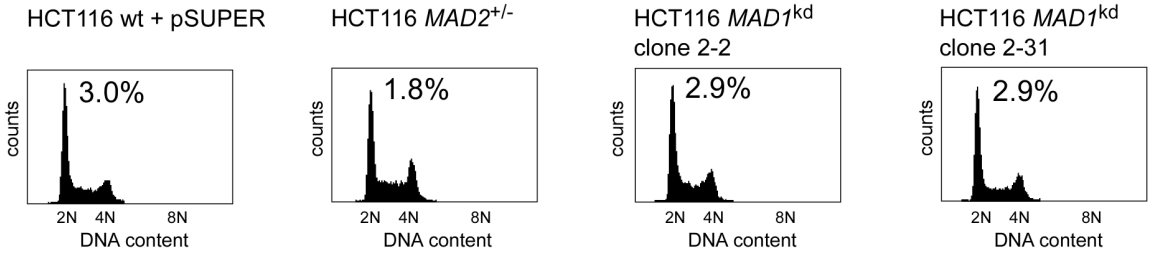

Figure 12: Mad1 downregulation does not alter normal cell cycle distribution of HCT116 *MAD1* knock down cell lines. Asynchronously growing HCT116 *MAD1* knock down cells (*MAD1*^{kd} clones 2-2, 2-31) were tested for cell cycle distribution. HCT116 wt + pSUPER cells (wt + pSUPER clone 1) and HCT116 *MAD2*$^{+/-}$ cells served as controls. DNA content distribution of the cell populations is presented as PI FACS profiles and the mitotic index determined by MPM2 FACS is given above the corresponding profiles.

HCT116 *MAD1* knock down cells and HCT116 *MAD2*$^{+/-}$ cells have an impaired spindle checkpoint response to spindle damaging agents

The spindle checkpoint is activated upon damage induced by spindle damaging agents. Nocodazole and the chemotherapeutically used *Vinca* alkaloids (e.g. vincristine, vinblastine) interfere with spindle dynamics and prevent generation of attachment and tension by depolymerizing the mitotic spindle at high doses. Taxanes (e.g. taxol, docetaxel) interfere with spindle dynamics and stabilize the microtubules at high doses. Since microtubules capture kinetochores by a stochastic process of growth and shrinkage (dynamic instability) and pull chromosomes to the spindle poles by shrinkage, microtubule stabilization interferes with the generation of tension between kinetochores (Jordan and Wilson 2004). Monastrol inhibits the motor protein Eg5 responsible for centrosome migration. The result of monastrol treatment is a monopolar spindle leading to a lack of tension between kinetochores (Mayer *et al.* 1999). Chromosome alignment is disturbed by spindle damaging agents, cells arrest in metaphase and die later by apoptosis (Jordan and Wilson 2004, Zhou and Giannakakou 2005). Cells treated with spindle damaging agents leave the spindle checkpoint-mediated mitotic arrest after prolonged spindle checkpoint

activation even if they possess a functional spindle checkpoint, a process termed mitotic slippage, which is accelerated in spindle checkpoint impaired cells (Chen *et al.* 2003).

The contribution of Mad1 to mounting and maintenance of mitotic arrest upon various kinds of spindle damage was assessed. HCT116 *MAD1*^{kd} cells, HCT116 *MAD2*$^{+/-}$, HCT116 wt and HCT116 *TP53*$^{-/-}$ cell lines were treated with 150 nM nocodazole, 100 nM taxol or 70 µM monastrol for 16 h and the mitotic arrest was monitored by MPM2 FACS analysis (Figure 13). Since the HCT116 wt + pSUPER clone 1 behaved similarly to HCT116 wt cells and the HCT116 *MAD1*^{kd} 2-2 cells behaved similarly to HCT116 *MAD1*^{kd} 2-31 cells the corresponding data was not shown. Treatment with nocodazole, taxol and monastrol yielded comparable results in each cell line (Figure 13). HCT116 wt and HCT116 *TP53*$^{-/-}$ cell lines exhibited an intact spindle checkpoint indicated by a maximal mitotic arrest of about 80% in response to the drugs after 16 h, which slowly decreased during time course measurements for 48 h in 8 h intervals (data not shown). HCT116 *TP53*$^{-/-}$ cells maintained the mitotic arrest approximately 8 h longer than HCT116 wt cells indicating that *TP53* is not required for mitotic arrest, but might be involved in mitotic slippage. The mitotic indices of HCT116 *MAD1*^{kd} and HCT116 *MAD2*$^{+/-}$ cell lines after 16 h were less than 50% of spindle checkpoint proficient cells and mitotic slippage was completed after 24 h of treatment – significantly faster than in the spindle checkpoint proficient cell lines.

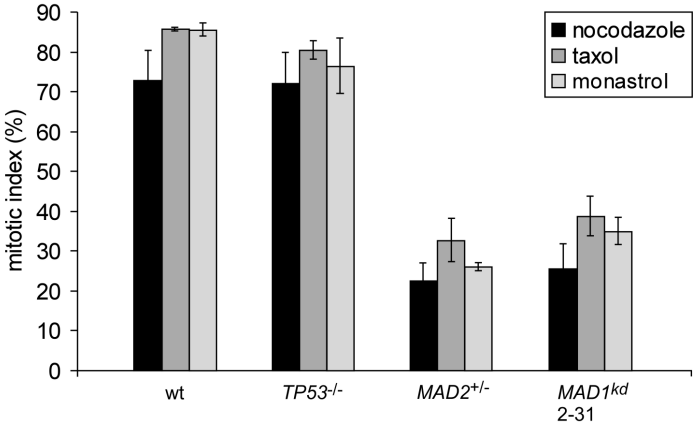

Figure 13: Spindle checkpoint impairment of HCT116 *MAD1* knock down cells or HCT116 *MAD2*$^{+/-}$ cells upon spindle damage. The ability of HCT116 *MAD1*^{kd} cells, *MAD2*$^{+/-}$ cells and the controls HCT116 wt and *TP53*$^{-/-}$ cells to arrest in mitosis upon treatment with 150 nM nocodazole, 100 nM taxol or 70 µM monastrol was determined by MPM2 FACS analysis after 16 h from at least three independent experiments.

Taken together, for the first time stable *MAD1* knock down cell lines were generated and characterized. Mad1 is required for spindle checkpoint function, since a reduction to 50-65% of the Mad1 protein levels in HCT116 wt cells impairs the mounting and maintenance of mitotic arrest upon spindle damage. The same reduction in Mad1 levels, however, does not impede normal growth of the cells. The mitotic arrest upon various kinds of spindle

damage, namely spindle depolymerization, spindle stabilization and a monopolar spindle, depends on normal levels of Mad1. Lowered Mad1 levels cause an impaired spindle checkpoint response leading to mitotic arrest defects, and premature mitotic slippage upon spindle damage. The experiments clearly show that *MAD1* and *MAD2* fulfill identical functions in the spindle checkpoint-mediated arrest upon challenge with various spindle damaging agents. The downregulation of either one is sufficient to induce mitotic arrest defects and premature mitotic slippage.

2. The spindle checkpoint and p53 suppress endoreduplication upon prolonged spindle damage

Polyploidization might be a first step on the road to cancer (Shackney *et al.* 1989). Subsequent losses or gains of chromosomes could generate aneuploid daughter cells (Lengauer *et al.* 1998, Duesberg and Li 2003, Rajagopalan *et al.* 2003). A possible result is the imbalance of tumor suppressor genes and oncogenes which can aid tumorigenesis (Weaver and Cleveland 2005). Especially an imbalance in checkpoint genes could impair the spindle checkpoint, the DNA damage checkpoints or other cell cycle checkpoints and thereby accelerate genomic changes resulting in malignant transformation (Duesberg and Li 2003). Polyploidy can be produced by a process called endoreduplication, the replication of DNA without completion of the subsequent mitosis, which produces cells with hyperdiploid DNA content (Weaver and Cleveland 2005). Endoreduplication can be reproduced under laboratory conditions by prolonged spindle damaging treatment of spindle checkpoint impaired or *TP53* negative cells (Minn *et al.* 1996). Mitotic slippage, i.e. unscheduled exit from mitotic arrest, occurs even in spindle checkpoint normal cells upon gradual weakening of the mitotic arrest induced by spindle damaging agents and the resulting tetraploid cells enter pseudo-G1 phase (Andreassen *et al.* 1996, Chen *et al.* 2003, Blagosklonny 2006, Brito and Rieder 2006). A so called tetraploidy checkpoint, or pseudo-G1 checkpoint, which is also termed postmitotic p53-dependent G1 checkpoint is implicated in preventing the replication of tetraploid cells, but its existence and mechanism of action remain disputed (Uetake and Sluder 2004, Wong and Stearns 2005, Blagosklonny 2006). Endoreduplication might promote malignant transformation. Therefore, I sought to understand which checkpoints and proteins prevent endoreduplication in mammalian cells. HCT116 cell lines were treated with nocodazole and the effects of checkpoint impairment due to reduced levels of *MAD1* or *MAD2* or the loss of *TP53* on mitotic slippage and endoreduplication were assessed.

Spindle checkpoint impairment or loss of *TP53* permit endoreduplication upon prolonged spindle damage

The functional interplay between the spindle checkpoint and the postmitotic p53-dependent G1 checkpoint in the prevention of endoreduplication upon spindle damage was investigated. HCT116 wt, HCT116 wt + pSUPER, HCT116 *TP53*$^{-/-}$, HCT116 *MAD2*$^{+/-}$

cells and HCT116 *MAD1*^{kd} cell clones 2-2 and 2-31 were treated with 150 nM nocodazole for up to 48 h (Figure 14a) or for up to 96 h in the case of HCT116 wt, HCT116 *TP53*$^{-/-}$ and HCT116 *MAD2*$^{+/-}$ cells (Figure 14c) and cells with hypertetraploid DNA content were identified by FACS analysis.

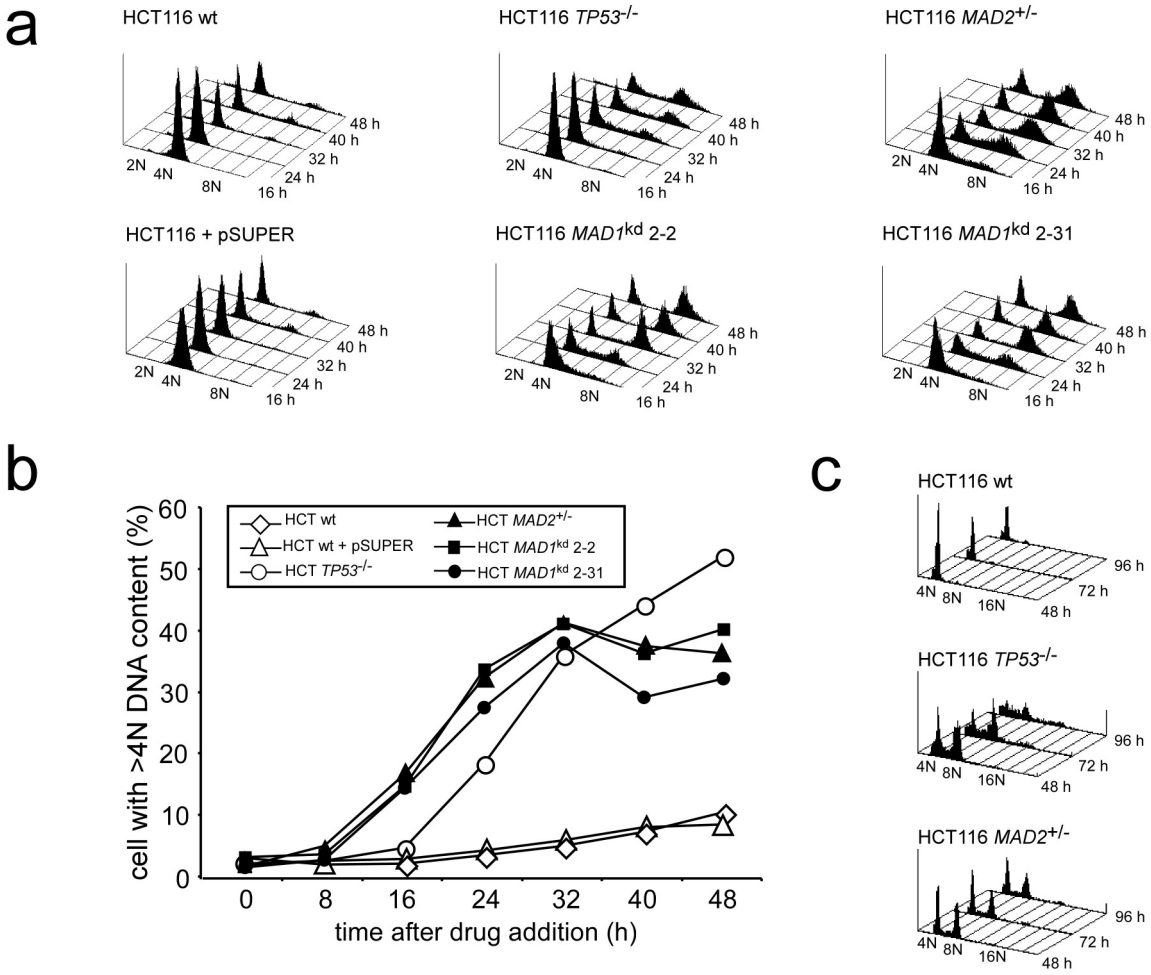

Figure 14: Spindle checkpoint impairment and loss of *TP53* allow endoreduplication upon prolonged spindle damage. a) The HCT116 wt cells, the HCT116 wt + pSUPER cells, HCT116 *TP53*$^{-/-}$ cells, HCT116 *MAD2*$^{+/-}$ cells and the *MAD1*^{kd} cell clones 2-2 and 2-31 were treated with 150 nM nocodazole in 8 h intervals for up to 48 h and their DNA content was determined by FACS analysis. Representative profiles are displayed. b) Quantitation of hypertetraploid cells of three experiments performed as in a). c) The HCT116 wt, HCT116 *TP53*$^{-/-}$ and HCT116 *MAD2*$^{+/-}$ cell lines were treated with 150 nM nocodazole for 48 h, 72 h and 96 h. Representative FACS profiles are displayed.

All spindle checkpoint impaired cell lines and the HCT116 *TP53*$^{-/-}$ cells exhibited endoreduplication, whereas the control cell lines did not endoreduplicate. Spindle checkpoint compromised cells endoreduplicated their DNA already after 16 h, whereas HCT116 *TP53*$^{-/-}$ cells began endoreduplication after 24 h (Figure 14a, b). This difference

can be attributed to the shortened mitotic arrest of spindle checkpoint impaired cell lines compared to spindle checkpoint normal cell lines. Nocodazole treatment for 96 h revealed further endoreduplication of HCT116 *TP53*$^{-/-}$ cells to 16N in contrast to the HCT116 *MAD2*$^{+/-}$ cells, which reached maximal ploidies of 8N (Figure 14c). This finding implied that spindle checkpoint impaired cells arrest after generation of 8N cells, an assumption that was tested by various methods. The quantitation of hypertetraploid cells treated as in Figure 14a showed a continued accumulation of hypertetraploid cells in the p53-negative HCT116 cell population, whereas spindle checkpoint compromised cell lines reached a maximum of 35% after 32 h of treatment (Figure 14b).

To investigate DNA synthesis in response to prolonged spindle damage in more detail, pulse labeling with BrdU of HCT116 wt, HCT116 wt + pSUPER, HCT116 *TP53*$^{-/-}$, HCT116 *MAD2*$^{+/-}$ cells and HCT116 *MAD1*^{kd} cell clones 2-2 and 2-31 treated with 150 nM nocodazole for up to 72 h was performed (Figure 15a). DNA synthesis in HCT116 *TP53*$^{-/-}$ cells started from a low level after 16 h (16%), peaked at 32 h (39%) and slowly declined during the next 40 h to a level comparable to that calculated for 20 h (23%). The high level of DNA synthesis even after 72 h of nocodazole treatment agrees well with the occurrence of 16 N cells after 96 h of treatment (Figure 14b) and suggests a continued cycling of the p53 deficient cells. The spindle checkpoint impaired cell lines, however, showed DNA synthesis already after 16 h (up to 33%), but DNA synthesis levels declined to that of control cell lines at 32 h (up to 17%) and remained low afterwards (up to 18%), indicating a stop of the cell cycle upon prolonged spindle damage. DNA synthesis in the control cell lines was below 15% after 16 h nocodazole treatment and slowly decreased after 32 h to a final value of 4% after 72 h (Figure 15a).

The activation of Cdk2/Cyclin E kinase complexes is a prerequisite for entry into S phase and, thus, for DNA replication and is inhibitable by p21 (Stewart *et al.* 1999). Detection of Cdk2 activity in a kinase assay indicates entry into S phase. Cdk2 was immunoprecipitated from HCT116 wt, HCT116 *TP53*$^{-/-}$ and HCT116 *MAD2*$^{+/-}$ cells treated with nocodazole for up to 50 h and the activity of Cdk2 was determined in a kinase assay (Figure 15b). Histone H1 was used as a substrate and the degree of its labeling with radioactive phosphate groups was quantified. An example for a kinase assay and immunoprecipitated Cdk2 on Western blot is shown in Figure 15c. The Cdk2 kinase activity of HCT116 *TP53*$^{-/-}$ cells treated with nocodazole for 18 h was set as 1.0-fold induction. HCT116 *TP53*$^{-/-}$ and HCT116 *MAD2*$^{+/-}$ cells showed almost the same kinase activity after 18 h of nocodazole treatment, but over the next 32 h Cdk2 activity in HCT116 *TP53*$^{-/-}$ cell lysates increased continuously, whereas

Cdk2 activity in HCT116 *MAD2*$^{+/-}$ cell lysates dropped to HCT116 wt levels after 36 h of treatment (Figure 15c). These results further support our finding that spindle checkpoint compromised cells endoreduplicate upon aberrant exit from mitosis, but arrest in the cell cycle subsequently, whereas p53 deficient cells cycle continuously in response to prolonged spindle damage.

Taken together, spindle checkpoint impairment allows endoreduplication upon early mitotic slippage from nocodazole-induced mitotic arrest. In contrast to spindle checkpoint compromised cells p53 deficient cells endoreduplicate after normal mitotic arrest and are able to traverse the cell cycle several times, each time replicating their DNA and entering mitosis without subsequent cytokinesis. Therefore a functional spindle checkpoint inducing prolonged mitotic arrest and functional p53 are necessary to prevent endoreduplication upon prolonged spindle damage.

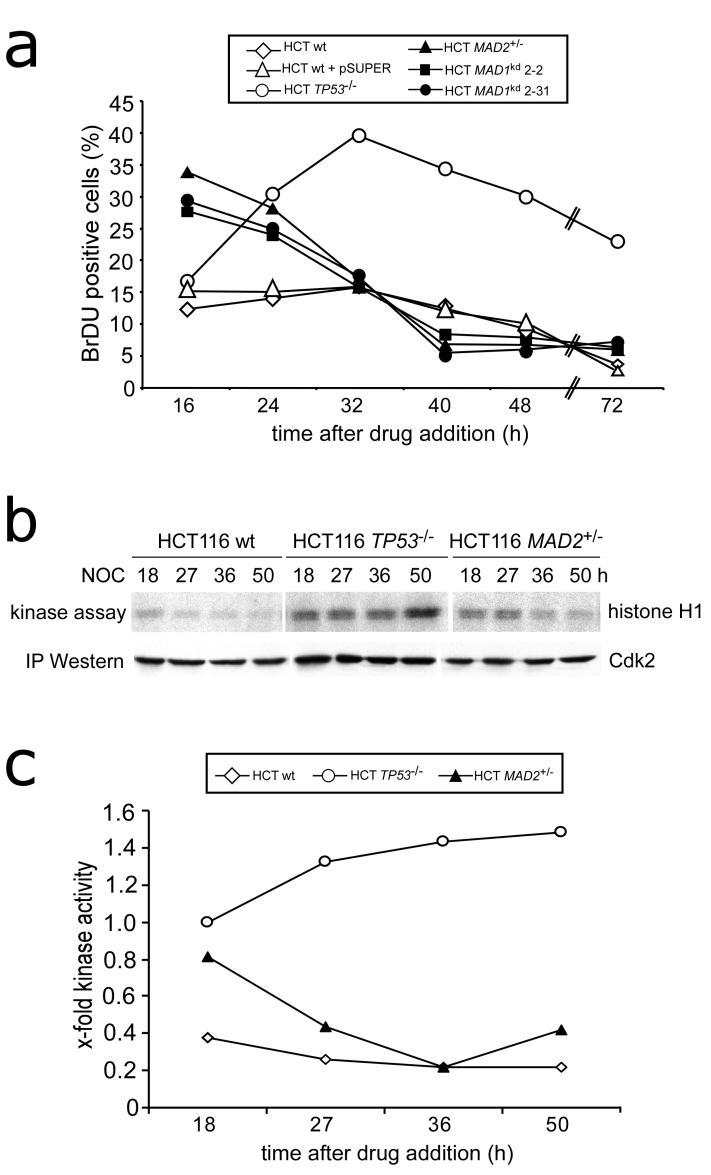

Figure 15: DNA synthesis and Cdk2 activation in endoreduplicating cells. a) HCT116 wt, HCT116 wt + pSUPER, HCT116 *TP53*$^{-/-}$, HCT116 *MAD2*$^{+/-}$ cells and *MAD1*^{kd} cell clones 2-2 and 2-31 were treated with 150 nM nocodazole for up to 72 h and new DNA synthesis was detected by BrdU FACS analysis. Mean values were calculated from at least three independent experiments. b), c) HCT116 wt, HCT116 *TP53*$^{-/-}$ and HCT116 *MAD2*$^{+/-}$ cell lines were treated with 150 nM nocodazole for up to 50 h and the activity of immunoprecipitated Cdk2 in histone H1 kinase assays was measured. One representative kinase assay and one Cdk2 IP Western blot are shown (b). The x-fold induction of Cdk2 activity (with the Cdk2 kinase activity of HCT116 *TP53*$^{-/-}$ cells treated with nocodazole for 18 h set as 1.0-fold induction) was calculated as mean value from two experiments (c).

A novel p53-dependent G2 checkpoint prevents re-entry of endoreduplicated cells into mitosis

To test whether polyploid cells can enter mitosis without cytokinesis, HCT116 wt, HCT116 wt + pSUPER, HCT116 *TP53*$^{-/-}$, HCT116 *MAD2*$^{+/-}$ cells and HCT116 *MAD1*^{kd} cell clones 2-2 and 2-31 were treated with nocodazole for up to 48 h and the percentage of octaploid mitotic cells was quantified (Figure 16). Starting from 24 h of nocodazole treatment onward the amount of octaploid mitotic cells in the HCT116 *TP53*$^{-/-}$ cell line rose steadily to 16% after 48 h, whereas in all other cell lines less than 3% of the cells were octaploid mitotic cells. These results clearly indicate that p53 is required to prevent mitotic entry of hypertetraploid cells and suggest the existence of a novel p53-dependent G2 checkpoint fulfilling this protective function.

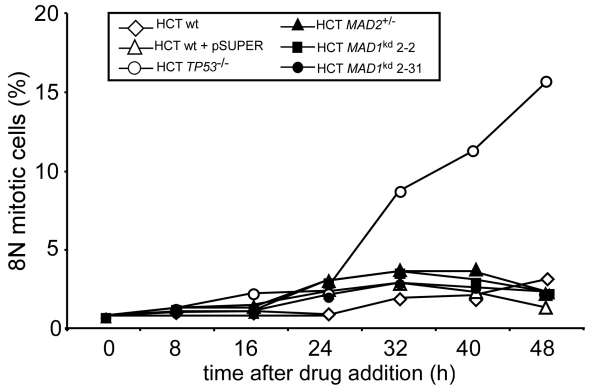

Figure 16: Endoreduplication is confined to one round in spindle checkpoint compromised cells but continues in *TP53*$^{-/-}$ cells. HCT116 wt, HCT116 wt + pSUPER, HCT116 *TP53*$^{-/-}$, HCT116 *MAD2*$^{+/-}$ cells and the *MAD1*^{kd} cell clones 2-2 and 2-31 were treated with 150 nM nocodazole for up to 48 h. The percentage of mitotic octaploid cells was determined by MPM2 FACS analysis and mean values from at least three independent experiments were calculated.

To uncover further components of the p53-dependent checkpoint preventing mitotic entry of octaploid cells I employed inhibitors of kinases involved in the DNA damage activated G2 checkpoint.

HCT116 wt, HCT116 *TP53*$^{-/-}$ and HCT116 *MAD2*$^{+/-}$ cells and the HCT116 *MAD1*^{kd} cell clone 2-31 were co-treated with nocodazole and the Chk1 kinase inhibitor UCN-01 for 32 h to test, if the percentage of mitotic octaploid cells could be enhanced by drug-induced weakening of the postulated novel G2 checkpoint. Indeed, UCN-01 increased the amount of octaploid mitotic cells in HCT116 *TP53*$^{-/-}$ cells from 7.7% to 13.9% (Figure 17a). However, UCN-01 treatment had no effect on the mitotic population in the other cell lines (Figure 17b). To test whether the ATM and ATR kinases, which act upstream of Chk1 in the DNA damage pathway, are involved, I co-treated cells with caffeine and nocodazole (Figure 17b). In fact, only in p53 deficient cells did ATM/ATR inhibition increase the rate of mitotic entry of octaploid cells.

The results strongly suggest the existence of a novel p53-dependent G2 checkpoint preventing entry of endoreduplicated cells into mitosis. The first identified components of the postmitotic G2 checkpoint might involve p53 and the kinases ATM, ATR and Chk1. Further analysis is required to confirm the involvement of these signaling components in this novel checkpoint.

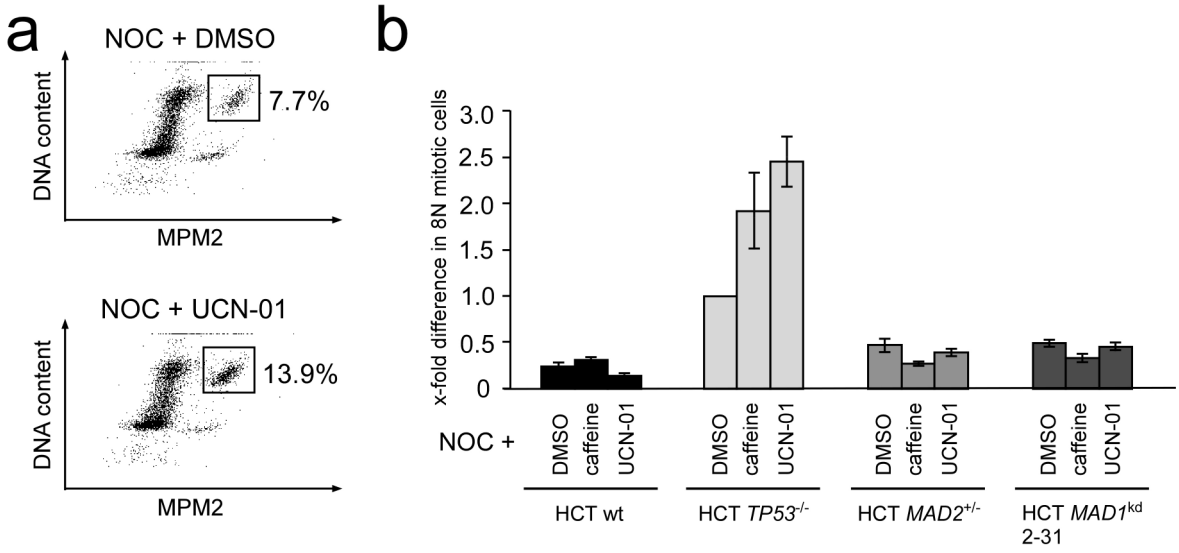

Figure 17: A novel p53-dependent G2 checkpoint is activated upon prolonged spindle damage. a) Mitotic entry of octaploid cells was determined by MPM2 FACS analysis in HCT116 *TP53*$^{-/-}$ cells treated with 150 nM nocodazole (NOC) and solvent (DMSO) or 100 nM UCN-01 for 32 h (the mitotic fraction is highlighted by boxes and quantified). b) Mitotic entry of octaploid cells was compared in HCT116 wt, HCT116 *TP53*$^{-/-}$ and HCT116 *MAD2*$^{+/-}$ cells and the *MAD1*^{kd} cell clone 2-31. The cell lines were treated with 150 nM nocodazole and DMSO, 1.2 mM caffeine or 100 nM UCN-01 for 32 h. The proportion of mitotic octaploid cells was determined by MPM2 FACS analysis and the mitotic entry rate of octaploid cells was calculated as x-fold of the control (the percentage of octaploid mitotic cells in the HCT116 *TP53*$^{-/-}$ cell population treated with nocodazole and solvent was set as 1.0-fold). The mean values and standard deviations from three independent experiments are shown.

p53 is stabilized upon prolonged mitotic arrest and p53 target genes are activated

p53 has been implicated as central player in the prevention of endoreduplication due to induction of cell cycle arrest by our findings and the results of others (Andreassen *et al.* 2003). Cell cycle arrest in G1 or G2 phase can be mediated via p53-dependent transactivation of *CDKN1A/WAF1* transcription (the gene encoding for the kinase inhibitor p21). It was suggested that p53 is activated by tetraploidy and not by mitotic defects

(Andreassen *et al.* 2001). I investigated the contribution of the spindle checkpoint in the prevention of endoreduplication by testing whether spindle damage in mitosis or the tetraploid state upon mitotic slippage activated p53.

p53 and p21 protein accumulation was determined on Western blots of lysates from HCT116 wt, HCT116 wt + pSUPER, HCT116 *TP53*$^{-/-}$, HCT116 *MAD2*$^{+/-}$ cells and the HCT116 *MAD1*^{kd} cell clones 2-2 and 2-31 treated with 150 nM nocodazole for up to 48 h. The cells were also treated with 350 nM adriamycin for 8 h and 14 h as a positive control for p53 and p21 protein accumulation, since adriamycin induces DNA damage resulting in a p53-mediated G1 and G2 arrest and a p53-independent G2 arrest, which are mediated by p21 (Shapiro and Harper 1999).

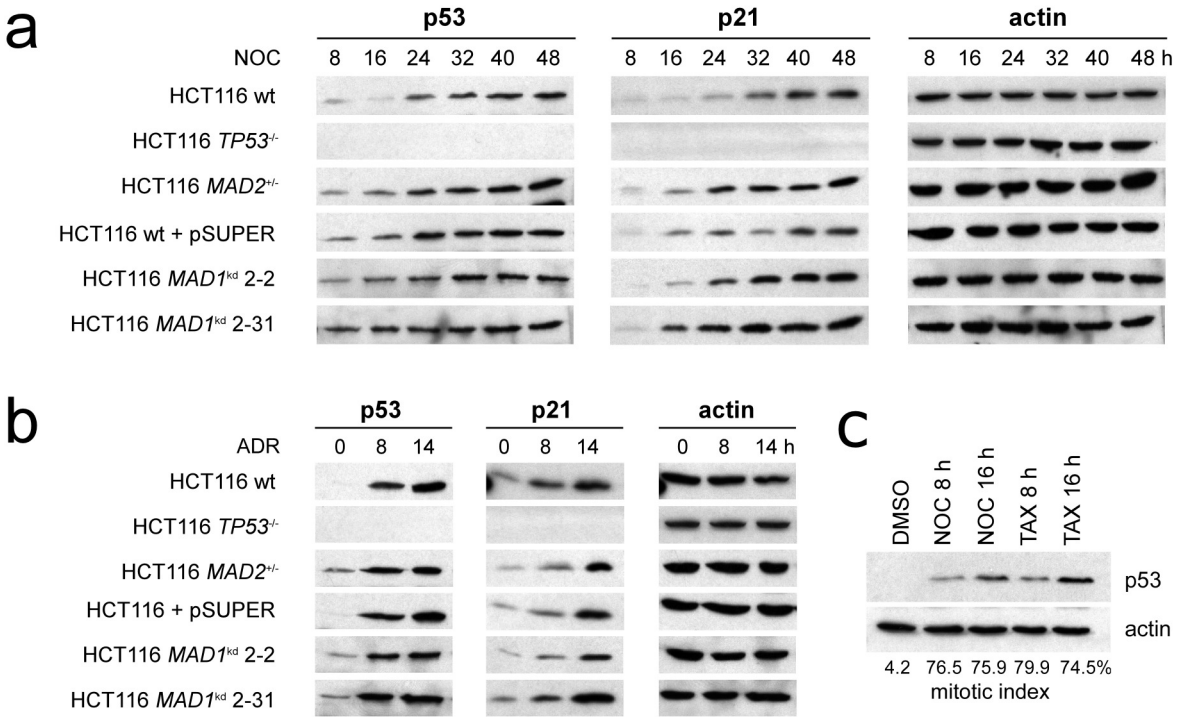

Figure 18: p53 is stabilized and p21 accumulates upon prolonged mitotic arrest. HCT116 wt, HCT116 wt + pSUPER, HCT116 *TP53*$^{-/-}$, HCT116 *MAD2*$^{+/-}$ cells and the HCT116 *MAD1*^{kd} cell clones 2-2 and 2-31 were treated with 150 nM nocodazole (NOC) in 8 h intervals for up to 48 h (a) or 350 nM adriamycin (ADR) for 8 h and 14 h (b). Lysates were analyzed by Western blotting with antibodies directed against p53, p21 and actin as a loading control. Representative blots are displayed. c) HCT116 wt cells were treated with 150 nM nocodazole (NOC) or 100 nM taxol (TAX) for 8 h or 16 h, a mitotic shake-off was performed and p53 stabilization was detected by Western blotting. One representative blot with actin as a loading control is shown and the mitotic indices are given below the blot (provided by Anne Kienitz).

In nocodazole treated cells p53 started to accumulate after 8 h and p53 levels rose steadily throughout the time course, whereas p21 accumulation followed with 8 h lag time,

beginning after 16 h of treatment (Figure 18a). The kinetics of p53 and p21 protein accumulation appeared to be similar in all *TP53*$^{+/+}$ cell lines regardless of their spindle checkpoint status. This result was at odds with the endoreduplication observed in spindle checkpoint compromised, but not in spindle checkpoint normal cells, but could be explained by the different time points of mitotic slippage. In adriamycin treated cells p53 accumulated strongly from 8 h to 14 h, whereas p21 accumulation was weakly visible after 8 h and more pronounced after 14 h of treatment (Figure 18b). To test whether p53 is stabilized already during mitotic arrest, HCT116 wt cells were treated with nocodazole or taxol for 8 h and 16 h, spindle depolymerizing and stabilizing agents, respectively. The amount of mitotic cells was adjusted to comparable mitotic indices by a mitotic shake-off of the treated cells (Figure 18c). The results revealed that p53 accumulation is an early event, beginning after 8 h in mitotically arrested cells independent of the nature of spindle damage.

Since no significant differences in p21 levels were detected in spindle checkpoint compromised cell lines compared to control cell lines, a more sensitive method to detect differences in p53-dependent gene expression was employed. Northern blots allowed quantification of *CDKN1A/WAF1* and *BAX* expression, p53 target genes for cell cycle arrest or apoptosis, respectively. *CDKN1A/WAF1* or *BAX* mRNA signal intensities were normalized on *GAPDH* signals and their expression was compared between nocodazole and adriamycin treated HCT116 wt and HCT116 *MAD2*$^{+/-}$ cell lines (Figure 19a). *CDKN1A/WAF1* mRNA was induced 4.3-fold in HCT116 wt cells after 48 h of nocodazole treatment compared to 2.9-fold in HCT116 *MAD2*$^{+/-}$ cells. *BAX* mRNA induction upon nocodazole treatment was 2.3-fold in HCT116 wt cells and 1.7x in HCT116 *MAD2*$^{+/-}$ cells. Significantly, control treatments with adriamycin showed no significant difference in *CDKN1A/WAF1* and *BAX* mRNA levels between HCT116 wt cells and HCT116 *MAD2*$^{+/-}$ cells.

ChIP assays were performed to prove that the difference in *CDKN1A/WAF1* and *BAX* mRNA levels in nocodazole treated HCT116 wt and HCT116 *MAD2*$^{+/-}$ cell lines was indeed attributable to the transactivation activity of p53. p53 crosslinked to the chromatin was immunoprecipitated and *CDKN1A/WAF1* and *CDC25C* (control) promoter fragments were amplified (Figure 19b). The *CDKN1A/WAF1* promoter signal upon nocodazole treatment was more pronounced in HCT116 wt than in HCT116 *MAD2*$^{+/-}$ cells. Adriamycin treatment was used as a positive control for both cell lines inducing a

CDKN1A/WAF1 promoter signal of similar strength in HCT116 wt and in HCT116 *MAD2*$^{+/-}$ cells.

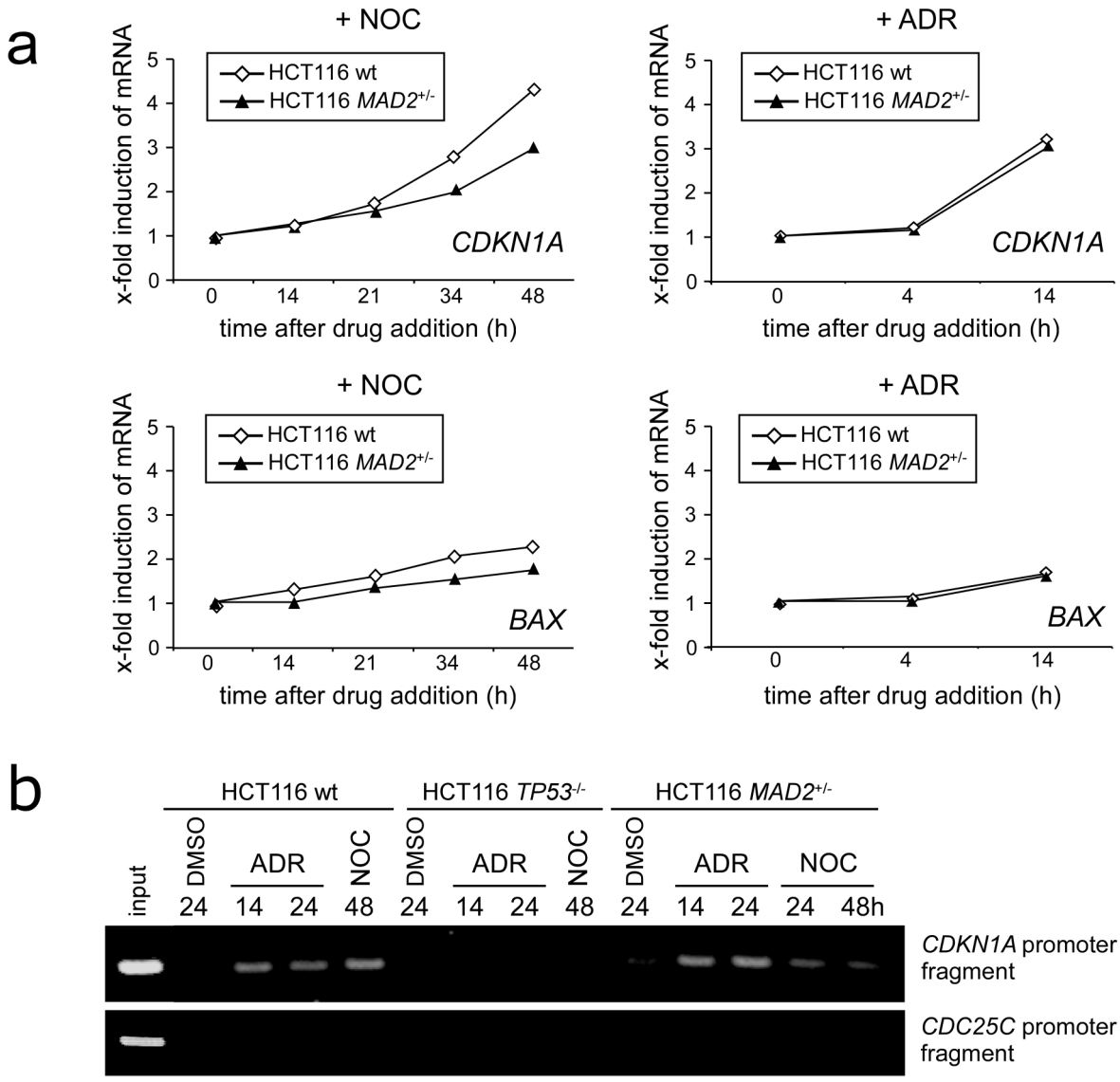

Figure 19: Differential transactivation of the *TP53* target genes *CDKN1A/WAF1* and *BAX* depends on spindle checkpoint and p53 status. a) HCT116 wt cells and HCT116 *MAD2*$^{+/-}$ cells were treated with 150 nM nocodazole (NOC) for up to 48 h, or with 350 nM adriamycin (ADR) for 4 h and 14 h and their RNA was isolated. The Northern blots were probed for mRNAs of *CDKN1A/WAF1* and *BAX*, and their signals normalized on *GAPDH* expression. Mean values from at least three independent experiments were calculated. Hybridization of probes directed against *CDKN1A/WAF1*, *BAX*, and *GAPDH* was performed at 55°C for 16 h, and the blots were washed twice at 55°C. The probe size was 1010 bp, 574 bp, and 905 bp, respectively. Positions - 80, 3, and 213 in the *CDKN1A/WAF1*, *BAX*, and *GAPDH* mRNAs were targeted. b) Lysates from HCT116 wt, HCT116 *TP53*$^{-/-}$ cells, and HCT116 *MAD2*$^{+/-}$ cells treated with 150 nM nocodazole for 24 h, or 48 h or with 350 nM adriamycin for 14 h and 24 h were used. p53 and the DNA fragments bound to it were immunoprecipitated after crosslinking with an antibody directed against p53 and the *CDKN1A/WAF1* and *CDC25C* promoter sequences were amplified by PCR. The PCR products were separated on a 1.5% agarose gel. One representative experiment is shown.

The *CDKN1A/WAF1* promoter signal upon nocodazole treatment was more pronounced in HCT116 wt than in HCT116 *MAD2*$^{+/-}$ cells. Adriamycin treatment was used as a positive control for both cell lines inducing a *CDKN1A/WAF1* promoter signal of similar strength in HCT116 wt and in HCT116 *MAD2*$^{+/-}$ cells. The *CDC25C* promoter was employed as a negative control. Its vacancy in the HCT116 wt and HCT116 *MAD2*$^{+/-}$ cell lysates and the vacancy of the *CDKN1A/WAF1* and *CDC25C* promoters in the HCT116 *TP53*$^{-/-}$ lysates confirmed the specificity for p53 in the assay.

Thus, we showed that prolonged spindle checkpoint activation induced by nocodazole-mediated spindle depolymerization or taxol-mediated spindle stabilization led to p53 protein accumulation already during mitotic arrest. p53 accumulation continued steadily for 48 h in nocodazole treated cells and p53 induced *CDKN1A/WAF1* and *BAX* expression. The transactivational capacity of p53 was reduced in nocodazole treated HCT116 *MAD2*$^{+/-}$ compared to HCT116 wt cells. Transcription of *CDKN1A/WAF1* and *BAX* upon nocodazole treatment was significantly lower in HCT116 *MAD2*$^{+/-}$ than in HCT116 wt cells, which might contribute to the inability of the spindle checkpoint compromised cells to arrest in G1 upon prolonged spindle damage.

Spindle damage-induced p53 accumulation is independent of the classical DNA damage pathway

Since p53 is stabilized and activated in response to spindle damage, I asked whether known components of the DNA damage checkpoint participate in this process. DNA damage activates ATM, ATR, Chk1 and Chk2 kinases, which are upstream regulators of p53, but can also act in a p53-independent pathway (Shiloh 2001). I tested whether one of these kinases was responsible for p53 activation upon prolonged spindle damage. Furthermore, a panel of stress kinase inhibitors was employed to detect other potential p53 activators. Caffeine is a well known inhibitor of ATM and ATR kinase activity (Blasina *et al.* 1999, Hall-Jackson *et al.* 1999). Pre-incubation with 1.2 mM caffeine did not affect p53 or p21 protein accumulation in HCT116 wt cells treated with nocodazole for 40 h, but abrogated p53 or p21 protein accumulation and p53-dependent cell cycle arrest upon control treatment with adriamycin as expected (Figure 20a). At a concentration of 100 nM the established Chk1 kinase inhibitor UCN-01 (Wang *et al.* 1996, Graves *et al.* 2000) did not influence p53 or p21 accumulation in HCT116 wt cells treated with either nocodazole

for 40 h or with adriamycin for 14 h, but abrogated p53-independent G2 cell cycle arrest upon control treatment with adriamycin (Figure 20b).

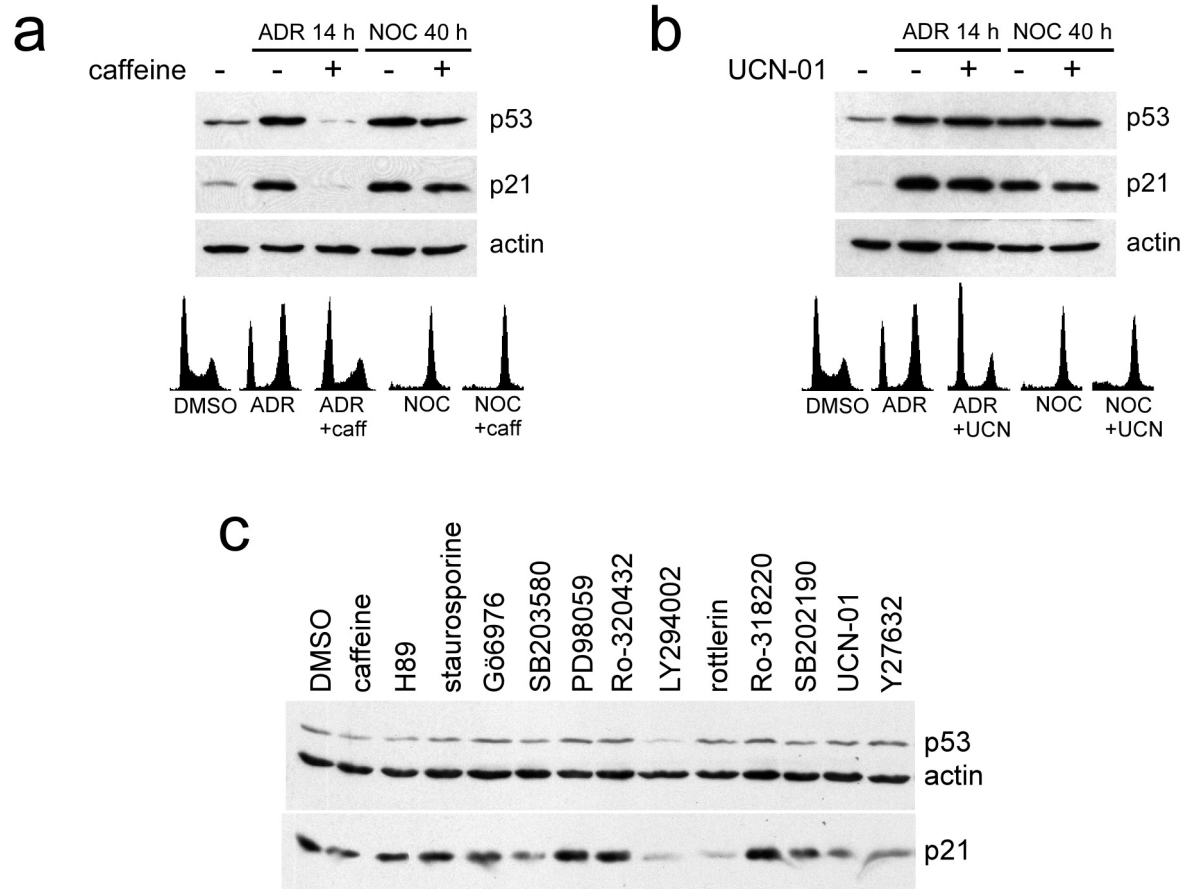

Figure 20: p53 is stabilized in response to spindle damage independent of ATM, ATR and Chk1. HCT116 wt cells were pre-incubated with DMSO, 1.2 mM caffeine (a) or 100 nM UCN-01 (b) for 2 h followed by treatment with 350 nM adriamycin for 14 h or 150 nM nocodazole for 40 h. Upper panels: Western blot analysis of p53, p21 and actin levels. Lower panels: PI FACS profiles of the same samples. Representative Western blots and FACS analyses are shown. c) A panel of protein kinase inhibitors was tested for their effects on p53 accumulation and p21 expression upon nocodazole treatment on a Western blot with actin as a loading control. HCT116 wt cells were treated with the kinase inhibitors for 2 h and subsequently with 150 nM nocodazole for 32 h. Kinase inhibitors: Inhibitors of the MAPK family: 50 µM PD98059 (inhibits MEK, ERK), 15 µM SB202190 (inhibits p38), 20 µM SB203580 (inhibits p38), inhibitor of PKA: 10 µM H89, inhibitors of PKC: 20 µM rottlerin, 1 µM Ro-318220, 200 nM Ro-320432, inhibitor of PI_3K: 50 µM LY294002, inhibitor of ROCK I and II: 10 µM Y27632, a broad spectrum inhibitor of kinases: 20 nM staurosporine, inhibitor of ATM/ATR: 1.2 mM caffeine, inhibitors of Chk1: 2 µM Gö6976 and 100 nM UCN-01. One Western blot representative of several experiments is shown.

An involvement of Chk2 in p53 activation upon prolonged spindle damage was investigated using the HCT116 *CHK2*$^{-/-}$ cell line (Jallepalli *et al.* 2003). HCT116 wt cells and HCT116 *CHK2*$^{-/-}$ cells were exposed to nocodazole for up to 48 h and p53 and p21

protein levels were determined by Western blotting. No differences in p53 or p21 accumulation between the cell lines were observed, suggesting that Chk2 does not play a role in p53 accumulation upon prolonged spindle damage (data not shown, experiment performed by Anne Kienitz). Likewise, ATM, ATR and Chk1 might not participate in p53 activation upon prolonged spindle damage. Therefore other kinases were investigated for their ability to promote p53 accumulation upon nocodazole treatment. HCT116 wt cells were treated with various kinase inhibitors for 2 h before 150 nM nocodazole was added for 32 h and p53 and p21 protein levels were checked on a Western blot. A panel of kinase inhibitors was used: Inhibitors of the MAPK family: 50 µM PD98059 (inhibits MEK, ERK), 15 µM SB202190 (inhibits p38) and 20 µM SB203580 (inhibits p38), the PKA inhibitor H89 at 10 µM, the PKC inhibitors rottlerin at 20 µM, Ro-318220 at 1 µM and Ro-320432 at 200 nM, the PI_3K inhibitor LY294002 at 50 µM, the ROCK I and II inhibitor Y27632 at 10 µM, the broad spectrum kinase inhibitor staurosporine at 20 nM, the ATM/ATR inhibitor caffeine at 1.2 mM, and the Chk1 inhibitors Gö6976 at 2 µM and UCN-01 at 100 nM. p53 and p21 accumulation was markedly reduced by treatment with LY294002 and p21 accumulation was diminished by rottlerin, whereas the other kinase inhibitors did not influence p53 accumulation and did reduce p21 accumulation only weakly (Figure 20c).

These results suggest that ATM, ATR, Chk1 and Chk2 do not participate in p53 activation upon prolonged spindle damage. The involvement of the kinases MEK, ERK, p38, PKA, PKC, ROCK I and ROCK II is also unlikely. However, the PI_3K inhibitor LY294002 reduced p53 and p21 accumulation, suggesting a role for PI_3K or other LY294002-sensitive kinases in p53 activation upon prolonged spindle damage. This interesting finding should be further investigated in future experiments.

In sum, endoreduplication takes place upon prolonged spindle damage in cells lacking functional p53 or an intact spindle checkpoint. A compromised spindle checkpoint allows endoreduplication only once, but continuous accumulation of p53 prevents further endoreduplication, whereas in *TP53*$^{-/-}$ cells endoreduplication continues unimpeded. p53 accumulation begins already during mitotic arrest and transactivates *CDKN1A/WAF1* (promoting arrest) and *BAX* (promoting apoptosis). These target genes are activated to a lesser extent in the spindle checkpoint impaired HCT116 *MAD2*$^{+/-}$ cells, thereby permitting transient evasion of pseudo-G1 arrest and apoptosis. Spindle damage-induced p53 stabilization might be independent of ATM, ATR, Chk1 and Chk2 kinases, but PI_3K might

aid p53 stabilization. A novel p53-dependent G2 checkpoint prevents entry of octaploid cells into mitosis. Its function might involve the checkpoint kinases ATM, ATR and Chk1.

3. Spindle damage-induced apoptosis is controlled by the spindle checkpoint and p53

The spindle checkpoint is activated by spindle damaging agents used in anti-cancer chemotherapy such as *Vinca* alkaloids (e.g. vincristine, vinblastine) or taxanes (e.g. docetaxel, paclitaxel), which interfere with spindle dynamics and at high doses depolymerize (Jordan *et al.* 1992) or stabilize the mitotic spindle (Jordan *et al.* 1996), respectively, and monastrol or KSP1 inhibitors that generate a monopolar spindle (Mayer *et al.* 1999, Tao *et al.* 2005, Schmidt and Bastians 2007). Despite their different effect on the mitotic spindle all spindle damaging agents interfere with chromosome alignment, resulting in spindle checkpoint-mediated cell cycle arrest in metaphase and subsequent cell death (Jordan and Wilson 2004). Though it is known for a long time that taxanes kill cancer cells by induction of apoptosis (Lanni *et al.* 1997, Blajeski *et al.* 2001), the signaling upon spindle damage is unclear (Bhalla 2003). Furthermore, little is known about spindle damaging agents with a different mechanism of action than taxol and how they induce cell death (Mollinedo and Gajate 2003, Schmidt and Bastians 2007). Therefore, we investigated the role of the spindle checkpoint for the induction of apoptosis in response to spindle damage.

Spindle damage-induced apoptosis depends on agent concentration, duration of treatment and cell line characteristics

The contribution of the spindle checkpoint proteins Mad1 and Mad2 and the DNA damage pathway components p53 and Chk2 to spindle damage-induced apoptosis was investigated. The concentration dependence of spindle damage-induced apoptosis was tested by measuring the sub G1 DNA content indicative of cell death. HCT116 wt, HCT116 *TP53*$^{-/-}$, HCT116 *CHK2*$^{-/-}$, HCT116 *MAD2*$^{+/-}$ cells and the HCT116 *MAD1*^{kd} cell clone 2-31 were treated for 48 h either with nocodazole concentrations of 150-500 nM, with taxol concentrations of 100-300 nM or with monastrol concentrations ranging from 10-100 µM (Figure 21a). The nocodazole and taxol concentrations tested had a similar effect, showing no concentration dependency of cell death. HCT116 *TP53*$^{-/-}$, HCT116 *MAD2*$^{+/-}$ cells and the *MAD1*^{kd} cell clone 2-31 were resistant to nocodazole or taxol treatment, whereas HCT116 wt and HCT116 *CHK2*$^{-/-}$ cells were sensitive. In contrast, monastrol-induced cell killing showed a clear concentration dependency. Concentrations exceeding 25 µM were

required to induce significant sub G1 populations and an increased agent concentration correlated with enhanced cell death.

Time-dependent analyses revealed that cell death upon spindle damage increased markedly during treatment for up to 72 h with nocodazole, taxol or monastrol (Figure 21b). Most importantly, upon all spindle damaging treatments HCT116 *TP53*$^{-/-}$, HCT116 *MAD2*$^{+/-}$ cells and the *MAD1*^{kd} cell clone 2-31 escaped from cell death, whereas the controls were susceptible to killing, suggesting that the spindle checkpoint might play an important role in mediating cell death in response to spindle damage.

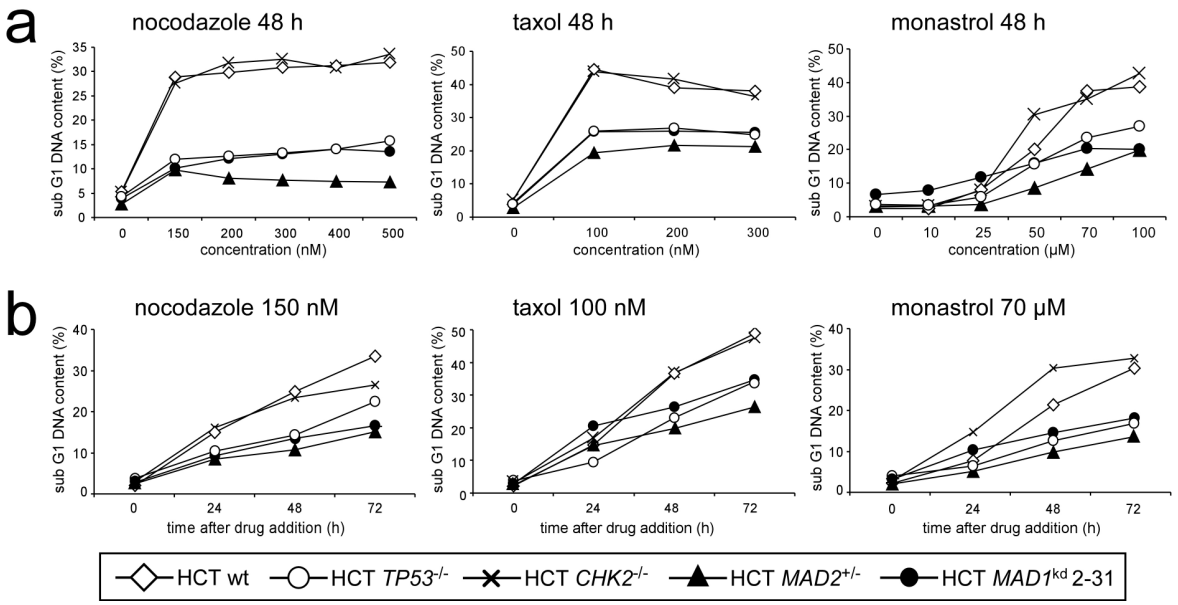

Figure 21: Spindle damage-induced apoptosis depends on agent concentration, duration of treatment and cell line characteristics. HCT116 wt, HCT116 *TP53*$^{-/-}$, HCT116 *CHK2*$^{-/-}$, HCT116 *MAD2*$^{+/-}$ cells and the HCT116 *MAD1*^{kd} cell clone 2-31 were treated with nocodazole concentrations of 150-500 nM, with taxol concentrations of 100-300 nM or with monastrol concentrations of 10-100 µM for 48 h (a) or with 150 nM nocodazole, 100 nM taxol or with 70 µM monastrol for 24 h, 48 h and 72 h (b). The mean values and standard deviations of at least three independent PI FACS analyses of sub-diploid DNA content were calculated.

To discern the roles of Mad1, Mad2 and p53 proteins in cell death upon spindle damaging drug treatment, apoptosis specific assays were employed. Determining the sub-diploid DNA content cannot be used to discriminate between apoptosis and other forms of cell death. Therefore, HCT116 wt, HCT116 *TP53*$^{-/-}$, HCT116 *MAD2*$^{+/-}$ cells and the HCT116 *MAD1*^{kd} cell clone 2-31 were treated with 150 nM nocodazole, 100 nM taxol or with 70 µM monastrol for 40 h to 48 h.

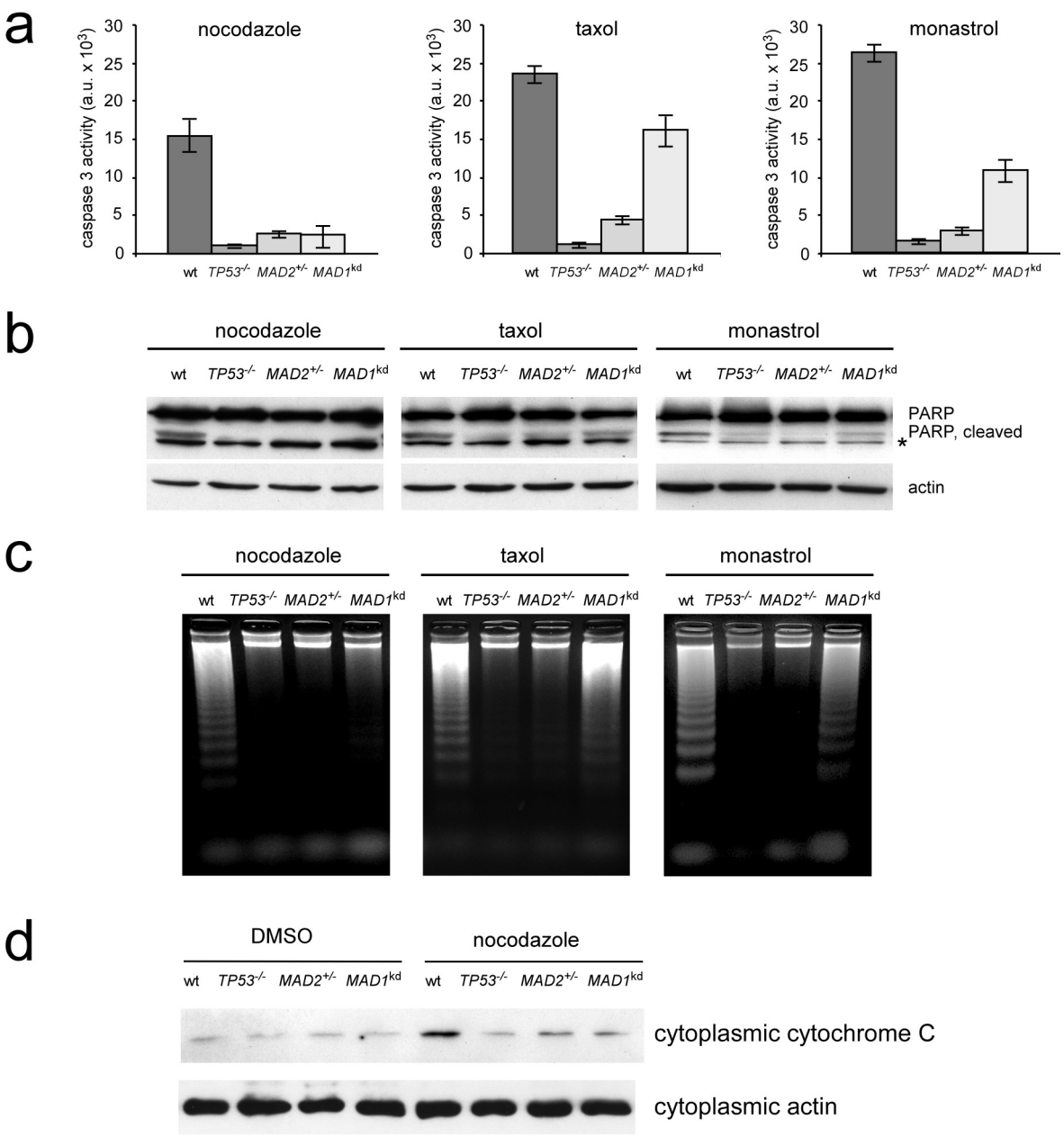

Figure 22: Spindle checkpoint proteins confer differential susceptibility to spindle damage-induced apoptosis. HCT116 wt, HCT116 *TP53*$^{-/-}$, HCT116 *MAD2*$^{+/-}$ cells and the HCT116 *MAD1*^{kd} cell clone 2-31 were treated with 150 nM nocodazole, 100 nM taxol or with 70 µM monastrol for 40 h (a) or 48 h (b, c, d). a) 1 x 10^5 cells per well were seeded 24 h prior to treatment. Caspase 3 activity was quantitatively determined using a fluorogenic peptide substrate. Background fluorescence of untreated cells was subtracted before mean values and standard deviations from three independent experiments were calculated. b) PARP cleavage was assessed by Western blotting (in collaboration with Anne Kienitz). The asterisk indicates a nonspecific cross-reacting band. Representative Western blots are displayed. c) Internucleosomal DNA cleavage was detected by a DNA laddering assay. Representative gels are shown. d) Cytochrome C release from mitochondria into the cytoplasm was revealed by subcellular fractionation and subsequent Western blotting of the cytoplasmic fraction. Actin was detected as a loading control. A representative Western blot is shown.

Hallmark parameters of apoptosis including caspase 3 activation, which was determined in a quantitative enzymatic assay (Figure 22a), PARP cleavage, which was assessed by Western blotting (Figure 22b) and internucleosomal DNA cleavage, which was detected by a DNA laddering assay (Figure 22c) were determined. Cytochrome C release from the mitochondria into the cytoplasm is characteristic for apoptosis executed by the intrinsic pathway and was detected by Western blotting of the cytoplasmic fraction of treated cells (Figure 22d). Caspase activation, PARP cleavage and DNA laddering induced by nocodazole, taxol and monastrol were very low in HCT116 *MAD2*$^{+/-}$ and HCT116 *TP53*$^{-/-}$ cells and high in HCT116 wt cells. These results clearly indicate that Mad2 is important for apoptosis induction upon spindle damage and that in HCT116 cells spindle damage-induced apoptosis is strictly p53-dependent. Surprisingly, HCT116 *MAD1*^{kd} cells were resistant to nocodazole-induced apoptosis, but partially susceptible to taxol and monastrol-induced apoptosis. HCT116 wt cells activated caspase 3 after nocodazole, taxol and monastrol treatment to 15000, 24000 and 26000 a.u. (activity given in arbitrary units), whereas HCT116 *MAD1*^{kd} cells induced caspase 3 to 2500, 16000 and 11000 a.u. (Figure 22a). Cytochrome C release indicated that nocodazole-induced apoptosis in HCT116 wt cells in particular via the intrinsic pathway of apoptosis, whereas HCT116 *TP53*$^{-/-}$, HCT116 *MAD2*$^{+/-}$ and HCT116 *MAD1*^{kd} cells escaped from nocodazole-induced apoptosis (Figure 22d).

Nocodazole- or taxol-induced apoptosis requires normal levels of spindle checkpoint proteins

To further investigate the contribution of the spindle checkpoint proteins to spindle damage-induced apoptosis, I used a different experimental system. The spindle checkpoint proteins Mad2, BubR1 and Bub1 were transiently downregulated by electroporation of shRNA vectors into HeLa cells. HeLa cells are sensitive to taxol-induced apoptosis despite their lack of functional p53 protein (Lanni *et al.* 1997).

To control spindle checkpoint impairment as an indicator of successful downregulation of the spindle checkpoint components 150 nM nocodazole or 100 nM taxol were added for 16 h and a MPM2 FACS analysis was performed (Figure 23a). Samples with a mitotic index below 30% were chosen for caspase 3 assays. Downregulation of *BUB1*, *BUB1B* or *MAD2* reduced caspase 3 activity upon nocodazole treatment to 56%, 31% or 30% of empty

vector control levels (Figure 23b). Downregulation of *BUB1B* or *MAD2* reduced caspase 3 activity upon taxol treatment to 51% or 43% of empty vector control levels (Figure 23c). Similar to the experiments using HCT116 cells theses results revealed that the major spindle checkpoint components *BUB1*, *BUB1B* and *MAD2* are each required for spindle damage-induced apoptosis in HeLa cells.

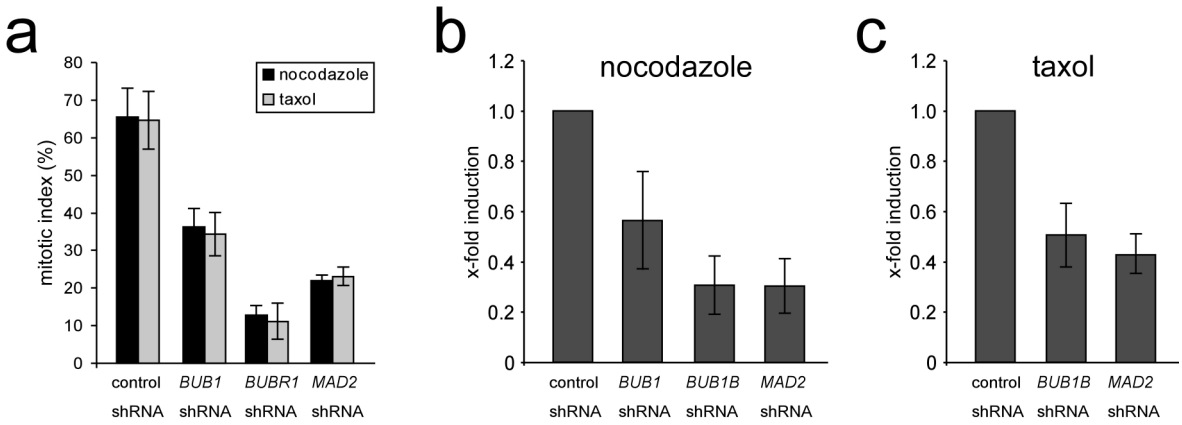

Figure 23: Reduced levels of spindle checkpoint proteins confer resistance to nocodazole or taxol. a) HeLa cells were transiently transfected with shRNA constructs directed against *BUB1*, *BUB1B* and *MAD2* and the empty vector as control. 15, 15, 7.5 and 7.5 µg plasmid, respectively, were used to electroporate 1.6 x 10^6 cells. 1 x 10^5 cells were seeded immediately after transfection. 24 h later 150 nM nocodazole or 100 nM taxol were added for 16 h and the mitotic index was determined by MPM2 FACS analysis. Mean values of three independent experiments are shown. b), c) 24 h post-transfection 150 nM nocodazole (b) or 100nM taxol (c) were added for 38 h and caspase 3 activity was measured in a fluorometric assay. Background fluorescence of untreated cells was subtracted before mean values and standard deviations from at least three independent experiments were calculated.

Surprisingly, in these experiments, a differential requirement of Mad1 and Mad2 for apoptosis induction by spindle damage was uncovered. Normal levels of Mad1 were required for nocodazole-induced apoptosis, but were largely dispensable for taxol- or monastrol-induced apoptosis. Mad2, however, was essential for a proapoptotic response to all three spindle damaging agents. Also, a strict dependency on p53 in spindle damage-induced apoptosis was found in HCT116 cells, but not in HeLa cells. In HeLa cells apoptosis induced by nocodazole required normal levels of Mad2, BubR1 and Bub1 and apoptosis induced by taxol normal levels of Mad2 and BubR1.

4. Reduced Mad2 levels confer resistance to topoisomerase inhibitor-induced apoptosis

Anti-cancer chemotherapy targets cell cycle checkpoints (Shapiro and Harper 1999, Eastman 2004, Kastan and Bartek 2004). Many members of the large group of anti-cancer drugs inflict DNA damage (Eastman 2004, Kastan and Bartek 2004), but the mitotic spindle is also a common target of chemotherapy (Jordan and Wilson 2004, Tao 2005, Weaver and Cleveland 2005, Zhou and Giannakakou 2005, Schmidt and Bastians 2007). Several agents can activate the DNA damage checkpoints. Inhibitors of topoisomerase I (e.g. camptothecin derivatives) or topoisomerase II (e.g. doxorubicin/adriamycin, VP-16/etoposide) cause DNA strand breaks that activate the DNA damage checkpoints via the kinases ATM, ATR, Chk1, Chk2 and the transcription factor p53 (Shiloh 2001, McGowan 2002). G1/S arrest depends on p53 signaling, whereas G2/M arrest can be activated by p53-dependent and p53-independent pathways. The nucleotide analogue 5-fluorouracil is a chemotherapeutic drug with a different mechanism of action. It inhibits DNA synthesis by depleting the intracellular dTTP pool leading to arrest in early S phase (Sampath *et al.* 2003). UV light produces mainly thymine dimers, which inhibit DNA replication and transcription (Smith *et al.* 2000).

I investigated whether the spindle checkpoint had a role in DNA damage-induced apoptosis in addition to its role in spindle damage-induced apoptosis. It is conceivable that some cells escape G2 arrest upon DNA damage, enter mitosis in the presence of DNA damage and die due to spindle checkpoint activation. Spindle checkpoint impaired cells, however, might escape apoptosis upon DNA damage. Furthermore, reduced *MAD2* levels confer resistance to various spindle damaging agents (nocodazole, taxol, monastrol), whereas a repression of *MAD1* only confers resistance to nocodazole. A similar functional difference as observed upon spindle damage might exist between *MAD1* and *MAD2* in apoptosis induction by topoisomerase inhibitors, 5-fluorouracil or UV light. To test this hypothesis, the role of the spindle checkpoint in apoptosis induction upon DNA damage was investigated in HCT116 *MAD2*$^{+/-}$ or HCT116 *MAD1*^{kd} cells. Employing HCT116 *TP53*$^{-/-}$ and HCT116 *CHK2*$^{-/-}$ cells allowed to study components of the DNA damage pathways.

Adriamycin-, 5-fluorouracil- or UV light-induced apoptosis depends on agent concentration, duration of treatment and cell line characteristics

It should be determined whether the spindle checkpoint proteins Mad1 or Mad2 have an additional role in apoptosis upon DNA damage similar to their different roles in spindle damage-induced apoptosis. HCT116 wt, HCT116 *TP53*$^{-/-}$, HCT116 *CHK2*$^{-/-}$, HCT116 *MAD2*$^{+/-}$ cells and the HCT116 *MAD1*^{kd} cell clone 2-31 were treated with different concentrations of adriamycin (500-2000 nM), of 5-fluorouracil (10-100 µg/ml) or different energies of UV light (50-100 J/m^2) for 48 h (Figure 24a) and cell death was determined by measuring the sub G1 DNA content. Time-dependent apoptosis upon treatment of the HCT116 cell lines for 24 h, 48 h and 72 h with 750 nM of adriamycin, 50 µg/ml of 5-fluorouracil or 50 J/m^2 of UV light was also tested (Figure 24b). Adriamycin treatment stimulated a differential behavior of the HCT116 cell lines. As expected, wild type cells were sensitive and *TP53*$^{-/-}$ cells were resistant to adriamycin-induced cell death (Bunz *et al.* 1998). HCT116 *CHK2*$^{-/-}$ cells were resistant to low adriamycin concentrations of 500 or 750 nM, but their sensitivity to higher concentrations increased until they died like HCT116 wt cells at the highest concentration of 2000 nM of adriamycin. Most surprisingly, reduced levels of *MAD2* led to resistance to adriamycin even at 2000 nM, but HCT116 *MAD1*^{kd} cells were sensitive to adriamycin-induced death at all concentrations (Figure 24a). Treatment with 750 nM adriamycin for up to 72 h showed resistance of HCT116 *TP53*$^{-/-}$, HCT116 *CHK2*$^{-/-}$ and HCT116 *MAD2*$^{+/-}$ cells and sensitivity of HCT116 wt and HCT116 *MAD1*^{kd} cells at all time points (Figure 24b). In agreement with previous observations (Kinsella and Smith 1998) 5-fluorouracil treatment killed all *TP53*$^{+/+}$ cell lines effectively at all concentrations (Figure 24a) and upon prolonged treatment (Figure 24b), whereas HCT116 *TP53*$^{-/-}$ cells were resistant. All HCT116 cell lines cells were similarly susceptible to killing by UV light with the exception of *TP53*$^{-/-}$ cells, which were less sensitive. Cell death increased with rising energies of 50-100 J/m^2 applied on the cells (Figure 24a) or prolonged treatment for up to 72 h (Figure 24b). Since, surprisingly, reduced *MAD2* levels conferred resistance to adriamycin treatment even at high drug concentrations, whereas HCT116 *MAD1*^{kd} cells were sensitive, it was tested whether HCT116 *MAD2*$^{+/-}$ cells were resistant not only to adriamycin, but also to etoposide, another topoisomerase II inhibitor widely used in chemotherapy. HCT116 wt and HCT116 *MAD2*$^{+/-}$ cells were treated with different concentrations of etoposide (50-200 µM) for 48 h to induce apoptosis (Figure 24c).

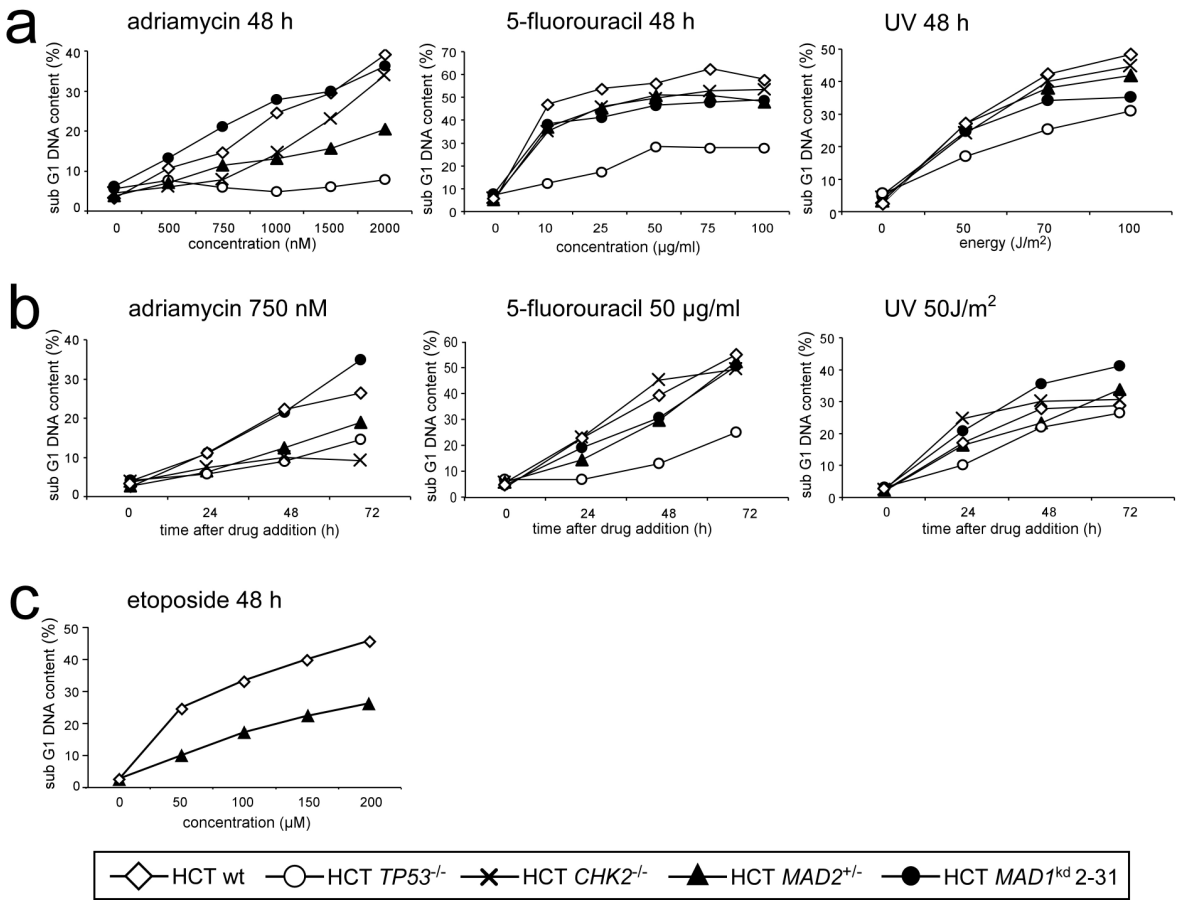

Figure 24: Apoptosis induction depends on agent concentration, duration of treatment and cell line characteristics. HCT116 wt, HCT116 *TP53*$^{-/-}$, HCT116 *CHK2*$^{-/-}$, HCT116 *MAD2*$^{+/-}$ cells and the *MAD1*^{kd} cell clone 2-31 were treated with DNA damage checkpoint activating agents and cell death was measured by determining the sub G1 DNA content by PI FACS analysis. The HCT116 cell lines indicated were treated with a) 500-2000 nM adriamycin (ADR), 10-100 µg/ml 5-fluorouracil (5-FU) or 50-100 J/m^2 UV light (UV) for 48 h, b) with 750 nM adriamycin, 50 µg/ml 5-fluorouracil or 50 J/m^2 UV light for 24 h, 48 h and 72 h or c) with 50-200µM etoposide for 48 h. Mean values were calculated from at least three independent experiments.

HCT116 *MAD2*$^{+/-}$ cells were similarly resistant to etoposide as to adriamycin treatment. At a concentration of 2 µM adriamycin, 40% of the HCT116 wt cell population, but only 20% of the HCT116 *MAD2*$^{+/-}$ cell population were dead. Similarly, at a concentration of 200 µM etoposide, 46% of the HCT116 wt cell population, but only 26% of the HCT116 *MAD2*$^{+/-}$ cell population were killed. The results clearly indicate a proapoptotic function of *MAD2* in HCT116 cells upon treatment with the topoisomerase II inhibitors adriamycin and etoposide.

p53 accumulates due to adriamycin, 5-fluorouracil or UV light treatment and is required for adriamycin- or 5-fluorouracil-, but not UV light-induced apoptosis

The surprising finding that reduced levels of *MAD2*, but not of *MAD1* conferred resistance to adriamycin-induced apoptosis should be confirmed and the role of p53 for differential apoptosis induction should be elucidated.

Since *TP53* is required for adriamycin-induced apoptosis in HCT116 cells, I checked whether p53 protein accumulation was reduced in HCT116 *MAD2*$^{+/-}$ cells compared to controls as a possible explanation for the observed resistance. HCT116 wt, HCT116 *TP53*$^{-/-}$, HCT116 *CHK2*$^{-/-}$, HCT116 *MAD2*$^{+/-}$ cells and the HCT116 *MAD1*^{kd} cell clone 2-31 were treated with adriamycin, 5-fluorouracil or UV light for 48 h. PARP cleavage indicative of apoptosis and p53 levels were detected on Western blots (Figure 25) and the results for the PARP cleavage confirmed the results of the sub G1 DNA content determination (Figure 24). The adriamycin-resistant cell lines HCT116 *TP53*$^{-/-}$, HCT116 *CHK2*$^{-/-}$ and HCT116 *MAD2*$^{+/-}$ and the 5-fluorouracil-resistant HCT116 *TP53*$^{-/-}$ cells showed almost no cleaved PARP fragment, whereas all samples clearly showed the full length fragment.

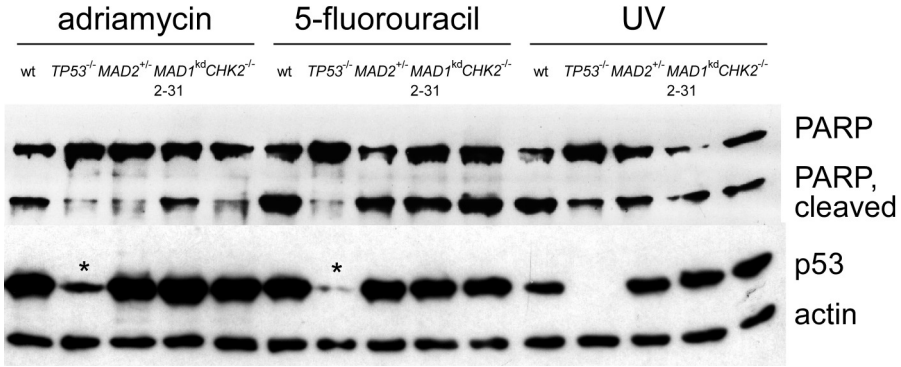

Figure 25: p53 accumulates due to adriamycin, 5-fluorouracil or UV light treatment and is required for adriamycin-, or 5-fluorouracil-, but not UV light-induced apoptosis. a) HCT116 wt, HCT116 *TP53*$^{-/-}$, HCT116 *MAD2*$^{+/-}$, HCT116 *CHK2*$^{-/-}$ cells and the *MAD1*^{kd} cell clone 2-31 were treated with 750 nM adriamycin, 50 µg/ml 5-fluorouracil or 50 J/m^2 UV light for 48 h. p53 accumulation, PARP cleavage and actin as a loading control were determined by Western blotting. The asterisk indicates a contamination with p53 containing sample from the neighboring lanes. One representative experiment is shown.

p53 accumulated in all treated HCT116 *TP53*$^{+/+}$ cell lines. The signal intensity depended on the treatment, but not on the cell line, as adriamycin induced the most pronounced p53

accumulation, UV light the least. The observed differences in apoptosis between the spindle checkpoint compromised cell lines cannot be attributed to differential p53 accumulation *per se*. However, differences in p53 activation influencing its transactivation or -repression abilities cannot be ruled out, as demonstrated for prolonged nocodazole treatment of HCT116 wt and HCT116 *MAD2*$^{+/-}$ cells (Figure 19).

Ovary cancer cell lines with reduced Mad2 protein levels are resistant to adriamycin treatment

To investigate the proapoptotic role of Mad2 in topoisomerase inhibitor-induced apoptosis in cancer cell lines with a intrinsic spindle checkpoint impairment, ovary cancer cell lines were employed that exhibit reduced levels of Mad1 or Mad2 protein (Wang *et al.* 2002). I assessed the apoptotic behavior of these ovarian cancer cell lines upon adriamycin treatment.

First, the spindle checkpoint status of the ovary cancer cell lines Ovca 420, 429, 432 and 433 was evaluated in one exploratory experiment. The cell lines were treated with 150 nM nocodazole or 100 nM taxol for 16 h and the mitotic index was determined by MPM2 FACS analysis (Figure 26a). All cell lines had a different capability to arrest in mitosis. The response of each cell line to either nocodazole or taxol treatment was almost identical. The spindle checkpoint response of Ovca 429 cells was stronger than that of the other cell lines. These results confirmed earlier characterizations of these cell lines obtained by cell counting (Wang *et al.* 2002). However, the cell growth of untreated cells, the time-dependent spindle checkpoint response to spindle damage or the Mad1, Mad2 and p53 protein levels were not checked. The four Ovca cell lines were treated with 500-2000 nM adriamycin for 48 h and apoptosis was quantified by sub G1 DNA content measurements in one exploratory experiment (Figure 26b). At a concentration of 2 µM adriamycin Ovca 429 cells died to 38%, whereas the Ovca 420, 432 and 433 cell lines displayed resistance to adriamycin-induced apoptosis with sub G1 values of 4%, 14% and 6%.

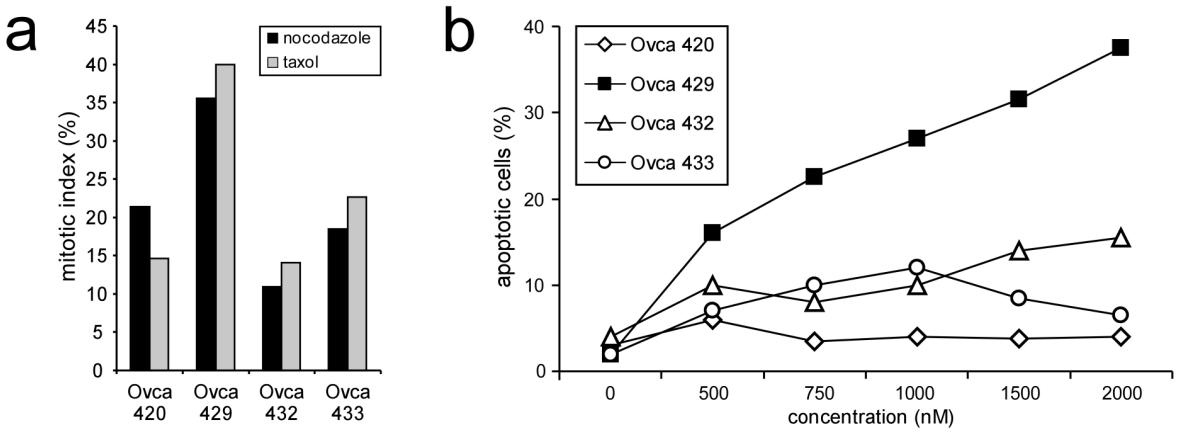

SCP status	-	+/-	-	-
Mad1 status	25%	100%	100%	100%
Mad2 status	25%	100%	25%	25%
p53 status	+	+	-	+

Figure 26: Susceptibility of ovarian cancer cell lines to adriamycin treatment. a) Ovca 420, 429, 432 and 433 cells were treated with 150 nM nocodazole or 100 nM taxol for 16 h. The mitotic index of one experiment determined by MPM2 FACS is presented. Mad1 and Mad2 protein levels and *TP53* status of the cell lines are indicated in the table below as given in the literature (Wang *et al.* 2002). b) Ovca 420, 429, 432 and 433 cells were treated with 500-2000 nM adriamycin for 48 h. Cell death was quantified from one experiment by determination of sub G1 DNA content.

Thus, similar to HCT116 *MAD2*$^{+/-}$ cells, ovary cancer cells with lowered Mad2 protein levels were also resistant to adriamycin-induced apoptosis. This supports a novel role of the spindle checkpoint protein Mad2 in topoisomerase inhibitor-induced apoptosis. Moreover, since Mad1 is dispensable for the proapoptotic role of Mad2, it seems possible that this novel function of Mad2 might be independent of the spindle checkpoint.

5. Apoptosis induction by G2 checkpoint abrogation is governed by pro- and antiapoptotic components of the spindle checkpoint

Given the fact that Mad2 has an important function in mediating apoptosis in response to spindle damage and topoisomerase inhibition, I evaluated another form of cell death known as "mitotic catastrophe". The induction of "mitotic catastrophe" by G2 checkpoint abrogation is a novel chemotherapeutic strategy to selectively target p53-deficient cells for killing (Kawabe 2004). To induce "mitotic catastrophe" under clinically relevant conditions cells were treated with the topoisomerase inhibitor adriamycin to arrest them in G2 and subsequently with the Chk1 inhibitor UCN-01 to induce mitotic entry in the presence of DNA damage. Since it is controversial which kind of cell death "mitotic catastrophe" constitutes and whether the time point of its execution lies in or after mitosis (Castedo *et al.* 2004, Okada and Mak 2004), I tested whether "mitotic catastrophe" constituted a special case of apoptosis and which apoptotic parameters were activated. The significance of various spindle checkpoint proteins in the induction of mitotic arrest or regulation of cell death upon induction of "mitotic catastrophe" by G2 checkpoint abrogation was investigated by employing shRNA-mediated and pharmacological inhibition of these proteins. Furthermore, new ways to improve chemotherapy-induced cancer cell killing by mitotic catastrophe were explored.

G2 checkpoint abrogation activates a spindle checkpoint-mediated mitotic arrest in topoisomerase inhibitor treated cells lacking functional p53

HCT116 wt and HCT116 *TP53*$^{-/-}$ cells were used to test the strategy of G2 checkpoint abrogation. Cells were treated with adriamycin and subsequently with UCN-01 or DMSO and the mitotic index was determined. Mitotic entry occurred only in HCT116 *TP53*$^{-/-}$ cells treated with adriamycin and UCN-01, whereas the HCT116 wt cells and adriamycin treated HCT116 wt and HCT116 *TP53*$^{-/-}$ cells remained arrested in G2 phase (Figure 27a). The percentage of mitotic cells in adriamycin and UCN-01 treated HCT116 *TP53*$^{-/-}$ cells rose from 8.5% after 3 h of UCN-01 treatment to 16% after 9 h (Figure 27a). Immuno-fluorescence staining of HCT116 *TP53*$^{-/-}$ cells treated with adriamycin for 14 h and UCN-01 for 6 h revealed spindle checkpoint activation, since Bub1 and BubR1 were localized at the kinetochores (Figure 27b). The chromosomes were condensed, but largely unaligned (Figure 27b). Forced mitotic entry was accompanied by an increase in the sub

G1 DNA content to a value of 15% after 12 h in adriamycin and UCN-01 treated HCT116 *TP53*$^{-/-}$ cells (Figure 27c). Upon prolonged adriamycin and UCN-01 treatment of *TP53*$^{-/-}$ cells a substantial proportion of the cells exited mitosis aberrantly, apparently underwent cytokinesis and finally died, whereas cells treated only with adriamycin maintained a tetraploid DNA content (Figure 27d).

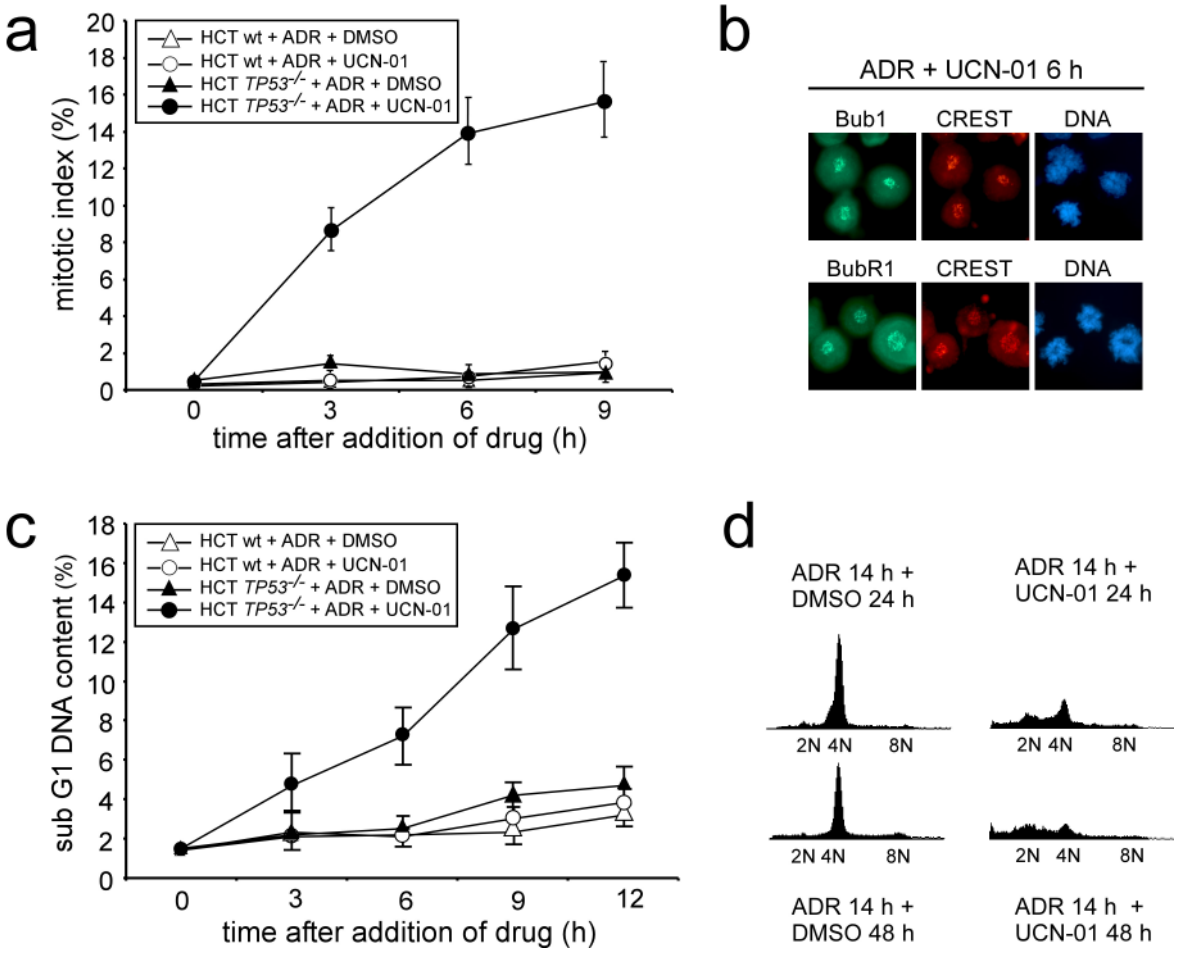

Figure 27: The spindle checkpoint mediates mitotic arrest in response to topoisomerase inhibitor and UCN-01 treatment. a) HCT116 wt and HCT116 *TP53*$^{-/-}$ cells were sequentially treated with 750 nM adriamycin for 14 h and 100 nM UCN-01 or DMSO for up to 9 h. The mitotic index was determined by MPM2 FACS analysis. Mean values and standard deviations were calculated from at least three independent experiments. b) HCT116 *TP53*$^{-/-}$ cells were treated with 750 nM adriamycin for 14 h followed by 100 nM UCN-01 for 6 h and immunofluorescence staining of Bub1 or BubR1 (green), the kinetochores (CREST, red) and the DNA (Hoechst 33258, blue) was performed. Representative results are shown. c) HCT116 wt and HCT116 *TP53*$^{-/-}$ cells were treated with 750 nM adriamycin for 14 h and UCN-01 or DMSO was added for up to 12 h. Apoptosis was measured by sub G1 PI FACS analysis. Mean values and standard deviations were calculated from at least three independent experiments. d) HCT116 *TP53*$^{-/-}$ cells were treated as in a), but UCN-01 or DMSO was administered for 24 h or 48 h. DNA content was measured by PI FACS analysis. Representative FACS profiles are shown.

After establishing UCN-01-mediated G2 checkpoint abrogation in HCT116 cells, I investigated the role of the spindle checkpoint in cell death upon G2 checkpoint abrogation. Since the HCT116 *MAD2*$^{+/-}$ and HCT116 *MAD1*^{kd} cells contain wild type *TP53*, the endogenous p53 protein was aimed to be inactivated by stable expression of a dominant negative fragment of p53. HCT116 wt, HCT116 *MAD2*$^{+/-}$ cells and the HCT116 *MAD1*^{kd} cell clone 2-31 were transfected with the pcDNA3-HA-p53DD vector carrying a neomycin resistance or an empty pcDNA3 vector. HCT116 wt and HCT116 *MAD2*$^{+/-}$ cells were additionally co-transfected with the pBabepuro vector and selected with 5 µg/ml puromycin, whereas the HCT116 *MAD1*^{kd} cells were selected with 300 µg/ml neomycin, because they already contained the pBabepuro vector. Transfection, selection and isolation of independent clones were performed as described for the generation of the HCT116 *MAD1*^{kd} cell clones (see chapter 1). Cell clones expressing the HA-tagged dominant negative fragment of p53 were identified by Western blotting with an antibody directed against the HA-tag (Figure 28a). One out of nine clones of HCT116 wt cells, two out of six clones of HCT116 *MAD2*$^{+/-}$ cells and two out of 13 HCT116 *MAD1*^{kd} cell clones did express the fragment and were tested with a functional assay for their ability to enter mitosis in the presence of DNA damage. The individual cell clones and empty vector controls were treated with 750 nM adriamycin for 14 h and 5 mM caffeine to inhibit ATM/ATR and thereby abrogate G2 arrest for 3 h or 6 h and the mitotic index was determined (Figure 28b). The expression levels of HA tagged p53 fragment and the rate of mitotic entry upon G2 checkpoint abrogation correlate only weakly. The empty vector controls showed a mitotic index below 1.4% and the positive control HCT116 *TP53*$^{-/-}$ cells displayed a mitotic index of 15.8%. The mitotic indices of the tested cell lines expressing the dominant negative fragment of p53 varied widely between these values, indicating that the generation of isogenic HCT116 cell lines with similar mitotic entry rates upon G2 checkpoint abrogation failed. Therefore, this experimental system was not suitable for the investigation of the role of the spindle checkpoint in cell death upon G2 checkpoint abrogation.

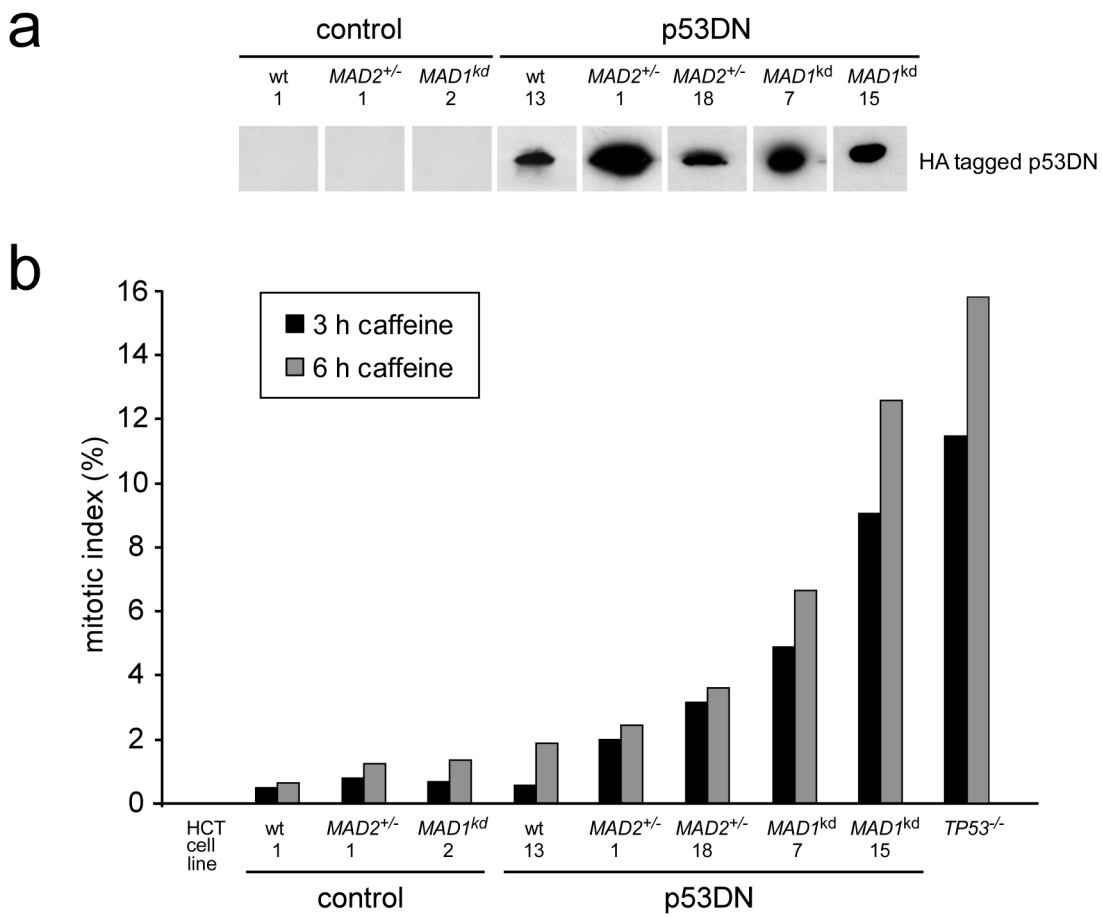

Figure 28: Test of HCT116 cell lines stably expressing a dominant negative p53 fragment for mitotic entry upon G2 checkpoint abrogation. a) HCT116 wt, HCT116 *MAD2*$^{+/-}$ and HCT116 *MAD1*^{kd} 2-31 clones expressing the dominant negative p53 fragment from the pcDNA3-HA-p53DD vector were identified by Western blotting with an anti-HA antibody. One representative experiment is shown. b) HCT116 wt, HCT116 *MAD2*$^{+/-}$ and HCT116 *MAD1*^{kd} 2-31 cells stably expressing the dominant negative p53 fragment or carrying the empty vector were treated sequentially with 750 nM adriamycin for 14 h and 5 mM caffeine for 3 h or 6 h. The mitotic index was determined by MPM2 FACS analysis. The cell lines containing the empty vector served as negative controls and HCT116 *TP53*$^{-/-}$ cells as positive controls for G2 checkpoint abrogation. One representative experiment is shown.

The mitotic entry rate upon G2 checkpoint abrogation in HCT116 *TP53*$^{-/-}$ cells was poor, therefore, the G2 checkpoint abrogation setup was also tested with other cancer cell lines lacking functional p53. HCT116 *TP53*$^{-/-}$, HeLa and HT29 cells were arrested in G2 phase with 300 nM adriamycin for 14 h and the arrest was abrogated by treatment with 100 nM UCN-01 for 6 h. The mitotic indices of HCT116 *TP53*$^{-/-}$, HeLa and HT29 cells were 10.6%, 45.5% or 79.1%, respectively (Figure 29). HT29 cells show a significantly prolonged mitotic arrest response to spindle damage which is uncommon for most cancer cell lines (data not shown). Based on these results I decided to use HeLa cells for subsequent experiments.

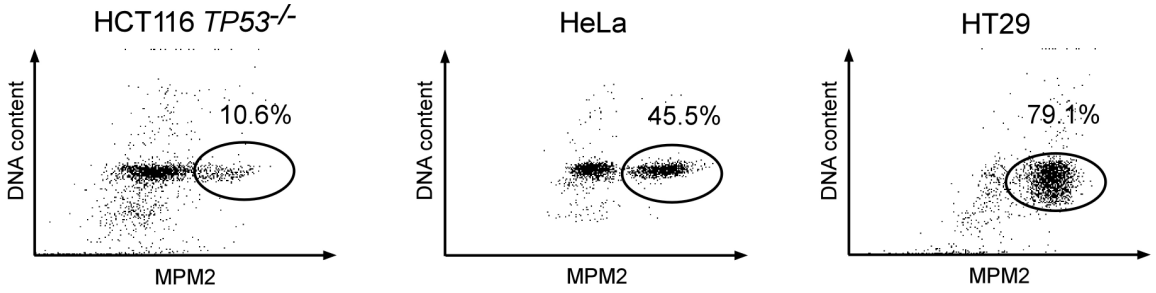

Figure 29: The efficiency of G2 DNA damage checkpoint abrogation by topoisomerase inhibitor and UCN-01 treatment is cell line-dependent. HCT116 *TP53*$^{-/-}$, HeLa and HT29 cells were treated with 300 nM adriamycin for 14 h, followed by treatment with 100 nM UCN-01 for 6 h. The mitotic index was determined by MPM2 FACS analysis and is indicated in the plots. Representative dot plots are displayed.

UCN-01-induced abrogation of the G2 DNA damage checkpoint activates the tension-sensing branch of the spindle checkpoint and induces a metaphase-like mitotic arrest

To investigate the mechanisms of G2 checkpoint abrogation and spindle checkpoint activation in HeLa cells, cells were arrested in G2 by treatment with 300 nM adriamycin and were forced to enter mitosis by treatment with 100 nM UCN-01. The mitotic index determined by MPM2 FACS analysis rose from 1.8% at 0 h to 67.1% at 9 h (Figure 30a). The appearance of Hoechst 33258 stained nuclei of UCN-01 treated cells changed from mitotically arrested after 4 h to apoptotic after 18 h (Figure 30b). Immunofluorescence studies of HeLa cells sequentially treated with adriamycin for 24 h and UCN-01 for 6 h revealed an activation of the spindle checkpoint, as mitotic checkpoint kinases Bub1 and BubR1 localized to the kinetochores (Figure 30c). Entry into mitosis was also accompanied by misaligned chromosomes, spindle deformations and centrosome splitting, which was previously associated with DNA damage (Hut *et al.* 2003; Figure 30d).

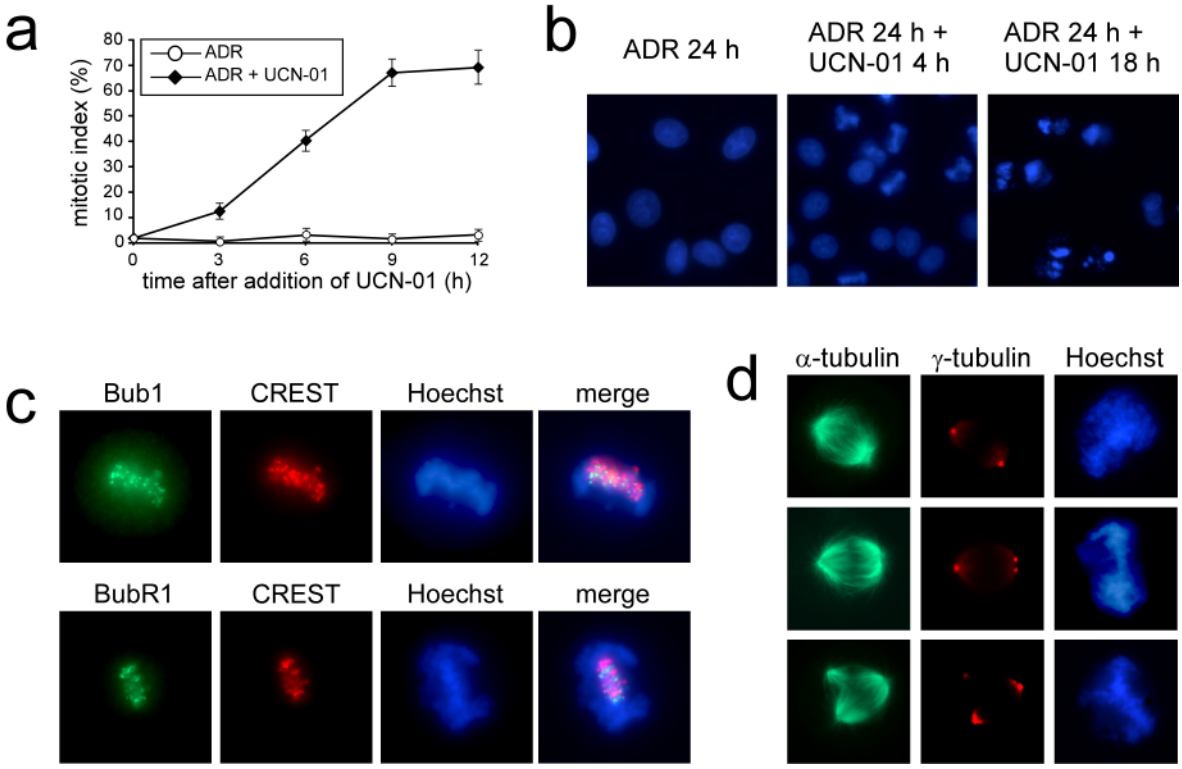

Figure 30: UCN-01-induced abrogation of the G2 checkpoint induces a metaphase-like mitotic arrest and activation of the spindle checkpoint. a) The development of the mitotic index upon sequential treatment of HeLa cells with 300 nM adriamycin (ADR) for 24 h and 100 nM UCN-01 for up to 12 h was determined by MPM2 FACS analysis. The mitotic indices and standard deviations were calculated from three independent experiments. b) Hoechst 33258 staining of nuclear DNA in fixed HeLa cells treated with 300 nM adriamycin for 24 h and 100 nM UCN-01 for 4 h or 18 h. A representative experiment is shown. c) Spindle checkpoint activation in HeLa cells after sequential treatment with 300 nM adriamycin for 24 h and 100 nM UCN-01 for 6 h was determined by immunofluorescence staining of mitotic kinases Bub1 or BubR1 (green), kinetochores (CREST, red) and DNA (Hoechst 33258, blue). A representative experiment is shown. d) HeLa cells were sequentially treated with 300 nM adriamycin for 24 h and 100 nM UCN-01 for 6 h and immunofluorescence staining of the mitotic spindle (α-tubulin, green), the centrosomes (γ-tubulin, red) and the DNA (Hoechst 33258, blue) was performed. A representative experiment is displayed.

The role of various spindle checkpoint components was elucidated by repression of *BUB1*, *BUB1B*, *MAD2*, *MPS1L1* and *survivin* by transient transfection of HeLa cells with shRNA constructs and pharmacological inhibition of Aurora B by the small molecule ZM447439. The effect on spindle checkpoint activity was evaluated by measurement of the mitotic index of cells control treated with 150 nM nocodazole or 100 nM taxol for 16 h (Figure 31b, c) and the repression of the spindle checkpoint components was determined on Western blot (Figure 31a). A degree of spindle checkpoint impairment comparable to that found in spindle checkpoint impaired cancer cell lines (i.e. a mitotic index of 15%-40%

after 16 h of treatment with 150 nM nocodazole or 100 nM taxol) was achieved by all treatments.

The spindle checkpoint impairment by repression of the spindle checkpoint components tested revealed that Bub1, BubR1, Mad2, Mps1, survivin and Aurora B were all required for mitotic arrest upon G2 checkpoint abrogation with 300 nM adriamycin and 100 nM UCN-01 (Figure 31c, e). The mitotic indices of these samples were at least as low as in the nocodazole and taxol treated controls. *MAD2* shRNA treated cells showed mitotic indices of 20.6%, 21.6% and 11.4% after 16 h of nocodazole, 16 h of taxol treatment or sequential treatment with adriamycin for 24 h and with UCN-01 for 12 h, compared to 66.0%, 72.3% and 66.4% in empty vector controls (Figure 31b, c).

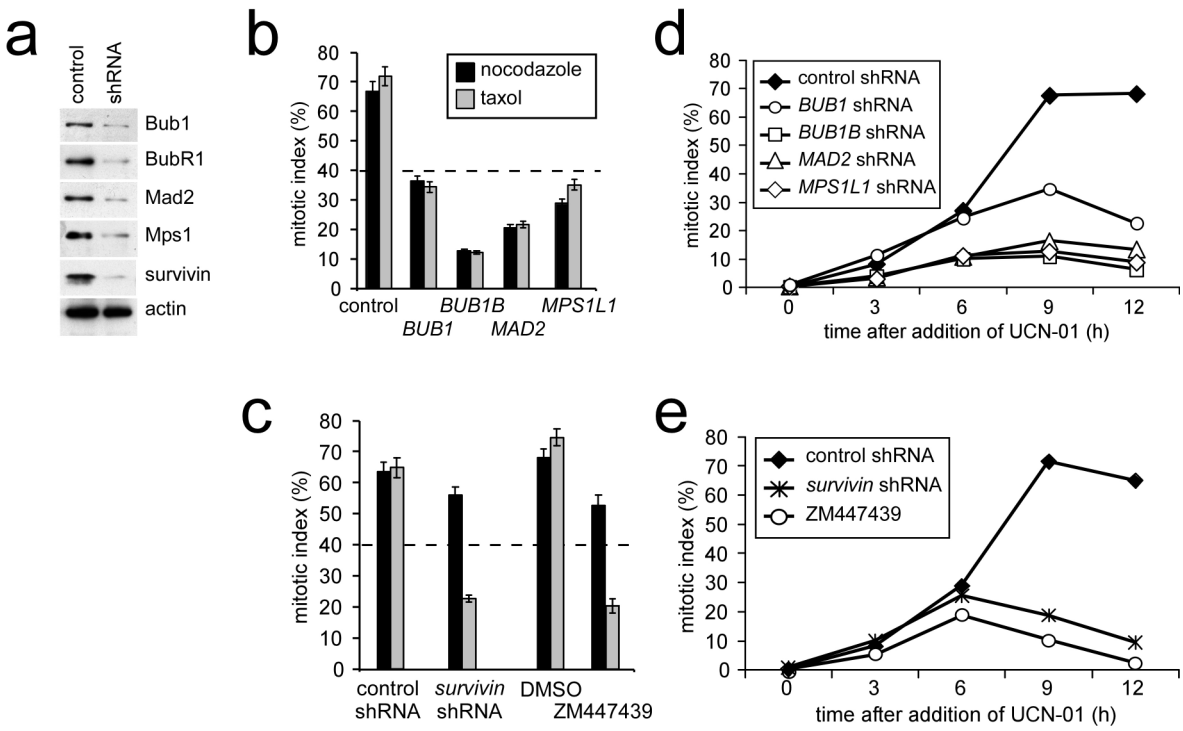

Figure 31: UCN-01-induced abrogation of the G2 DNA damage checkpoint activates the tension-sensing branch of the spindle checkpoint. a) The levels of the spindle checkpoint proteins indicated were detected by Western blotting in lysates from HeLa cells transfected with the corresponding shRNA constructs. Actin served as a loading control. A representative experiment is shown (performed in collaboration with Christian Hager). b)-e) HeLa cells transfected with the shRNA constructs or treated with 1 µM ZM447439 were treated with 150 nM nocodazole or 100 nM taxol for 16 h (b, c) or were sequentially treated with 300 nM adriamycin for 24 h and 100 nM UCN-01 for up to 12 h (d, e). The mitotic indices were measured by MPM2 FACS analysis and standard deviations were calculated from at least three independent experiments.

The effect of downregulation of *survivin* or inhibition of Aurora B suggests that the tension-sensing branch of the spindle checkpoint is required to sense the defects attributable to G2 checkpoint abrogation (Figure 31d, e).

The results clearly indicate that UCN-01-induced abrogation of the G2 DNA damage checkpoint in HeLa cells leads to severe mitotic defects, including spindle and centrosome damage. For the first time, I showed that G2 checkpoint abrogation activates the tension-sensing branch of the spindle checkpoint and evokes a metaphase-like mitotic arrest, that depends on Bub1, BubR1, Mad2, Mps1, survivin and Aurora B.

UCN-01-mediated abrogation of the G2 DNA damage checkpoint induces apoptosis

UCN-01-mediated G2 checkpoint abrogation leads to mitotic catastrophe and it is still unclear whether this form of cell death is related to apoptosis (Okada and Mak 2004).

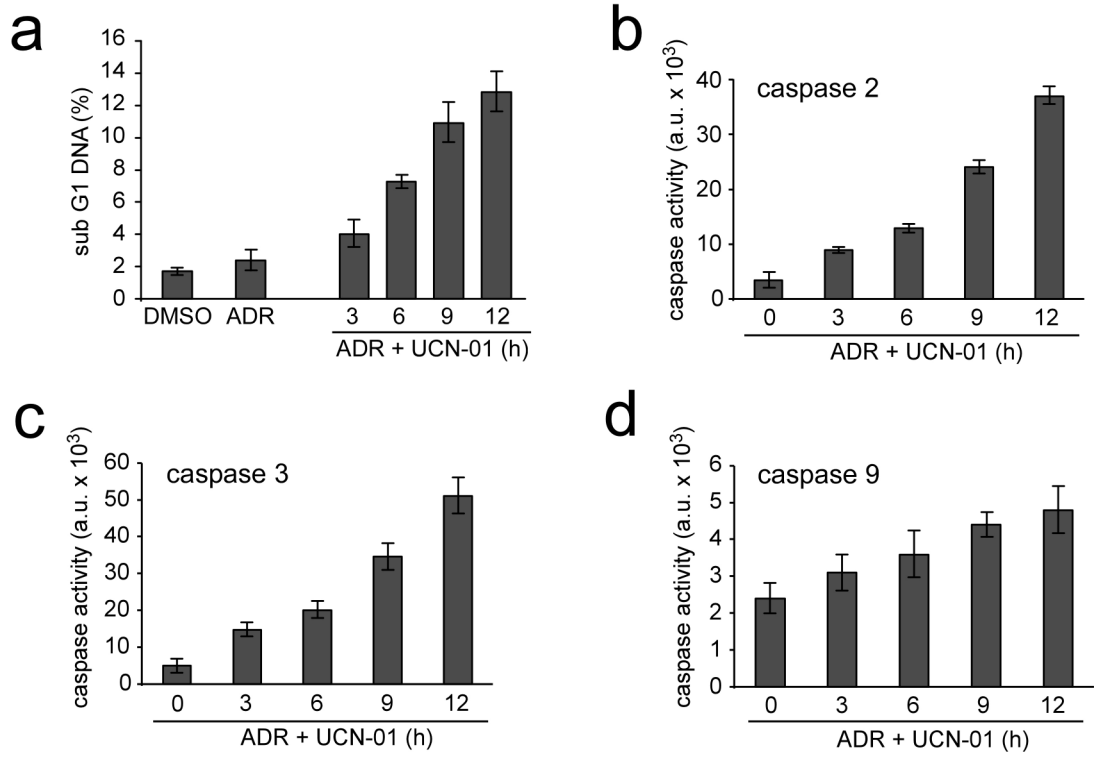

Figure 32: G2 checkpoint abrogation by UCN-01 activates caspases. a) Cell death upon sequential treatment of HeLa cells with 300 nM adriamycin for 24 h and 100 nM UCN-01 for up to 12 h was determined by measuring the sub G1 DNA content by PI FACS analysis. The graphs and standard deviations were calculated from at least three independent experiments. b)-d) 1 x 10^5 cells were seeded 24 h prior to treatment and caspase 2, 3 and 9 activity was determined fluorometrically in living cells treated as in a). Mean values and standard deviations from three independent experiments were calculated.

HeLa cells arrested in G2 phase by adriamycin for 24 h were treated with UCN-01 for up to 12 h. Determination of the sub G1 DNA content showed that cells start to die after G2 checkpoint abrogation, following mitotic entry (Figure 32a). The percentage of cells with a sub G1 DNA content of 14% is rather low after 12 h of treatment, but nevertheless suggests an early response to G2 checkpoint abrogation. To investigate whether the observed cell death was indeed apoptosis, a caspase activity assay in living cells was employed. The measurement of caspase activity in HeLa cells upon adriamycin and UCN-01 treatment revealed an activation of caspase 2, 3 and 9 (Figure 32b).

To investigate whether apoptosis is initiated in mitosis, HeLa cells were treated with adriamycin and UCN-01 and a shake-off was carried out after 12 h. Cells were accumulated in mitosis up to 75%. Clearly, caspase 2, 3 and 9 activation was detected in mitotic cell populations, whereas the non-mitotic cell population or G2 arrested cells displayed only minor caspase activities (Figure 33a). Caspase 2 and 3 were activated about tenfold in the mitotic population compared to the control samples. Caspase 9 activity was low and only 2.5-fold higher than in control cells, which might be explained by the usually very low values obtained when using caspase 9 substrates. Hallmark parameters of the intrinsic pathway of apoptosis were detected in mitotic and control cell populations. Subcellular fractionation allowed the isolation and Western blotting of cytoplasmic proteins. Cytochrome C release from the mitochondria into the cytoplasm was detected in the mitotic cell lysate but not in the controls, including mitotically arrested cells treated with nocodazole for 8 h (Figure 33b), excluding the possibility that mitotic cells show cytochrome C release *per se*. Similarly, PARP cleavage (Figure 33c) and DNA laddering (Figure 33d) were predominantly detectable in mitotic cell lysates by Western blotting and agarose gel electrophoresis, respectively.

The results demonstrate that cell death upon G2 checkpoint abrogation can be defined as apoptosis executed during mitosis via the intrinsic pathway of apoptosis. They also suggest an early induction of apoptosis upon mitotic entry, pointing to a different mechanism of apoptosis induction than during spindle damage-induced apoptosis, which is dependent on a prolonged mitotic arrest and subsequent slippage.

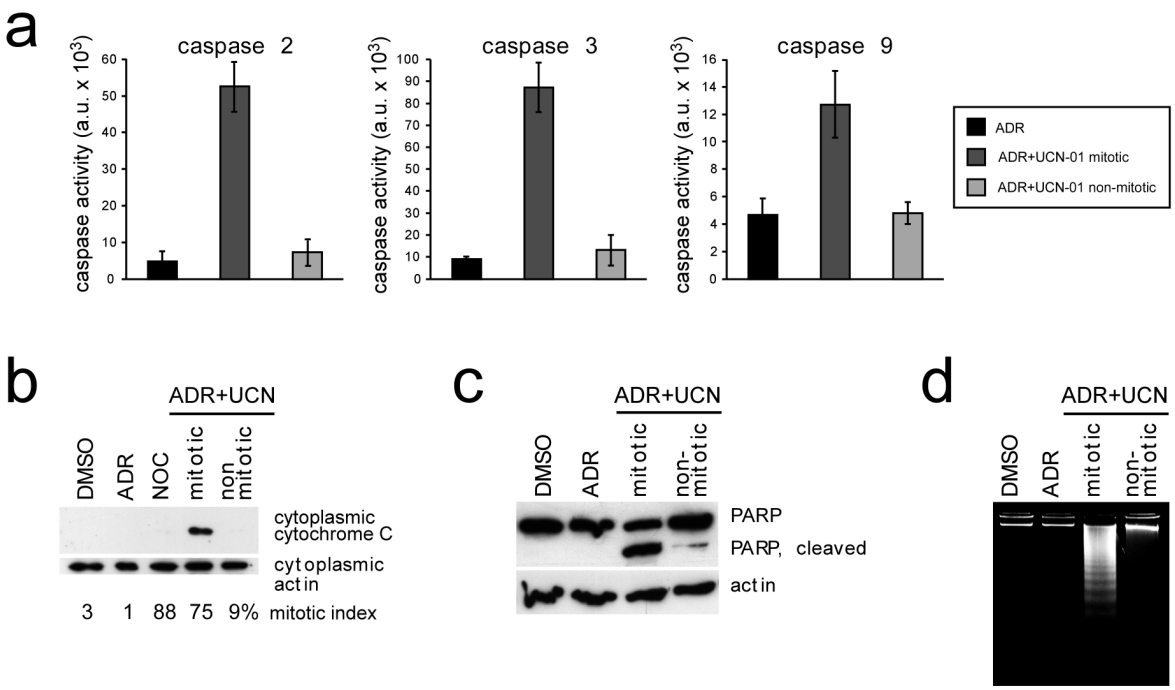

Figure 33: UCN-01-mediated abrogation of the G2 DNA damage checkpoint induces mitochondria-associated apoptosis in mitotic cells. HeLa cells were sequentially treated with 300 nM adriamycin for 24 h and 100 nM UCN-01 for 12 h (a, b) or 24 h (c, d) and a shake-off was performed to obtain cell populations either enriched in mitotic or in non-mitotic cells. Controls were incubated with DMSO, 300 nM adriamycin for 36 h or 48 h or 150 nM nocodazole for 8 h. a) Caspase 2, 3 and 9 activities in 1 x 10^5 cells were measured and mean values and standard deviations from three independent experiments were calculated. Western blots of b) cytochrome C release from mitochondria and c) PARP cleavage or d) the gel of an internucleosomal DNA laddering assay from one representative experiment are displayed.

Mad2 has a proapoptotic role in UCN-01-induced cell death

The spindle checkpoint mediates the UCN-01-induced mitotic arrest upon G2 checkpoint abrogation. Therefore, I tested whether the spindle checkpoint proteins contributed not only to the induction of mitotic arrest, but also to mitotic apoptosis. *MAD2*, *BUB1B* and *BUB1* expression was repressed in HeLa cells by transient transfection with shRNA constructs as described before (Figure 31).

The percentage of apoptotic figures in transfected HeLa cells treated with adriamycin and subsequently with UCN-01 for 18 h was counted after fixation and DNA staining of the cells (Figure 34a). The amount of dead cells after 18 h of UCN-01 treatment was comparable to the empty vector control in cell populations with reduced *BUB1* or *BUB1B* levels, but reduced by 56% in cells depleted of *MAD2*. Those cells that escaped from apoptosis showed multinuclei (Figure 34a).

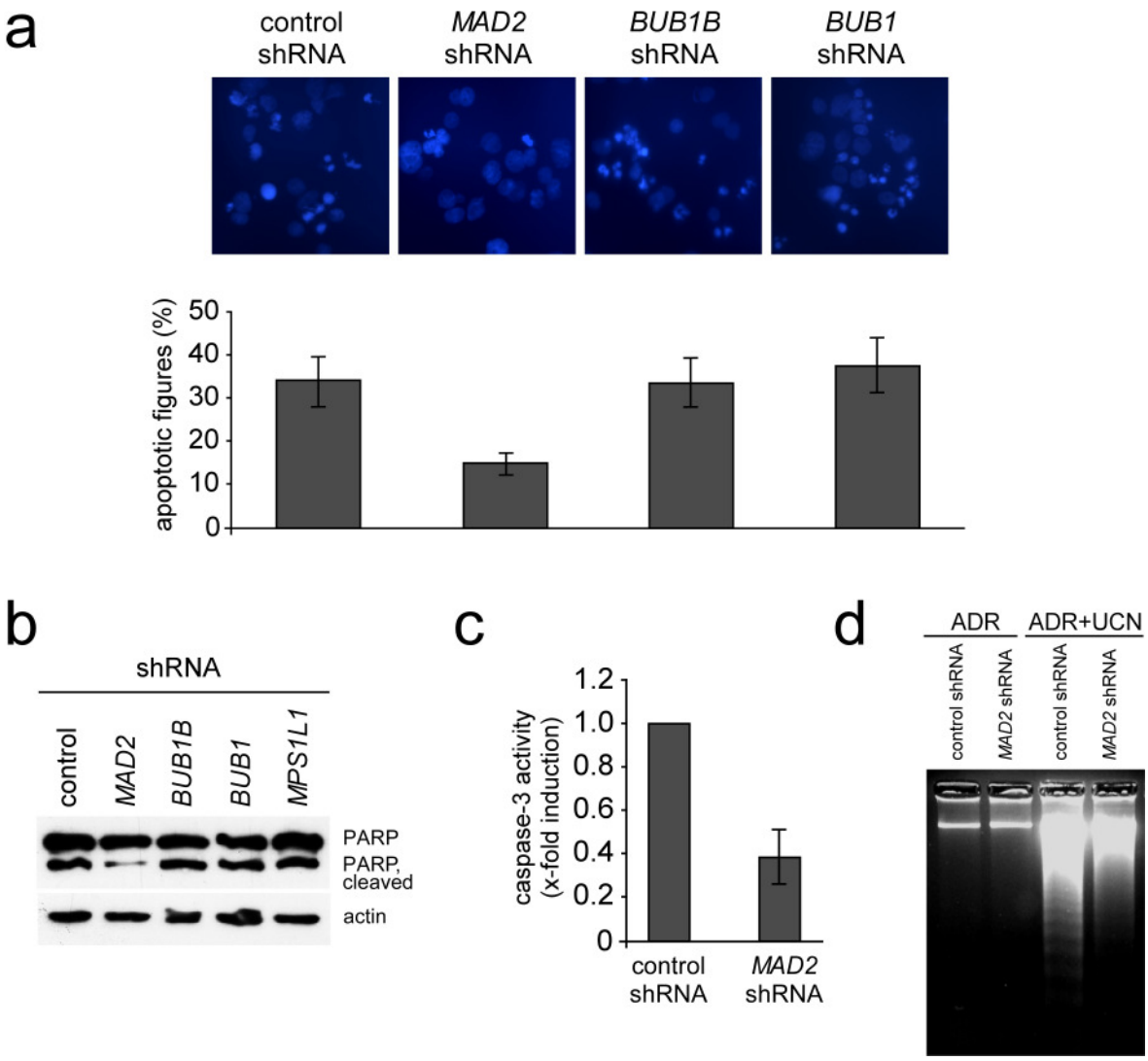

Figure 34: Mad2 is required for apoptosis upon UCN-01-induced abrogation of the G2 DNA damage checkpoint. HeLa cells were transiently transfected with shRNAs targeting the spindle checkpoint components indicated and were sequentially treated with 300 nM adriamycin for 24 h and 100 nM UCN-01 for a) 18 h or b)-d) 24 h. a) Microscopic quantitation of fixed and Hoechst 33258 stained HeLa cells transiently transfected with shRNAs and treated with adriamycin and UCN-01. At least 1500 cells from three independent experiments were evaluated. b) A Western blot of PARP cleavage and actin as a loading control of one representative experiment performed as in a) is shown. c) The caspase 3 activity of 1 x 10^5 HeLa cells transfected with control or *MAD2* shRNA upon G2 checkpoint abrogation was determined fluorometrically and mean values and standard deviations were calculated from at least three independent experiments. d) Cells were treated as in c), the internucleosomal DNA laddering was detected and one representative experiment is displayed.

Furthermore, PARP cleavage was reduced in cells with decreased *MAD2* levels, but not in lysates from cells with diminished levels of *BUB1B*, *BUB1* and *MPS1L1* compared to empty vector controls (Figure 34b). The caspase 3 activity in *MAD2* shRNA treated HeLa cells was reduced by 60% (Figure 34c) and a DNA laddering assay also confirmed the

proapoptotic effect of Mad2 (Figure 34d). The results clearly indicate a proapoptotic function of Mad2 in apoptosis upon G2 checkpoint abrogation. Surprisingly, however, BubR1, Bub1 and Mps1 were dispensable for apoptosis induction upon G2 checkpoint abrogation. In contrast, UCN-01-induced mitotic arrest required normal levels of Mad2, BubR1, Bub1 and Mps1.

A survivin-dependent survival pathway restrains apoptosis in UCN-01-induced abrogation of the G2 checkpoint

Since survivin and Aurora B are required to mediate the mitotic arrest induced by UCN-01, I asked whether the chromosomal passenger proteins also participate in mediating apoptotic signals. Overexpression of survivin and Aurora B, which are both part of the larger chromosomal passenger complex (Bolton *et al.* 2002, Honda *et al.* 2003), is found in many human tumors and correlates with chemotherapy resistance and advanced stages of cancer (Keen and Taylor 2004), suggesting an antiapoptotic role of these proteins. Genetic ablation of *survivin* (Li *et al.* 1999) or pharmacological inhibition of Aurora B kinase by ZM447439 (Ditchfield *et al.* 2003), Hesperadin (Hauf *et al.* 2003) or VX-680 (Harrington *et al.* 2004) leads to a block in cell division resulting in polyploidy and to apoptosis induction. The influence of reduced survivin levels or reduced Aurora B activity on members of the bcl-2 family, which control mitochondrial apoptosis (Wei *et al.* 2001, Willis *et al.* 2003), was studied in the following experiments. Bcl-2 is an antiapoptotic protein, which is often overexpressed in cancer (Willis *et al.* 2003) and protects against spindle damage-induced apoptosis in its phosphorylated state (Deng *et al.* 2004). Bax and bak on the other hand are proapoptotic bcl-2 family proteins and often fulfill redundant functions (Wei *et al.* 2001).

When HeLa cells were treated with adriamycin, I found that survivin levels were elevated when compared with asynchronously growing cells, which is consistent with a cell cycle regulated expression. Significantly, I found a dramatic further increase of survivin protein upon mitotic entry induced by UCN-01 (Figure 35a). Interestingly, the increase in survivin accumulation correlated with a strong bcl-2 hyperphosphorylation (Figure 35a). Survivin levels and bcl-2 hyperphosphorylation levels were markedly reduced upon G2 checkpoint abrogation in HeLa cells transfected with the shRNA plasmid targeting *survivin* (Figure 35a), implicating survivin in the regulation of bcl-2 phosphorylation.

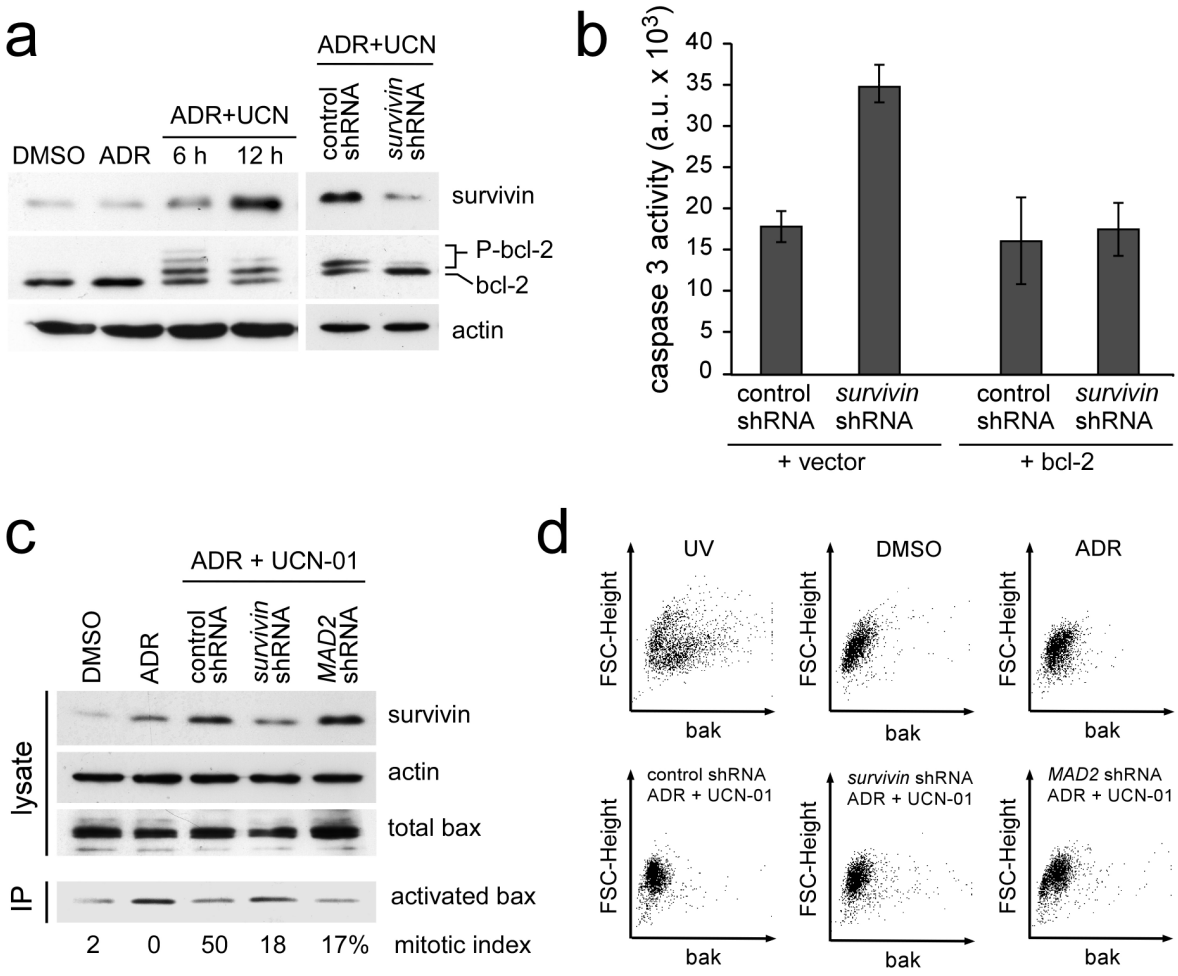

Figure 35: Survivin restrains apoptosis upon UCN-01-induced abrogation of the G2 DNA damage checkpoint. HeLa cells transfected with shRNA expressing constructs targeting *survivin* or *MAD2* or cells overexpressing *BCL2* were sequentially treated with 300 nM adriamycin for 24 h and 100 nM UCN-01 for 12 h (a, b) or 6 h (c, d). Untransfected HeLa cells were treated with DMSO or 300 nM adriamycin for 24 h and subsequently with 100 nM UCN-01 or DMSO for 6 h or 12 h. a) Survivin and bcl-2 were detected by Western blotting. One representative blot with actin as a loading control is shown. b) Caspase 3 activity was measured fluorometrically in 1 x 10^5 HeLa cells expressing shRNAs targeting *survivin* in the presence or absence of *BCL2* overexpression, upon treatment with adriamycin and UCN-01. Mean values and standard deviations were calculated from four independent experiments. c) Bax and survivin were detected in whole cell lysates by Western blotting, whereas activated bax was immunoprecipitated with the conformation-specific antibody 6A7 (Calbiochem). Representative blots are shown. d) Activated bak was detected with the conformation-specific TC-100 antibody (Calbiochem) by FACS analysis of cells treated as in c) or as a positive control with 200 J/m^2 UV light for 12 h. Representative dot plots are shown.

The effect of diminished survivin levels and of bcl-2 overexpression on the rate of apoptosis was monitored with caspase 3 activity assays. Lowered survivin levels enhanced apoptosis 1.7-fold compared to controls (Figure 35b). Moreover, bcl-2 overexpression counteracted the proapoptotic effect of the loss of survivin completely, indicating that

survivin might positively regulate bcl-2 phosphorylation to suppress apoptosis (Figure 35b). The antiapoptotic effect of survivin and bcl-2 might be mediated by counteracting the activation of the proapoptotic proteins bax and bak. Therefore, the activation bax or of bak was investigated by immunoprecipitation of activated bax or detection of activated bak in FACS analysis. Bax and survivin were detected by Western blotting of whole cell lysates, whereas activated bax was immunoprecipitated with a conformation-specific antibody (Figure 35c). Bax was found in an inactive conformation in asynchronously growing cells and in an activated state in adriamycin treated cells as expected (Figure 35c). Surprisingly, however, bax was deactivated in cells treated with adriamycin and subsequently with UCN-01 (Figure 35c). Lowered survivin levels led to a reactivation of bax in adriamycin and UCN-01 exposed cells, whereas bax remained inactive in the presence of lowered Mad2 levels (Figure 35c). Total bax levels remained almost unchanged, regardless of the various treatments. Survivin levels were low in untreated cells, enhanced in adriamycin treated cells and highest in cells also treated with UCN-01. Surprisingly, survivin levels remained high in the cell population with lowered Mad2 levels with a mitotic index of only 17% compared to a mitotic index of 50% in controls, supporting a non-mitotic antiapoptotic function of survivin. In these experiments, bak was found not to be activated under any of these conditions, but upon treatment with UV light, which served as a positive control, with a second cell population appearing to the right of the negative population (Figure 35d). Taken together, these results suggest that mitotic apoptosis is promoted by Mad2 and restrained by a survivin-dependent survival pathway that activates bcl2 and inactivates bax.

Pharmacological interference with the survivin-dependent mitotic survival pathway potentiates apoptosis upon UCN-01-induced abrogation of the G2 checkpoint

The detection of survivin's antiapoptotic function in apoptosis upon G2 checkpoint abrogation gave rise to the idea that pharmacological inhibition of this pathway might significantly enhance apoptosis in UCN-01 treated cells. Since no small molecule inhibitors of survivin were available at the time, I targeted other components of the signaling pathway, Aurora B and Cdk1. It has been shown that Aurora B's complex formation with survivin stimulates its kinase activity (Bolton *et al.* 2002, Wheatley *et al.* 2004). Pharmacological inhibition of Aurora B by ZM447439 prompts mitotic exit

(Morrow *et al.* 2005), as does roscovitine-mediated inhibition of Cdk1 activity (Blagden and de Bono 2005). Roscovitine could abrogate the survivin-dependent survival pathway by inhibiting Cdk1, which confers a stabilizing phosphorylation to survivin (O'Connor *et al.* 2000).

HeLa cells were treated with adriamycin for 24 h and subsequently with UCN-01 for 6 h or 12 h. For Aurora B inhibition 1 µM ZM447439 (ZM) was added prior to 12 h of UCN-01 treatment. To allow mitotic entry HeLa cells were treated with adriamycin and UCN-01 for 6 h, before roscovitine (RV), an inhibitor with the same specificity for Cdk1 and Cdk2, or purvalanol A (PU), which has a tenfold higher specificity for Cdk1 over Cdk2, were added for 6 h. Western blotting revealed decreased survivin levels and a loss of bcl-2 phosphorylation in cells co-treated with either Cdk1 or Aurora B inhibitors (Figure 36a).

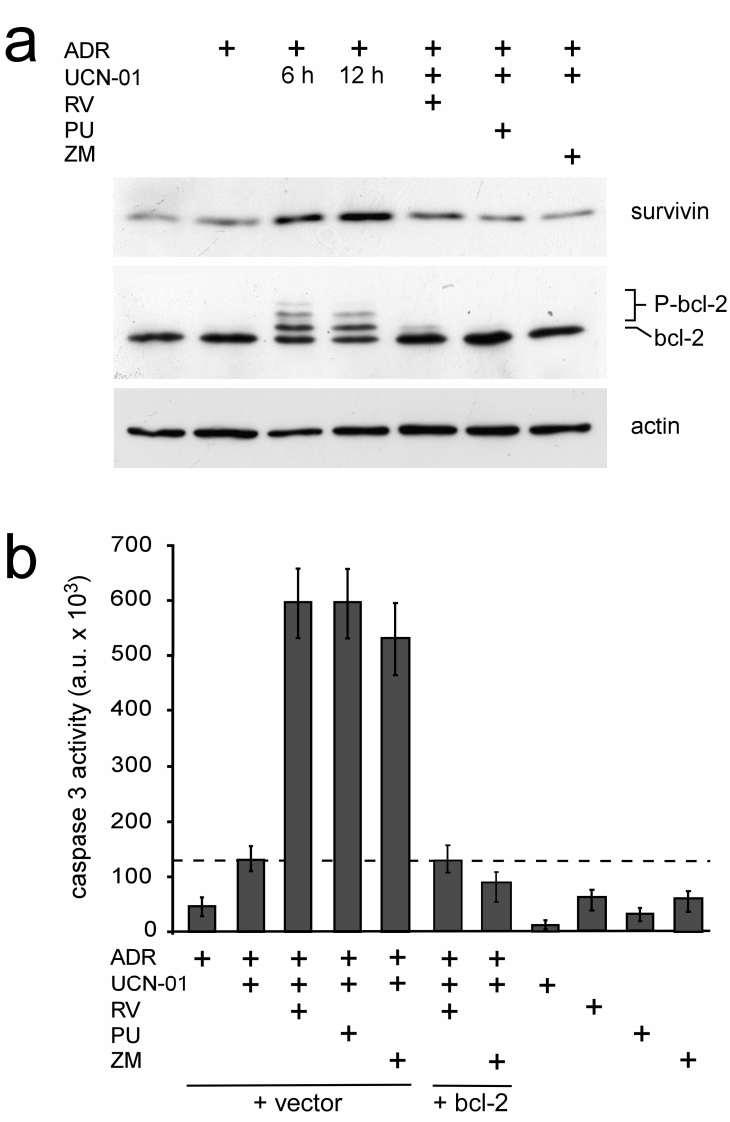

Figure 36: Pharmacological inhibition of the mitotic survivin-dependent survival pathway potentiates apoptosis upon G2 checkpoint abrogation. HeLa cells were sequentially treated with 300 nM adriamycin for 24 h and 100 nM UCN-01 for 6 h or 12 h. For Aurora B inhibition 1 µM ZM447439 (ZM) was added prior to UCN-01. For Cdk1 inhibition cells were treated with adriamycin for 24 h and with UCN-01 for 6 h before 20 µM roscovitine (RV) or 10 µM purvalanol A (PU) were added for 6 h. a) Survivin levels and bcl-2 phosphorylation were detected by Western blotting. One representative blot is shown. b) 1 x 10^5 HeLa cells were treated as in a) in the presence or absence of *BCL2* overexpression. Caspase 3 activity was measured and mean values and standard deviations from three independent experiments were calculated.

The consequences of Aurora B or Cdk1 inhibition for apoptosis induction by G2 checkpoint abrogation were investigated by caspase 3 activity assays. Caspase activity was enhanced 6.0-fold or 4.3-fold upon treatment with Cdk1 or Aurora B inhibitors, respectively (Figure 36b). The potentiation of caspase 3 activity by roscovitine or ZM447439 was completely suppressed by bcl-2 overexpression (Figure 36b), indicating that apoptosis upon G2 checkpoint abrogation is mitochondria-dependent. These results clearly show that apoptosis induced by G2 checkpoint abrogation can be greatly enhanced by inhibition of the survival pathway, thus suggesting a highly improved combination therapy.

The enhancement of apoptosis upon G2 checkpoint abrogation by inhibition of Cdk1 was investigated with respect to the temporal dynamics of caspase 2 and 3 activation. HeLa cells were sequentially treated with adriamycin for 24 h and UCN-01 for 6 h to allow mitotic entry before roscovitine was added for 2 h, 4 h and 6 h. After 4 h of roscovitine treatment the caspase activities exceeded the values for the 12 h treatment with UCN-01, but it took 6 h of roscovitine treatment to induce a strong increase in caspase 2 and 3 activity (Figure 37). These findings indicate that apoptosis induced by Cdk1 inhibition is a comparably slow response given the fact that the cells are synchronized in mitosis before roscovitine treatment by the previous block in G2 with adriamycin and release of the arrested cells with UCN-01. Roscovitine might inhibit mitotic entry via Cdk1 inhibition in adriamycin and UCN-01 treated cells, which are still arrested in G2 at the time of roscovitine addition. However, the mitotic index after 4 h of roscovitine treatment exceeds that after 2 h, suggesting that some cells are able to enter mitosis after roscovitine addition.

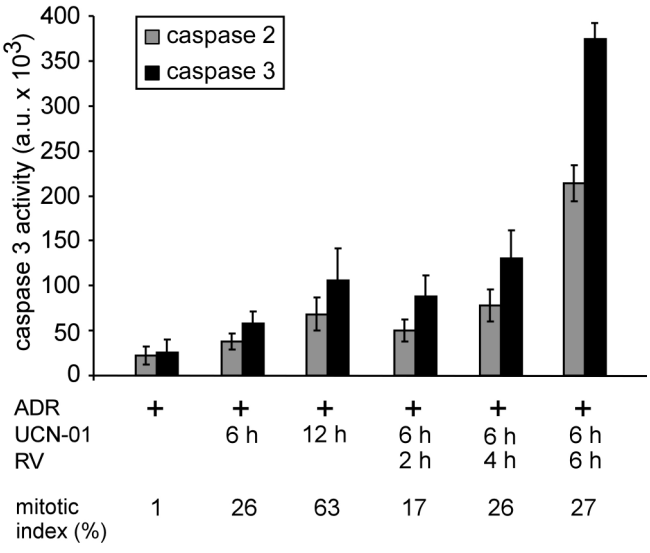

Figure 37: Pharmacological Cdk1 inhibition enhances apoptosis upon G2 checkpoint abrogation. 1 x 10^5 HeLa cells were treated with 300 nM adriamycin (ADR) for 24 h and subsequently with 100 nM UCN-01 for 6 h to allow mitotic entry, before roscovitine (RV) was added for up to 6 h. Mean values of caspase 2 and caspase 3 activity measurements and standard deviations were calculated from at least three independent experiments. The mitotic indices determined by MPM2 FACS analysis are indicated below.

Inhibition of transcription potentiates apoptosis upon UCN-01-induced abrogation of the G2 checkpoint

Apoptosis can be executed independent or dependent on transcription and translation (Martin *et al.* 1990, Saelens *et al.* 2001, Holcik and Sonenberg 2005). Therefore, I investigated the effect of inhibitors of transcription or translation on apoptosis upon G2 checkpoint abrogation in roscovitine treated cells. HeLa cells were treated with adriamycin and UCN-01 for 6 h to allow mitotic entry, before roscovitine (RV) was added for 2 h, followed by addition of the inhibitors of transcription or translation or DMSO for 4 h. As shown before, roscovitine increased the caspase 3 activity induced by G2 checkpoint abrogation 6.3-fold (Figure 38). Inhibition of global transcription by α-amanitin-oleate or actinomycin D partially suppressed the roscovitine-mediated increase of G2 checkpoint abrogation-induced apoptosis (Figure 38). However, inhibition of translation by cycloheximide, hygromycin or puromycin enhanced caspase 3 activity (Figure 38).

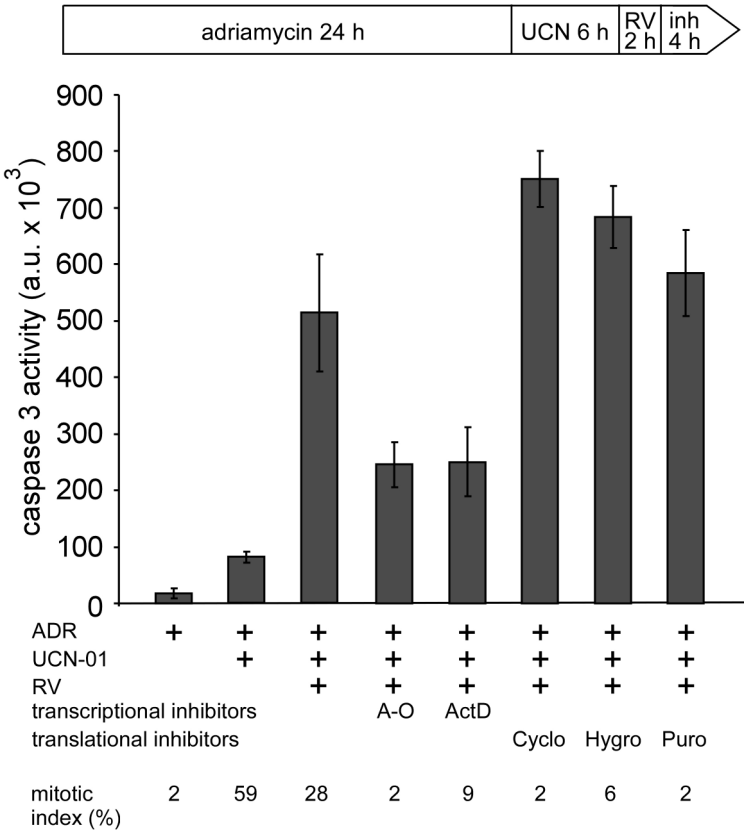

Figure 38: Transcription is required for enhanced apoptosis triggered by Cdk1 inhibition upon G2 checkpoint abrogation. HeLa cells were sequentially treated with 300 nM adriamycin for 24 h and 100 nM UCN-01 for 6 h to allow mitotic entry, then 20 µM roscovitine (RV) was added for 2 h, subsequently the inhibitors indicated or DMSO for 4 h. Caspase 3 assays of 1 x 10^5 cells were performed and the mean values and standard deviations from at least three independent experiments were calculated. Transcriptional inhibitors: 10 µM α-amanitin-oleate (A-O), 10 µg/ml actinomycin D (ActD). Translational inhibitors: 50 µg/ml cycloheximide (Cyclo), 1 mg/ml hygromycin (Hygro), 40 µg/ml puromycin (Puro). Mitotic indices determined by MPM2 FACS analysis are indicated below.

Surprisingly, inhibitors of transcription or of translation had opposite effects on apoptosis induced by the combination treatment of G2 checkpoint abrogation and survival pathway inhibition. It is conceivable, that the transcriptional inhibitors prevent transcription of pro-apoptotic genes, thereby partially protecting the cells from apoptosis. In contrast, the inhibitors of translation might prevent the translation of housekeeping mRNAs already present in the cell before the proapoptotic treatment, thereby depriving the cells of essential proteins. Further analysis is required to resolve the role of transcription and translation in G2 checkpoint-mediated apoptosis.

Inhibition of MAP kinases potentiates apoptosis upon UCN-01-induced abrogation of the G2 DNA damage checkpoint

The family of MAP kinases can be activated by stress or growth signals and can influence cell survival and death (Roux and Blenis 2004) and is therefore an attractive candidate for the positive or negative regulation of apoptosis upon G2 checkpoint abrogation. I tested several inhibitors of MAP kinase family members for their effect on caspase 3 activation upon G2 checkpoint abrogation.

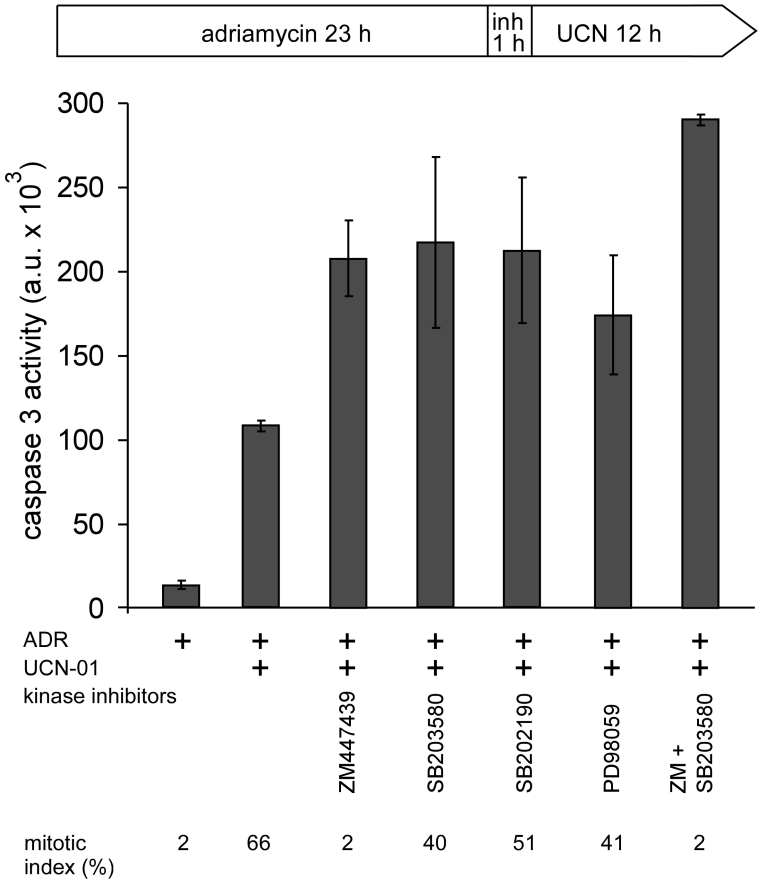

Figure 39: Pharmacological inhibition of MAP kinases enhances apoptosis upon G2 checkpoint abrogation. 1 x 10^5 HeLa cells were sequentially treated with 300 nM adriamycin for 24 h and 100 nM UCN-01 for 12 h. 40 µM SB203580 (a p38 inhibitor), 20 µM SB202190 (a p38 inhibitor), 50 µM PD98059 (a MEK, ERK inhibitor) and 1 µM ZM447439 were added 1 h prior to UCN-01. Mean values and standard deviations from at least three independent caspase 3 assays were calculated. Mitotic indices determined by MPM2 FACS analysis are indicated below.

40 µM SB203580 (a p38 inhibitor), 20 µM SB202190 (a p38 inhibitor) and 50 µM PD98059 (a MEK/ERK inhibitor) were added prior to UCN-01 treatment and enhanced apoptosis to the same extent as the Aurora B kinase inhibitor ZM447439 at 1 µM as a positive control for apoptosis potentiation. The different inhibitors increased caspase 3 activity about 1.6-2.0-fold (Figure 39). The combination of ZM447439 and SB203580 further increased caspase 3 activity (Figure 39). These results suggest that the MAP kinase pathway might be an antiapoptotic regulator of mitotic cell death.

Kinase inhibitors and shRNA constructs have differential effects on cytokinesis and mitotic arrest upon G2 checkpoint abrogation

To gain more insight into the mechanisms of mitotic apoptosis and enhanced mitotic apoptosis upon combination of UCN-01 with Aurora B or MAP kinase inhibitors, the characteristics of the mitotic arrest induced upon G2 checkpoint abrogation were compared to the mitotic arrest induced by the spindle damaging agents nocodazole and taxol. Furthermore, the effect of reduced levels of spindle checkpoint proteins or the inhibition of Cdk1, Aurora B or of MAP kinase p38 on cytokinesis or apoptosis was studied.

To investigate the role of Aurora B in signaling upon G2 checkpoint abrogation in more detail HeLa cells were pre-incubated with 0, 0.5, 1 and 2 µM ZM447439 for 1 h and subsequently treated with nocodazole or taxol for 16 h. Alternatively, HeLa cells were treated with 300 nM adriamycin for 24 h and the ZM447439 concentrations were added 1 h prior to UCN-01, which was added for 12 h.

As expected, inhibition of Aurora B affected the tension sensing branch of the spindle checkpoint more effectively than the one sensing attachment (see also Figure 31). In fact, much lower doses of ZM447439 were needed for the inhibition of spindle checkpoint signaling upon spindle stabilization by taxol than upon spindle depolymerization by nocodazole (Figure 40a). A half-maximal effect of ZM447439 was observed at about 1 µM in the presence of nocodazole, but at about 0.5 µM in the presence of taxol (Figure 40a). Spindle checkpoint signaling upon G2 checkpoint abrogation was dependent on the tension-sensitive arm of the spindle checkpoint (Figure 31e, Figure 40a, b). The mitotic arrest upon UCN-01 treatment was less stable than the one induced by nocodazole or taxol. This was indicated by the fact that 0.5 µM of ZM447439 was sufficient to induce almost complete escape from the mitotic arrest (Figure 40b).

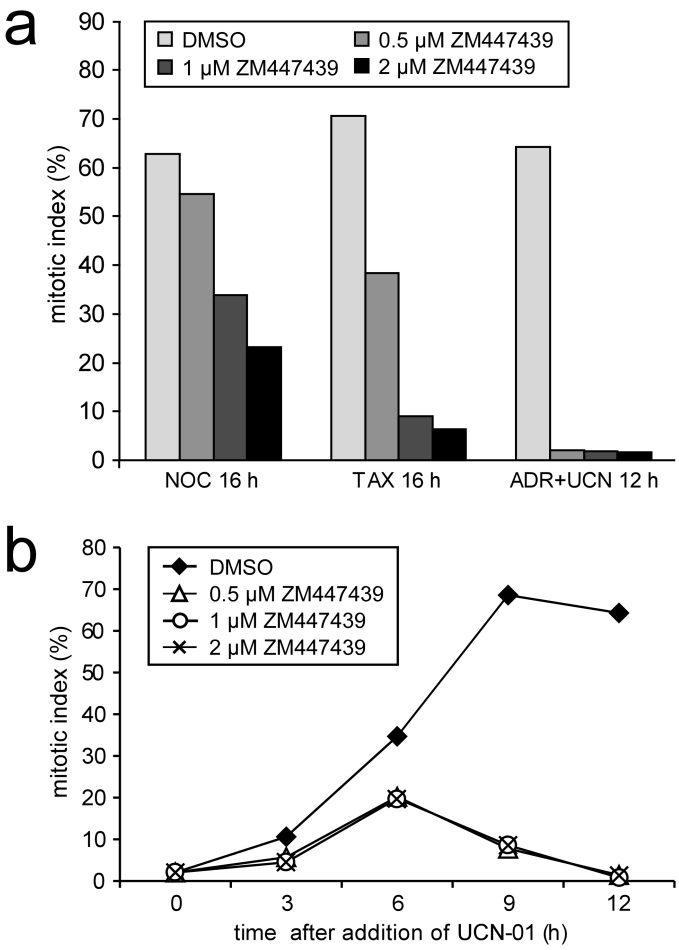

Figure 40: The Aurora B kinase inhibitor ZM447439 decreases the mitotic index upon G2 checkpoint abrogation more strongly than upon taxol- or nocodazole-induced spindle checkpoint activation. a) HeLa cells were pre-incubated with 0, 0.5, 1 and 2 µM ZM447439 for 1 h and were subsequently treated with 150 nM nocodazole (NOC) or 100 nM taxol (TAX) for 16 h. HeLa cells were treated with 300 nM adriamycin for 24 h and 100 nM UCN-01 for 12 h (a) or up to 12 h (b). 0, 0.5, 1 and 2 µM ZM447439 were added 1 h prior to UCN-01. The mitotic indices were determined by MPM2 FACS analyses and mean values were calculated from three independent experiments.

To clarify the role of p38 MAP kinase in signaling upon G2 checkpoint abrogation, HeLa cells were sequentially treated with adriamycin and UCN-01 for up to 12 h and 40 µM SB203580 were added 1 h prior to UCN-01.

SB203580 treatment reduced the mitotic arrest upon G2 checkpoint abrogation from 69.5% after 9 h of UCN-01 treatment to 39.2% (Figure 41a). HeLa cells were pre-incubated with 40 µM SB203580 for 1 h and subsequently treated with 150 nM nocodazole or 100 nM taxol for up to 12 h. Nocodazole or taxol treated cell populations maintained the mitotic arrest in the presence of SB203580 throughout the time course (Figure 41b). This argues for a role of p38 MAPK in spindle checkpoint signaling upon G2 checkpoint abrogation, but not in spindle damage-induced mitotic arrest and indicates that p38 does not interfere with mitotic entry.

Despite their different effects on mitotic arrest induced by G2 checkpoint abrogation or spindle damaging agents ZM447439 and SB203580 potentiated caspase 3 activity to the same extent upon adriamycin and UCN-01 treatment (see Figure 39).

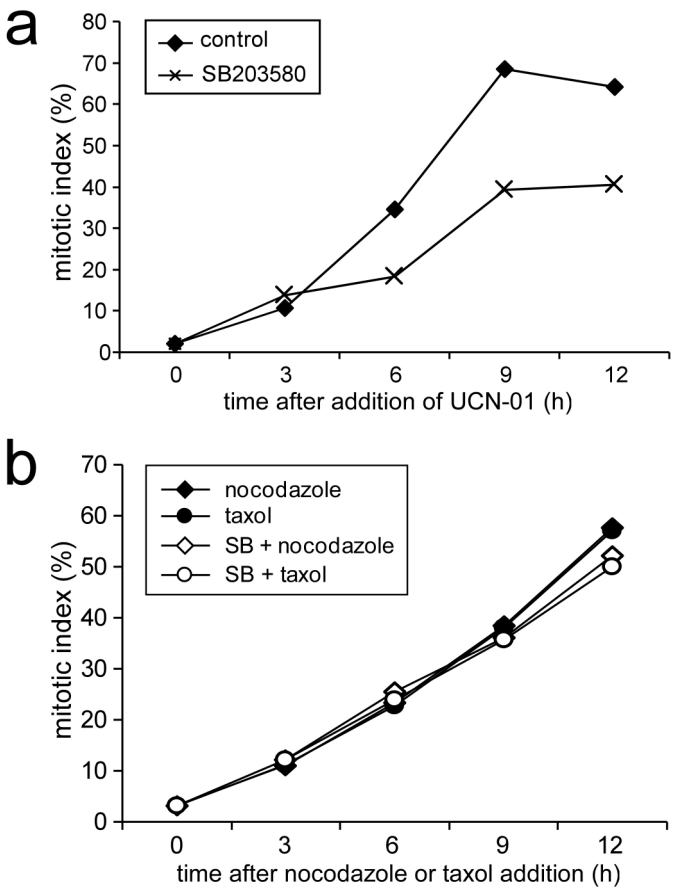

Figure 41: The MAP kinase inhibitor SB203580 decreases the mitotic index upon G2 checkpoint abrogation, but not upon spindle damage. a) HeLa cells were treated with 300 nM adriamycin for 24 h and 100 nM UCN-01 for up to 12 h. 40 µM SB203580 were added 1 h prior to UCN-01. The mitotic indices were determined by MPM2 FACS analyses and mean values were calculated from three independent experiments. b) HeLa cells were pre-incubated with 40 µM SB203580 (SB) for 1 h and subsequently treated with 150 nM nocodazole or 100 nM taxol for up to 12 h. The mitotic indices were determined and calculated as in a).

It has been postulated that the suppression of cytokinesis induces apoptosis due to a tetraploidy checkpoint acting in the postmitotic G1 phase (Andreassen *et al.* 2003). The conditions leading to cytokinesis defects in combination with G2 checkpoint abrogation were investigated and it was tested whether the execution of cytokinesis and apoptosis were interdependent. The effect of shRNA-mediated reduction in spindle checkpoint protein levels on cytokinesis upon G2 checkpoint abrogation was determined by FACS analyses. Sequential treatment of HeLa cells with adriamycin and UCN-01 for 12 h revealed that weakening the mitotic arrest resulted in reduced mitotic indices (Figure 31, Figure 42). Large 2N peaks indicated cytokinesis in cell populations with lowered levels of *BUB1*, *BUB1B*, *MAD2* and *MPS1L1* (Figure 42a). Enhanced cytokinesis might therefore be a direct consequence of spindle checkpoint weakening upon G2 checkpoint abrogation and did correlate with low apoptosis induction (Figure 34, Figure 42a). In contrast, treatment with various kinase inhibitors or shRNA-mediated repression of *survivin* led to accelerated mitotic exit, i.e. a reduction of the mitotic index, unaltered or slightly increased cytokinesis and greatly increased caspase 3 activity. These treatments increase sub G1 values in PI FACS analysis – with the notable exception of Aurora B inhibition and

survivin repression – underscoring the higher specificity of the caspase 3 assays for apoptosis detection compared to FACS analysis.

The Cdk1 inhibitors roscovitine and purvalanol A, Aurora B inhibition or repression of *survivin* effectively induced mitotic exit, while the MAPK inhibitor p38 induced only partial spindle checkpoint abrogation (Figure 42b). Cytokinesis levels upon these treatments were identical or lower than in control treated cells (Figure 42b).

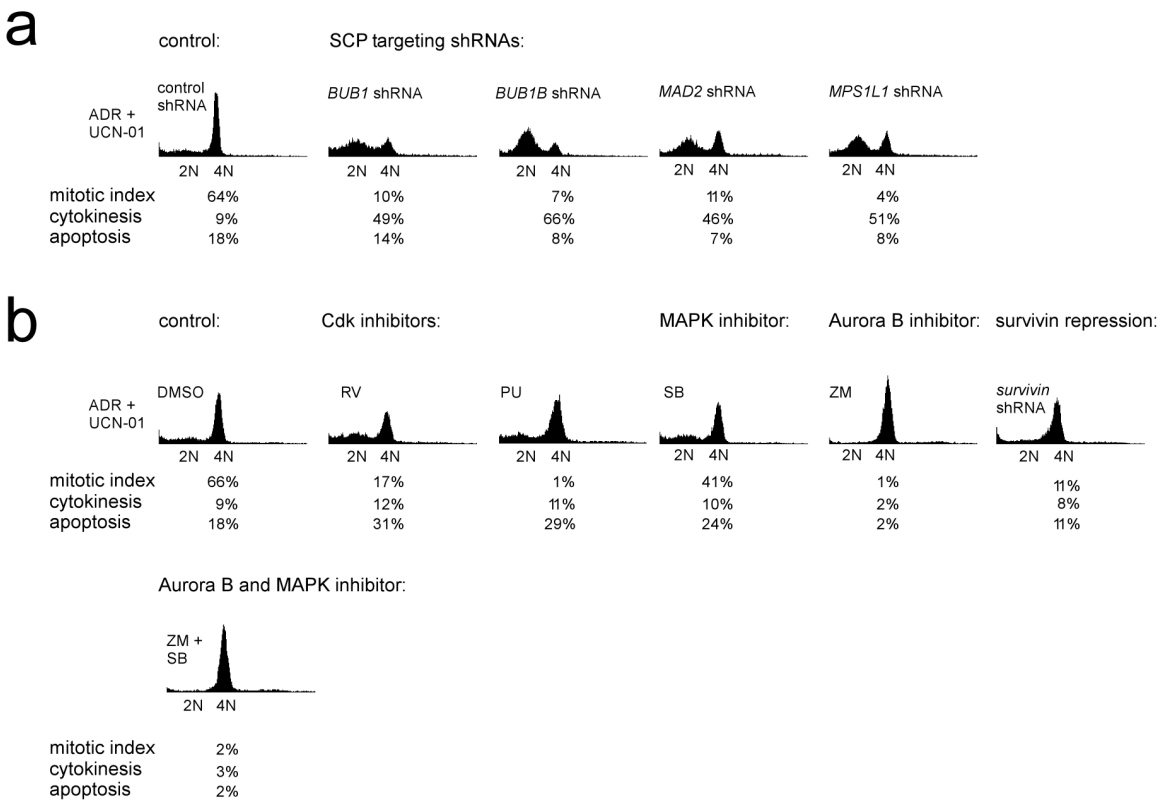

Figure 42: Suppression of cytokinesis and enhanced apoptosis upon G2 checkpoint abrogation might be positively correlated. a) HeLa cells transfected for 24 h with the shRNA constructs indicated were sequentially treated with 300 nM adriamycin for 24 h and 100 nM UCN-01 for 12 h. The DNA content was determined by PI FACS analysis and the mitotic index was measured by MPM2 FACS analysis. Representative FACS profiles are shown, the mitotic indices, percentage of cells that underwent cytokinesis (2N peak, measured as PI FACS) and the number of dead cells (apoptosis, measured as sub G1 FACS) are indicated. b) HeLa cells were treated with 300 nM adriamycin for 24 h and 100 nM UCN-01 for 6 h before 20 µM roscovitine (RV) or 10 µM purvalanol A (PU) were added for 6 h. HeLa cells were sequentially treated with 300 nM adriamycin for 24 h, 1 µM ZM447439 (ZM) or 40 µM SB203580 (SB), or both agents together for 1 h and 100 nM UCN-01 for 12 h. *Survivin* was repressed by shRNA treatment as described in a). All parameters were determined and are displayed as in a).

Aurora B inhibition led to the lowest values for 2N cells, p38 inhibition to the highest (Figure 42b). Interestingly, the combination of G2 checkpoint abrogation with p38 and Aurora B inhibitors yielded the same results as treatment with Aurora B inhibitor alone

with regard to MPM2, sub G1 and cytokinesis values (Figure 42b), but led to enhanced caspase 3 activity (Figure 39). These results indicate that accelerated mitotic exit induced by lowered levels of *BUB1*, *BUB1B*, *MAD2* and *MPS1L1* correlates with cytokinesis and low levels of apoptosis upon G2 checkpoint abrogation, whereas inhibition of Cdk1, Aurora B, reduced levels of *survivin* and p38 inhibition inhibit cytokinesis and enhance apoptosis.

In sum, I demonstrated that G2 checkpoint abrogation by adriamycin and UCN-01 treatment is an efficient strategy to target cells lacking functional p53, which kills cells upon mitotic entry by the intrinsic pathway of apoptosis. Apoptosis upon G2 checkpoint abrogation is promoted by a novel, probably spindle checkpoint-independent proapoptotic activity of Mad2 and restrained by the antiapoptotic activity of survivin, Aurora B, Cdk1 and bcl-2. Therefore, cell death could be strongly enhanced by pharmacological inhibition of Aurora B or Cdk1 or by genetic ablation of *survivin* leading to a mitotic activation of bax. MAP kinase inhibition also increased caspase 3 activation upon G2 checkpoint abrogation and acted synergistically with Aurora B kinase inhibition, suggesting a combination treatment, which could induce apoptosis more effectively. These findings strongly argue for an improvement of adriamycin and UCN-01-mediated G2 CP abrogation chemotherapy by combination with other agents targeting the survival pathway to potentiate apoptosis.

6. Targeting the spindle checkpoint induces apoptosis in cancer cells

Resistance of cancer cells to chemotherapy is a widespread and serious problem (Lee and Schmitt 2003). The experiments described in the preceding chapters demonstrated that impairment of the spindle checkpoint can confer resistance to spindle and DNA damaging agents, many of them commonly used for chemotherapy. A possible strategy to overcome this resistance could be to abrogate the spindle checkpoint, since it is essential for cell viability (Kalitsis *et al.* 2000, Michel *et al.* 2001, Kops *et al.* 2004, Iwanaga *et al.* 2007). Therefore, our lab aimed to identify pharmacological inhibitors of the spindle checkpoint. In fact, Gö6976, an indolocarbolozole compound structurally related to UCN-01, was identified as a potent spindle checkpoint abrogator in a screen for kinase inhibitors abrogating mitotic arrest (manuscript in preparation).

Severe repression of Bub1, BubR1 or Mad2 induces apoptosis

To confirm that severe spindle checkpoint impairment *per se* leads to apoptosis HeLa cells were transiently transfected with shRNA constructs targeting *BUB1*, *BUB1B* and *MAD2*. The degree of repression of the targeted spindle checkpoint proteins was monitored by an assay determining the functionality of the spindle checkpoint.

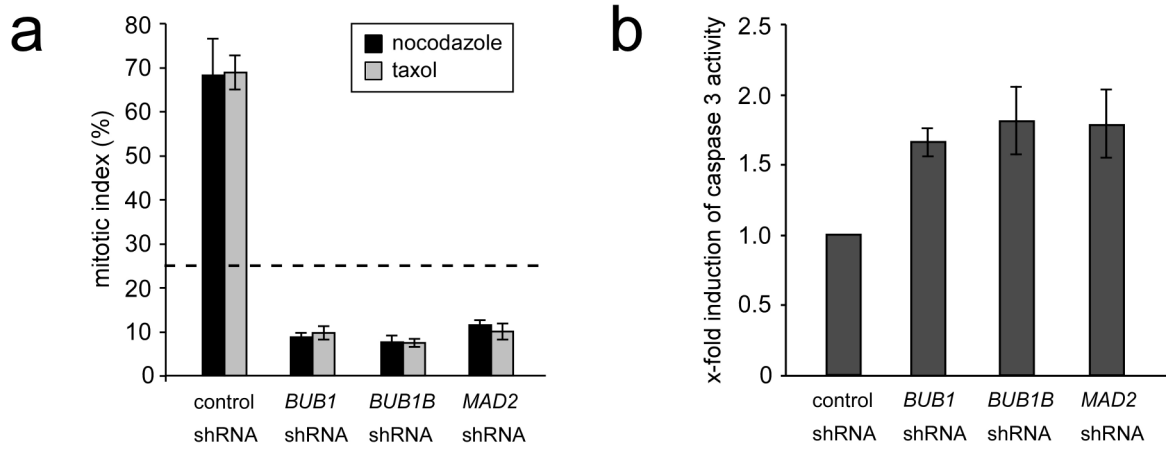

Figure 43: Severe repression of spindle checkpoint components induces spontaneous apoptosis. HeLa cells were transiently transfected with shRNA constructs targeting *BUB1*, *BUB1B* and *MAD2*. a) 24 h post transfection the cells were treated with 150 nM nocodazole or 100 nM taxol for 16 h and the mitotic index was determined to control the inhibition of spindle checkpoint activity. Mean values and standard deviations from at least three independent experiments were determined. b) Caspase 3 activity of 1 x 10^5 cells was measured 48 h post transfection. The mean values and standard deviations from at least three independent experiments were calculated.

The mitotic arrest of the transfected cells was measured by MPM2 FACS analysis after exposure to 150 nM nocodazole or 100 nM taxol for 16 h (Figure 43a). Depending on the amount of shRNA transfected (data not shown) the mitotic indices were significantly lower than in previous experiments (about 10% instead of 15-40%) and therefore indicated sufficiently low spindle checkpoint protein levels to ensure lethality (Figure 43a). Caspase 3 activation was measured 48 h after transfection and found to be significantly increased compared to the empty vector control (Figure 43b) verifying that severe repression of spindle checkpoint function leads to the induction of apoptosis.

Gö6976 overrides the spindle checkpoint independent of Cdk1

HCT116 wt cells had been used to identify Gö6976 as a novel spindle checkpoint abrogator. It should be tested whether Gö6976 had the same effect on mitotic arrest of spindle checkpoint impaired or *TP53*$^{-/-}$ cells. The mitotic indices of HCT116 wt, HCT116 *TP53*$^{-/-}$, HCT116 *MAD2*$^{+/-}$ cells and the HCT116 *MAD1*^{kd} cell clone 2-31 treated simultaneously with 150 nM nocodazole and 2 µM Gö6976 or DMSO for 16 h were determined by MPM2 FACS analysis (Figure 44a). Gö6976 reduced spindle checkpoint activation significantly in all cell lines. HCT116 wt and HCT116 *TP53*$^{-/-}$ cells arrested at levels normally seen upon nocodazole treatment of the spindle checkpoint compromised HCT116 cell lines. These cells, however, had an even further reduced spindle checkpoint response upon co-treatment with Gö6976 than after nocodazole treatment alone. Since Gö6976 impairs mitotic arrest and inhibition of Cdk1 during mitotic arrest results in exit from the arrest (Blagden and de Bono 2005), Cdk1 was tested as possible mitotic target of Gö6976. For the *in vitro* samples Cdk1/Cyclin B complexes were co-immunoprecipitated from nocodazole treated cells and incubated with the inhibitors for 30 min (see experimental scheme, left panel, Figure 44b). Incubation with 150 nM nocodazole and 200 µM ALLN to prevent mitotic exit in the presence of Gö6976, UCN-01 or roscovitine was carried out to determine inhibition of Cdk1 in living cells (see experimental scheme, right panel, Figure 44b). Gö6976 did not reduce Cdk1 kinase activity towards histone H1 in the *in vitro* assay and by only 9% in the *in vivo* assay. UCN-01, the negative control for Gö6976, did not diminish kinase activity in the *in vitro* assay and by just 8% in the *in vivo* assay, whereas the positive control roscovitine strongly inhibited Cdk1 (Figure 44b). These results suggest that Gö6976 overrides the spindle checkpoint independent of Cdk1 inhibition.

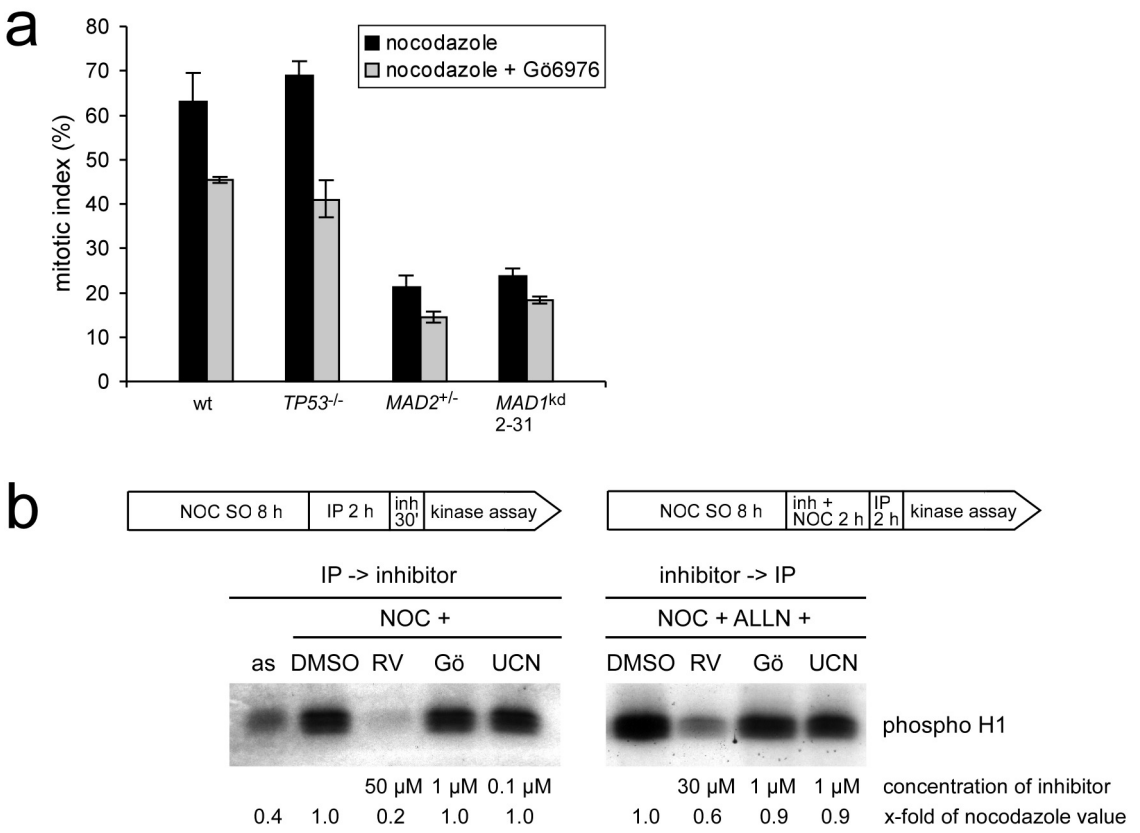

Figure 44: Gö6976 overrides the mitotic spindle checkpoint. a) HCT116 wt, HCT116 *TP53*$^{-/-}$, HCT116 *MAD2*$^{+/-}$ cells and the HCT116 *MAD1*^{kd} cell clone 2-31 were treated sequentially with 150 nM nocodazole for 14 h and 2 µM Gö6976 or DMSO for 2 h and the mitotic index was determined by MPM2 FACS analysis. Mean values from at least three independent experiments were calculated. b) HeLa cells were treated as indicated in the experimental scheme. For the *in vitro* samples Cdk1/Cyclin B complexes were coimmunoprecipitated from nocodazole treated shake-off cells with the Cyclin B antibody and incubated with the inhibitors at concentrations of 50 µM roscovitine (RV), 1 µM Gö6976 (Gö) or 100 nM UCN-01 (UCN) for 30 min (left panel). Incubation with 150 nM nocodazole and 200 µM ALLN to prevent mitotic exit in the presence of 30 µM RV, 1 µM Gö6976 or 1 µM UCN-01 was done with living cells for the *in vivo* samples prior to the Cdk1/Cyclin B coimmunoprecipitation with the Cyclin B antibody (GNS-1, Santa Cruz, right panel). Cdk1 activity was determined in histone H1 kinase assays. One representative experiment is shown.

Gö6976 induces apoptosis in HCT116 cells

To test whether Gö6976 induces apoptosis and whether this effect depended on traversal through mitosis, Gö6976 was added to HCT116 wt cells 7 h after release from a double thymidine block just before cells entered mitosis and apoptosis was measured 7 h or 14 h later. Gö6976 induced caspase 3 activity in a concentration-dependent manner in fluorometric caspase 3 assays. 2, 10 and 20 µM Gö6976 led to a 1.3-fold, 3.0-fold and 4.2-fold increase in caspase 3 activity. Moreover, treatment with roscovitine prevented Cdk1-mediated entry into mitosis and the activation of caspase 3 in response to Gö6976 (Figure

45a). Other hallmarks of apoptosis including PARP cleavage (Figure 45b) and DNA laddering (Figure 45c) were detectable after 14 h of Gö6976 treatment. Thus, the induction of apoptosis in response to pharmacological spindle checkpoint abrogation requires progression through mitosis.

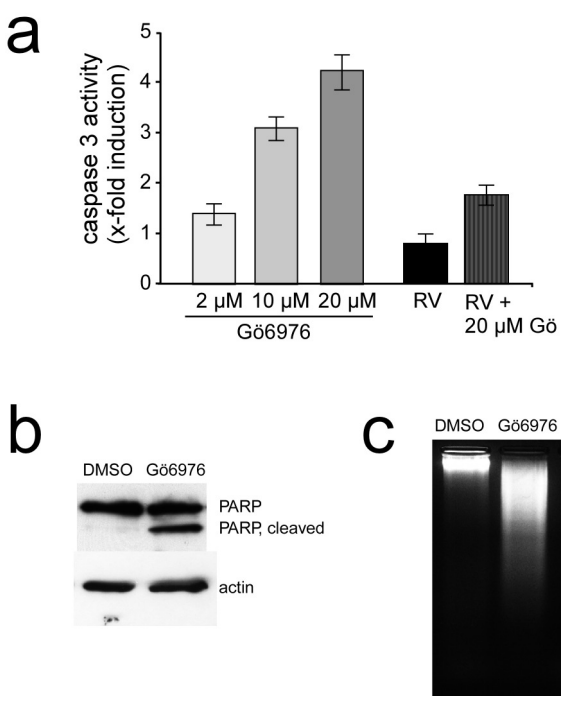

Figure 45: Spindle checkpoint inhibition by Gö6976 results in the induction of apoptosis. 1 x 10^5 HCT116 wt cells synchronized at G1/S were released for 7 h and then treated with Gö6976 for 7 h or 14 h. a) Caspase 3 activation was measured in a quantitative fluorometric assay after 7 h treatment with 2, 10 or 20 µM Gö6976 or 30 µM roscovitine (RV) combined with DMSO or 20 µM Gö6976. Mean values and standard deviations from three independent experiments are shown. b) PARP cleavage was detected on a Western blot. The result from one representative experiment is presented. c) Internucleosomal DNA laddering was detected in a DNA laddering assay. The result from one representative experiment is shown.

A broad panel of human cancer cell lines is sensitive to Gö6976-mediated apoptosis

To exclude a cell line specific effect, a panel of human cancer cell lines was investigated for sensitivity towards Gö6976 treatment and compared with non-cancerous cells. A panel of cancer cell lines originating from different tissues and two non-cancerous cell lines were treated with 15 µM Gö6976 for 24 h and the activation of caspase 3 was determined in several experiments. The following cell lines including two non-transformed cell lines were tested: BJ-tert and HUVEC (human immortalized fibroblast and untransformed endothel cell lines, respectively), Ovca 429 and A2780 (ovary cancer), U2OS and SaOS-2 (osteosarcoma), A549 and H1299 (lung cancer), T47D (breast cancer), HeLa and C33A (cervix cancer) and four colon carcinoma cell lines: CaCo-2, SW-620, HT29 and HCT116 cells. Caspase 3 activity was induced in all cancer cell lines, indicating their susceptibility to Gö6976-induced apoptosis, whereas the non-cancerous cell lines did induce caspase 3 activity very weakly (Figure 46). The degree of caspase 3 induction, however, varied

greatly between the cancer cell lines from different tissues and between cell lines from the same tissue. HeLa, A549, Ovca429 and SW-620 cells were the most sensitive cell lines with caspase activation values of 44000, 35000, 29000 and 28000, whereas all other cancer cell lines exhibited inductions between 6000 and 20000 a.u. (Figure 46). In contrast, the non-cancerous cell lines showed caspase 3 activities below 4000 a.u. (Figure 46). Half of the cancer cell lines evaluated were above and half were below the mean value for all cancer cell lines tested for their reaction to Gö6976. Besides for their origin from different tissues, the cancer cell lines had been chosen for their differences in functionality of p53 and spindle checkpoint to get an impression, if Gö6976-mediated apoptosis would display selectivity for these features. However, the lack of p53 did not correlate with sensitivity to Gö6976. A correlation between normal spindle checkpoint status and Gö6976 sensitivity was apparent for the three most sensitive cell lines (HeLa, A549 and Ovca429 cells).

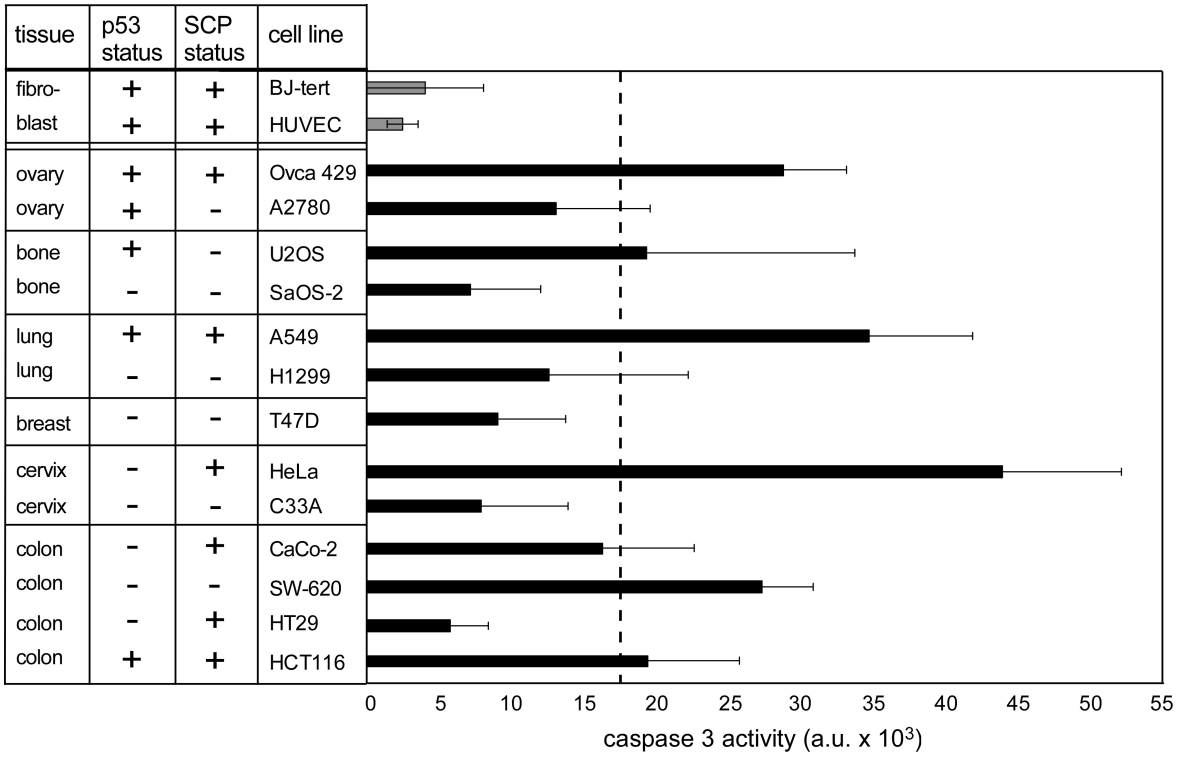

Figure 46: Various human cancer cell lines are sensitive to Gö6976-induced apoptosis. 6 x 10^4 cells of the indicated cell lines were seeded 24 h prior to treatment and were subsequently treated with 15 µM Gö6976 for 24 h. Caspase 3 activation was determined, the background values were subtracted and mean values and standard deviations from at least three independent experiments were calculated. The top cell lines (BJ-tert, HUVEC) are non-cancerous fibroblast cell lines, all other cell lines are cancer cell lines. The p53 and spindle checkpoint status of all cell lines is given as reported in the literature.

However, as the cancer cell lines tested probably contain a lot more alterations to genes and cell cycle checkpoints than the known impairments of p53 or spindle checkpoint status, it is possible that many other unknown factors govern sensitivity to Gö6976-induced apoptosis.

To shed light on the role of spindle checkpoint function in Gö6976-mediated apoptosis, the isogenic HCT116 *MAD2*$^{+/-}$ cells and the HCT116 *MAD1*^{kd} clone 2-31 cells were compared to HCT116 wt cells. The HCT116 cell lines were synchronized at G1/S by a double thymidine block, released for 7 h and treated with Gö6976 concentrations of 2.5, 5, 10, 15 and 20 µM and caspase 3 activity was determined. Interestingly, both spindle checkpoint impaired cell lines, HCT116 *MAD2*$^{+/-}$ cells and HCT116 *MAD1*^{kd} cells, were slightly more sensitive to Gö6976 treatment than the HCT116 wt cells (Figure 47), suggesting that Gö6976-induced apoptosis in HCT116 cells can be even more effective in spindle checkpoint impaired cells than in spindle checkpoint proficient cells.

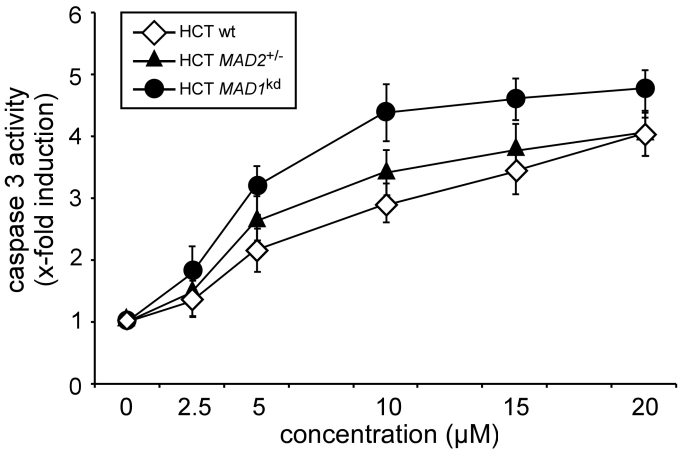

Figure 47: Gö6976-induced apoptosis in HCT116 cell lines is enhanced by spindle checkpoint impairment. 1 x 10^5 doubly thymidine blocked HCT116 wt, HCT116 *MAD2*$^{+/-}$ and HCT116 *MAD1*^{kd} cell clones 2-31 were released for 7 h and then treated with Gö6976 for 7 h. The x-fold induction of caspase 3 activity and the standard deviation were calculated from values of least three independent experiments.

Taken together, the feasibility of spindle checkpoint abrogation as a strategy to overcome chemotherapy resistance was successfully demonstrated by the use of the newly identified pharmacological spindle checkpoint abrogator Gö6976. Treatment with Gö6976 mimics the lethal effect of severe repression of spindle checkpoint proteins. Gö6976 reduces the mitotic arrest in spindle checkpoint normal cells, but also in spindle checkpoint compromised cells and induces apoptosis upon passage through mitosis. It displays some selectivity for apoptosis induction in cancer cells over non-cancerous cells, suggesting to use it as a lead compound for anti-cancer drug development.

Discussion

1. Comparison of stable colon cancer cell lines with reduced Mad1 and Mad2 levels

In human cancers the expression levels of multiple genes associated with spindle checkpoint function or mitosis are altered mainly by epigenetic mechanisms, but amplifications and point mutations have also been described, for instance in *MAD1*, *MAD2, BUB1*, *BUB1B* and *PLK1* (Perez de Castro *et al.* 2007). Numerous cases of Mad2 up- or downregulation in cancers originating from various organs were reported (Li and Benezra 1996, Takahashi *et al.* 1999, Wang *et al.* 2000, Wang *et al.* 2002, Hernando *et al.* 2004, Sze *et al.* 2004, Wu *et al.* 2004, Fung *et al.* 2007). In ovary cancer Mad1 and Mad2 protein levels are reduced (Wang *et al.* 2002), whereas both are increased in breast cancers (Yuan *et al.* 2006). *MAD2* expression was elevated in renal cancer, while *MAD1* expression was lowered (Pinto *et al.* 2007). Interestingly, a *MAD1* polymorphism found in several cancer cell lines might decrease protein interaction with Mad2 and spindle checkpoint signaling (Iwanaga *et al.* 2002).

To compare the consequences of partial downregulation of *MAD1* to those of *MAD2* a stable human cancer cell line expressing reduced levels of *MAD1* was created for the first time. Its characterization revealed several similarities to the effects of *MAD2* downregulation, but also some significant differences. The mitotic spindle checkpoint-induced mounting and also the maintenance of a mitotic arrest is Mad1-dependent. Mad1 is required for mitotic arrest upon treatment with diverse pharmacological inhibitors of spindle dynamics or spindle bipolarity like nocodazole, taxol or monastrol. The spindle checkpoint impairment induced by *MAD1* downregulation leads to a lower overall arrest level and a shortened arrest time, which is associated with premature mitotic slippage. Interestingly, higher levels of Mad2 than of Mad1 are required for full spindle checkpoint function, since a reduction to 70-80% of wild typic Mad2 levels has the same detrimental effect on mitotic arrest proficiency as a reduction of Mad1 levels to 50-65% of the wild type. However, in spite of an impaired spindle checkpoint the overall growth rate is unchanged in untreated HCT116 *MAD1* knockdown and HCT116 *MAD2*$^{+/-}$ cell populations compared to the parental cell line. Spindle checkpoint impairment in HCT116 *MAD1* knockdown cells is accompanied by aneuploidization and continuous chromosomal instability (Kienitz *et al.* 2005) to a similar degree as in HCT116 *MAD2*$^{+/-}$ cells (Michel *et*

al. 2001). However, in contrast to the consequences of reduced Mad2 levels, mitotic timing during an undisturbed mitosis is unaltered in *MAD1* knockdown cells. Only cells with lowered Mad2 levels show premature sister chromatid separation (Kienitz *et al.* 2005), probably due to insufficient inhibition of the proteolytic degradation of securin, whereas chromatid cohesion is intact in *MAD1* knockdown cells.

Mad1 and Mad2 in cancerogenesis and chemotherapy resistance

Mad2 might have at least two distinct functions in mitosis, firstly in conjunction with Mad1 in the spindle checkpoint and secondly as mitotic timer in a kinetochore-independent manner (Meraldi *et al.* 2004), whereas Mad1's only known function in mitosis is spindle checkpoint-related. Since there is only a partial overlap of Mad1 and Mad2 functions, a tumor cell might gain a selective advantage by their concomitant deregulation. Indeed, simultaneous reduction of Mad1 and Mad2 levels is found in human ovarian cancer cell lines (Wang *et al.* 2002), but so far there is no large scale investigation of concomitant Mad1 and Mad2 deregulation in different cancer types. As I could show, Mad2 acts as a proapoptotic protein upon treatments with chemicals targeting the mitotic spindle or topoisomerase II, thus, its downregulation confers resistance to such chemotherapies. It is possible, that Mad1 and Mad2 have additional functions in mitosis, the spindle checkpoint and beyond, but so far evidence for this is scarce and is mainly reported for yeast. Mad1 and Mad2 are localized to nuclear pores during interphase in *S. cerevisiae* and human cells and Mad1 might actively mediate nuclear transport, whereas Mad2 is believed to be sequestered at nuclear pores (Campbell *et al.* 2001, Iouk *et al.* 2002). Furthermore, Mad2 delays mitotic entry in the presence of unreplicated DNA in fission yeast as component of the DNA replication checkpoint (Sugimoto *et al.* 2004). In *S. cerevisiae* DNA damage-induced spindle checkpoint and MEN activation via Mad2, Bub3 and the BubR1 homolog Mad3 provides time for various repair attempts and results in gross chromosomal rearrangements, which are typically found in cancer cells (Myung *et al.* 2004). Furthermore, reduced levels of BubR1 cause premature aging and infertility in mice (Baker *et al.* 2004) and concomitant downregulation of *BUB3* and *RAE1* also accelerates aging in mice (Baker *et al.* 2006). Since homozygous deletions of various spindle checkpoint genes are lethal during murine embryogenesis and in most human cell lines, their products appear to be essential for survival, probably by ensuring a correct mitosis (Kops *et al.* 2005, Perera *et al*. 2007). Significantly, mice heterozygous for Mad1 (Iwanaga *et al.* 2007) or

Mad2 (Michel *et al.* 2001) develop spontaneous tumors. However, mice heterozygous for other spindle checkpoint genes like Bub3, BubR1, CENP-E and Rae1 (Baker *et al.* 2004, Dai *et al.* 2004, Baker *et al.* 2006, Weaver *et al.* 2007) only develop tumors upon exposure to cancerogenic chemicals, indicating that Mad1 and Mad2 play a more prominent role in the inhibition of cancerogenesis than many other known spindle checkpoint proteins. Mad2 downregulation is found in various human tumors, including breast, lung, nasopharyngeal and ovarian cancers, hepatomas and testicular germ cell tumors (Li and Benezra 1996, Takahashi *et al.* 1999, Wang *et al.* 2000, Wang *et al.* 2002, Sze *et al.* 2004, Fung *et al.* 2007) and is correlated with spindle checkpoint impairment and chemotherapy resistance. One mechanism conferring resistance to apoptosis by reduced Mad2 levels is the upregulation of antiapoptotic bcl-2 relative to proapoptotic bax (Du *et al.* 2006) leading to resistance against vincristine and cisplatin. Surprisingly, not only downregulation, but also overexpression of Mad2 can contribute to cancerogenesis, suggesting that fine-tuning of Mad2 expression is essential to preserve the nontransformed state of a cell. Recent experiments with inducible Mad2 overexpression in transgenic mice showed that transient Mad2 overexpression is sufficient to produce aneuploidy and other mitotic defects like anaphase bridges and chromosome breaks and to induce various tumors (Sotillo *et al.* 2007). Interestingly, in contrast to many other studied oncogenes sustained Mad2 overexpression is not required for tumor maintenance (Sotillo *et al.* 2007). Inducible mouse models could also help to further characterize the contribution of Mad1 to cancerogenesis and tumor maintenance. Even homozygous deletion of spindle checkpoint genes can be mimicked in such animal models, as recently shown for Bub1, where it leads to lethal mitoses when inactivated in postimplantation embryos or sterility when inactivated in adult males (Perera *et al*. 2007). Interestingly, *MAD1* expression levels can be regulated by the tumor suppressor p53, although contradicting reports regarding its up- or downregulation exist (Iwanaga and Jeang 2002, Chun and Jin 2003). It was also reported that p53 can repress expression of *MAD2* and regulate expression of other cell cycle-related genes (Zhao *et al.* 2000). *MAD2* expression can be increased by loss of the tumor suppressor Rb or overexpression of the oncogene E2F (Hernando *et al.* 2004). Defects in the Rb pathway are common in human solid tumors, but future studies have to determine the real frequency of changes in *MAD2* levels correlated with Rb pathway defects. Thus, at least in some instances spindle checkpoint impairment leading to aneuploidy, chromosomal instability and cancerogenesis can be generated by alteration of spindle checkpoint protein expression levels. Altered gene expression can be caused by

mutations in oncogenes or tumor suppressor genes or their promoters (Rajagopalan *et al.* 2003, Kops *et al.* 2005) or epigenetic mechanisms (Shichiri *et al.* 2002, Perez de Castro *et al*. 2007), whereas aneuploidization can affect the expression levels of numerous unmutated genes simultaneously. Aneuploidization and its effect on gene expression is one of the most prominent features of cancer cells (Duesberg and Li 2003, Bharadwaj and Yu 2004, Kops *et al*. 2005) and poses an alternative explanation for the frequent spindle checkpoint impairment found in cancer cells, which often lack detectable mutations in known spindle checkpoint genes. The loss or gain of whole chromosomes or large parts thereof leads to the absence or additional presence of large groups of genes in the genome of a cell and therefore to dramatic changes in gene dosage of all these genes, which could also directly or indirectly affect spindle checkpoint components. In an ingenious experiment artificial trisomies were generated by injection of various chromosomes into human immortalized epithelial or cancer cells and global gene expression was determined using cDNA arrays. Interestingly, in all cases transcription was significantly upregulated not only regarding the trisomic, but also numerous other chromosomes, which might induce large-scale changes of the cell's properties leading to malignant transformation (Upender *et al.* 2004). However, it cannot be excluded that as yet unknown spindle checkpoint genes are mutated in spindle checkpoint impaired cancers. Projects like MitoCheck aiming to identify all genes – especially all kinases and their targets – involved in mitosis and spindle checkpoint signaling should help to close this gap in current knowledge (http://www.mitocheck.org). Furthermore, extensive studies on human cell cycle regulators (Mukherji *et al.* 2006) and on the phosphoproteome of the mitotic spindle (Nousiainen *et al.* 2006) have confirmed previous data and added numerous new potential players to the list of putative and established proteins involved in these processes. Analysis of gene expression patterns on mRNA and protein levels in various cancer cell lines or tumor samples could elucidate the frequency of expression changes in spindle checkpoint genes. The expression data could be correlated to spindle checkpoint impairment, aneuploidy, tumor stage and chemotherapy response and help to assess the actual significance of spindle checkpoint genes in human cancer.

2. The role of a functional spindle checkpoint and p53 in preventing polyploidization upon prolonged spindle damage

The contribution of polyploidy and aneuploidy to cancerogenesis is incompletely understood, but polyploidy seems to precede aneuploidy in this process (Shackney *et al*. 1989, Borel *et al.* 2000, Meraldi *et al*. 2002, Margolis *et al*. 2003). Spindle damaging agents induce prolonged mitotic arrest, which is followed by spindle checkpoint adaptation, i.e. checkpoint inactivation and mitotic exit, which is commonly termed mitotic slippage. Mitotic arrest in the presence of spindle damage results in cytokinesis failure and entry of tetraploid cells into G1 phase. The pseudo-G1 or tetraploidy checkpoint inhibits entry into S phase and endoreduplication of the DNA to higher ploidies in a p53-dependent manner (Minn *et al.* 1996, Lanni and Jacks 1998). Premature mitotic slippage occurs in spindle checkpoint impaired cells and depends on Cyclin B destruction (Brito and Rieder 2006).

Elucidation of pseudo-G1 checkpoint mechanisms

There are significant differences in the checkpoints inducing arrest before S phase and before mitosis. The pseudo-G1 or tetraploidy checkpoint depends on the accumulation and activation of p53 during a prolonged spindle checkpoint-mediated arrest leading to the transcriptional activation of the Cdk inhibitor *CDKN1A/WAF1* (p21; Lanni and Jacks 1998). Accumulation of p21 then inhibits entry into S phase and therefore prevents DNA replication in cells possessing both, an intact spindle checkpoint and functional p53. Simultaneously, transcription of the proapoptotic gene *BAX* is activated by p53, but the p21-induced arrest protects the cells from immediate execution of apoptosis. In our exploratory experiments accumulation and activation of p53 upon spindle damage – and probably upon a failed mitosis in general – appears to be independent of the ATM, ATR, Chk1 and Chk2 kinases involved in DNA damage signaling, although a recent report indicates a role for ATM (Oricchio *et al.* 2006). Northern blot data revealed a reduced expression of *CDKN1A/WAF1* and *BAX* in HCT116 *MAD2*$^{+/-}$ cells compared to wild typic cells, suggesting that the transactivation activity of p53 might be compromised in spindle checkpoint impaired cells, whereas the rate of p53 accumulation upon spindle or DNA damage appeared to be unchanged in spite of the different time points of mitotic slippage in the two cell lines. A certain level of p53 might be required to induce G1 arrest upon

mitotic slippage and this level might not be reached in spindle checkpoint impaired cells with shortened mitotic arrest timespans. Therefore spindle checkpoint impaired cells will enter S phase, but since accumulation of p53 continues after mitotic slippage in all following cell cycle phases, sufficient levels of p53 to arrest endoreduplicated cells before the next mitosis are also achieved in spindle checkpoint impaired cells (Figure 48).

Previous studies have shown distinct phosphorylation patterns of p53 upon spindle damage and upon different kinds of DNA damage (Stewart *et al.* 2001, Lavin and Gueven 2006), including the phosphorylation of p53 after spindle damage at serine 15, which we could also show after nocodazole treatment (data not shown). To find the upstream kinases or other factors responsible for p53 activation and accumulation upon spindle damage, inhibitors and nocodazole were added sequentially to HCT116 wt cells and reduced accumulation of p21 was used as a read-out for inhibition of p53 activation. The phosphatidylinositol-3 kinase (PI_3K) inhibitor LY294002 strongly inhibited the stabilization and, thus, accumulation of p53 and the *CDKN1A/WAF1* expression, suggesting a role for PI_3K or a PI_3K-related kinase in p53 signaling upon spindle damage. However, it was not tested whether LY294002 might induce a G2 arrest inhibiting mitotic entry and the p53 accumulation accompanying it. The PI_3K pathway regulates multiple aspects of an undisturbed or disturbed cell cycle. Among its most prominent functions is the positive regulation of the transition from quiescence to proliferation and from G1 to S phase, while less is known about the role of PI_3 kinases in G2/M transition and upon DNA damage (Garcia *et al.* 2006). The PI_3K pathway also regulates transcription factors, e.g. members of the Fox family or p53. G2 progression and mitotic entry depends on FoxO (forkhead box containing protein, O subfamily)-mediated expression of *CCNB1* and *PLK1*, while FoxM1 (forkhead box containing protein, M subfamily 1) couples DNA synthesis and mitosis and mediates expression of *CCNB1* and *CENPF*, ensuring G2 and mitotic progression (Laoukili *et al.* 2005, Garcia *et al.* 2006). Cancerogenesis via PI_3K pathway deregulation occurs mainly through suppression of inhibitory phosphatases like PTEN (phosphatase and tensin homolog deleted on chromosome 10), a tumor suppressor which is mutated in 50% of human cancers (Cantley and Neel 1999) and through increased activation of the PI_3K pathway, e.g. via its downstream target Akt/PKB (Garcia *et al.* 2006). Constitutively active Akt was reported to override DNA damage-induced G2 arrest (Kandel *et al.* 2002) and to promote cell survival by inactivating bad, whereas expression of dominant negative Akt increased apoptosis in taxol treated ovary cancer cells (Chang *et al.* 2003). Thus, in analogy to abrogation of DNA damage-induced G2 arrest by PI_3K

inhibition, the treatment of mitotically arrested cells with the PI_3K inhibitor LY294002 could override the spindle checkpoint. Interestingly, Akt-mediated phosphorylation of Mdm2 promotes p53 degradation and Akt-mediated phosphorylation of p21 suppresses its cell cycle inhibitory function via translocation to the cytoplasm (Kandel *et al.* 2002). Taken together, modulation of the PI_3K pathway has to be carefully evaluated for its involvement in spindle checkpoint-mediated mitotic arrest and apoptosis upon spindle damage. The effect of PI_3K inhibitors could be a matter of sequence: On one hand, mitotic entry or mitotic arrest might be impaired by PI_3K inhibitors, which would present an unwanted outcome, because apoptosis might be suppressed under these circumstances. On the other hand, treatment of cells with PI_3K inhibitors upon prolonged spindle checkpoint arrest might be proapoptotic, because it would preserve bad activation. Rottlerin also led to reduced p53 and p21 levels in nocodazole treated cells, but is not suitable for future studies due to its broad inhibitory spectrum. Although spindle damage-induced p53 activation is known for a long time, it remained a mystery how the signaling between an activated spindle checkpoint and p53 occurred, until a recent publication identified BubR1 as a major kinase that phosphorylates p53 upon mitotic damage. BubR1 confers activating and stabilizing phosphorylations to p53's serine residues 15 and 46, but not to serine 9 or 20 (Ha *et al.* 2007). p53 and BubR1 interact directly through their N-termini, which might prevent Mdm2 binding and consequently degradation of p53, although this remains to be tested (Ha *et al.* 2007). Upon prolonged nocodazole-induced spindle damage *TP53*$^{-/-}$ cells expressing reduced levels of BubR1 showed a synergistic increase in rereplication compared to cells with either a loss of p53 or reduced levels of BubR1, indicating that concomitant loss of p53 and normal spindle checkpoint function can dramatically enhance the occurrence of premalignant phenotypes (Ha *et al.* 2007). Further experiments could identify additional components of the pathway signaling to p53 upon mitotic perturbations by using pharmacological inhibitors of kinases or other enzymes, they could employ mutants of other genes or use siRNA technology to downregulate their expression. Cell lines harboring mutants of *TP53* that retain transactivating or transrepressive potential or are transcriptionally inactive could also be helpful to elucidate the spectrum of p53 target genes and their gene expression pattern in response to spindle damage could be analyzed with microarrays. Mass spectrometric analysis of posttranslational modifications of p53 could also be performed.

The novel postmitotic G2 checkpoint

Spindle checkpoint impaired cells undergo premature mitotic slippage upon spindle damage and are able to replicate their DNA to octaploidy. However, they do not reach the next mitosis or the subsequent S phase, whereas p53-negative cells do not arrest and reach higher ploidies. Thus, a novel p53-dependent checkpoint acting in G2 inhibits mitotic entry of endoreduplicated cells which originated from a failed mitosis. It was not investigated whether this G2 arrest upon mitotic failure and rereplication was resolved later, i.e. cells then resumed to traverse the cell cycle and if they incurred a lethal amount of damage or survived. Therefore, future experiments like colony formation assays should address long-term survival in spindle checkpoint impaired cells upon spindle damage.

In contrast to the tetraploidy checkpoint, the newly identified p53-dependent G2 checkpoint is inhibitable by caffeine and UCN-01, which target ATM/ATR and Chk1 kinases. The finding that spindle checkpoint impaired cells endoreduplicate their DNA only once was puzzling at first, but can be explained be the existence of the novel postmitotic G2 checkpoint. Apparently the level of activated p53 is insufficient in spindle checkpoint impaired cells to prevent entry into S phase and subsequent DNA replication, thus generating octaploid cells from the tetraploid cells that slipped out of the spindle damage-induced mitotic arrest (Figure 48). It is conceivable that to induce p53-dependent postmitotic G2 arrest, either lower p53 levels are required than to induce G1 arrest, or p53 accumulation during S phase continues to levels sufficient to induce G2 arrest. The next step in characterizing this checkpoint pathway is the identification of its signaling components, which should employ a wide variety of methods like detailed previously (Andreassen *et al.* 1996, Chen *et al.* 2003, Blagosklonny 2006) for the uncovering of components of the pseudo-G1 checkpoint. The question which level of p53 protein is required for functioning of the postmitotic G2 checkpoint could be addressed by manipulating p53 accumulation with inducible or repressible p53 expression systems.

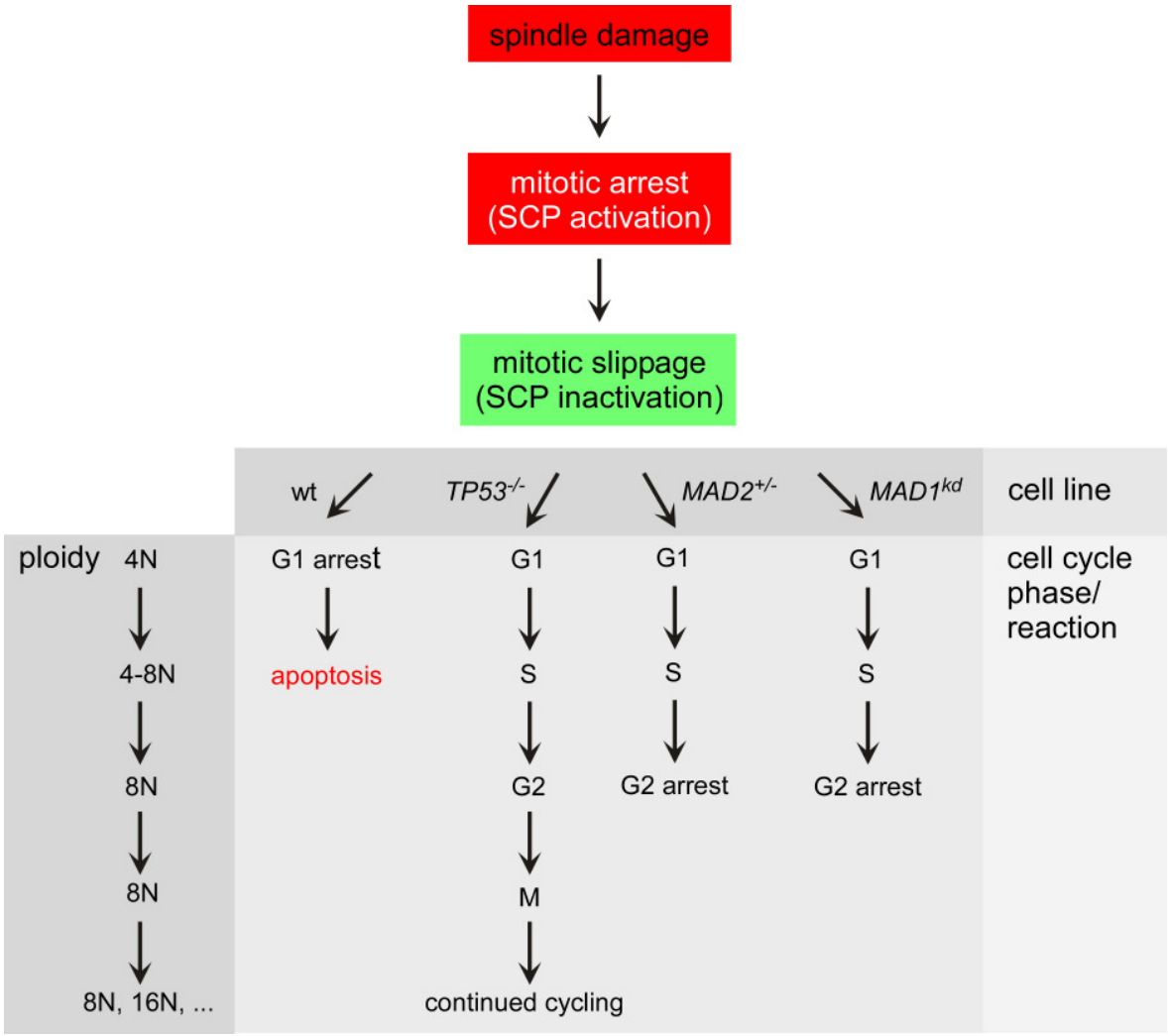

Figure 48: Activation of several cell cycle checkpoints prevents polyploidization by induction of cell cycle arrest and apoptosis upon spindle damage. Spindle damage induces mitotic arrest via the spindle checkpoint. Mitotic arrest is resolved by an adaptation process leading to mitotic slippage, which occurs prematurely in spindle checkpoint impaired cells, e.g. with lowered *MAD1* or *MAD2* levels, but not in p53 deficient cells. Wild typic cells die by apoptosis upon mitotic slippage after prolonged mitotic arrest. In spindle checkpoint impaired cells premature mitotic slippage leads to insufficient accumulation of p53 in G1, allowing DNA replication. Continuous p53 accumulation in spindle checkpoint impaired cells throughout the subsequent S phase induces arrest in G2 via activation of the novel p53-dependent postmitotic G2 checkpoint. However, p53 negative cells will continue to traverse the cell cycle and reach higher ploidies than spindle checkpoint impaired cells, because they will neither arrest in G1 nor in G2 upon mitotic failure.

Polyploidy in cancerogenesis and chemotherapy

The postmitotic G1 and G2 checkpoints probably present additional failsafe mechanisms to protect animal cells from the propagation of polyploid cells. Polyploid HCT116 cells were generated by transient treatment with nocodazole. Our unpublished data indicate that populations of mainly polyploid HCT116 wild typic or of p53-negative cells revert to

euploidy after several weeks of culture, probably by slowed growth of polyploid cells compared to the euploid cell fraction of the population or by apoptotic cell death, as recently reported (Castedo *et al.* 2006). Polyploidization plays an important role in plant speciation, where it often contributes to better growth and production of larger seeds, and has been proposed in the early evolution of animal species (Storchova and Pellman 2004, Otto 2007). In contrast to plants, most animal species seem to tolerate polyploidy quite badly or only in cells from specialized tissues like megakaryocytes with ploidies up to 128N or in stressed or damaged organs like the liver, heart and esophagus (Storchova and Pellman 2004, Nguyen and Ravid 2006). Animal cells do apparently have evolved several checkpoints to prevent polyploidization, which implies that polyploidization is potentially harmful to the organism and has to be avoided, especially as a first step in cancerogenesis (Margolis *et al*. 2003).

Fujiwara and colleagues report that only tetraploid, but not diploid *TP53*$^{-/-}$ cells from murine mammary epithelium induced tumors in nude mice in the absence of carcinogens and were transformed by carcinogens *in vitro* (Fujiwara *et al.* 2005). A huge methodological problem is the almost universal lack of data from the progression of individual tumors in humans, which might help clarify the process of cancerogenesis from its earliest stage of just one or a few transformed cells to its latest stages. A notable exception is Barrett's esophagus, a premalignant condition, which can develop into cancer at a low rate and pace. Interestingly, biopsy samples taken at regular intervals reveal early loss of p53 and development of tetraploidy and subsequently aneuploidy (Storchova and Pellman 2004). Other steps to understand the process of cancerogenesis in its entirety are research on human colon carcinoma (Lengauer *et al.* 1997, Rajagopalan *et al.* 2003), the creation of diverse cancer-prone mouse models and investigation of cancer stem cells. It is conceivable that the limits to polyploidization are cell type- and species-specific. Theoretically, the changes in the ratios between nuclear surface and nuclear volume and between nuclear volume and cytoplasmic volume would limit cell viability, as would the alterations in diffusion-dependent cellular processes. For instance, a twofold increase in cell volume would correspond to an approximate increase in the surface of subcellular structures of 1.4-fold and in the length of linear structures of 1.2-fold (Storchova and Pellman 2004), thus, nucleocytoplasmic and subcellular transport processes could be severely affected. The described changes could also influence the chemotherapeutic treatment of cancer cells, but are poorly investigated. Drug uptake and removal from the cell by MDR pumps or diffusion might both be reduced due to the smaller ratio between

cell surface and cell volume in polyploid cells. Whether intracellular drug concentrations are increased or decreased in polyploid cells or if cellular physiology is altered in these cells is so far only poorly studied. A comparison of diploid, aneuploid and tetraploid human colon carcinomas indicates higher levels of microsatellite instability in tetraploid tumors and altered gene expression (Sun 2006). Another report found a higher resistance to several DNA damaging drugs and γ- and UVC-radiation in tetraploidized colon carcinoma cell lines, HCT116 and RKO cells, which was p53-dependent (Castedo *et al.* 2006). Although only a small set of genes was expressed differently in the tetraploidized cell lines compared to their diploid parental cell lines, 41% of those genes were regulated by p53, pointing to a specific dysregulation of p53 target genes in tetraploid cells (Castedo *et al.* 2006), which might be exploited by future chemotherapies. However, many chemotherapeutic drugs are a double-edged sword, since they can induce poly- or aneuploidy, leading on the one hand to cell death of a part of the cancer cell population, but on the other hand to the generation of secondary tumors or more aggressive tumors from primary cancer cells that escaped cell death. Cancer cell lines with mixed ploidies, e.g. U2OS cells (human osteosarcoma cells), might be a good tool to study these effects, because their polyploid subpopulations might have circumvented the mechanisms protecting against polyploidy.

Polyploidy and checkpoint signaling

Controversy persists about the exact trigger for the postmitotic G1 checkpoint, which apparently does not sense tetraploidy, an aberrant centrosome number or a failed cytokinesis, or about its existence *per se* (Uetake and Sluder 2004, Wong and Stearns 2005). Uetake and Sluder hypothesize that cleavage failure is either essentially nonexistent in the living organism or not sufficient by itself to cause problems (Uetake and Sluder 2004). Wong and Stearns suspect artifacts of drug treatment were interpreted as actions of a tetraploidy checkpoint (Wong and Stearns 2005). Both groups question the existence of a tetraploidy checkpoint in mammalian somatic cells, but it is conceivable that cancer cells are more likely to undergo a postmitotic G1 arrest in response to the massive disturbances caused by chemotherapeutic drugs. Much more data gathered in carefully designed experiments is needed to elucidate this issue. However, a simple explanation resolving the issue of the trigger for a postmitotic G1 arrest might be the prolonged duration of mitosis, which promotes the accumulation of p53 (Blagosklonny 2006). Various mitotic defects

like spindle damage, centrosome malfunction, prolonged mitotic delay and tetraploidization might lead to the same outcome: prolonged mitosis, p53 accumulation and priming of p53 for action on target genes upon exit from mitosis, when transcription is again possible (Blagosklonny 2006). Early reports stated a role of p53 in spindle checkpoint signaling, but were soon revoked. HeLa cells, which lack functional p53, arrest as strongly in mitosis as HCT116 cells with functional p53. Indeed, we found that HCT116 *TP53*$^{-/-}$ cells arrest slightly longer upon various spindle damages than their wild typic counterparts and do not accumulate p21 upon nocodazole treatment. p21 inhibits Cdk1 activity and might therefore promote mitotic exit of arrested cells when present at sufficient levels. However, some reports claim that the Cyclin B level is the crucial factor in the maintenance of mitotic arrest (Brito and Rieder 2006). Cyclin B is a repression target of p53 in G2 phase, which is on the one hand directly repressed by p53 and on the other hand indirectly by three transcriptional target genes of p53, *CDKN1A* (p21), *GADD45* and *14-3-3σ* (Zhao *et al.* 2000, Taylor and Stark 2001). Therefore prolonged mitotic arrest in HCT116 *TP53*$^{-/-}$ cells would be in line with my expectations regarding the role of p53 in modulating mitotic slippage. The question how p21 accumulation during mitotic arrest is possible when it is generally believed that transcription and translation in mitosis are shut down – with the exception of IRES-mediated transcription – is so far unanswered. It could be that transcription is shut down completely during a normal mitosis, but that some selected mRNAs are transcribed upon prolonged mitotic arrest as part of an adaptation process facilitating cell survival. An alternative explanation could be that the fraction of cells expressing p21 – at a given time during nocodazole treatment – has already slipped out of the mitotic arrest and expresses p21 very strongly. Immunofluorescence or FACS costainings with antibodies directed against mitotic proteins and p21 could clarify this issue.

Lack of p53 is insufficient to induce polyploidy or aneuploidy *per se* (Bunz *et al.* 1998). Therefore, additional factors must play a significant role in these processes. Prime candidates for these additional factors are spindle checkpoint components, as I have shown here. Interestingly, *MAD2* mRNA levels drop 20% during nocodazole-induced mitotic arrest and subsequent slippage in HCT116 wt and *MAD2*$^{+/-}$ cells (data not shown), possibly contributing to p21-mediated mitotic slippage by weakening spindle checkpoint signaling. Indeed, cDNA array data showed a p53-dependent repression of spindle checkpoint genes *BUB1*, *BUB1B*, *CCNB1/2*, *CDC20*, *HEC1*, *MAD2*, *MPS1L1*, *PTTG1* (encoding securin) and other genes whose products are involved in cell cycle progression or DNA replication,

e.g. DNA topoisomerase IIα and primase (Zhao *et al.* 2000, Bhonde *et al.* 2006). Furthermore, *survivin* is a direct repression target of p53 (Hoffmann *et al.* 2002) and survivin overexpression represses transcription and accelerates degradation of p53 (Wang *et al.* 2004), thereby stabilizing its own increased expression levels. Survivin levels are elevated during mitosis (Li *et al.* 1998), spindle damage-induced mitotic arrest (Chen *et al.* 2003) and after G2 checkpoint abrogation (our data). Thus, the interaction of p53 and survivin warrants further investigation in spindle damaged cells. My unpublished results indicate a prolonged mitotic arrest in nocodazole treated HCT116 knockout cell lines of *TP53* or *CDKN1A/WAF1* compared to the wild type, suggesting that mitotic slippage in HCT116 cells is promoted by p53 and some of its target genes. However, p53-independent regulation of *CDKN1A/WAF1*, *14-3-3-σ* or other factors might also play a role in mitotic slippage, since $TP53^{-/-}$ cells maintain mitotic arrest a little longer than wild type cells, but eventually slip out of the arrest as well. Interestingly, HT29 cells, which express mutated *TP53* (Huang *et al.* 1994), maintain mitotic arrest upon spindle damage more than three times longer than HCT116 cells. HCT116 cells expressing wild typic *TP53* arrest for a shorter time than HCT116 cells lacking *TP53*, indicating that p53 accelerates mitotic slippage. Mutated *TP53* in HT29 cells might exert a dominant negative effect and, thus, delay mitotic slippage more strongly compared to cells lacking *TP53* entirely. Cdk1 small molecule inhibitors can induce mitotic slippage and augment apoptosis in taxol treated HeLa cells and in Eg5/KSP inhibitor treated HT29 cells (O'Connor *et al.* 2002, Tao *et al.* 2005). We could abrogate mitotic arrest induced by nocodazole, taxol or an Eg5/KSP inhibitor by Cdk1 inhibition with purvalanol A and induce apoptosis in chemoresistant HT29 cells, albeit to a lesser extent than in HCT116 wt and HeLa cells, as evidenced by PARP cleavage on Western blot and sub G1 FACS analysis (our unpublished observations). Thus, the combination of spindle damaging agents and Cdk inhibitors could pose a promising chemotherapeutic strategy against chemotherapy-resistant cells with high rates of mitotic arrest in response to spindle damage.

Interestingly, a most recent report states that prolonged nocodazole-, taxol- or monastrol-induced mitotic arrest of cancer cells can generate DNA strand breaks in mitosis. These strand breaks can also occur spontaneously in spindle checkpoint impaired cancer cells with reduced *CENPE* or elevated *MAD2* expression and even in untransformed cells, if they undergo a prolonged mitosis (Dalton *et al.* 2007, Sotillo *et al.* 2007). The DNA strand breaks activate an ATM-dependent DNA damage response after mitotic exit independently of cell death and can lead to altered karyotypes, which might promote cancerogenesis and

influence responses to chemotherapy (Dalton *et al.* 2007). Conversely, replication stress led to sustained mitotic arrest and apoptosis in a fraction of p53-deficient mouse embryonic fibroblasts (Duensing *et al.* 2006). These findings indicate that spindle checkpoint activation and DNA damage are more closely linked than previously thought, although further investigations are needed to elucidate the mechanisms underlying linking them.

In sum, human cells possess at least three distinct checkpoints to prevent the propagation of polyploid cells: the mitotic spindle checkpoint, the pseudo-G1 or tetraploidy checkpoint and the postmitotic G2 checkpoint (Figure 48). Loss of functional p53 has severe consequences, since p53 is a main part of the barrier to polyploidization and subsequent aneuploidization. Spindle checkpoint impairment leads to aneuploidization and chromosomal instability (Rajagopalan *et al.* 2003), which in turn can promote loss of p53. At least half of all human tumors lack functional p53 (Vousden and Lu 2002) and the majority have spindle checkpoint defects (Bharadwaj and Yu 2004). Thus, cancerogenesis, cancer and defects in the prevention of polyploidization and aneuploidization are intimately linked (Kops *et al.* 2005). Unfortunately, the coupling of spindle checkpoint and p53 functionality means that loss of either one can already have severe consequences for the organism, making cancerogenesis much more likely. Loss of both, the spindle checkpoint and p53, probably primes a cell for malignant transformation and will also confer resistance to many chemotherapies. For instance, in early passage *TP53*$^{-/-}$ mouse embryonic fibroblasts, which are karyotypically and centrosomally unstable, *BUB1B* expression is low and spindle checkpoint function is impaired. However, upon prolonged culture, BubR1 levels rise and the population is aneuploid, but karyotypically homogenous and stable, and spindle checkpoint function is restored (Oikawa *et al.* 2005). Thus, transient spindle checkpoint impairment in conjunction with genetic alterations that favour transformation like loss of *TP53* can induce aneuploidy. The observed reversion to a functional spindle checkpoint via upregulation of a spindle checkpoint component might be a way for cancer cells to preserve an advantageous karyotype and might explain the genomic convergence seen in cultured cells and tumors (Oikawa *et al.* 2005). These results support the hypothesis that the observed upregulation of spindle checkpoint components in cancers originating from various tissues might represent a compensation mechanism of cancers for deleterious spindle checkpoint defects (Yuan *et al.* 2006). However, overexpression of spindle checkpoint components like *MAD2* can also disrupt spindle checkpoint function (Hernando *et al.* 2004) and prove to be cancerogenic (Sotillo *et al.*

2007). Thus, further investigation into the fine-tuning of spindle checkpoint signaling is required to assess the effect of altered spindle checkpoint gene expression in cancer. It is also conceivable that spindle checkpoint impairment might not be inherently lethal, but that the resulting accumulation of damage could trigger apoptosis. Interestingly, a recent study provides evidence for this hypothesis. Loss of *TP53* can compensate for the lethality of *MAD2* loss in murine embryonic fibroblasts (Burds *et al.* 2005), suggesting that simultaneous impairment of the spindle checkpoint and p53 could provide a survival advantage also to cancer cells. However, to eliminate such cancer cells, effective chemotherapeutic strategies exploiting the unique checkpoint defects of p53 negative cells or complete inhibition of the spindle checkpoint could be envisioned, as described in chapters 5 and 6 of the results section.

3. Spindle checkpoint integrity is required for spindle damage-induced apoptosis

Spindle damaging agents are widely used in cancer chemotherapy, but their mechanism of action in cell killing by apoptosis induction is still incompletely understood. The impact of spindle checkpoint functionality and of several of its components and of functional p53 on the efficacy of spindle damaging agents to induce apoptosis in cancer cells was investigated. A main determinant of apoptosis induction is the duration of mitotic arrest upon spindle damage. Mitotic arrest depends on normal levels of each of the spindle checkpoint proteins Mad1, Mad2, BubR1 and Bub1 and several more not tested here. Surprisingly, however, the induction of apoptosis is governed by specific spindle checkpoint proteins upon different types of spindle damage. Mad2 is required for cell death upon treatment with nocodazole, taxol and monastrol, which alter spindle dynamics or polarity, respectively. In contrast, Mad1 is needed for nocodazole-induced apoptosis, but is dispensable for apoptosis upon taxol or monastrol treatment (Figure 49). p53 is absolutely required for apoptosis induction by spindle damaging agents in HCT116 colon carcinoma cells, whereas HeLa cervix carcinoma cells induce apoptosis effectively despite lacking functional p53. Therefore the role of p53 in spindle damage-induced apoptosis is likely to be cell- or cancer type-specific and dependent on other factors like components of apoptotic or cell cycle arrest signaling pathways as well.

Spindle damage-induced apoptosis is dependent on prolonged mitotic arrest followed by mitotic slippage

My experiments with HeLa cells show that apoptosis is induced upon mitotic slippage after at least 24 h of nocodazole or taxol treatment. However, in mitotically arrested cells with normal or reduced levels of Mad2, BubR1 or Bub1, only basal levels of caspase 3 activity can be detected. So far this effect has not been resolved, but mounting evidence points to the existence of a cytoprotective mechanism acting in mitosis in form of a survival pathway comprising survivin and bcl-2. While survivin's main function in untransformed cells lies in the regulation of mitosis, it is probably promoting survival in many cancer cell lines (Altieri 2006) and its levels peak in mitosis (Li *et al.* 1998). Bcl-2 is phosphorylated at several residues upon mitotic arrest and some of these phosphorylations have been shown to either enhance bcl-2's antiapoptotic properties and or its resistance against

proteolytic degradation (Breitschopf *et al*. 2000, Deng *et al.* 2004), but it was also reported that the level of bcl-2 expression in mitochondria rather than its phosphorylation state could regulate the sensitivity of cancer cells to taxol *in vitro* (Brichese *et al*. 2002). Upon mitotic slippage, survivin levels drop dramatically due to loss of a stabilizing Cdk1-mediated phosphorylation (Li *et al.* 1998, O'Connor *et al.* 2000, Shin *et al.* 2003) and mitotic bcl-2 phosphorylation is also lost, leading to increased apoptosis. Furthermore, transcription of proapoptotic proteins can be carried out in pseudo-G1 phase following mitotic slippage and accelerate apoptosis in these cells (Blagosklonny 2006). Interestingly, several recent reports link caspases, mitosis and the spindle checkpoint. An inhibitory phosphorylation at threonine 125 conferred by Cdk1/Cyclin B keeps caspase 9 activity in check during mitosis and upon spindle damage (Allan and Clarke 2007), while caspase 3 expression and activation at the G2/M transition in unstressed cells could enable immediate action upon extensive damage in mitosis (Hsu *et al.* 2006). Furthermore, caspase 3-dependent cleavage of Bub1 and BubR1 during an undisturbed mitosis or upon treatment with spindle damaging agents promotes mitotic slippage and caspase-insensitive mutants of both proteins increase apoptotic cell death in tetraploid cells by prolonging mitotic arrest (Baek *et al*. 2005, Kim *et al.* 2005). Since these hints have yet to give rise to a model linking spindle checkpoint proteins and apoptotic proteins, survivin is to date the only well documented spindle checkpoint protein with ties to the apoptotic machinery. Our results indicate a proapoptotic role of Mad2 upon spindle damage, which could be tested in various assays to find a connection between Mad2 and its activation of proapoptotic or inhibition of antiapoptotic proteins. Direct interactions could be detectable by immunoprecipitation and purification of complexes from cancer cells or an approach via a yeast two-hybrid system. An interaction of Mad2 and survivin is conceivable, since these proteins come into close proximity at the kinetochore. However, Mad2's links to apoptosis could be indirect and mediated via a complex pathway involving several proteins and comprising many signaling steps.

Differential roles of spindle checkpoint proteins in spindle damage-induced apoptosis

Our new finding is that differential sensitivity to taxol- or monastrol-induced apoptosis is dependent on Mad1 or Mad2. Future experiments might help to clarify the role of all known spindle checkpoint proteins in response to spindle damaging agents with different

modes of action like *Vinca* alkaloids or Eg5 inhibitors. Nocodazole is not used as a medication, but *Vinca* alkaloids like vincristines and vinblastines employ a similar mechanism of action and are commonly used anticancer agents. Eg5 inhibitors induce a monopolar spindle and a resulting lack of tension due to a lack of amphitelic attachment of the mitotic spindle and are therefore mechanistically similar to taxol in terms of spindle checkpoint activation and apoptosis induction. The drug-induced monopolar spindle itself appears to be intact at superficial inspection, but is probably less stable than its bipolar counterpart (our unpublished observations).

It will be of great interest to reconcile the observed differences in the requirement of spindle checkpoint components for the induction of mitotic arrest on the one hand and the requirement of a subset of specific spindle checkpoint components for spindle damage-induced apoptosis on the other hand. For instance, both Mad1 and Mad2 are required for the induction of mitotic arrest upon nocodazole, taxol and monastrol treatment, but while either Mad1 or Mad2 downregulation confer resistance to nocodazole, only reduced levels of Mad2 protect cells also against taxol- or monastrol-induced apoptosis. Therefore, not the spindle checkpoint proficiency *per se*, but the status of individual spindle checkpoint components might be of great prognostic value in cancer chemotherapy (Figure 49). One explanation for the observed differences might be the existence of at least three different categories of spindle checkpoint proteins: 1. Proteins with a function in spindle checkpoint signaling inducing mitotic arrest (e.g. Bub1, Bub3). 2. Proteins with a function in spindle checkpoint signaling inducing mitotic arrest and a role in kinetochore independent mitotic timing (e.g. Mad2, BubR1). 3. Proteins with a function in spindle checkpoint signaling inducing mitotic arrest and positively or negatively regulating apoptosis upon treatment with spindle damaging agents (e.g. Mad2, survivin). For survivin it has been shown, that its mitotic and prosurvival functions are separable, because they depend on the subcellular localization of survivin governed by a nuclear export signal (Colnaghi *et al*. 2006). Some evidence points to a similar role of its subcellular localization for the Mad2 protein. It was reported that mislocalization of the Mad1/Mad2 complex by the viral Tax protein from the nucleus to the cytoplasm correlates with spindle checkpoint impairment and resistance to chemotherapeutic agents in adult T-cell leukemia cell lines (Kasai *et al*. 2003). The same mislocalization pattern for Mad2 was reported for tissue samples and spindle checkpoint impairment was found in 75% of the investigated cell lines derived from testicular germ cell tumors, which also showed reduced *MAD2* expression levels (Fung *et al.* 2007). However, the authors of both papers do not explain how Mad1/Mad2 localization to the

cytoplasm could negatively affect spindle checkpoint function, since the nucleus is dissolved in mitosis. Also, it has to be noted that the proapoptotic role of Mad2 in spindle damage-induced apoptosis might stem from Mad2's terminal position in spindle checkpoint signaling, but might also indicate a putative spindle checkpoint independent function in apoptosis.

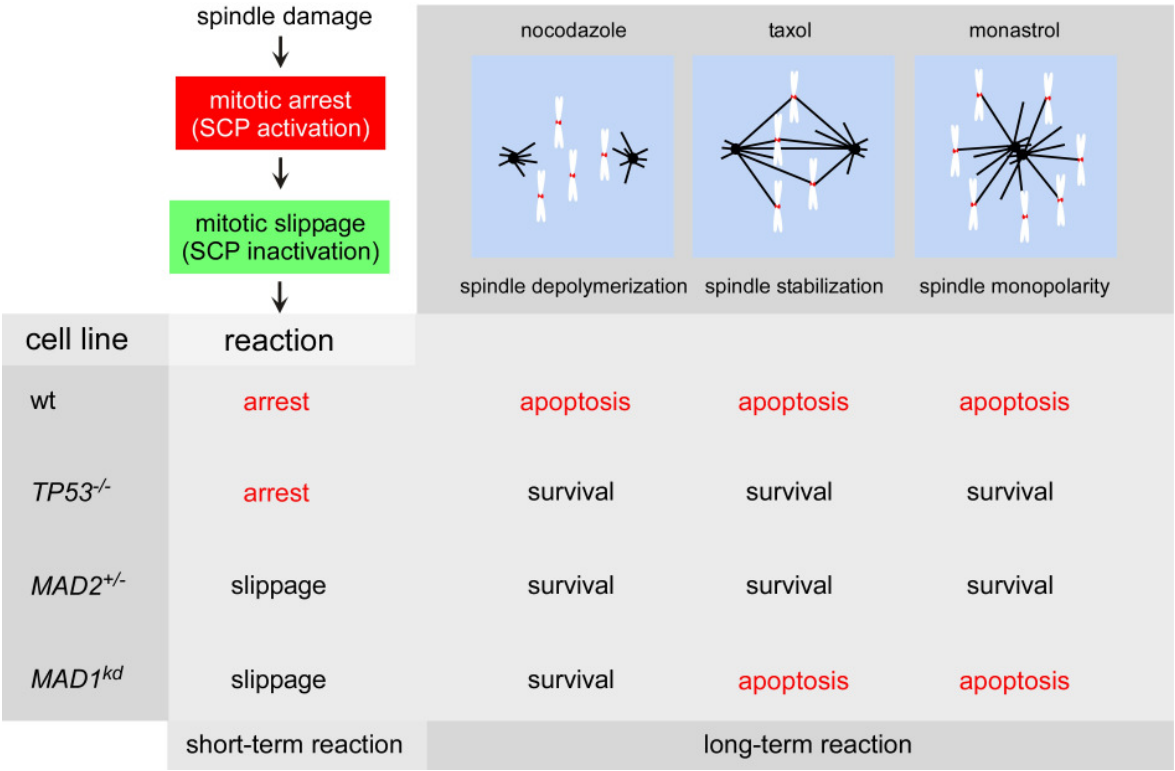

Figure 49: Spindle damage-induced apoptosis is differentially regulated by Mad1 and Mad2. In HCT116 cell lines different kinds of spindle damage, i.e. spindle depolymerization, spindle stabilization and a monopolar spindle, induce mitotic arrest followed by mitotic slippage. The mitotic arrest is shortened in *MAD1* knockdown and in *MAD2*$^{+/-}$ cells, but not in wild typic and *TP53*$^{-/-}$ cells (short-term reaction, 16 h). HCT116 wt cells are sensitive to all kinds of spindle damage, whereas HCT116 *TP53*$^{-/-}$ cells are resistant. Lowered levels of Mad2 confer resistance to all kinds of spindle damage, whereas reduced levels of Mad1 confer resistance to nocodazole-induced spindle depolymerization, but not to taxol-induced spindle stabilization or monastrol-induced spindle monopolarity (long-term reaction, 48 h). This suggests that not the ability of a cancer to induce and maintain mitotic arrest by spindle checkpoint activation, but rather the distinct apoptosis-inducing properties of the spindle checkpoint components determine chemotherapy responsivity.

Apoptosis induction due to altered spindle dynamics was most intensely studied for taxol. However, the mechanisms of apoptosis induction by various agents impinging on spindle dynamics are still only poorly understood. Apparently, at higher doses of these agents, cell killing depends on spindle checkpoint-mediated mounting of a prolonged mitotic arrest and

subsequent mitotic slippage, while at lower doses cell death occurs independent of the spindle checkpoint or traversal through mitosis (Wang *et al.* 2000). Spindle disruption leads to intrinsic apoptosis, which mainly depends on members of the bcl-2 family. Bax and/or bak are activated by conformational changes and translocate to the mitochondria, bim is released from microtubules, bad is activated by phosphorylation and each of these alterations inhibits bcl-2 and bcl-X_L, tipping the scales toward apoptosis (Bhalla 2003). Apoptosis induction by Eg5/KSP inhibitors employs similar mechanisms (Tao *et al.* 2005, Tao *et al.* 2007, Vijapurkar *et al.* 2007). Spindle damage induces stress kinases, but their relative contribution to activation or inhibition of apoptosis remains controversial (Bhalla 2003, Mollinedo and Gajate 2003). The mechanism of apoptosis induction upon spindle damage remains largely unresolved and might differ depending on the kind of spindle damage and its extent. Future experiments have to uncover the links between the spindle checkpoint and apoptosis, characterize the signaling pathways involved and discriminate between different cases or different amounts of spindle damage. This could be achieved by employing isogenic cell systems, chemical compounds with different modes of action on the mitotic apparatus and monitoring of apoptotic signaling over time, preferably in single cells, not in cell populations.

4. Normal Mad2 levels are required for topoisomerase inhibitor-induced apoptosis

DNA damaging agents are chemotherapeutics with a longstanding history in cancer therapy and employ diverse modes of action. Some of them are closely dependent on functional p53 to induce apoptosis. However, very little was known about the role of the spindle checkpoint in the action of DNA damaging drugs. Therefore I investigated the significance of Mad1 and Mad2 in apoptosis induction upon topoisomerase inhibition by adriamycin or etoposide, UV crosslinking and a 5-fluorouracil-mediated block in DNA synthesis in the isogenic HCT116 cell system. Since DNA damage signaling mainly depends on ATM, ATR, Chk1 and Chk2 kinases and p53, HCT116 *CHK2*$^{-/-}$ and *TP53*$^{-/-}$ cells were included as controls. Surprisingly, topoisomerase II inhibitor-induced apoptosis was significantly reduced in HCT116 *MAD2*$^{+/-}$ cells, but not in HCT116 *MAD1* knockdown cells.

Reduced Mad2 levels do not influence DNA damage generation upon topoisomerase inhibition

Adriamycin resistance of HCT116 *MAD2*$^{+/-}$ cells was not due to reduced DNA damage levels in the first place, since immunofluorescence stainings of HCT116 wt and HCT116 *MAD2*$^{+/-}$ cells against phospho-H2AX as a marker of DNA double strand breaks showed the same intensity, which increased in both cell lines upon treatment in a concentration-dependent manner (data not shown). In contrast, it was reported that *TP53*-deficient mouse embryonic fibroblasts accumulate lower levels of DNA damage upon adriamycin or etoposide treatment resulting in reduced apoptosis, thus, lower levels of initial DNA damage trigger a weaker response (Dunkern *et al.* 2003). Since the initial damage triggering apoptosis in adriamycin treated HCT116 *MAD2*$^{+/-}$ cells is identical to wild typic cells and the level of apoptotic response is decreased in HCT116 *MAD2*$^{+/-}$ cells we followed p53-dependent *CDKN1A/WAF1* and *BAX* transcription as a readout for p53 trans-activational ability. We treated the cell lines for only 14 h and did not observe significant differences between HCT116 *MAD2*$^{+/-}$ cells and wild typic cells, but these might have become apparent upon prolonged adriamycin treatment and extended observation time like shown for nocodazole treated cells.

Significance of spindle checkpoint status for DNA damage-induced apoptosis

The spindle checkpoint might play a role in DNA damage-induced apoptosis by eliminating damaged cells, which escape the G1 or G2 arrests mediated by components of the DNA damage pathways and subsequently enter mitosis. DNA damage in mitosis has been shown to trigger cell death by mitotic catastrophe depending on the spindle checkpoint, in particular its components Mad2 and BubR1 (Nitta *et al*. 2004). Thus, cancer cells with an impaired spindle checkpoint might escape apoptosis upon DNA damage by slipping through mitosis. This, however, is probably not the case in our cell system, since HCT116 *MAD1* knockdown and HCT116 *MAD2*$^{+/-}$ cells show reduced mitotic arrest, but only HCT116 *MAD2*$^{+/-}$ cells display resistance to topoisomerase inhibitor-generated apoptosis. Therefore, an alternative explanation could be that DNA damage-induced apoptosis is similar to apoptosis induced by spindle damaging agents, where functional differences between Mad1 and Mad2 were also observed. Topoisomerase II inhibition by adriamycin or etoposide might interfere with the generation of tension similar to taxol or monastrol and activate the same signaling pathways, which depend on normal levels of Mad2, but not on Mad1, to kill cells by apoptosis. Our preliminary findings in ovary cancer cells with reduced levels of Mad2 corroborate our results gained in HCT116 cell lines. A requirement for normal levels of Mad2 and BubR1 in topoisomerase inhibitor-induced mitotic catastrophe has been reported by Nitta and colleagues (Nitta *et al*. 2004). HeLa cell populations with siRNA-induced spindle checkpoint deficiencies formed colonies at a rate of 5-10% upon DNA damage (Nitta *et al*. 2004), thus, colony formation assays might help to assess long-term survival of cells with specific spindle checkpoint deficiencies like lowered Mad1 or Mad2 levels.

In preliminary experiments with ovary carcinoma cell lines I could show a correlation between the reported Mad1 and Mad2 protein levels with sensitivity to adriamycin-induced apoptosis. Cell lines with lowered Mad2 levels were less susceptible to adriamycin than the cell line with wild typic Mad1 and Mad2 content. However, it has to be noted that even this control cell line arrested maximally to 40% upon nocodazole or taxol treatment and does not possess a fully functional spindle checkpoint by our standards. The other cell lines showed an even lower mitotic index of 20%, only half of the control, which is the value obtained with HCT116 *MAD2*$^{+/-}$ cells, in which the correlation between decreased Mad2 levels and adriamycin resistance was first observed. The role of other spindle checkpoint proteins in DNA damage-induced apoptosis is still unknown, but might be similar to the

situation in cells undergoing mitotic catastrophe, where cells enter mitosis with damaged DNA.

A possible spindle checkpoint-independent proapoptotic role of Mad2

The significance of the duration of mitotic arrest and of mitotic slippage for the induction of apoptosis upon treatment with DNA damaging agents in comparison to the findings on spindle damage-induced apoptosis could not be addressed satisfactorily. I could not observe an accumulation of mitotic cells upon adriamycin treatment of HCT116 wt and HCT116 *MAD2*$^{+/-}$ cells by employing MPM2-FACS analysis (data not shown). There are several possible explanations for the lack of a detectable population of mitotic cells: 1. Low rates of cells enter mitosis at a given moment and do not arrest in mitosis. 2. Epitopes conferring MPM2 positivity are destroyed, as observed for adriamycin and UCN-01 treated cells after prolonged treatment (data not shown). 3. Mitotic arrest is not executed and is not required for the induction of apoptosis in topoisomerase inhibitor treated cells, therefore cells might die directly upon entry into mitosis, which would keep the amount of mitotic cells very low. 4. Traversal through mitosis is not required for the induction of apoptosis in topoisomerase inhibitor treated cells, and, thus, cells might die independently from mitosis. Thus, it may be speculated that the proapoptotic role of Mad2 upon topoisomerase inhibitor-induced apoptosis is not only independent of kinetochores, but also of mitosis itself. It could be that Mad2's diverse functions in mitosis and the spindle checkpoint and its proapoptotic function are separable. Mislocalization of survivin from the cytoplasm to the nucleus sensitizes cancer cells to radiation-induced apoptosis (Colnaghi *et al*. 2006). In analogy to survivin's localization-dependent mitotic and apoptosis-related functions, Mad2 might behave similarly. Expression of tagged Mad2 proteins, Mad2 immunofluorescence analyses or subcellular fractionation experiments might provide some information on the localization of Mad2 and whether complex formation with Mad1 occurs upon DNA damage or not.

To answer whether DNA damage in mitosis might induce cell death independent of the spindle checkpoint, cells arrested in mitosis with nocodazole were treated with adriamycin. No effect on DNA integrity was seen by immunofluorescence detection of phospho-H2AX, chromosome spreading or determination of cell death by sub G1 FACS measurements (data not shown). Adriamycin induces DNA double strand breaks by inhibition of topoisomerase II enzymatic activity and might, therefore, not induce DNA

damage in mitotically arrested cells with already completely condensed chromatin. Future experiments should directly induce DNA double strand breaks in mitotic cells by γ-irradiation or a radiomimetic chemical. However, for the following experiments I chose to induce DNA damage before mitosis by G2 checkpoint abrogation, because this strategy has clinical significance as a novel chemotherapeutic regimen.

5. Pharmacological G2 checkpoint abrogation induces apoptosis and is affected by pro- and antiapoptotic spindle checkpoint components

G2 checkpoint abrogation is a promising strategy to specifically target tumor cells lacking functional p53, while sparing p53-proficient untransformed cells (Kawabe 2004). In contrast to cells expressing functional p53, which arrest in G1 and G2 upon DNA damage, p53 negative cells can only arrest in G2 in a p53-independent manner. This G2 arrest can be abrogated by pharmacological inhibition of Chk1 by UCN-01 and cell death is executed by mitotic catastrophe. “Mitotic catastrophe” or “mitotic cell death” is occurring during or after a faulty mitosis and the mechanisms and the nature of this form of cell death are largely unknown (Okada and Mak 2004).

G2 checkpoint abrogation activates a spindle checkpoint-dependent mitotic arrest

Upon mitotic entry in the presence of DNA damage HCT116 *TP53*$^{-/-}$ cells and HeLa cells activate the spindle checkpoint as evidenced by kinetochore localization of Bub1 and BubR1 and they arrest in a prometaphase-like state. It is known that DNA damage can result in centrosome splitting, which then gives rise to multipolar spindles and promotes the generation of aneuploid daughter cells (Hut *et al*. 2003). Thus, the observed multipolar spindles in cells upon G2 checkpoint abrogation could be caused by centrosome splitting. ShRNA-mediated downregulation shows that the spindle checkpoint proteins Mad2, Bub1, BubR1 and Mps1 are needed for mitotic arrest. In addition, experiments applying the Aurora B kinase inhibitor ZM447439 or downregulating *survivin* by shRNA indicate that the mitotic arrest upon G2 checkpoint abrogation is due to a lack of tension between kinetochores and depends on the chromosomal passenger complex. Chromosome congression at the metaphase plate suggests that most kinetochores are attached to the spindle. It is conceivable that chromatids are able to attach their kinetochores to spindle fibers, but are unable to generate tension between them due to multiple breaks in their DNA induced by adriamycin-mediated inhibition of topoisomerase II. During G2 topoisomerase II decatenates chromosomes and compacts chromatin, processes that have to be completed before the onset of mitosis to allow proper chromosome segregation and to avoid catastrophic – in most cases lethal and in some cases cancerogenic – consequences like chromosome breaks (Cortes *et al*. 2003). Surprising differences in apoptosis induction

depending on the trigger activating the spindle checkpoint – attachment or tension – were reported by Bozko and colleagues. They observed a correlation between increased apoptosis and reduced survivin levels in human leukemia cells upon cotreatment with the DNA alkylating agent melphalan, caffeine and nocodazole, whereas cells treated with melphalan, caffeine and taxol showed decreased apoptosis and increased survivin levels (Bozko *et al.* 2005).

Plk1 kinase inhibition could be a promising chemotherapeutic strategy. A combination of G2 checkpoint abrogation with Plk1 inhibition might be more useful than therapy with Plk1 inhibitors alone, because it might lead to synergistic effects in cell killing. The effect of Plk1 downregulation could not be studied due to experimental constraints. ShRNA-mediated Plk1 downregulation requires traversal through the cell cycle to manifest itself, which takes a minimum of one day in an unsynchronized cell population. Then the cells arrest in mitosis due to lowered Plk1 levels, making it impossible to arrest cells in G2 before letting them enter mitosis by Chk1 inhibition. Thus, a pharmacological Plk1 inhibitor would have been desirable, because it could have been administered after the adriamycin treatment, but was not available to me at the time.

Furthermore, HCT116 cells were not suitable to study mitotic catastrophe in more detail, because the fraction of cells entering mitosis upon G2 checkpoint abrogation comprised only about 15% of the cells even in populations of cells carrying a homozygous deletion of *TP53*. Therefore, further experiments on mitotic catastrophe were done with HeLa cells. HeLa cells are also preferable to HT29 cells, which reach an even higher mitotic index than HeLa cells upon G2 checkpoint abrogation, but are resistant to most apoptosis-inducing agents. Therefore, to study sufficient amounts of apoptotic cells, HeLa cells were used for further experiments. Several combinations of DNA damaging agents or anti-metabolites and UCN-01 were recently undergoing clinical tests (Blagden and de Bono 2005, Kortmansky *et al.* 2005, Lara *et al.* 2005, Hotte *et al.* 2006, Perez *et al.* 2006, Sampath *et al.* 2006). Our unpublished experiments show that combinations of adriamycin or etoposide with UCN-01, caffeine or wortmannin, inhibitors of Chk1, ATM/ATR or ATM/DNA-PK/PI_3K kinases, respectively, all induce mitotic entry in HCT116 *TP53*$^{-/-}$ or HCT116 *CDKN1A/WAF1*$^{-/-}$ cells, but not in HCT116 wt cells. These data prove that G2 checkpoint abrogation via inhibition of DNA damage checkpoint kinases is specific for cells lacking functional p53 or p21, and that p53-dependent G2 arrest is mediated by its transcriptional target p21 in HCT116 cells. They also show a preference for p53-negative over wild typic cells, which is desirable for anticancer chemotherapy, as it confers

specificity to the treatment and therefore leads to less side effects on non-cancerous tissues. In fact, this would be one of the great advantages of G2 checkpoint abrogation as a chemotherapeutic strategy over many traditional drug regimens.

Pro- and antiapoptotic pathways regulate apoptosis induced by G2 checkpoint abrogation

Mad2's prominent role as a novel proapoptotic protein was strengthened further by the experiments centered on mitotic catastrophe. Not only does Mad2 induce apoptosis upon spindle or DNA damage, but also upon DNA damage in mitosis, probably by activating bax, while bak remains inactive (Figure 50a, b, c). Bax and bak are proapoptotic proteins acting in the intrinsic pathway of apoptosis and directly influence mitochondrial permeability (Wei *et al*. 2001, Willis *et al*. 2003, Reed 2006). Survivin and Aurora B kinase counteract mitotic apoptosis in concert with phosphorylated bcl-2 (Figure 50a, b, c). Mitotic apoptosis is enhanced by shRNA-mediated downregulation of *survivin* or pharmacological inhibition of Aurora B or Cdk1 kinases (Figure 50b, c), which might confer a stabilizing phosphorylation to survivin (O'Connor *et al*. 2000), indicating the presence of an active prosurvival pathway in mitosis. Recent findings link Chk1-mediated phosphorylation of Aurora B to enhancing Aurora B's kinase activity *in vitro* (Zachos *et al*. 2007), suggesting that UCN-01 might not only abrogate G2 arrest by inhibiting Chk1, but might also weaken the antiapoptotic properties of the chromosomal passenger protein complex by preventing the Chk1-mediated phosphorylation of Aurora B. A mutant of Aurora B that is constitutively mimicking phosphorylation or lack thereof at the Chk1 phosphorylation site could be used to test this hypothesis. Zachos and colleagues propose that Chk1 augments spindle checkpoint function and is needed for regulation of Aurora B and BubR1 in the presence of a weakened kinetochore signal and for susceptibility to taxol-induced apoptosis (Zachos *et al*. 2007). In contrast to G2 checkpoint abrogation, the opposite effect can be observed in taxol treated cells, where Chk1 inhibition confers resistance to taxol be weakening the spindle checkpoint, shortening mitotic arrest and inducing premature mitotic slippage (Zachos *et al*. 2007). These results are corroborating our findings on spindle checkpoint impairment and resistance to spindle damaging agents. However, they are in contrast to our findings regarding mitotic catastrophe, because UCN-01 abrogated the G2 arrest, but not the subsequent spindle checkpoint-mediated mitotic arrest. Mitotic arrest should be abrogated by UCN-01, if Chk1 is a *bona fide*

spindle checkpoint component. Thus, either Chk1 augments spindle checkpoint function only under certain spindle checkpoint activating conditions or UCN-01 selectively abrogates G2 arrest, because Chk1 might not be accessible to UCN-01 in mitosis or higher concentrations of UCN-01 than the ones we used are required for spindle checkpoint abrogation. It remains to be determined which proteins might be part of G2 or mitotic complexes containing Chk1 and whether they have distinct sensitivities to UCN-01-mediated inhibition of Chk1 kinase activity.

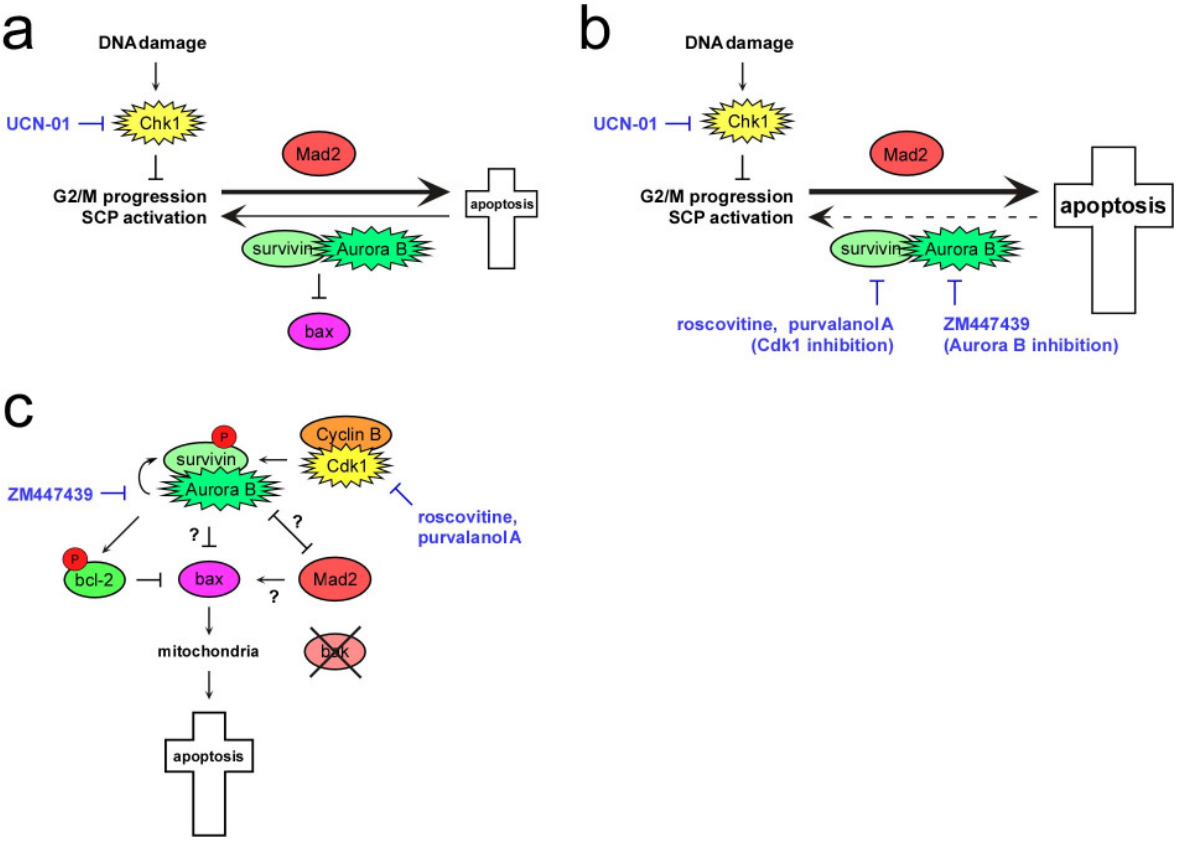

Figure 50: Mitotic catastrophe induced by G2 checkpoint abrogation is regulated by pro- and antiapoptotic pathways. a) DNA damage-induced G2 arrest is abrogated by Chk1 inhibition leading to mitotic entry in the presence of DNA damage. The spindle checkpoint is activated and apoptosis is induced by a proapoptotic pathway comprising Mad2 and bax. An antiapoptotic pathway comprising Aurora B, survivin and bcl-2 slows the execution of apoptosis down. b) Pharmacological abrogation of the antiapoptotic pathway enhances apoptosis by direct inhibition of Aurora B or indirect inhibition of survivin by inhibiting a stabilizing Cdk1-mediated phosphorylation. c) The antiapoptotic complex comprising Aurora B and survivin is controlled and stabilized by Aurora B- and Cdk1-mediated phosphorylation of survivin and survivin-mediated regulation of Aurora B activity and localization of the complex. The specific interactions between several components of the pro- and antiapoptotic pathways remain to be determined, but bcl-2 acts antiapoptotically, Mad2 and bax act proapoptotically and bak does not take part in mitotic apoptosis. Active kinases are indicated as spiked symbols.

Survivin and maybe borealin and INCENP are likely to be the regulatory subunits to the catalytic subunit Aurora B in the chromosomal passenger protein complex (Vader *et al*. 2006). They depend on each other for complex formation and subcellular localization (Wheatley and McNeish 2005). Survivin acts as a substrate, a regulator of kinase activity and an adaptor for substrates of Aurora B (Wheatley and McNeish 2005). Vader and colleagues speculate that the specific and particularly dynamic localization of the chromosomal passenger protein complex might depend on specific ligands localized at the target structures and on the composition of chromosomal passenger protein complex proteins as ligands for these receptors (Vader *et al*. 2006). Phosphorylation, ubiquitination or truncation mutants of chromosomal passenger proteins could be used to investigate this matter further. Furthermore, a complex with different composition than the chromosomal passenger complex could be acting during mitotic apoptosis, which could be identified by coimmunoprecipitations and chromatography. I could show that overexpression of bcl-2 protects HeLa cells from enhanced apoptosis by pharmacological inhibition of Aurora B or Cdk1, but not from basal levels of apoptosis induced by G2 checkpoint abrogation itself (Figure 50c). Bcl-2 overexpression is found in many human tumors (Bettaieb *et al*. 2003, Willis *et al*. 2003) and can contribute to a more aggressive phenotype and cell survival upon chemotherapeutic treatments inducing apoptotic or nonapoptotic forms of cell death (Kim *et al*. 2006), although it has to be noted that these effects are cell type-specific and antiproliferative properties of bcl-2 in human and murine cancers have also been observed (Zinkel *et al*. 2006). Several strategies to chemotherapeutically target bcl-2 and related antiapoptotic proteins are pursued, e.g. antisense oligonucleotides, peptidic and non-peptidic BH3 domain mimetics and the pharmacological modulation of posttranslational modifications (Bettaieb *et al*. 2003, Fesik 2005). Future studies might elucidate whether the pro- and antiapoptotic pathways identified to act during mitotic catastrophe are also active during an undisturbed mitosis or during spindle damage-induced apoptosis. Indeed, a mitotic survival pathway has first been described for taxol treated cancer cells (O'Connor *et al.* 2002).

The role of transcription and translation in mitotic apoptosis upon G2 checkpoint abrogation

Interestingly, pharmacological inhibitors alter the degree of mitotic apoptosis not only by inhibition of mitotic kinases like Aurora B and Cdk1, but also by inhibition of

transcription, translation and MAP kinases. Inhibition of transcription in cells treated with adriamycin, UCN-01 and the Cdk1 inhibitor roscovitine leads to a significant decrease in apoptosis compared to cells treated with the three agents alone. In fact, the roscovitine-mediated enhancement of apoptosis is halved by the addition of transcriptional inhibitors. Surprisingly, if translational inhibitors are added upon treatment with adriamycin, UCN-01 and roscovitine, apoptosis is increased compared to treatment with the three agents alone. These opposite effects of inhibitors of transcription or translation seem puzzling at first, but might be explained by a requirement for newly transcribed mRNAs for the full activation of apoptosis. This effect can be seen in cells treated with spindle damaging agents, where full-fledged apoptosis occurs upon mitotic slippage, while only basal levels of apoptosis are reached during mitotic arrest. The newly transcribed mRNAs would have to be translated to enhance apoptosis, therefore inhibition of translation should be antiapoptotic. That this is not the case might be attributable to the lack of translation of essential mRNAs already present in the cell before the proapoptotic treatment, posing a challenge for the cell that possibly outweighs the antiapoptotic effect of the lack of translation of proapoptotic mRNAs. However, these findings are only a first step and require further investigation to elucidate the role of transcription and translation in mitotic apoptosis.

The role of MAP kinases in mitotic apoptosis upon G2 checkpoint abrogation

The family of MAP kinases has multiple functions upon activation by growth or stress signals that can stimulate either cell survival or cell death (Roux and Blenis 2004). Important members of MAP kinase subfamilies are p38, ERK and JNK. Three inhibitors of MAP kinases, which inhibit p38 (SB202190, SB203580) or ERK/MEK (PD98059), were tested on adriamycin and UCN-01 treated cells and all enhance apoptosis to a similar extent as the Aurora B inhibitor ZM447439. ERK/MEK inhibition with PD98059 and concomitant G2 checkpoint abrogation had a synergistic effect on caspase 3 activity. ERK1 and 2 kinases are implicated in the regulation of early G2 ensuring timely mitotic entry, they are overexpressed in many cancers and activated by various spindle damaging agents (Mollinedo and Gajate 2003, Shinohara *et al.* 2006). Pharmacological suppression of taxol-mediated ERK activation augments apoptosis, indicating that ERK promotes cell survival (MacKeigan *et al.* 2000). Thus, ERK might also be part of the same or a parallel survival pathway as survivin, Aurora B and Cdk1 in taxol (O'Connor *et al.* 2002) or

adriamycin and UCN-01 treated cells. JNK is activated by various spindle damaging agents and enhances apoptosis upon such treatments (Mollinedo and Gajate 2003). Thus, maintenance of JNK signaling and not its inhibition is probably also desirable upon G2 checkpoint abrogation. Indeed, caspase 3 activity upon G2 checkpoint abrogation was reduced 30% by JNK inhibition with 500 nM SP600125 in preliminary experiments (data not shown). Apoptosis is significantly increased upon concomitant p38 inhibition and G2 checkpoint abrogation and is accompanied by a partial mitotic exit. Combination of the p38 inhibitor SB203580 with the Aurora B inhibitor ZM447439 strongly increases mitotic exit and furthers apoptosis upon G2 checkpoint abrogation. The synergistic effect might indicate that p38 and Aurora B are part of parallel survival pathways or of the same pathway, which is not fully activated at the drug concentrations used for each of the kinases. In contrast, the reports on the effects of p38 inhibition on taxol-induced apoptosis are contradictory and most argue against a role of p38 (Mollinedo and Gajate 2003). A recent report challenges the reported role for p38 in spindle checkpoint-mediated mitotic arrest (Takenaka *et al.* 1998, Cha *et al.* 2007) and I, too, did not observe an effect of p38 inhibition on nocodazole- or taxol-induced mitotic arrest, while apoptosis was not investigated upon these treatments. However, mitotic arrest upon G2 checkpoint abrogation is reduced by the p38 inhibitor SB203580. This suggests a role of p38 in spindle checkpoint signaling upon DNA damage in mitosis, but not upon spindle damage and indicates that p38 does not regulate mitotic entry, at least in cells treated with spindle damaging drugs. Interestingly, topoisomerase II and HDAC inhibitors and diverse other stresses in G2 lead to global changes in chromatin topology triggering p38 activation via a number of different pathways and arrest cells at the G2/M transition by a so-called antephase checkpoint (Mikhailov *et al.* 2004). Such a kinase-mediated response could react more rapidly to perceived damage than a partially transcription-based system like the classical G2 DNA damage checkpoint. P38 confers an inhibitory phosphorylation to Cdc25B, thus keeping Cdk1/Cyclin B inactive and inhibiting mitotic entry, a mechanism reported for stressed (Mikhailov *et al.* 2004) and unstressed cells alike (Cha *et al.* 2007). Conflicting reports on p38 in G2 and spindle checkpoint signaling exist, which are probably attributable to differences in the roles of p38 and other MAP kinases in cell cycle regulation in different cell types and organisms and due to treatment with diverse substances (MacCorkle and Tan 2005). It is conceivable that p38 is activated by adriamycin treatment and remains activated upon G2 checkpoint abrogation, but that p38 does not induce a firm G2 arrest, explaining why Chk1 inhibition is sufficient to override

the G2 checkpoint. The role of MAP kinases and other components of the numerous stress kinase pathways in cell cycle progression and checkpoint signaling awaits further elucidation. Future experiments should address the respective roles and relationships of the chromosomal passenger proteins, MAP kinases and components of the apoptotic machinery like bcl-2 and bax in mitotic apoptosis upon G2 checkpoint abrogation and evaluate the therapeutic potential of their modulation. Indeed, MAP kinase inhibitors have been proposed as potential enhancers of apoptosis induced by established chemotherapeutics, e.g. taxanes, *Vinca* alkaloids, topoisomerase I and II inhibitors and cisplatin (Dent and Grant 2001).

Comparison of apoptosis induced by spindle damage or by DNA damage in mitosis

Recent reports shed some light on the mechanisms of apoptosis induction upon treatment with Eg5/KSP inhibitors. The mitotic kinesin motor protein Eg5/KSP establishes spindle bipolarity by moving the duplicated centrosomes to opposite sides of the cell (Blangy *et al.* 1995), consequently, its inhibition results in a monoastral spindle, which leads to spindle checkpoint-mediated mitotic arrest. Its is expected that Eg5/KSP inhibitors act solely on mitotic cells, because Eg5 has no known function outside mitosis, and might, thus, avoid the side effects associated with interference with microtubule stability, which also affect quiescent cells. Prolonged Eg5/KSP inhibitor-induced mitotic arrest kills cells upon slippage out of mitosis via activation of the intrinsic pathway of apoptosis (Tao *et al.* 2005) and is reported to be effective in taxol-sensitive and -insensitive ovary carcinoma cell lines (Marcus *et al.* 2005). Eg5/KSP inhibitor-induced apoptosis is executed via activation of bax, phosphorylation of bcl-X_L, activation of caspase 3 and cleavage of PARP (Tao *et al.* 2005, Tao *et al.* 2007, Vijapurkar *et al.* 2007). It does not require protein translation and p53 activation, but additional activation of the Fas death receptor pathway via p53 can further enhance Eg5/KSP inhibitor-induced cell death (Tao *et al.* 2005, Tao *et al.* 2007, Vijapurkar *et al.* 2007). Apoptosis induction by various spindle damaging agents like taxol, epothilones, *Vinca* alkaloids or nocodazole depends mainly on proapoptotic regulation of components of the bcl-2 family (Bhalla 2003, Mollinedo and Gajate 2003). Many prominent stress kinases are activated upon spindle damage, but their relative contribution to activation or inhibition of apoptosis remains controversial. Several reports indicate that ERK acts antiapoptotic, JNK acts proapoptotic and p38 does not play a critical role in

response to various spindle damaging agents (Bhalla 2003, Mollinedo and Gajate 2003). However, it has to be noted that in most experiments mitotic cell populations were not separated from nonmitotic upon spindle damage-induced mitotic arrest, although Deacon and colleagues could show distinct activation patterns of several proteins for the two populations in nocodazole treated cells (Deacon *et al.* 2003). Thus, I investigated mitotic and nonmitotic fractions of adriamycin and UCN-01 treated cells and found significant apoptosis induction to be restricted to mitotically arrested cells. As we could show, spindle damage-induced apoptosis depends on a sufficient duration of the mitotic arrest followed by mitotic slippage. While the levels of apoptosis during mitotic arrest are minimal, they rise sharply upon mitotic exit. In contrast, cells entering mitosis in the presence of DNA damage upon G2 checkpoint abrogation die during mitotic arrest. Apoptotic parameters rise with a lag time of about three hours in adriamycin and UCN-01 treated HeLa cells, indicating that apoptosis is not executed immediately or that its level is below the detection threshold of the methods employed. My unpublished results showed that the strength of mitotic arrest upon G2 checkpoint abrogation depends on the amount of DNA damage: low concentrations of adriamycin lead to a leaky G2 arrest as evidenced by the occurrence of mitotic cells in MPM2 FACS analysis (data not shown). The combination of low doses of adriamycin with UCN-01 leads to a shortened mitotic arrest resulting in a prominent G1 peak in FACS measurements indicating cytokinesis of the slipped cells. The resulting daughter cells probably die later due to unrepaired DNA damage, aneuploidization or the consequences of severing chromosome bridges by cytokinesis. The effect of different adriamycin concentrations on mitotic arrest, but not on cell death, was tested. Future experiments could address this issue, in particular the effect of clinically relevant doses of all inhibitors employed. For instance, the combination of UCN-01 with lower doses of adriamycin than the ones employed by us might be as effective as the combination with high doses, provided that the consequences of a faulty cytokinesis are as lethal as apoptosis executed directly in mitotic cells. Live cell imaging could be used to follow the fate of individual cells upon the described treatments.

With the exception of Aurora B and survivin inhibition, which suppress cytokinesis, the inhibitors of transcription, translation and MAP kinases and the shRNA-mediated downregulation of spindle checkpoint genes lead to spindle checkpoint impairment and cytokinesis upon G2 checkpoint abrogation, similar to weak spindle checkpoint activation due to decreased mitotic damage created by lower adriamycin concentrations. The resulting G1 peak is broader and not as clearly defined as in untreated cells, suggesting that

the DNA content of these newly divided cells is not uniformly 2N, but might be higher or lower in substantial parts of the population. This might be the consequence of chromosome bridges, uneven divisions due to multipolar spindles or the existence of incorrectly attached chromosomes. Such mitotic defects might endanger the long-term survival of the affected cells and colony formation assays would be particularly helpful to analyze the efficiency of different chemotherapy regimens based on G2 checkpoint abrogation. Immunofluorescence experiments could determine the exact timing of apoptosis induction in cells undergoing mitotic apoptosis and elucidate which cellular alterations trigger apoptosis. The components of the pro- and antiapoptotic pathways, their interactions and their mechanisms of action await further experimental clarification. In particular the proapoptotic function of Mad2 remains to be elucidated and proteins linking Mad2 to the apoptotic machinery have to be identified. Since Mad2 downregulation confers resistance to apoptosis induced by various treatments, it is conceivable that Mad2 upregulation sensitizes cells to apoptosis *per se* or to apoptosis induced by chemotherapeutic drugs. Indeed, cisplatin-resistant nasopharyngeal cancer cells characterized by reduced *MAD2* levels were successfully sensitized to cisplatin by ectopic *MAD2* expression (Cheung *et al*. 2005). *MAD2* upregulation has been reported in gastric cancers (Wu *et al.* 2004), neuroblastomas and bladder cancers (Hernando *et al*. 2004), but apparently these cancer cells have acquired some other alterations counterbalancing a possible proapoptotic or cell cycle arresting effect of overexpressed Mad2. Therefore further experiments are required to uncover the pro- and antiapoptotic pathways involved in cellular reactions to altered Mad2 expression levels. Their results might shed more light on cancerogenesis and better predict chemotherapy outcomes. Simultaneous treatment with p38 and Aurora B inhibitors induced mitotic exit, but suppressed cytokinesis and enhanced caspase 3 activity significantly. Similarly, future experiments could evaluate whether cells with reduced Mad2 levels could be sensitized to apoptosis upon G2 checkpoint abrogation by pharmacological Aurora B inhibition leading to abortive cytokinesis.

Another possible way to enhance apoptosis upon G2 checkpoint abrogation could be the combination of newly developed survivin inhibitors, which should have a similar effect as Aurora B or Cdk1 inhibitors. The selectivity of survivin or bcl-2 inhibitors for cancer cells might even be higher than that of several other inhibitors since *survivin* and *BCL2* are highly expressed in many cancers (Bettaieb *et al.* 2003, Keen and Taylor 2004, Fesik 2005).

Also, a combination of Aurora B inhibitors with UCN-01 might prove useful in cancer chemotherapy (Vogel *et al.* 2007). Aurora B and Chk1 inhibition could be synergistic by several ways. 1. Chk1 inhibition leads to premature mitotic entry of cells with incompletely replicated DNA (Furnari *et al.* 2003, Zeng *et al.* 1998), which can be interpreted as DNA damage that is further potentiated by progression through mitosis. Aurora B inhibition then abrogates the spindle checkpoint and cells exit mitosis with DNA damage. Therefore apoptosis by Chk1 inhibition is enhanced by subsequent Aurora B inhibition. 2. Aurora B inhibition leads to tetraploidization (Keen and Taylor 2004). Chk1 inhibition preferentially kills tetraploid cells (Vitale *et al.* 2007), therefore apoptosis by Aurora B inhibition is enhanced by subsequent Chk1 inhibition. 3. By G2 checkpoint abrogation plus Aurora B inhibition, as described above, DNA damage is potentiated in mitosis and apoptosis is increased by inhibition of the Aurora B-dependent survival pathway.

6. Pharmacological inactivation of the spindle checkpoint induces apoptosis in cancer cells

Resistance to chemotherapy is a frequent problem in the therapy of cancer (Lee and Schmitt 2003) and its mechanisms are still incompletely understood, making it difficult to combat. However, our results clearly indicate a prominent role for a functional spindle checkpoint in successful chemotherapeutic cell killing. While a functional spindle checkpoint often participates in the induction of apoptosis in response to spindle damage, DNA damage and DNA damage in mitosis, a partially impaired spindle checkpoint confers resistance to these treatments. To circumvent this mechanism of resistance, we set out to pharmacologically mimic the lack of spindle checkpoint signaling to a degree which is lethal for the cell as seen in HeLa cells with markedly reduced levels of *BUB1*, *BUB1B* or *MAD2*. The indolocarbazole compound Gö6976 was first identified by our lab as a spindle checkpoint abrogating drug in mitotically arrested cells upon spindle damage. Interestingly, single treatment with Gö6976 produces spindle damage leading to a transient delay in mitosis (data not shown), which is then abrogated by Gö6976 (Figure 51a). These dual effects of Gö6976 might explain why it effectively induces apoptosis in a wide variety of cancer cell lines.

Gö6976 abrogates the spindle checkpoint

Gö6976 is closely related to UCN-01 and both are derived from staurosporine, a broad-spectrum kinase inhibitor. The inhibitory spectrum of Gö6976 and UCN-01 is more selective than that of staurosporine and is distinct but overlapping. Both were originally identified as PKC kinase inhibitors and UCN-01 entered clinical trials under this premise. Furthermore, Gö6976 and UCN-01 abrogate DNA damage-induced G2 arrest in p53 negative cells by inhibition of Chk1 kinase, the principal kinase responsible for G2 arrest. Gö6976, but not UCN-01, overrides the spindle checkpoint without inhibiting Cdk1. Interestingly, Gö6976 inhibits mitotic arrest more efficiently upon sequential treatment with nocodazole and Gö6976 than upon parallel treatment with the same substances (data not shown). UCN-01 appears not to affect mitotic arrest at the concentrations tested, although a role for Chk1 in the spindle checkpoint was recently proposed (Zachos *et al*. 2007), therefore Chk1 is probably not the target of Gö6976 in mitosis. The mitotic target of

Gö6976 remains to be determined, but is likely to be a mitotic kinase, e.g. from the Aurora family, and not one of the kinases already known to be inhibited by Gö6976.

Gö6976 kills cancer cells by inducing mitochondrial apoptosis

Several assays detecting caspase 3 activity were performed on Gö6976 treated cancer cells. Caspase 3 activity was determined directly in a fluorimetric enzymatic assay and indirectly as PARP cleavage or DNA laddering. FACS analysis of synchronized living cells upon Gö6976 treatment revealed that apoptosis is executed via the intrinsic pathway of apoptosis as evidenced by permeabilization of mitochondria to TMRE dye (data not shown). Cell cycle synchronization experiments showed that a single traversal through a faulty mitosis is sufficient to trigger apoptosis in Gö6976 treated HCT116, H1299 and U2OS cell lines (data not shown). Immunostaining of mitotic cells revealed multiple spindle defects induced by Gö6976 like lagging chromosomes, asymmetric and deformed spindles (data not shown). Therefore it is unlikely that Gö6976 kills cells independently of mitosis, and underscores that Gö6976 is the first spindle checkpoint abrogator described for use as a single agent for cancer chemotherapy. Cdk1 inhibition could have a similar effect, but in contrast to Cdk1 inhibitors, Gö6976 does not interfere with mitotic entry. To overcome the problem of G2 arrest induced by Cdk1 inhibition, cancer cells would first have to be treated with spindle checkpoint activating drugs, which work preferentially in spindle checkpoint proficient cells. Thus, such a combination treatment with spindle damaging agents and Cdk1 inhibitors would encounter the same difficulties facing established chemotherapies, several of which rely on a functional spindle checkpoint. Furthermore, Cdk inhibitors lack specificity, they inhibit several kinases at once. Thus, specificity for a single Cdk can only be achieved by arresting cells in a cell cycle phase, where only one Cdk is active, e.g. Cdk1 in mitosis, and then administering the Cdk inhibitor.

Tests of Gö6976 on a panel of cancer cell lines from various tissues showed that half of the tested cell lines induce a high level of apoptosis and the other half is at least sensitive to Gö6976 when compared to non-cancerous human control cell lines. Non-cancerous cells are probably spared from Gö6976-induced apoptosis, because cancer cells often display a generally higher sensitivity to apoptosis, impaired cell cycle checkpoint responses and an increased proliferation rate, all of which might sensitize them, e.g. to proteasome inhibitors, since the proteasome is essential for the degradation of cell cycle and apoptosis regulators (Richardson *et al*. 2005). An obvious correlation between sensitivity to Gö6976-

induced apoptosis and spindle checkpoint status or p53 status of the cell lines could not be found, but the numerous alterations accumulated during cancerogenesis in each of the cell lines makes a thorough analysis difficult. Therefore, I employed the isogenic HCT116 cell system to investigate the role of the spindle checkpoint or p53 in Gö6976-mediated apoptosis. Spindle checkpoint impaired HCT116 *MAD2*$^{+/-}$ or HCT116 Mad1 knockdown cells are indeed at least as sensitive to Gö6976 than wild typic cells, proving that Gö6976 could be effective against cells resistant to various spindle damaging agents (Figure 51b). However, results on the role of p53 in Gö6976-mediated apoptosis were inconclusive (data not shown) and it should be noted that the requirement for functional p53 in spindle damage-induced apoptosis is cell line-dependent.

b

	spindle checkpoint status			
treatment	fully functional	partially functional	non-functional	reaction
no drug	survival	survival	apoptosis	
conventional spindle damaging drug	apoptosis	survival		
Gö6976	apoptosis	apoptosis		

Figure 51: A novel spindle checkpoint abrogator induces apoptosis regardless of spindle checkpoint status. a) Gö6976 induces spindle damage, leading to a transient delay in mitosis and to apoptosis in cancer cells. b) Conventional spindle damaging agents rely on a fully functional spindle checkpoint to successfully induce apoptosis and cannot kill spindle checkpoint impaired cells. Gö6976 treatment mimics the complete loss of the spindle checkpoint with lethal consequences to all treated cancer cells, thus overcoming chemotherapy resistance of cells with reduced spindle checkpoint function.

Spindle checkpoint abrogation as a novel mechanism of apoptosis induction presents a promising alternative to current chemotherapies. Especially Gö6976's ability to not only kill chemotherapy-resistant spindle checkpoint impaired cells, but the prospect of enhanced killing of these cells compared to spindle checkpoint proficient cells is very promising. The

observed effects of Gö6976 prove the feasibility of this strategy in anticancer treatment in principle. Gö6976 might serve as a model substance to study apoptosis caused by spindle checkpoint abrogation and as a lead structure to develop new drugs with higher specific activities, which are required for use as a drug. Specific spindle checkpoint abrogators with a mechanism of action similar to Gö6976, which do not require mitotic arrest mediated by other agents as a prerequisite for the induction of apoptosis, are rare. So far, small molecule inhibitors of the mitotic kinase Mps1 have been reported for yeast and for human cells, but induction of apoptosis upon Mps1 inhibition was not investigated (Dorer *et al.* 2005, Schmidt *et al.* 2005). Interestingly, nocodazole- or taxol-induced mitotic arrest upon inhibition of Mps1 is abrogated in cancer cells, but not in BJ-tert cells, suggesting that untransformed cells possess an additional Mps1-independent spindle checkpoint pathway (Schmidt *et al.* 2005). Thus, like Gö6976 Mps1 inhibitors might confer cancer cell selectivity, an advantage for potential chemotherapeutic use.

Literature

Abrieu A; Magnaghi-Jaulin L; Kahana JA; Peter M; Castro A; Vigneron S; Lorca T; Cleveland DW; Labbé JC (2001) Mps1 is a kinetochore-associated kinase essential for the vertebrate mitotic checkpoint. *Cell,* **106,** 83-93.

Acquaviva C; Pines J (2006) The anaphase-promoting complex/cyclosome: APC/C. *J Cell Sci,* **119,** 2401-4.

Allan LA; Clarke PR (2007) Phosphorylation of caspase-9 by CDK1/cyclin B1 protects mitotic cells against apoptosis. *Mol Cell,* **26,** 301-10.

Altieri DC (2006) The case for survivin as a regulator of microtubule dynamics and cell-death decisions. *Curr Opin Cell Biol ,* **18,** 609-15.

Anand S; Penrhyn-Lowe S; Venkitaraman AR (2003) AURORA-A amplification overrides the mitotic spindle assembly checkpoint, inducing resistance to Taxol. *Cancer Cell,* **3,** 51-62.

Andreassen PR; Lohez OD; Lacroix FB; Margolis RL (2001) Tetraploid state induces p53-dependent arrest of nontransformed mammalian cells in G1. *Mol Biol Cell,* **12,** 1315-28.

Andreassen PR; Lohez OD; Margolis RL (2003) G2 and spindle assembly checkpoint adaptation, and tetraploidy arrest: implications for intrinsic and chemically induced genomic instability. *Mutat Res,* **532,** 245-53.

Andreassen PR; Martineau SN; Margolis RL (1996) Chemical induction of mitotic checkpoint override in mammalian cells results in aneuploidy following a transient tetraploid state. *Mutat Res,* **372,** 181-94.

Antignani A; Youle RJ (2006) How do Bax and Bak lead to permeabilization of the outer mitochondrial membrane? *Curr Opin Cell Biol,* **18,** 685-9.

Baek KH; Shin HJ; Jeong SJ; Park JW; McKeon F; Lee CW; Kim CM (2005) Caspases-dependent cleavage of mitotic checkpoint proteins in response to microtubule inhibitor. *Oncol Res,* **15,** 161-8.

Baker DJ; Jeganathan KB; Cameron JD; Thompson M; Juneja S; Kopecka A; Kumar R; Jenkins RB; de Groen PC; Roche P; van Deursen JM (2004) BubR1 insufficiency causes early onset of aging-associated phenotypes and infertility in mice. *Nat Genet,* **36,** 744-9.

Baker DJ; Jeganathan KB; Malureanu L; Perez-Terzic C; Terzic A; van Deursen JM (2006) Early aging-associated phenotypes in Bub3/Rae1 haploinsufficient mice. *J Cell Biol,* **172,** 529-40.

Bartek J; Lukas C; Lukas J (2004) Checking on DNA damage in S phase. *Nat Rev Mol Cell Biol,* **5,** 792-804.

Belmont LD; Hyman AA; Sawin KE; Mitchison TJ (1990) Real-time visualization of cell cycle-dependent changes in microtubule dynamics in cytoplasmic extracts. *Cell,* **62,** 579-89.

Bentley AM; Normand G; Hoyt J; King RW (2007) Distinct sequence elements of cyclin B1 promote localization to chromatin, centrosomes, and kinetochores during mitosis. *Mol Biol Cell,* **18,** 4847-58.

Bettaieb A; Dubrez-Daloz L; Launay S; Plenchette S; Rebe C; Cathelin S; Solary E (2003) Bcl-2 proteins: targets and tools for chemosensitisation of tumor cells. *Curr Med Chem Anticancer Agents,* **3,** 307-18.

Bhalla KN (2003) Microtubule-targeted anticancer agents and apoptosis. *Oncogene,* **22,** 9075-86.

Bharadwaj R; Yu H (2004) The spindle checkpoint, aneuploidy, and cancer. *Oncogene,* **23,** 2016-27.

Bhonde MR; Hanski ML; Budczies J; Cao M; Gillissen B; Moorthy D; Simonetta F; Scherübl H; Truss M; Hagemeier C; Mewes HW; Daniel PT; Zeitz M; Hanski C (2006) DNA damage-induced expression of p53 suppresses mitotic checkpoint kinase hMps1: the lack of this suppression in p53MUT cells contributes to apoptosis. *J Biol Chem,* **281,** 8675-85.

Blagden S; de Bono J (2005) Drugging cell cycle kinases in cancer therapy. *Curr Drug Targets,* **6,** 325-35.

Blagosklonny MV (2006) Prolonged mitosis versus tetraploid checkpoint: how p53 measures the duration of mitosis. *Cell Cycle,* **5,** 971-5.

Blajeski AL; Kottke TJ; Kaufmann SH (2001) A multistep model for paclitaxel-induced apoptosis in human breast cancer cell lines. *Exp Cell Res,* **270,** 277-88.

Blangy A; Lane HA; d'Hérin P; Harper M; Kress M; Nigg EA (1995) Phosphorylation by p34cdc2 regulates spindle association of human Eg5, a kinesin-related motor essential for bipolar spindle formation in vivo. *Cell,* **83,** 1159-69.

Blasina A; Price BD; Turenne GA; McGowan CH (1999) Caffeine inhibits the checkpoint kinase ATM. *Curr Biol,* **9,** 1135-8.

Blow JJ; Tanaka TU (2005) The chromosome cycle: coordinating replication and segregation. Second in the cycles review series. *EMBO Rep,* **6,** 1028-34.

Bode AM; Dong Z (2004) Post-translational modification of p53 in tumorigenesis. *Nat Rev Cancer,* **4,** 793-805.

Bolton MA; Lan W; Powers SE; McCleland ML; Kuang J; Stukenberg PT (2002) Aurora B kinase exists in a complex with survivin and INCENP and its kinase activity is stimulated by survivin binding and phosphorylation. *Mol Biol Cell,* **13,** 3064-77.

Borel F; Lohez OD; Lacroix FB; Margolis RL (2002) Multiple centrosomes arise from tetraploidy checkpoint failure and mitotic centrosome clusters in p53 and RB pocket protein-compromised cells. *Proc Natl Acad Sci U S A,* **99,** 9819-24.

Boveri, T. (1914). *Zur Frage der Entstehung maligner Tumoren.* Jena: Gustav Fischer Verlag.

Bozko P; Sabisz M; Larsen AK; Skladanowski A (2005) Cross-talk between DNA damage and cell survival checkpoints during G2 and mitosis: pharmacologic implications. *Mol Cancer Ther,* **4,** 2016–25.

Breitschopf K; Haendeler J; Malchow P; Zeiher AM; Dimmeler S (2000) Posttranslational modification of Bcl-2 facilitates its proteasome-dependent degradation: molecular characterization of the involved signaling pathway. *Mol Cell Biol,* **20,** 1886-96.

Brichese L; Barboule N; Heliez C; Valette A (2002) Bcl-2 phosphorylation and proteasome-dependent degradation induced by paclitaxel treatment: consequences on sensitivity of isolated mitochondria to Bid. *Exp Cell Res,* **278,** 101-11.

Brito DA; Rieder CL (2006) Mitotic checkpoint slippage in humans occurs via cyclin B destruction in the presence of an active checkpoint. *Curr Biol,* **16,** 1194-200.

Broker LE; Kruyt FA; Giaccone G (2005) Cell death independent of caspases: a review. *Clin Cancer Res,* **11,** 3155-62.

Brooks CL; Gu W (2003) Ubiquitination, phosphorylation and acetylation: the molecular basis for p53 regulation. *Curr Opin Cell Biol,* **15,** 164-71.

Brooks TA; Minderman H; O'Loughlin KL; Pera P; Ojima I; Baer MR; Bernacki RJ (2003) Taxane-based reversal agents modulate drug resistance mediated by P-glycoprotein, multidrug resistance protein, and breast cancer resistance protein. *Mol Cancer Ther,* **2,** 1195-205.

Brummelkamp TR; Bernards R; Agami R (2002) A system for stable expression of short interfering RNAs in mammalian cells. *Science,* **296,** 550-3.

Budihardjo I; Oliver H; Lutter M; Luo X; Wang X (1999) Biochemical pathways of caspase activation during apoptosis. *Annu Rev Cell Dev Biol,* **15,** 269-90.

Buffin E; Lefebvre C; Huang J; Gagou ME; Karess RE (2005) Recruitment of Mad2 to the kinetochore requires the Rod/Zw10 complex. *Curr Biol,* **15,** 856-61.

Bunz F; Dutriaux A; Lengauer C; Waldman T; Zhou S; Brown JP; Sedivy JM; Kinzler KW; Vogelstein B (1998) Requirement for p53 and p21 to sustain G2 arrest after DNA damage. *Science,* **282,** 1497-501.

Burds AA; Lutum AS; Sorger PK (2005) Generating chromosome instability through the simultaneous deletion of Mad2 and p53. *Proc Natl Acad Sci U S A,* **102,** 11296-301.

Cahill DP; Kinzler KW; Vogelstein B; Lengauer C (1999) Genetic instability and darwinian selection in tumours. *Trends Cell Biol,* **9,** M57-60.

Cahill DP; Lengauer C; Yu J; Riggins GJ; Willson JK; Markowitz SD; Kinzler KW; Vogelstein B (1998) Mutations of mitotic checkpoint genes in human cancers. *Nature,* **392,** 300-3.

Campbell MS; Chan GK; Yen TJ (2001) Mitotic checkpoint proteins HsMAD1 and HsMAD2 are associated with nuclear pore complexes in interphase. *J Cell Sci,* **114,** 953-63.

Cantley LC; Neel BG (1999) New insights into tumor suppression: PTEN suppresses tumor formation by restraining the phosphoinositide 3-kinase/AKT pathway. *Proc Natl Acad Sci U S A,* **96,** 4240-5.

Carter SL, E.A., Kohane IS; Harris LN; Szallasi Z, Harris LN; Szallasi Z, and Szallasi Z, (2006) A signature of chromosomal instability inferred from gene expression profiles predicts clinical outcome in multiple human cancers. *Nat Genet,* **38,** 1043-8.

Castedo M; Coquelle A; Vivet S; Vitale I; Kauffmann A; Dessen P; Pequignot MO; Casares N; Valent A; Mouhamad S; Schmitt E; Modjtahedi N; Vainchenker W; Zitvogel L; Lazar V; Garrido C; Kroemer G (2006) Apoptosis regulation in tetraploid cancer cells. *EMBO J,* **25,** 2584-95.

Castedo M; Perfettini JL; Roumier T; Valent A; Raslova H; Yakushijin K; Horne D; Feunteun J; Lenoir G; Medema R; Vainchenker W; Kroemer G (2004) Mitotic catastrophe constitutes a special case of apoptosis whose suppression entails aneuploidy. *Oncogene,* **23,** 4362-70.

Castro A; Bernis C; Vigneron S; Labbe JC; Lorca T (2005) The anaphase-promoting complex: a key factor in the regulation of cell cycle. *Oncogene,* **24,** 314-25.

Castro A; Vigneron S; Bernis C; Labbe JC; Prigent C; Lorca T (2002) The D-Box-activating domain (DAD) is a new proteolysis signal that stimulates the silent D-Box sequence of Aurora-A. *EMBO Rep,* **3,** 1209-14.

Cazales M; Schmitt E; Montembault E; Dozier C; Prigent C; Ducommun B (2005) CDC25B phosphorylation by Aurora-A occurs at the G2/M transition and is inhibited by DNA damage. *Cell Cycle,* **4,** 1233-8.

Cha H; Wang X; Li H; Fornace AJ Jr (2007) A functional role for p38 MAP kinase in modulating mitotic transit in the absence of stress. *J Biol Chem,* **282,** 22984-92.

Chan GK; Jablonski SA; Starr DA; Goldberg ML; Yen TJ (2000) Human Zw10 and ROD are mitotic checkpoint proteins that bind to kinetochores. *Nat Cell Biol,* **2,** 944-7.

Chang F; Lee JT; Navolanic PM; Steelman LS; Shelton JG; Blalock WL; Franklin RA; McCubrey JA (2003) Involvement of PI3K/Akt pathway in cell cycle progression, apoptosis, and neoplastic transformation: a target for cancer chemotherapy. *Leukemia,* **17,** 590-603.

Chen JG; Yang CP; Cammer M; Horwitz SB (2003) Gene expression and mitotic exit induced by microtubule-stabilizing drugs. *Cancer Res,* **63,** 7891-9.

Chen Q; Zhang X; Jiang Q; Clarke PR; Zhang C (2008) Cyclin B1 is localized to unattached kinetochores and contributes to efficient microtubule attachment and proper chromosome alignment during mitosis. *Cell Res,* **18,** 268-80.

Chen RH (2002) BubR1 is essential for kinetochore localization of other spindle checkpoint proteins and its phosphorylation requires Mad1. *J Cell Biol,* **158,** 487-96.

Chen RH; Shevchenko A; Mann M; Murray AW (1998) Spindle checkpoint protein Xmad1 recruits Xmad2 to unattached kinetochores. *J Cell Biol,* **143,** 283-95.

Chen RH; Waters JC; Salmon ED; Murray AW (1996) Association of spindle assembly checkpoint component XMAD2 with unattached kinetochores. *Science,* **274,** 242-6.

Chen Y; Riley DJ; Chen PL; Lee WH (1997) HEC, a novel nuclear protein rich in leucine heptad repeats specifically involved in mitosis. *Mol Cell Biol,* **17,** 6049-56.

Cheng M; Olivier P; Diehl JA; Fero M; Roussel MF; Roberts JM; Sherr CJ (1999) The p21(Cip1) and p27(Kip1) CDK 'inhibitors' are essential activators of cyclin D-dependent kinases in murine fibroblasts. *EMBO J,* **18,** 1571-83.

Cheung HW; Jin DY; Ling MT; Wong YC; Wang Q; Tsao SW; Wang X (2005) Mitotic arrest deficient 2 expression induces chemosensitization to a DNA-damaging agent, cisplatin, in nasopharyngeal carcinoma cells. *Cancer Res,* **65,** 1450-8.

Chieffi P; Cozzolino L; Kisslinger A; Libertini S; Staibano S; Mansueto G; De Rosa G; Villacci A; Vitale M; Linardopoulos S; Portella G; Tramontano D (2006) Aurora B expression directly correlates with prostate cancer malignancy and influence prostate cell proliferation. *Prostate,* **66,** 326-33.

Chipuk JE; Bouchier-Hayes L; Kuwana T; Newmeyer DD; Green DR (2005) PUMA couples the nuclear and cytoplasmic proapoptotic function of p53. *Science,* **309,** 1732-5.

Christophorou MA; Ringshausen I; Finch AJ; Swigart LB; Evan GI (2006) The pathological response to DNA damage does not contribute to p53-mediated tumour suppression. *Nature,* **443,** 214-7.

Chun AC; Jin DY (2003) Transcriptional regulation of mitotic checkpoint gene MAD1 by p53. *J Biol Chem,* **278,** 37439-50.

Chung E; Chen RH (2003) Phosphorylation of Cdc20 is required for its inhibition by the spindle checkpoint. *Nat Cell Biol,* **5,** 748-53.

Colnaghi R; Connell CM; Barrett RM; Wheatley SP (2006) Separating the anti-apoptotic and mitotic roles of survivin. *J Biol Chem,* **281,** 33450-6.

Cooke CA; Heck MM; Earnshaw WC (1987) The inner centromere protein (INCENP) antigens: movement from inner centromere to midbody during mitosis. *J Cell Biol,* **105,** 2053-67.

Cortes F; Pastor N; Mateos S; Dominguez I (2003) Roles of DNA topoisomerases in chromosome segregation and mitosis. *Mutat Res,* **543,** 59-66.

Dai W; Wang Q; Liu T; Swamy M; Fang Y; Xie S; Mahmood R; Yang YM; Xu M; Rao CV (2004) Slippage of mitotic arrest and enhanced tumor development in mice with BubR1 haploinsufficiency. *Cancer Res,* **64,** 440-5.

Dalton WB; Nandan MO; Moore RT; Yang VW (2007) Human cancer cells commonly acquire DNA damage during mitotic arrest. *Cancer Res,* **67,** 11487-92.

Davis DA; Sarkar SH; Hussain M; Li Y; Sarkar FH 6:22. (2006) Increased therapeutic potential of an experimental anti-mitotic inhibitor SB715992 by genistein in PC-3 human prostate cancer cell line. *BMC Cancer,* **6,** .

De Antoni A; Pearson CG; Cimini D; Canman JC; Sala V; Nezi L; Mapelli M; Sironi L; Faretta M; Salmon ED; Musacchio A (2005) The Mad1/Mad2 complex as a template for Mad2 activation in the spindle assembly checkpoint. *Curr Biol,* **15,** 214-25.

Deacon K; Mistry P; Chernoff J; Blank JL; Patel R (2003) p38 Mitogen-activated protein kinase mediates cell death and p21-activated kinase mediates cell survival during chemotherapeutic drug-induced mitotic arrest. *Mol Biol Cell,* **14,** 2071-87.

Degenhardt K; Mathew R; Beaudoin B; Bray K; Anderson D; Chen G; Mukherjee C; Shi Y; Gelinas C; Fan Y; Nelson DA; Jin S; White E (2006) Autophagy promotes tumor cell survival and restricts necrosis, inflammation, and tumorigenesis. *Cancer Cell,* **10,** 51-64.

Deng X; Gao F; Flagg T; May WS Jr (2004) Mono- and multisite phosphorylation enhances Bcl2's antiapoptotic function and inhibition of cell cycle entry functions. *Proc Natl Acad Sci U S A,* **101,** 153-8.

Dent P; Grant S (2001) Pharmacologic interruption of the mitogen-activated extracellular-regulated kinase/mitogen-activated protein kinase signal transduction pathway: potential role in promoting cytotoxic drug action. *Clin Cancer Res,* **7,** 775-83.

Di Nicolantonio F; Mercer SJ; Knight LA; Gabriel FG; Whitehouse PA; Sharma S; Fernando A; Glaysher S; Di Palma S; Johnson P; Somers SS; Toh S; Higgins B; Lamont A; Gulliford T; Hurren J; Yiangou C; Cree IA (2005) Cancer cell adaptation to chemotherapy. *BMC Cancer,* **5,** .

Ditchfield C; Johnson VL; Tighe A; Ellston R; Haworth C; Johnson T; Mortlock A; Keen N; Taylor SS (2003) Aurora B couples chromosome alignment with anaphase by targeting BubR1, Mad2, and Cenp-E to kinetochores. *J Cell Biol,* **161,** 267-80.

Ditchfield C; Keen N; Taylor SS (2005) The Ipl1/Aurora kinase family: methods of inhibition and functional analysis in mammalian cells. *Methods Mol Biol,* **296,** 371-81.

Donehower LA; Harvey M; Slagle BL; McArthur MJ; Montgomery CA Jr; Butel JS; Bradley A (1992) Mice deficient for p53 are developmentally normal but susceptible to spontaneous tumours. *Nature,* **356,** 215-21.

Dorer RK; Zhong S; Tallarico JA; Wong WH; Mitchison TJ; Murray AW (2005) A small-molecule inhibitor of Mps1 blocks the spindle-checkpoint response to a lack of tension on mitotic chromosomes. *Curr Biol,* **15,** 1070-6.

Draviam VM; Stegmeier F; Nalepa G; Sowa ME; Chen J; Liang A; Hannon GJ; Sorger PK; Harper JW; Elledge SJ (2007) A functional genomic screen identifies a role for TAO1 kinase in spindle-checkpoint signalling. *Nat Cell Biol,* **9,** 556-64.

Du Y; Yin F; Liu C; Hu S; Wang J; Xie H; Hong L; Fan D (2006) Depression of MAD2 inhibits apoptosis of gastric cancer cells by upregulating Bcl-2 and interfering mitochondrion pathway. *Biochem Biophys Res Commun,* **345,** 1092-8.

Duensing A; Teng X; Liu Y; Tseng M; Spardy N; Duensing S (2006) A role of the mitotic spindle checkpoint in the cellular response to DNA replication stress. *J Cell Biochem,* **99,** 759-69.

Duesberg P; Li R (2003) Multistep carcinogenesis: a chain reaction of aneuploidizations. *Cell Cycle,* **2,** 202-10.

Dunkern TR; Wedemeyer I; Baumgartner M; Fritz G; Kaina B (2003) Resistance of p53 knockout cells to doxorubicin is related to reduced formation of DNA strand breaks rather than impaired apoptotic signaling. *DNA Repair (Amst),* **2,** 49-60.

Dutertre S; Cazales M; Quaranta M; Froment C; Trabut V; Dozier C; Mirey G; Bouché JP; Theis-Febvre N; Schmitt E; Monsarrat B; Prigent C; Ducommun B (2004) Phosphorylation of CDC25B by Aurora-A at the centrosome contributes to the G2-M transition. *J Cell Sci,* **117,** 2523-31.

Eastman A (2004) Cell cycle checkpoints and their impact on anticancer therapeutic strategies. *J Cell Biochem,* **91,** 223-31.

Eckelman BP; Salvesen GS; Scott FL (2006) Human inhibitor of apoptosis proteins: why XIAP is the black sheep of the family. *EMBO Rep,* **7,** 988-94.

Eckerdt F; Yuan J; Strebhardt K (2005) Polo-like kinases and oncogenesis. *Oncogene,* **24,** 267-76.

Elowe S; Hümmer S; Uldschmid A; Li X; Nigg EA (2007) Tension-sensitive Plk1 phosphorylation on BubR1 regulates the stability of kinetochore microtubule interactions. *Genes Dev,* **21,** 2205-19.

Evans T; Rosenthal ET; Youngblom J; Distel D; Hunt T (1983) Cyclin: a protein specified by maternal mRNA in sea urchin eggs that is destroyed at each cleavage division. *Cell,* **33,** 389-96.

Fang G; Yu H; Kirschner MW (1998) The checkpoint protein MAD2 and the mitotic regulator CDC20 form a ternary complex with the anaphase-promoting complex to control anaphase initiation. *Genes Dev,* **12,** 1871-83.

Fesik SW (2005) Promoting apoptosis as a strategy for cancer drug discovery. *Nat Rev Cancer,* **5,** 876-85.

Fischle W; Tseng BS; Dormann HL; Ueberheide BM; Garcia BA; Shabanowitz J; Hunt DF; Funabiki H; Allis CD (2005) Regulation of HP1-chromatin binding by histone H3 methylation and phosphorylation. *Nature,* **438,** 1116-22.

Folkman J (1995) Angiogenesis in cancer, vascular, rheumatoid and other disease. *Nat Med,* **1,** 27–31.

Fujiwara T; Bandi M; Nitta M; Ivanova EV; Bronson RT; Pellman D (2005) Cytokinesis failure generating tetraploids promotes tumorigenesis in p53-null cells. *Nature,* **437,** 1043-7.

Fung MK; Cheung HW; Wong HL; Yuen HF; Ling MT; Chan KW; Wong YC; Cheung AL; Wang X (2007) MAD2 expression and its significance in mitotic checkpoint control in testicular germ cell tumour. *Biochim Biophys Acta,* **1773,** 821-32.

Fung TK; Ma HT; Poon RYC (2007) Specialized Roles of the Two Mitotic Cyclins in Somatic Cells: Cyclin A as an Activator of M Phase–promoting Factor. *Mol Biol Cell,* **18,** 1861–1873.

Furnari B; Rhind N; Russell P (1997) Cdc25 mitotic inducer targeted by chk1 DNA damage checkpoint kinase. *Science,* **277,** 1495-7.

García Z; Kumar A; Marqués M; Cortés I; Carrera AC (2006) Phosphoinositide 3-kinase controls early and late events in mammalian cell division. *EMBO J,* **25,** 655-61.

Gassmann R; Carvalho A; Henzing AJ; Ruchaud S; Hudson DF; Honda R; Nigg EA; Gerloff DL; Earnshaw WC (2004) Borealin: a novel chromosomal passenger required for stability of the bipolar mitotic spindle. *J Cell Biol,* **166,** 179-91.

Geley S; Kramer E; Gieffers C; Gannon J; Peters JM; Hunt T (2001) Anaphase-promoting complex/cyclosome-dependent proteolysis of human cyclin A starts at the beginning of mitosis and is not subject to the spindle assembly checkpoint. *J Cell Biol,* **153,** 137-48.

Giet R; Prigent C (1999) Aurora/Ipl1p-related kinases, a new oncogenic family of mitotic serine-threonine kinases. *J Cell Sci,* **112,** 3591-601.

Giles GI; Sharma RP (2005) Topoisomerase enzymes as therapeutic targets for cancer chemotherapy. *Med Chem,* **1,** 383-94.

Gizatullin F; Yao Y; Kung V; Harding MW; Loda M; Shapiro GI (2006) The Aurora kinase inhibitor VX-680 induces endoreduplication and apoptosis preferentially in cells with compromised p53-dependent postmitotic checkpoint function. *Cancer Res,* **66,** 7668-77.

Glotzer M (2001) Animal cell cytokinesis. *Annu Rev Cell Dev Biol,* **17,** 351-86.

Golsteyn RM; Schultz SJ; Bartek J; Ziemiecki A; Ried T; Nigg EA (1994) Cell cycle analysis and chromosomal localization of human Plk1, a putative homologue of the mitotic kinases Drosophila polo and Saccharomyces cerevisiae Cdc5. **107,** 1509-17.

Gomez-Lazaro M; Fernandez-Gomez FJ; Jordán J (2004) p53: twenty five years understanding the mechanism of genome protection. *J Physiol Biochem,* **60,** 287-307.

Gong D; Pomerening JR; Myers JW; Gustavsson C; Jones JT; Hahn AT; Meyer T; Ferrell JE Jr (2007) Cyclin A2 regulates nuclear-envelope breakdown and the nuclear accumulation of cyclin B1. *Curr Biol,* **17,** 85-91.

Grabsch H; Takeno S; Parsons WJ; Pomjanski N; Boecking A; Gabbert HE; Mueller W (2003) Overexpression of the mitotic checkpoint genes BUB1, BUBR1, and BUB3 in gastric cancer--association with tumour cell proliferation. *J Pathol,* **200,** 16-22.

Graves PR; Yu L; Schwarz JK; Gales J; Sausville EA; O'Connor PM; Piwnica-Worms H (2000) The Chk1 protein kinase and the Cdc25C regulatory pathways are targets of the anticancer agent UCN-01. *J Biol Chem,* **275,** 5600-5.

Guertin DA; Trautmann S; McCollum D (2002) Cytokinesis in eukaryotes. *Microbiol Mol Biol Rev,* **66,** 155-78.

Ha GH; Baek KH; Kim HS; Jeong SJ; Kim CM; McKeon F; Lee CW (2007) p53 activation in response to mitotic spindle damage requires signaling via BubR1-mediated phosphorylation. *Cancer Res ,* **67,** 7155-64.

Habedanck R; Stierhof YD; Wilkinson CJ; Nigg EA (2005) The Polo kinase Plk4 functions in centriole duplication. *Nat Cell Biol,* **7,** 1140-6.

Habu T; Kim SH; Weinstein J; Matsumoto T (2002) Identification of a MAD2-binding protein, CMT2, and its role in mitosis. *EMBO J,* **21,** 6419-28.

Hall-Jackson CA; Cross DA; Morrice N; Smythe C (1999) ATR is a caffeine-sensitive, DNA-activated protein kinase with a substrate specificity distinct from DNA-PK. *Oncogene,* **18,** 6707-13.

Hanahan D (1985). DNA cloning, a practical approach. Oxford-Washington D.C., USA: Glover DM, IRL Press.

Hanahan D; Weinberg RA (2000) The hallmarks of cancer. *Cell,* **100,** 57-70.

Hanks S; Coleman K; Reid S; Plaja A; Firth H; Fitzpatrick D; Kidd A; Méhes K; Nash R; Robin N; Shannon N; Tolmie J; Swansbury J; Irrthum A; Douglas J; Rahman N (2004) Constitutional aneuploidy and cancer predisposition caused by biallelic mutations in BUB1B. *Nat Genet,* **36,** 1159-61.

Hari M; Loganzo F; Annable T; Tan X; Musto S; Morilla DB; Nettles JH; Snyder JP; Greenberger LM (2006) Paclitaxel-resistant cells have a mutation in the paclitaxel-binding region of beta-tubulin (Asp26Glu) and less stable microtubules. *Mol Cancer Ther,* **5,** 270-8.

Harrington EA; Bebbington D; Moore J; Rasmussen RK; Ajose-Adeogun AO; Nakayama T; Graham JA; Demur C; Hercend T; Diu-Hercend A; Su M; Golec JM; Miller KM (2004) VX-680, a potent and selective small-molecule inhibitor of the Aurora kinases, suppresses tumor growth in vivo. *Nat Med,* **10,** 262-7.

Hartwell LH; Culotti J; Pringle JR; Reid BJ (1974) Genetic control of the cell division cycle in yeast. *Science,* **183,** 46-51.

Hauf S; Cole RW; LaTerra S; Zimmer C; Schnapp G; Walter R; Heckel A; van Meel J; Rieder CL; Peters JM (2003) The small molecule Hesperadin reveals a role for Aurora B in correcting kinetochore-microtubule attachment and in maintaining the spindle assembly checkpoint. *J Cell Biol,* **161,** 281-94.

Hernando E; Nahle Z; Juan G; Diaz-Rodriguez E; Alaminos M; Hemann M; Michel L; Mittal V; Gerald W; Benezra R; Lowe SW; Cordon-Cardo C (2004) Rb inactivation promotes genomic instability by uncoupling cell cycle progression from mitotic control. *Nature,* **430,** 797-802.

Herrmann M; Lorenz HM; Voll R; Grunke M; Woith W; Kalden JR (1994) A rapid and simple method for the isolation of apoptotic DNA fragments. *Nucleic Acids Res,* **22,** 5506-7.

Hirota T; Kunitoku N; Sasayama T; Marumoto T; Zhang D; Nitta M; Hatakeyama K; Saya H (2003) Aurora-A and an interacting activator, the LIM protein Ajuba, are required for mitotic commitment in human cells. *Cell,* **114,** 585-98.

Hirota T; Lipp JJ; Toh BH; Peters JM (2005) Histone H3 serine 10 phosphorylation by Aurora B causes HP1 dissociation from heterochromatin. *Nature,* **438,** 1176-80.

Hoeijmakers JH (2001) Genome maintenance mechanisms for preventing cancer. *Nature,* **411,** 366-74.

Hoffman WH; Biade S; Zilfou JT; Chen J; Murphy M (2002) Transcriptional repression of the anti-apoptotic survivin gene by wild type p53. *J Biol Chem,* **277,** 3247-57.

Holcik M; Sonenberg N (2005) Translational control in stress and apoptosis. *Nat Rev Mol Cell Biol,* **6,** 318-27.

Honda R; Korner R; Nigg EA (2003) Exploring the functional interactions between Aurora B, INCENP, and survivin in mitosis. *Mol Biol Cell,* **14,** 3325-41.

Hotte SJ; Oza A; Winquist EW; Moore M; Chen EX; Brown S; Pond GR; Dancey JE; Hirte HW (2006) Phase I trial of UCN-01 in combination with topotecan in patients with advanced solid cancers: a Princess Margaret Hospital Phase II Consortium study. *Ann Oncol,* **17,** 334-40.

Howell BJ; McEwen BF; Canman JC; Hoffman DB; Farrar EM; Rieder CL; Salmon ED (2001) Cytoplasmic dynein/dynactin drives kinetochore protein transport to the spindle poles and has a role in mitotic spindle checkpoint inactivation. *J Cell Biol,* **155,** 1159-72.

Hoyer-Hansen M; Bastholm L; Szyniarowski P; Campanella M; Szabadkai G; Farkas T; Bianchi K; Fehrenbacher N; Elling F; Rizzuto R; Mathiasen IS; Jaattela M (2007) Control of macroautophagy by calcium, calmodulin-dependent kinase kinase-beta, and Bcl-2. *Mol Cell,* **25,** 193-205.

Hoyt MA; Totis L; Roberts BT (1991) S. cerevisiae genes required for cell cycle arrest in response to loss of microtubule function. *Cell,* **66,** 507-17.

Hsu SL; Yu CT; Yin SC; Tang MJ; Tien AC; Wu YM; Huang CY (2006) Caspase 3, periodically expressed and activated at G2/M transition, is required for nocodazole-induced mitotic checkpoint. *Apoptosis,* **11,** 765-71.

Huang F; Hsu S; Yan Z; Winawer S; Friedman E (1994) The capacity for growth stimulation by TGF beta 1 seen only in advanced colon cancers cannot be ascribed to mutations in APC, DCC, p53 or ras. *Oncogene,* **9,** 3701-6.

Hut HM; Lemstra W; Blaauw EH; Van Cappellen GW; Kampinga HH; Sibon OC (2003) Centrosomes split in the presence of impaired DNA integrity during mitosis. *Mol Biol Cell,* **14,** 1993-2004.

Hutchison M; Berman KS; Cobb MH (1998) Isolation of TAO1, a protein kinase that activates MEKs in stress-activated protein kinase cascades. *J Biol Chem,* **273,** 28625-32.

Inoue H; Nojima H; Okayama H (1990) High efficiency transformation of Escherichia coli with plasmids. *Gene,* **96,** 23-8.

Iouk T; Kerscher O; Scott RJ; Basrai MA; Wozniak RW (2002) The yeast nuclear pore complex functionally interacts with components of the spindle assembly checkpoint. *J Cell Biol,* **159,** 807-19.

Iwanaga Y; Chi YH; Miyazato A; Sheleg S; Haller K; Peloponese JM Jr; Li Y; Ward JM; Benezra R; Jeang KT (2007) Heterozygous deletion of mitotic arrest-deficient protein 1 (MAD1) increases the incidence of tumors in mice. *Cancer Res,* **67,** 160-6.

Iwanaga Y; Jeang KT (2002) Expression of mitotic spindle checkpoint protein hsMAD1 correlates with cellular proliferation and is activated by a gain-of-function p53 mutant. *Cancer Res,* **62,** 2618-24.

Jacks T; Remington L; Williams BO; Schmitt EM; Halachmi S; Bronson RT; Weinberg RA (1994) Tumor spectrum analysis in p53-mutant mice. *Curr Biol,* **4,** 1-7.

Jallepalli PV: Lengauer C; Vogelstein B; Bunz F (2003) The Chk2 tumor suppressor is not required for p53 responses in human cancer cells. *J Biol Chem,* **278,** 20475-9.

Jensen PB; Sehested M (1997) DNA topoisomerase II rescue by catalytic inhibitors: a new strategy to improve the antitumor selectivity of etoposide. *Biochem Pharmacol,* **54,** 755-9.

Jin Z; El-Deiry WS (2005) Overview of cell death signaling pathways. *Cancer Biol Ther,* **4,** 139-63.

Johnson DG; Walker CL (1999) Cyclins and cell cycle checkpoints. *Annu Rev Pharmacol Toxicol,* **39,** 295-312.

Johnson VL; Scott MI; Holt SV; Hussein D; Taylor SS (2004) Bub1 is required for kinetochore localization of BubR1, Cenp-E, Cenp-F and Mad2, and chromosome congression. *J Cell Sci,* **117,** 1577-89.

Jordan MA; Thrower D; Wilson L (1992) Effects of vinblastine, podophyllotoxin and nocodazole on mitotic spindles. Implications for the role of microtubule dynamics in mitosis. *J Cell Sci,* **102,** 401-16.

Jordan MA; Wendell K; Gardiner S; Derry WB; Copp H; Wilson L (1996) Mitotic block induced in HeLa cells by low concentrations of paclitaxel (Taxol) results in abnormal mitotic exit and apoptotic cell death. *Cancer Res,* **56,** 816-25.

Jordan MA; Wilson L (2004) Microtubules as a target for anticancer drugs. *Nat Rev Cancer,* **4,** 253-65.

Juin P; Hueber AO; Littlewood T; Evan G (1999) c-Myc-induced sensitization to apoptosis is mediated through cytochrome c release. *Genes Dev,* **13,** 1367-81.

Kalitsis P; Earle E; Fowler KJ; Choo KH (2000) Bub3 gene disruption in mice reveals essential mitotic spindle checkpoint function during early embryogenesis. *Genes Dev,* **14,** 2277-82.

Kallio MJ; McCleland ML; Stukenberg PT; Gorbsky GJ (2002) Inhibition of aurora B kinase blocks chromosome segregation, overrides the spindle checkpoint, and perturbs microtubule dynamics in mitosis. *Curr Biol,* **12,** 900-5.

Kandel ES; Skeen J; Majewski N; Di Cristofano A; Pandolfi PP; Feliciano CS; Gartel A; Hay N (2002) Activation of Akt/protein kinase B overcomes a G(2)/m cell cycle checkpoint induced by DNA damage. *Mol Cell Biol,* **22,** 7831-41.

Karess R (2005) Rod-Zw10-Zwilch: a key player in the spindle checkpoint. *Trends Cell Biol,* **15,** 386-92.

Kasai T; Iwanaga Y; Iha H; Jeang KT (2002) Prevalent loss of mitotic spindle checkpoint in adult T-cell leukemia confers resistance to microtubule inhibitors. *J Biol Chem,* **277,** 5187-93.

Kastan MB; Bartek J (2004) Cell-cycle checkpoints and cancer. *Nature,* **432,** 316-23.

Kawabe T (2004) G2 checkpoint abrogators as anticancer drugs. *Mol Cancer Ther,* **3,** 513-9.

Keen N; Taylor S (2004) Aurora-kinase inhibitors as anticancer agents. *Nat Rev Cancer,* **4,** 927-36.

Kerr JF; Wyllie AH; Currie AR (1972) Apoptosis: a basic biological phenomenon with wide-ranging implications in tissue kinetics. *Br J Cancer,* **26,** 239-57.

Kienitz A; Vogel C; Morales I; Muller R; Bastians H (2005) Partial downregulation of MAD1 causes spindle checkpoint inactivation and aneuploidy, but does not confer resistance towards taxol. *Oncogene,* **24,** 4301-4310.

Kim M; Murphy K; Liu F; Parker SE; Dowling ML; Baff W; Kao GD (2005) Caspase-mediated specific cleavage of BubR1 is a determinant of mitotic progression. *Mol Cell Biol,* **25,** 9232-48.

Kim R; Emi M; Tanabe K; Murakami S; Uchida Y; Arihiro K (2006) Regulation and interplay of apoptotic and non-apoptotic cell death. *J Pathol,* **208,** 319-26.

Kinsella AR; Smith D (1998) Tumor resistance to antimetabolites. *Gen Pharmacol,* **30,** 623-6.

Kitajima TS; Hauf S; Ohsugi M; Yamamoto T; Watanabe Y (2005) Human Bub1 defines the persistent cohesion site along the mitotic chromosome by affecting Shugoshin localization. *Curr Biol,* **15,** 353-9.

Kops GJ; Foltz DR; Cleveland DW (2004) Lethality to human cancer cells through massive chromosome loss by inhibition of the mitotic checkpoint. *Proc Natl Acad Sci USA,* **101,** 8699-704.

Kops GJ; Weaver BA; Cleveland DW (2005) On the road to cancer: aneuploidy and the mitotic checkpoint. *Nat Rev Cancer,* **5,** 773-85.

Kortmansky J; Shah MA; Kaubisch A; Weyerbacher A; Yi S; Tong W; Sowers R; Gonen M; O'reilly E; Kemeny N; Ilson DI; Saltz LB; Maki RG; Kelsen DP; Schwartz GK (2005) Phase I trial of the cyclin-dependent kinase inhibitor and protein kinase C inhibitor 7-hydroxystaurosporine in combination with Fluorouracil in patients with advanced solid tumors. *J Clin Oncol,* **23,** 1875-84.

Kramer A; Mailand N; Lukas C; Syljuasen RG; Wilkinson CJ; Nigg EA; Bartek J; Lukas J (2004) Centrosome-associated Chk1 prevents premature activation of cyclin-B-Cdk1 kinase. *Nat Cell Biol,* **6,** 884-91.

Kroemer G; Martin SJ (2005) Caspase-independent cell death. *Nat Med,* **11,** 725-30.

Krystyniak A; Garcia-Echeverria C; Prigent C; Ferrari S (2006) Inhibition of Aurora A in response to DNA damage. *Oncogene,* **25,** 338-48.

Lanni JS; Jacks T (1998) Characterization of the p53-dependent postmitotic checkpoint following spindle disruption. *Mol Cell Biol,* **18,** 1055-64.

Lanni JS; Lowe SW; Licitra EJ; Liu JO; Jacks T (1997) p53-independent apoptosis induced by paclitaxel through an indirect mechanism. *Proc Natl Acad Sci U S A,* **94,** 9679-83.

Laoukili J; Kooistra MR; Brás A; Kauw J; Kerkhoven RM; Morrison A; Clevers H; Medema RH (2005) FoxM1 is required for execution of the mitotic programme and chromosome stability. *Nat Cell Biol,* **7,** 126-36.

Lara PN Jr; Mack PC; Synold T; Frankel P; Longmate J; Gumerlock PH; Doroshow JH; Gandara DR (2005) The cyclin-dependent kinase inhibitor UCN-01 plus cisplatin in advanced solid tumors: a California cancer consortium phase I pharmacokinetic and molecular correlative trial. *Clin Cancer Res,* **11,** 4444-50.

Lavin MF; Gueven N (2006) The complexity of p53 stabilization and activation. *Cell Death Differ,* **13,** 941-50.

Le Cam L; Linares LK; Paul C; Julien E; Lacroix M; Hatchi E; Triboulet R; Bossis G; Shmueli A; Rodriguez MS; Coux O; Sardet C (2006) E4F1 is an atypical ubiquitin ligase that modulates p53 effector functions independently of degradation. *Cell,* **127,** 775-88.

Lee S; Schmitt CA (2003) Chemotherapy response and resistance. *Curr Opin Genet Dev,* **13,** 90-6.

Lengauer C; Kinzler KW; Vogelstein B (1997) Genetic instability in colorectal cancers. *Nature,* **386,** 623-7.

Lengauer C; Kinzler KW; Vogelstein B (1998) Genetic instabilities in human cancers. *Nature,* **396,** 643-9.

Lens SM; Vader G; Medema RH (2006) The case for Survivin as mitotic regulator. *Curr Opin Cell Biol,* **18,** 616-22.

Lens SM; Wolthuis RM; Klompmaker R; Kauw J; Agami R; Brummelkamp T; Kops G; Medema RH (2003) Survivin is required for a sustained spindle checkpoint arrest in response to lack of tension. *EMBO J,* **22,** 2934-47.

Li F; Ackermann EJ; Bennett CF; Rothermel AL; Plescia J; Tognin S; Villa A; Marchisio PC; Altieri DC (1999) Pleiotropic cell-division defects and apoptosis induced by interference with survivin function. *Nat Cell Biol,* **1,** 461-6.

Li F; Ambrosini G; Chu EY; Plescia J; Tognin S; Marchisio PC; Altieri DC (1998) Control of apoptosis and mitotic spindle checkpoint by survivin. *Nature,* **396,** 580-4.

Li JJ; Li SA (2006) Mitotic kinases: the key to duplication, segregation, and cytokinesis errors, chromosomal instability, and oncogenesis. *Pharmacol Ther,* **111,** 974-84.

Li R; Murray AW (1991) Feedback control of mitosis in budding yeast. *Cell,* **66,** 519-31.

Li Y; Benezra R (1996) Identification of a human mitotic checkpoint gene: hsMAD2. *Science,* **274,** 246-8.

Liang XH; Jackson S; Seaman M; Brown K; Kempkes B; Hibshoosh H; Levine B (1999) Induction of autophagy and inhibition of tumorigenesis by beclin 1. *Nature,* **402,** 672-6.

Lindqvist A; van Zon W; Rosenthal CK; Wolthuis RMF (2007) Cyclin B1–Cdk1 Activation Continues after Centrosome Separation to Control Mitotic Progression. *PLoS Biol,* **5,** e123.

Loeb LA (2001) A mutator phenotype in cancer. *Cancer Res,* **61,** 3230-9.

Losada A; Hirano M; Hirano T (2002) Cohesin release is required for sister chromatid resolution, but not for condensin-mediated compaction, at the onset of mitosis. *Genes Dev,* **16,** 3004-16.

Luo X; Tang Z; Rizo J; Yu H (2002) The Mad2 spindle checkpoint protein undergoes similar major conformational changes upon binding to either Mad1 or Cdc20. *Mol Cell,* **9,** 59-71.

MacCorkle RA; Tan TH (2005) Mitogen-activated protein kinases in cell-cycle control. *Cell Biochem Biophys,* **43,** 451-61.

MacKeigan JP; Collins TS; Ting JP (2000) MEK inhibition enhances paclitaxel-induced tumor apoptosis. *J Biol Chem,* **275,** 38953-6.

Malumbres M; Barbacid M (2005) Mammalian cyclin-dependent kinases. *Trends Biochem Sci,* **30,** 630-41.

Manfredi MG; Ecsedy JA; Meetze KA; Balani SK; Burenkova O; Chen W; Galvin KM; Hoar KM; Huck JJ; LeRoy PJ; Ray ET; Sells TB; Stringer B; Stroud SG; Vos TJ; Weatherhead GS; Wysong DR; Zhang M; Bolen JB; Claiborne CF (2007) Antitumor activity of MLN8054, an orally active small-molecule inhibitor of Aurora A kinase. *Proc Natl Acad Sci U S A,* **104,** 4106-11.

Mani A; Gelmann EP (2005) The ubiquitin-proteasome pathway and its role in cancer. *J Clin Oncol,* **23,** 4776-89.

Mao Y; Abrieu A; Cleveland DW (2003) Activating and silencing the mitotic checkpoint through CENP-E-dependent activation/inactivation of BubR1. *Cell,* **114,** 87-98.

Marcus AI; Peters U; Thomas SL; Garrett S; Zelnak A; Kapoor TM; Giannakakou P (2005) Mitotic kinesin inhibitors induce mitotic arrest and cell death in Taxol-resistant and -sensitive cancer cells. *J Biol Chem,* **280,** 11569-77.

Margolis RL; Lohez OD; Andreassen PR (2003) G1 tetraploidy checkpoint and the suppression of tumorigenesis. *J Cell Biochem,* **88,** 673-83.

Martin SJ; Lennon SV; Bonham AM; Cotter TG (1990) Induction of apoptosis (programmed cell death) in human leukemic HL-60 cells by inhibition of RNA or protein synthesis. *J Immunol,* **145,** 1859-1867.

Marumoto T; Honda S; Hara T; Nitta M; Hirota T; Kohmura E; Saya H (2003) Aurora-A kinase maintains the fidelity of early and late mitotic events in HeLa cells. *J Biol Chem,* **278,** 51786-95.

Marumoto T; Zhang D; Saya H (2005) Aurora-A - a guardian of poles. *Nat Rev Cancer,* **5,** 42-50.

Masuda A; Maeno K; Nakagawa T; Saito H; Takahashi T (2003) Association between mitotic spindle checkpoint impairment and susceptibility to the induction of apoptosis by anti-microtubule agents in human lung cancers. *Am J Pathol,* **163,** 1109-16.

Mayer TU; Kapoor TM; Haggarty SJ; King RW; Schreiber SL; Mitchison TJ (1999) Small molecule inhibitor of mitotic spindle bipolarity identified in a phenotype-based screen. *Science,* **286,** 971-4.

McGowan CH (2002) Checking in on Cds1 (Chk2): A checkpoint kinase and tumor suppressor. *Bioessays,* **24,** 502-11.

Meraldi P; Draviam VM; Sorger PK (2004) Timing and checkpoints in the regulation of mitotic progression. *Dev Cell,* **7,** 45-60.

Meraldi P; Honda R; Nigg EA (2002) Aurora-A overexpression reveals tetraploidization as a major route to centrosome amplification in p53-/- cells. *EMBO J,* **21,** 483-92.

Meraldi P; Honda R; Nigg EA (2004) Aurora kinases link chromosome segregation and cell division to cancer susceptibility. *Curr Opin Genet Dev,* **14,** 29-36.

Meraldi P; Sorger PK (2005) A dual role for Bub1 in the spindle checkpoint and chromosome congression. *EMBO J,* **24,** 1621-33.

Michel L; Benezra R; Diaz-Rodriguez E (2004) MAD2 dependent mitotic checkpoint defects in tumorigenesis and tumor cell death: a double edged sword. *Cell Cycle,* **3,** 990-2.

Michel LS; Liberal V; Chatterjee A; Kirchwegger R; Pasche B; Gerald W; Dobles M; Sorger PK; Murty VV; Benezra R (2001) MAD2 haplo-insufficiency causes premature anaphase and chromosome instability in mammalian cells. *Nature,* **409,** 355-9.

Mikhailov A; Shinohara M; Rieder CL (2004) Topoisomerase II and histone deacetylase inhibitors delay the G2/M transition by triggering the p38 MAPK checkpoint pathway. *J Cell Biol,* **166,** 517-26.

Minn AJ; Boise LH; Thompson CB (1996) Expression of Bcl-xL and loss of p53 can cooperate to overcome a cell cycle checkpoint induced by mitotic spindle damage. *Genes Dev,* **10,** 2621-31.

Mitchison T; Kirschner M (1984) Dynamic instability of microtubule growth. *Nature,* **312,** 237-42.

Mollinedo F; Gajate C (2003) Microtubules, microtubule-interfering agents and apoptosis. *Apoptosis,* **8,** 413-50.

Momand J; Jung D; Wilczynski S; Niland J (1998) The MDM2 gene amplification database. *Nucleic Acids Res,* **26,** 3453-9.

Morgenstern JP; Land H (1990) Advanced mammalian gene transfer: high titre retroviral vectors with multiple drug selection markers and a complementary helper-free packaging cell line. *Nucleic Acids Res,* **18,** 3587-96.

Morrow CJ; Tighe A; Johnson VL; Scott MI; Ditchfield C; Taylor SS (2005) Bub1 and aurora B cooperate to maintain BubR1-mediated inhibition of APC/CCdc20. *J Cell Sci,* **118,** 3639-52.

Mukherji M; Bell R; Supekova L; Wang Y; Orth AP; Batalov S; Miraglia L; Huesken D; Lange J; Martin C; Sahasrabudhe S; Reinhardt M; Natt F; Hall J; Mickanin C; Labow M; Chanda SK; Cho CY; Schultz PG (2006) Genome-wide functional analysis of human cell-cycle regulators. *Proc Natl Acad Sci U S A,* **103,** 14819-24.

Myung K; Smith S; Kolodner RD (2004) Mitotic checkpoint function in the formation of gross chromosomal rearrangements in Saccharomyces cerevisiae. *Proc Natl Acad Sci U S A,* **101,** 15980-5.

Nakajima H; Toyoshima-Morimoto F; Taniguchi E; Nishida E (2003) Identification of a consensus motif for Plk (Polo-like kinase) phosphorylation reveals Myt1 as a Plk1 substrate. *J Biol Chem,* **278,** 25277-80.

Nettles JH; Li H; Cornett B; Krahn JM; Snyder JP; Downing KH (2004) The binding mode of epothilone A on alpha,beta-tubulin by electron crystallography. *Science,* **305,** 866-9.

Nguyen HG; Ravid K (2006) Tetraploidy/aneuploidy and stem cells in cancer promotion: The role of chromosome passenger proteins. *J Cell Physiol,* **208,** 12-22.

Nigg EA (2001) Mitotic kinases as regulators of cell division and its checkpoints. *Nat Rev Mol Cell Biol,* **2,** 21-32.

Nitta M; Kobayashi O; Honda S; Hirota T; Kuninaka S; Marumoto T; Ushio Y; Saya H (2004) Spindle checkpoint function is required for mitotic catastrophe induced by DNA-damaging agents. *Oncogene,* **23,** 6548-58.

Noble ME; Endicott JA; Johnson LN (2004) Protein kinase inhibitors: insights into drug design from structure. *Science,* **303,** 1800-5.

Nousiainen M; Silljé HH; Sauer G; Nigg EA; Körner R (2006) Phosphoproteome analysis of the human mitotic spindle. *Proc Natl Acad Sci U S A,* **103,** 5391-6.

Nurse P (1975) Genetic control of cell size at cell division in yeast. *Nature,* **256,** 547-51.

O'Connor DS; Grossman D; Plescia J; Li F; Zhang H; Villa A; Tognin S; Marchisio PC; Altieri DC (2000) Regulation of apoptosis at cell division by p34cdc2 phosphorylation of survivin. *Proc Natl Acad Sci U S A,* **97,** 13103-7.

O'Connor DS; Wall NR; Porter AC; Altieri DC (2002) A p34(cdc2) survival checkpoint in cancer. *Cancer Cell,* **2,** 43-54.

Oikawa T; Okuda M; Ma Z; Goorha R; Tsujimoto H; Inokuma H; Fukasawa K (2005) Transcriptional control of BubR1 by p53 and suppression of centrosome amplification by BubR1. *Mol Cell Biol,* **25,** 4046-61.

Okada H; Mak TW (2004) Pathways of apoptotic and non-apoptotic death in tumour cells. *Nat Rev Cancer,* **4,** 592-603.

Oricchio E; Saladino C; Iacovelli S; Soddu S; Cundari E (2006) ATM is activated by default in mitosis, localizes at centrosomes and monitors mitotic spindle integrity. *Cell Cycle,* **5,** 88-92.

Ozben T (2006) Mechanisms and strategies to overcome multiple drug resistance in cancer. *FEBS Lett,* **580,** 2903-9.

Palframan WJ; Meehl JB; Jaspersen SL; Winey M; Murray AW (2006) Anaphase inactivation of the spindle checkpoint. *Science,* **313,** 680-4.

Panaretakis T; Pokrovskaja K; Shoshan MC; Grand D (2002) Activation of Bak, Bax, and BH3-only proteins in the apoptotic response to doxorubicin. *J Biol Chem,* **277,** 44317-44326.

Pennati M; Folini M; Zaffaroni N (2007) Targeting survivin in cancer therapy: fulfilled promises and open questions. *Carcinogenesis,* **28,** 1133-9.

Perera D; Tilston V; Hopwood JA; Barchi M; Boot-Handford RP; Taylor SS (2007) Bub1 maintains centromeric cohesion by activation of the spindle checkpoint. *Dev Cell,* **13,** 566-79.

Perez RP; Lewis LD; Beelen AP; Olszanski AJ; Johnston N; Rhodes CH; Beaulieu B; Ernstoff MS; Eastman A (2006) Modulation of cell cycle progression in human tumors: a pharmacokinetic and tumor molecular pharmacodynamic study of cisplatin plus the Chk1 inhibitor UCN-01 (NSC 638850). *Clin Cancer Res,* **12,** 7079-85.

Perez de Castro I; de Carcer G; Malumbres M (2007) A Census of Mitotic Cancer Genes: New Insights into Tumor Cell Biology and Cancer Therapy. *Carcinogenesis,* **28,** 899-912.

Petermann E; Caldecott KW (2006) Evidence that the ATR/Chk1 pathway maintains normal replication fork progression during unperturbed S phase. *Cell Cycle,* **5,** 2203-9.

Peters GJ; van der Wilt CL; van Moorsel CJ; Kroep JR; Bergman AM; Ackland SP (2000) Basis for effective combination cancer chemotherapy with antimetabolites. *Pharmacol Ther,* **87,** 227-53.

Pfleger CM; Kirschner MW (2000) The KEN box: an APC recognition signal distinct from the D box targeted by Cdh1. *Genes Dev,* **14,** 655-65.

Pines J (2006) Mitosis: a matter of getting rid of the right protein at the right time. *Trends Cell Biol,* **16,** 55-63.

Pinto M; Soares MJ; Cerveira N; Henrique R; Ribeiro FR; Oliveira J; Jerónimo C; Teixeira MR (2007) Expression changes of the MAD mitotic checkpoint gene family in renal cell carcinomas characterized by numerical chromosome changes. *Virchows Arch,* **450,** 379-85.

Pray TR; Parlati F; Huang J; Wong BR; Payan DG; Bennett MK; Issakani SD; Molineaux S; Demo SD (2002) Cell cycle regulatory E3 ubiquitin ligases as anticancer targets. *Drug Resist Updat,* **5,** 249-58.

Rajagopalan H; Nowak MA; Vogelstein B; Lengauer C (2003) The significance of unstable chromosomes in colorectal cancer. *Nat Rev Cancer,* **3,** 695-701.

Rape M; Reddy SK; Kirschner MW (2006) The processivity of multiubiquitination by the APC determines the order of substrate degradation. *Cell,* **124,** 89-103.

Reddy SK; Rape M; Margansky WA; Kirschner MW (2007) Ubiquitination by the anaphase-promoting complex drives spindle checkpoint inactivation. *Nature,* **446,** 921-5.

Reed JC (2006) Proapoptotic multidomain Bcl-2/Bax-family proteins: mechanisms, physiological roles, and therapeutic opportunities. *Cell Death Differ,* **13,** 1378-86.

Richardson PG; Mitsiades C; Hideshima T; Anderson KC (2005) Proteasome inhibition in the treatment of cancer. *Cell Cycle,* **4,** 290-6.

Rieder CL; Cole RW; Khodjakov A; Sluder G (1995) The checkpoint delaying anaphase in response to chromosome monoorientation is mediated by an inhibitory signal produced by unattached kinetochores. *J Cell Biol,* **130,** 941-8.

Rivera T; Losada A (2006) Shugoshin and PP2A, shared duties at the centromere. *Bioessays,* **28,** 775-9.

Ross DD; Doyle LA (2004) Mining our ABCs: pharmacogenomic approach for evaluating transporter function in cancer drug resistance. *Cancer Cell,* **6,** 105-7.

Roux PP; Blenis J (2004) ERK and p38 MAPK-Activated Protein Kinases: a Family of Protein Kinases with Diverse Biological Functions. *Microbiol Mol Biol Rev,* **68,** 320-344.

Saelens X; Kalai M; Vandenabeele P (2001) Translation inhibition in apoptosis: caspase-dependent PKR activation and eIF2-alpha phosphorylation. *J Biol Chem,* **276,** 41620-8.

Sampath D; Cortes J; Estrov Z; Du M; Shi Z; Andreeff M; Gandhi V; Plunkett W (2006) Pharmacodynamics of cytarabine alone and in combination with 7-hydroxystaurosporine (UCN-01) in AML blasts in vitro and during a clinical trial. *Blood,* **107,** 2517-24.

Sampath D; Rao VA; Plunkett W (2003) Mechanisms of apoptosis induction by nucleoside analogs. *Oncogene,* **22,** 9063-74.

Sancar A; Lindsey-Boltz LA; Unsal-Kacmaz K; Linn S (2004) Molecular mechanisms of mammalian DNA repair and the DNA damage checkpoints. *Annu Rev Biochem,* **73,** 39-85.

Schmidt M; Bastians H (2007) Mitotic drug targets and the development of novel anti-mitotic anticancer drugs. *Drug Resist Updat,* **10,** 162-81.

Schmidt M; Budirahardja Y; Klompmaker R; Medema RH (2005) Ablation of the spindle assembly checkpoint by a compound targeting Mps1. *EMBO Rep,* **9,** 866-72.

Schreiber V; Dantzer F; Ame JC; de Murcia G (2006) Poly(ADP-ribose): novel functions for an old molecule. *Nat Rev Mol Cell Biol,* **7,** 517-28.

Scolnick DM; Halazonetis TD (2000) Chfr defines a mitotic stress checkpoint that delays entry into metaphase. *Nature,* **406,** 430-5.

Shackney SE; Smith CA; Miller BW; Burholt DR; Murtha K; Giles HR; Ketterer DM; Pollice AA (1989) Model for the genetic evolution of human solid tumors. *Cancer Res,* **49,** 3344-54.

Shapiro GI (2006) Cyclin-dependent kinase pathways as targets for cancer treatment. *J Clin Oncol.,* **24,** 1770-83.

Shapiro GI; Harper JW (1999) Anticancer drug targets: cell cycle and checkpoint control. *J Clin Invest,* **104,** 1645-53.

Sherr CJ; Roberts JM (1999) CDK inhibitors: positive and negative regulators of G1-phase progression. *Genes Dev,* **13,** 1501-12.

Sherr CJ; Roberts JM (2004) Living with or without cyclins and cyclin-dependent kinases. *Genes Dev,* **18,** 2699-711.

Shichiri M; Yoshinaga K; Hisatomi H; Sugihara K; Hirata Y (2002) Genetic and epigenetic inactivation of mitotic checkpoint genes hBUB1 and hBUBR1 and their relationship to survival. *Cancer Res,* **62,** 13-7.

Shiloh Y (2001) ATM and ATR: networking cellular responses to DNA damage. *Curr Opin Genet Dev,* **11,** 71-7.

Shin HJ; Baek KH; Jeon AH; Park MT; Lee SJ; Kang CM; Lee HS; Yoo SH; Chung DH; Sung YC; McKeon F; Lee CW (2003) Dual roles of human BubR1, a mitotic checkpoint kinase, in the monitoring of chromosomal instability. *Cancer Cell,* **4,** 483-97.

Shinohara M; Mikhailov AV; Aguirre-Ghiso JA; Rieder CL (2006) Extracellular signal-regulated kinase 1/2 activity is not required in mammalian cells during late G2 for timely entry into or exit from mitosis. *Mol Biol Cell,* **17,** 5227-40.

Slattery SD; Moore RV; Brinkley BR; Hall RM (2007) Aurora-C and Aurora-B share phosphorylation and regulation of cenp-A and borealin during mitosis. *Cell Cycle,* **7,** .

Smith ML; Ford JM; Hollander MC; Bortnick RA; Amundson SA; Seo YR; Deng CX; Hanawalt PC; Fornace AJ Jr (2000) p53-mediated DNA repair responses to UV radiation: studies of mouse cells lacking p53, p21, and/or gadd45 genes. *Mol Cell Biol,* **20,** 3705-14.

Sotillo R; Hernando E; Diaz-Rodriguez E; Teruya-Feldstein J; Cordon-Cardo C; Lowe SW; Benezra R (2007) Mad2 overexpression promotes aneuploidy and tumorigenesis in mice. *Cancer Cell,* **11,** 9-23.

Steegmaier M; Hoffmann M; Baum A; Lenart P; Petronczki M; Krssak M; Gurtler U; Garin-Chesa P; Lieb S; Quant J; Grauert M; Adolf GR; Kraut N; Peters JM; Rettig WJ (2007) BI 2536, a potent and selective inhibitor of polo-like kinase 1, inhibits tumor growth in vivo. *Curr Biol,* **17,** 316-22.

Stegmeier F; Rape M; Draviam VM; Nalepa G; Sowa ME; Ang XL; McDonald ER 3rd; Li MZ; Hannon GJ; Sorger PK; Kirschner MW; Harper JW; Elledge SJ (2007) Anaphase initiation is regulated by antagonistic ubiquitination and deubiquitination activities. *Nature,* **446,** 876-81.

Stevaux O; Dyson NJ (2002) A revised picture of the E2F transcriptional network and RB function. *Curr Opin Cell Biol,* **14,** 684-91.

Stewart ZA; Leach SD; Pietenpol JA (1999) p21(Waf1/Cip1) inhibition of cyclin E/Cdk2 activity prevents endoreduplication after mitotic spindle disruption. *Mol Cell Biol,* **19,** 205-15.

Stewart ZA; Pietenpol JA (2001) p53 Signaling and cell cycle checkpoints. *Chem Res Toxicol,* **14,** 243-63.

Storchova Z; Pellman D (2004) From polyploidy to aneuploidy, genome instability and cancer. *Nat Rev Mol Cell Biol,* **5,** 45-54.

Stucke VM; Silljé HH; Arnaud L; Nigg EA (2002) Human Mps1 kinase is required for the spindle assembly checkpoint but not for centrosome duplication. *EMBO J.,* **21,** 1723-32.

Sudakin V; Chan GK; Yen TJ (2001) Checkpoint inhibition of the APC/C in HeLa cells is mediated by a complex of BUBR1, BUB3, CDC20, and MAD2. *J Cell Biol,* **154,** 925-36.

Sudo T; Nitta M; Saya H; Ueno NT (2004) Dependence of paclitaxel sensitivity on a functional spindle assembly checkpoint. *Cancer Res,* **64,** 2502-8.

Sugimoto I; Murakami H; Tonami Y; Moriyama A; Nakanishi M (2004) DNA replication checkpoint control mediated by the spindle checkpoint protein Mad2p in fission yeast. *J Biol Chem,* **279,** 47372-8.

Sun XF (2006) Clinicopathological and biological features of DNA tetraploid colorectal cancers. *Cancer J,* **12,** 501-6.

Swenson KI; Farrell KM; Ruderman JV (1986) The clam embryo protein cyclin A induces entry into M phase and the resumption of meiosis in Xenopus oocytes. *Cell,* **47,** 861-70.

Sze KM; Ching YP; Jin DY; Ng IO (2004) Association of MAD2 expression with mitotic checkpoint competence in hepatoma cells. *J Biomed Sci,* **11,** 920-7.

Takahashi T; Haruki N; Nomoto S; Masuda A; Saji S; Osada H; Takahashi T (1999) Identification of frequent impairment of the mitotic checkpoint and molecular analysis of the mitotic checkpoint genes, hsMAD2 and p55CDC, in human lung cancers. *Oncogene,* **18,** 4295-300.

Takai N; Hamanaka R; Yoshimatsu J; Miyakawa I (2005) Polo-like kinases (Plks) and cancer. *Oncogene,* **24,** 287-91.

Takenaka K; Moriguchi T; Nishida E (1998) Activation of the protein kinase p38 in the spindle assembly checkpoint and mitotic arrest. *Science,* **280,** 599-602.

Tang CJ; Lin CY; Tang TK (2006) Dynamic localization and functional implications of Aurora-C kinase during male mouse meiosis. *Dev Biol,* **290,** 398-410.

Tang Z; Bharadwaj R; Li B; Yu H (2001) Mad2-Independent inhibition of APCCdc20 by the mitotic checkpoint protein BubR1. *Dev Cell,* **1,** 227-37.

Tao W (2005) The mitotic checkpoint in cancer therapy. *Cell Cycle,* **4,** 1495-9.

Tao W; South VJ; Diehl RE; Davide JP; Sepp-Lorenzino L; Fraley ME; Arrington KL; Lobell RB (2007) An inhibitor of the kinesin spindle protein activates the intrinsic apoptotic pathway independently of p53 and de novo protein synthesis. *Mol Cell Biol,* **27,** 689-98.

Tao W; South VJ; Zhang Y; Davide JP; Farrell L; Kohl NE; Sepp-Lorenzino L; Lobell RB (2005) Induction of apoptosis by an inhibitor of the mitotic kinesin KSP requires both activation of the spindle assembly checkpoint and mitotic slippage. *Cancer Cell,* **8,** 49-59.

Taylor SS; Ha E; McKeon F (1998) The human homologue of Bub3 is required for kinetochore localization of Bub1 and a Mad3/Bub1-related protein kinase. *J Cell Biol,* **142,** 1-11.

Taylor SS; McKeon F (1997) Kinetochore localization of murine Bub1 is required for normal mitotic timing and checkpoint response to spindle damage. *Cell,* **89,** 727-35.

Taylor SS; Scott MI; Holland AJ (2004) The spindle checkpoint: a quality control mechanism which ensures accurate chromosome segregation. *Chromosome Res,* **12,** 599-616.

Taylor WR; Stark GR (2001) Regulation of the G2/M transition by p53. *Oncogene,* **20,** 1803-15.

Thompson CB (1995) Apoptosis in the pathogenesis and treatment of disease. *Science,* **267,** 1456-62.

Toledo F; Wahl GM (2006) Regulating the p53 pathway: in vitro hypotheses, in vivo veritas. *Nat Rev Cancer,* **6,** 909-23.

Uetake Y; Sluder G (2004) Cell cycle progression after cleavage failure: mammalian somatic cells do not possess a "tetraploidy checkpoint". *J Cell Biol,* **165,** 609-15.

Uhlmann F (2003) Chromosome cohesion and separation: from men and molecules. *Curr Biol,* **13,** R104-14.

Upender MB; Habermann JK; McShane LM; Korn EL; Barrett JC; Difilippantonio MJ; Ried T (2004) Chromosome transfer induced aneuploidy results in complex dysregulation of the cellular transcriptome in immortalized and cancer cells. *Cancer Res,* **64,** 6941-9.

Vader G; Medema RH; Lens SM (2006) The chromosomal passenger complex: guiding Aurora-B through mitosis. *J Cell Biol,* **173,** 833-7.

van Vugt MA; Medema RH (2005) Getting in and out of mitosis with Polo-like kinase-1. *Oncogene,* **24,** 2844-59.

van Vugt MA; van de Weerdt BC; Vader G; Janssen H; Calafat J; Klompmaker R; Wolthuis RM; Medema RH (2004) Polo-like kinase-1 is required for bipolar spindle formation but is dispensable for anaphase promoting complex/Cdc20 activation and initiation of cytokinesis. *J Biol Chem,* **279,** 36841-54.

van de Weerdt BC; Medema RH (2006) Polo-like kinases: a team in control of the division. *Cell Cycle,* **5,** 853-64.

Vaux DL; Cory S; Adams JM (1988) Bcl-2 gene promotes haemopoietic cell survival and cooperates with c-myc to immortalize pre-B cells. *Nature,* **335,** 440-2.

Vigneron S; Prieto S; Bernis C; Labbe JC; Castro A; Lorca T (2004) Kinetochore localization of spindle checkpoint proteins: who controls whom? *Mol Biol Cell,* **15,** 4584-96.

Vijapurkar U; Wang W; Herbst R (2007) Potentiation of kinesin spindle protein inhibitor-induced cell death by modulation of mitochondrial and death receptor apoptotic pathways. *Cancer Res,* **67,** 237-45.

Vischioni B; Oudejans JJ; Vos W; Rodriguez JA; Giaccone G (2006) Frequent overexpression of aurora B kinase, a novel drug target, in non-small cell lung carcinoma patients. *Mol Cancer Ther,* **5,** 2905-13.

Vitale I; Galluzzi L; Vivet S; Nanty L; Dessen P; Senovilla L; Olaussen KA; Lazar V; Prudhomme M; Golsteyn RM; Castedo M; Kroemer G (2007) Inhibition of Chk1 Kills Tetraploid Tumor Cells through a p53-Dependent Pathway. *PLoS ONE,* **2,** e1337.

Vogel C; Hager C; Bastians H (2007) Mechanisms of mitotic cell death induced by chemotherapy-mediated G2 checkpoint abrogation. *Cancer Res,* **67,** 339-45.

Vogel C; Kienitz A; Hofmann I; Muller R; Bastians H (2004) Crosstalk of the mitotic spindle assembly checkpoint with p53 to prevent polyploidy. *Oncogene,* **23,** 6845-6853.

Vogel C; Kienitz A; Müller R; Bastians H (2005) The mitotic spindle checkpoint is a critical determinant for topoisomerase-based chemotherapy. *J Biol Chem,* **280,** 4025-4028.

Vousden KH; Lu X (2002) Live or let die: the cell's response to p53. *Nat Rev Cancer,* **2,** 594-604.

Wang D; Lippard SJ (2005) Cellular processing of platinum anticancer drugs. *Nat Rev Drug Discov,* **4,** 307-20.

Wang H; Hu X; Ding X; Dou Z; Yang Z; Shaw AW; Teng M; Cleveland DW; Goldberg ML; Niu L; Yao X (2004) Human Zwint-1 specifies localization of Zeste White 10 to kinetochores and is essential for mitotic checkpoint signaling. *J Biol Chem,* **279,** 54590-8.

Wang HK; Morris-Natschke SL; Lee KH (1997) Recent advances in the discovery and development of topoisomerase inhibitors as antitumor agents. *Med Res Rev,* **17,** 367-425.

Wang Q; Fan S; Eastman A; Worland PJ; Sausville EA; O'Connor PM (1996) UCN-01: a potent abrogator of G2 checkpoint function in cancer cells with disrupted p53. *J Natl Cancer Inst,* **88,** 956-65.

Wang X; Jin DY; Ng RW; Feng H; Wong YC; Cheung AL; Tsao SW (2002) Significance of MAD2 expression to mitotic checkpoint control in ovarian cancer cells. *Cancer Res,* **62,** 1662-8.

Wang X; Jin DY; Wong YC; Cheung AL; Chun AC; Lo AK; Liu Y; Tsao SW (2000) Correlation of defective mitotic checkpoint with aberrantly reduced expression of MAD2 protein in nasopharyngeal carcinoma cells. *Carcinogenesis,* **21,** 2293-7.

Wang Y; O'Brate A; Zhou W; Giannakakou P (2005) Resistance to microtubule-stabilizing drugs involves two events: beta-tubulin mutation in one allele followed by loss of the second allele. *Cell Cycle,* **4,** 1847-53.

Wang Z; Fukuda S; Pelus LM (2004) Survivin regulates the p53 tumor suppressor gene family. *Oncogene,* **23,** 8146-53.

Warnke S; Kemmler S; Hames RS; Tsai HL; Hoffmann-Rohrer U; Fry AM; Hoffmann I (2004) Polo-like kinase-2 is required for centriole duplication in mammalian cells. *Curr Biol,* **14,** 1200-7.

Wassmann K; Liberal V; Benezra R (2003) Mad2 phosphorylation regulates its association with Mad1 and the APC/C. *EMBO J,* **22,** 797-806.

Weaver BA; Cleveland DW (2005) Decoding the links between mitosis, cancer, and chemotherapy: The mitotic checkpoint, adaptation, and cell death. *Cancer Cell,* **8,** 7-12.

Weaver BA; Silk AD; Montagna C; Verdier-Pinard P; Cleveland DW (2007) Aneuploidy acts both oncogenically and as a tumor suppressor. *Cancer Cell,* **11,** 25-36.

Wei MC; Zong WX; Cheng EH; Lindsten T; Panoutsakopoulou V; Ross AJ; Roth KA; MacGregor GR; Thompson CB; Korsmeyer SJ (2001) Proapoptotic BAX and BAK: a requisite gateway to mitochondrial dysfunction and death. *Science,* **292,** 727-30.

Weichert W; Denkert C; Schmidt M; Gekeler V; Wolf G; Köbel M; Dietel M; Hauptmann S (2004) Polo-like kinase isoform expression is a prognostic factor in ovarian carcinoma. *Br J Cancer,* **90,** 815-21.

Wheatley SP; Henzing AJ; Dodson H; Khaled W; Earnshaw WC (2004) Aurora-B phosphorylation in vitro identifies a residue of survivin that is essential for its localization and binding to inner centromere protein (INCENP) in vivo. *J Biol Chem,* **279,** 5655-60.

Wheatley SP; McNeish IA (2005) Survivin: a protein with dual roles in mitosis and apoptosis. *Int Rev Cytol,* **247,** 35-88.

Williams BC; Li Z; Liu S; Williams EV; Leung G; Yen TJ; Goldberg ML (2003) Zwilch, a new component of the ZW10/ROD complex required for kinetochore functions. *Mol Biol Cell,* **14,** 1379-91.

Willis S; Day CL; Hinds MG; Huang DC (2003) The Bcl-2-regulated apoptotic pathway. *J Cell Sci,* **116,** 4053-6.

Winkles JA; Alberts GF (2005) Differential regulation of polo-like kinase 1, 2, 3, and 4 gene expression in mammalian cells and tissues. *Oncogene,* **24,** 260-6.

Woessner R; Corrette C; Allen S; Hans J; Zhao Q; Aicher T; Lyssikatos J; Robinson J; Poch G; Hayter L; Cox A; Lee P; Winkler J; Koch K; Wallace E (2007) ARRY-520, a KSP Inhibitor with Efficacy and Pharmacodynamic Activity in Animal Models of Solid Tumors. *Proc Am Ass Cancer Res,* Abstr. 1433.

Wong C; Stearns T (2005) Mammalian cells lack checkpoints for tetraploidy, aberrant centrosome number, and cytokinesis failure. *BMC Cell Biol,* **6,** 6.

Wu CW; Chi CW; Huang TS (2004) Elevated level of spindle checkprotein MAD2 correlates with cellular mitotic arrest, but not with aneuploidy and clinicopathological characteristics in gastric cancer. *World J Gastroenterol,* **10,** 3240-4.

Wu Y; Mehew JW; Heckman CA; Arcinas M; Boxer LM (2001) Negative regulation of bcl-2 expression by p53 in hematopoietic cells. *Oncogene,* **20,** 240-51.

Yamaguchi H; Bhalla K; Wang HG (2003) Bax plays a pivotal role in thapsigargin-induced apoptosis of human colon cancer HCT116 cells by controlling Smac/Diablo and Omi/HtrA2 release from mitochondria. Cancer Res 63, 1483-1489. *Cancer Res,* **63,** 1483-1489.

Yan X; Cao L; Li Q; Wu Y; Zhang H; Saiyin H; Liu X; Zhang X; Shi Q; Yu L (2005) Aurora C is directly associated with Survivin and required for cytokinesis. *Genes Cells,* **10,** 617-26.

Yang M; Li B; Tomchick DR; Machius M; Rizo J; Yu H; Luo X (2007) p31comet blocks Mad2 activation through structural mimicry. *Cell,* **131,** 744-55.

Yee KS; Vousden KH (2005) Complicating the complexity of p53. *Carcinogenesis,* **26,** 1317-22.

Yen TJ; Compton DA; Wise D; Zinkowski RP; Brinkley BR; Earnshaw WC; Cleveland DW (1991) CENP-E, a novel human centromere-associated protein required for progression from metaphase to anaphase. *EMBO J,* **10,** 1245-54.

Yoon YM; Baek KH; Jeong SJ; Shin HJ; Ha GH; Jeon AH; Hwang SG; Chun JS; Lee CW (2004) WD repeat-containing mitotic checkpoint proteins act as transcriptional repressors during interphase. *FEBS Lett,* **575,** 23-9.

Yu H (2006) Structural activation of Mad2 in the mitotic spindle checkpoint: the two-state Mad2 model versus the Mad2 template model. *J Cell Biol,* **173,** 153-7.

Yu X; Minter-Dykhouse K; Malureanu L; Zhao WM; Zhang D; Merkle CJ; Ward IM; Saya H; Fang G; van Deursen J; Chen J (2005) Chfr is required for tumor suppression and Aurora A regulation. *Nat Genet,* **37,** 401-6.

Yuan B; Xu Y; Woo JH; Wang Y; Bae YK; Yoon DS; Wersto RP; Tully E; Wilsbach K; Gabrielson E (2006) Increased expression of mitotic checkpoint genes in breast cancer cells with chromosomal instability. *Clin Cancer Res,* **12,** 405-10.

Zachos G; Black EJ; Walker M; Scott MT; Vagnarelli P; Earnshaw WC; Gillespie DA (2007) Chk1 is required for spindle checkpoint function. *Dev Cell,* **12,** 247-60.

Zeng Y, F.K., Wu Z; Moreno S; Piwnica-Worms H; Enoch T, Moreno S; Piwnica-Worms H; Enoch T, Piwnica-Worms H; Enoch T, and Enoch T, (1998) Replication checkpoint requires phosphorylation of the phosphatase Cdc25 by Cds1 or Chk1. *Nature,* **395,** 507-10.

Zhang W; Fletcher L; Muschel RJ (2005) The role of Polo-like kinase 1 in the inhibition of centrosome separation after ionizing radiation. *J Biol Chem,* **280,** 42994-9.

Zhao R; Gish K; Murphy M; Yin Y; Notterman D; Hoffman WH; Tom E; Mack DH; Levine AJ (2000) Analysis of p53-regulated gene expression patterns using oligonucleotide arrays. *Genes Dev,* **14,** 981-93.

Zhou J; Giannakakou P (2005) Targeting microtubules for cancer chemotherapy. *Curr Med Chem Anticancer Agents,* **5,** 65-71.

Zinkel S; Gross A; Yang E (2006) BCL2 family in DNA damage and cell cycle control. *Cell Death Differ,* **13,** 1351-9.

Appendix

Abbreviations

A	ampere
Act D	actinomycin D
adr	adriamycin
au	arbitrary units
A-O	α-amanitin oleate
BSA	bovine serum albumin
bp	base pairs
BrdU	bromodeoxyuridine
°C	degree Celsius
cDNA	complementary DNA
caspase	cysteine aspartate protease
CIN	chromosome instability
cm	centimeter
cpm	counts per minute
Cyclo	cycloheximide
cyt C	cytochrome C
Da	Dalton
DEPC	diethylpyrocarbonate
DMEM	Dulbecco's modified Eagle's medium
DMSO	dimethyl sulfoxide
DNA	desoxyribonucleic acid
EDTA	ethylendiaminetetraacetatic acid
EGM-2	epithelial growth medium 2
E. coli	Escherichia coli
et al.	et alteres: and others
FACS	fluorescence activated cell sorting
F	Farad
f	femto ($1x10^{-15}$)
FSC	forward scatter
g	gram(s)

Gö	Gö6976
h	hour(s)
HUVEC	human umbilical vein epithelial cells
Hygro	hygromycin
IF	immunofluorescence
IMT	Institute for Molecular Biology and Tumour Research, Philipps-University Marburg, Marburg, Germany
IP	immunoprecipitation
k	kilo
kb	kilo base pair(s)
LB	lysogeny broth
µ	micro ($1x10^{-6}$)
m	milli ($1x10^{-3}$)
M	molarity
MCS	multiple cloning site
min	minute(s)
MIN	microsatellite instability
mon	monastrol
MPM2	mitotic protein monoclonal 2
mRNA	messenger RNA
n	nano ($1x10^{-9}$)
NB	Northern blot(ting)
noc	nocodazole
OD	optical density
p	pico ($1x10^{-12}$)
PARP	poly ADP ribose polymerase
PBS	phosphate buffered saline
PCR	polymerase chain reaction
pen/strep	penicillin/streptomycin
pH	negative decadic logarithm of H^+ ion concentration
PI	propidium iodide
PU	purvalanol A
Puro	puromycin
RNA	ribonucleic acid

RNase	ribonuclease
rpm	rotations per minute
RPMI	Roswell Park Memorial Institute 1640
RV	roscovitine
SDS	sodium dodecyl sulfate
sec	second(s)
SSC	sideward scatter
SSC	sodium chloride-sodium citrate
TAE	tris-acetate EDTA
tax	taxol
Tris	tris(hydroxymethyl)aminomethane
UCN	UCN-01
UV	ultraviolet
V	volt(s)
WB	Western blot(ting)
ZM	ZM447439

Acknowledgements

It is impossible to acknowledge all the influences and persons, who helped me to come to this point in life, but I want to thank everyone who helped to shape this work by providing me with the education, the intellectual challenges and the working opportunities required to pursue an academic career.

My sincere thanks are due to professor Dr. Rolf Müller for the excellent scientific environment at the IMT.

I am deeply grateful to my supervisor PD Dr Holger Bastians for giving me the opportunity to explore the fascinating subject, for the good working conditions and fruitful and extensive discussions.

My special thanks for their excellent collaboration in experiments are due to Anne Kienitz and Christian Hager.

I thank PD Dr Heike Krebber for stimulating discussions.

I warmly thank the past and present members of the Bastians lab, in particular Irmgard Hofmann, Ivonne Morales, Anne Kienitz, Verena Grodd, Christian Hager, Ailine Stolz and Norman Ertych, who accompanied me during my thesis with helpful discussions, good humor and through the challenges of everyday lab life. Their great ability for team work is highly appreciated.

I wish to thank the past and present members of the Krebber lab, in particular Merle Windgassen, Melanie Jauernig, Thomas Groß, Dorothée Sturm, Alexandra Hackmann, Claudia Baierlein and Tobias Sorg for a good time and helpful discussions.

I am grateful to the past and present members of the IMT groups Müller, Eilers, Bauer, Suske, Lutz and Gaubatz, in particular Michael Wanzel, Tobias Otto, Alexandra Sapetschnig, Imme Krüger, Kerstin Nau, Markus Rieck, Sabine Müller-Brüsselbach, Uschi Eilers, Guntram Suske and Wolfgang Meißner.

I am indebted to secretary Ulrike Schülke and technical assistants Klaus Weber and Bernhard Wilke. While the former tirelessly and cheerfully helped me to navigate administrative matters, the latter always lended a screwdriver or a helping hand, when needed.

My warm thanks are due to my friends, a cosmopolitan crowd of different creeds and professions, which keep my life interesting: Insa Stroman, Claudia Bergin, Karin Bologa, Julia Hamori, Salvatore Manmana, Françoise Debierre-Grockiego, Margret Adam, Rainer Wiegmann, Christine Richter, Ulrike Kreysler.

I am deeply grateful to my brother Bennet, my parents Dorothea and Peter Vogel and my aunt Urte Dehn, who taught me the sense of dedication required for my profession. They always believed in me and helped me to think outside the box.

Last but not least I want to thank André Wedell, a versatile mind with pitch black humor and the patience to accompany me through all the ups and downs of academia and life outside the ivory tower.

Academic teachers

Ruprecht-Karls-Universität Heidelberg, Heidelberg, Germany:

Bautz, Behnke, Bock, Bock, Braunbeck, Buselmeier, Comba, Dobberstein, Dubbers, Erbar, Foerste, Fuchs, Gehring, Geier, Gleiter, Hassel, Henkel, Herrmann, Hüttemann, Huttner, Irngartinger, Jantzen, Jentsch, Krautter, Kreß, Leins, Leitz, Lorra, Moeller, Müller, Nullmeier, Rausch, Riedel, Schill, Schneider, Schölzer, Soldati, Stitt, Storch, Thiele, Ulmschneider, Vogt, Warnatz, Weber, Weinhold, Zimmermann.

Georg-August-Universität Göttingen, Göttingen, Germany:

Aufermann, Bartels, Bohlander, Burfeind, Drehwald, Dröge-Laser, Engel, Fritz, Gatz, Gradstein, Günther, Hofmann, Kessler, Klaus, Kolmar, Korte, Kramer, Kriete, Laccone, Meins, Reiß, Rupke, Sterner, Wilke, Zoll.

Universiteit Leiden, Leiden, the Netherlands:

Hooykaas, Nagelkerke, Offringa, Van de Water.

Philipps-Universität Marburg, Marburg, Germany:

Bastians, Krebber, Müller.

Curriculum Vitae

Name: Celia Jill Vogel
Address: Steinweg 35a, 35037 Marburg, Germany
Telephone: +49-6421-590634
E-mail: celia.vogel@gmx.net

Date of Birth: 28.03.1977
Place of Birth: Oldenburg (Oldb.), Germany
Marital Status: single

Higher education and academic record

1989-1996 Herbartgymnasium Oldenburg, Germany

21.05.1996 Abitur (A-levels)

10.1996-07.1998 study of biology at the Ruprecht-Karls-Universität Heidelberg, Germany

18.07.1998 Vordiplom (Associate degree)

10.1998-03.2002 study of biology at the Georg-August-Universität Göttingen, Germany

10.1998-09.1999 study of biology at the Georg-August-Universität Göttingen, Germany

10.1999-03.2000 research project and study of biology at the Universiteit Leiden, the Netherlands, funded by the Erasmus programme

04.2000-03.2002 study of biology at the Georg-August-Universität Göttingen, Germany

11.03.2002 Graduation as Diplom-Biologin (Master of Biological Sciences). Diploma thesis: „Functional analyses of a novel chromatin binding protein" at the Institute for Human Genetics, Medical Faculty, Georg-August-Universität Göttingen, Germany

06.2002-12.2007 PhD student, Institute for Molecular Biology and Tumor Research (IMT), PD Dr. H. Bastians, Philipps-Universität Marburg, Germany

10.2003-09.2005 study of human biology at the Philipps-Universität Marburg, Germany

06.2002-10.2006 experimental work for the PhD thesis: "The role of the Mitotic Spindle Checkpoint in Chemotherapy-Induced Apoptosis"

01.-12.2007 experimental work on characterization of novel spindle checkpoint activating compounds for anti-cancer chemotherapy: collaboration with Altana PharmaAG as part of the TransMIT center for "Cell Cycle Associated Targets for Chemotherapy" (PD Dr. H. Bastians at the IMT, Philipps-Universität Marburg)

05.-12.2007 experimental work for the revision of a paper on a novel spindle checkpoint function of components of DNA damage checkpoints

Publications

Vogel C*; Kienitz A*; Hofmann I; Müller R; Bastians H (2004) Crosstalk of the mitotic spindle assembly checkpoint with p53 to prevent polyploidy. *Oncogene,* **23,** 6845-6853.

Vogel C*; Kienitz A*; Müller R; Bastians H (2005) The mitotic spindle checkpoint is a critical determinant for topoisomerase-based chemotherapy. *J Biol Chem,* **280,** 4025-4028.

Kienitz A*; Vogel C*; Morales I; Müller R; Bastians H (2005) Partial downregulation of MAD1 causes spindle checkpoint inactivation and aneuploidy, but does not confer resistance towards taxol. *Oncogene,* **24,** 4301-4310.

Vogel C; Hager C; Bastians H (2007) Mechanisms of mitotic cell death induced by chemotherapy-mediated G2 checkpoint abrogation. *Cancer Res,* **67,** 339-45.

Small molecule targeting of the mitotic spindle checkpoint as a novel approach for anti cancer therapy. Manuscript in preparation.

*: co-authorship

Research Communications and Posters

Deutsche Krebshilfe, Meeting on Apoptosis 2004, Bonn, Germany
Kienitz A.; Vogel C.; Hofmann I.; Müller R.; Bastians H. (2004) Crosstalk of the mitotic spindle assembly checkpoint with p53.

ELSO Conference 2005, Dresden, Germany
Vogel C.; Kienitz A.; Müller R.; Bastians H. (2005) Functional crosstalk of the mitotic spindle checkpoint with apoptotic pathways.

ELSO Conference 2005, Dresden, Germany
Kienitz A.; Vogel C.; Grodd V.; Bastians H. (2005) Pharmacological targeting of the mitotic spindle checkpoint: a novel strategy for anticancer therapy.

Annual meeting of the Society for Biochemistry and Molecular Biology 2005, Berlin/Potsdam, Germany
Vogel C.; Kienitz A.; Grodd V.; Bastians H. (2005) Pharmacological targeting of the mitotic spindle checkpoint as a novel approach for anti-cancer treatment.

ChemBioNet Meeting Europe 2005, Frankfurt am Main, Germany
Kienitz A.; Grodd V.; Vogel C.; Bastians H. (2005) Small molecule targeting of the mitotic spindle checkpoint as a novel approach for anti cancer treatment.

Annual meeting of the German Society for Cell Biology 2006, Braunschweig, Germany
Kienitz A.; Vogel C.; Grodd V.; Stolz A.; Bastians H. (2006) A chemical biology approach to the spindle checkpoint: a tool to investigate the mechanisms of checkpoint activation and implications for anti cancer treatment. *Eur. J. Cell Biol.* **85S1**, Suppl. 56.

German Society for Cell Biology, 8th Young Scientist Meeting "Cell biology of cancer" 2006, Heidelberg, Germany
Kienitz A.; Grodd V.; Stolz A.; Vogel C.; Bastians H. (2006) Pharmacological targeting of the mitotic spindle checkpoint: a novel strategy for cancer therapy

7th International Chromosome Segregation and Aneuploidy Workshop 2007, Naantali, Finland
Vogel C., Kienitz A., Grodd V., Stolz A., Scheffler K., Bastians H. (2007) Small molecule targeting of the mitotic spindle checkpoint: a novel concept for anti-cancer therapy?

Oral presentations

German Society for Cell Biology, 8th Young Scientist Meeting "Cell biology of cancer" 2006, Heidelberg, Germany
Vogel, C.; Hager C.; Bastians H. (2006) Mitotic cell death induced by chemotherapy mediated G2 checkpoint abrogation: mechanisms and improvements

Ehrenwörtliche Erklärung

Ich erkläre ehrenwörtlich, dass ich die dem Fachbereich Medizin Marburg zur Promotionsprüfung eingereichte Arbeit mit dem Titel “The Role of the Mitotic Spindle Checkpoint in Chemotherapy-Induced Apoptosis” im Institut für Molekularbiologie und Tumorforschung (Geschäftsführender Direktor: Prof. Dr. Rolf Müller) unter Leitung von Herrn PD Dr. Holger Bastians ohne sonstige Hilfe selbst durchgeführt und bei der Abfassung der Arbeit keine anderen als die in der Dissertation aufgeführten Hilfsmittel benutzt habe. Ich habe bisher an keinem in- oder ausländischen Medizinischen Fachbereich ein Gesuch um Zulassung zur Promotion eingereicht, noch die vorliegende oder eine andere Arbeit als Dissertation vorgelegt.
Die vorliegende Arbeit wurde in folgenden Publikationsorganen Cancer Research, Journal of Biological Chemistry und Oncogene veröffentlicht (siehe: Publications).

Marburg, den 28.03.2008, Celia Vogel